UNIVERSITAT DE BARCELONA

Physical Cosmology in the Epoch of Large Surveys

Ali Rida Khalife

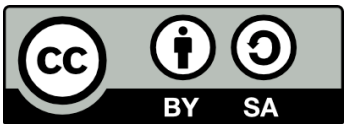

Tesi doctoral

Physical Cosmology in the Epoch of Large Surveys

Autor: Ali Rida Khalife

Director: Raúl Jiménez

UNIVERSITAT DE BARCELONA

Physical Cosmology in the Epoch of Large Surveys

Programa de doctorat en física

Línia de recerca en astronomia i astrofísica

Autor: Ali Rida Khalife

Director: Raúl Jiménez

Tutor: Alberto Manrique Oliva

Lloc on s'ha dut a terme la tesi

UNIVERSITAT DE BARCELONA

Ali Rida Khalifeh, *Physical Cosmology in the Epoch of Large Surveys*,
PhD Thesis
Barcelona, Spain
December 01, 2021

Cover Image:

DECLARATION

This thesis is presented following the regulations of the University of Barcelona (Aprovada pel CdG en sessió del 16 de març de 2012 i modificada pel CdG de data 9 de maig i 19 de juliol de 2012, 29 de maig i 3 d'octubre de 2013, 17 de juliol de 2014, 16 de juliol de 2015, 15 de juny i 21 de novembre de 2016, 5 de desembre de 2017, 4 de maig de 2018, 15 de maig de 2019 i 22 de juliol de 2019, 6 de marçde 2020 i 22 d'abril 2020). The listed regulations allow for the presentation of a PhD thesis as a "compendia of published articles". According to the regulations, the thesis must contain a minimum of three published or accepted articles. This thesis contains the published version of five articles, which is sufficient to allow its presentation. It also contains one additional article, submitted but not yet accepted for publication at the moment of thesis presentation.

Barcelona, Spain, December 01, 2021

Ali Rida Khalifeh

...to my beloved grandmother, my queen, the late Najlah Amin Hamzeh.

ABSTRACT

Our understanding of the Universe has advanced tremendously in the past few decades. Having a well established theory of gravity, General Relativity(GR), laid the ground for a successful model for the Universe, ΛCDM. However, despite the fact that GR and ΛCDM passed numerous observational tests, there are still some fundamental open questions about them that need to be explored. It is therefore the objective of this thesis to highlight some of these questions by exploring them from a theoretical perspective, in addition to presenting current and future means of exploring them observationally.

This thesis includes five parts. In the first part, the Introduction, I will present an overview about the basic concepts in GR and ΛCDM that are needed to understand the following parts, in addition to some historical background.

The second part is on testing an essential assumption in Cosmology, the *Copernican Principle*, which states that the Universe is homogeneous and isotropic on large scales. Theoretically, by distinguishing between line-of-sight and transverse expansion rates in the most general spacetime possible, one can constrain deviations from the Copernican Principle. Observationally, this is done using polarization of Cosmic Microwave Background(CMB) photons that have been inverse-Compton scattered by galaxy clusters. The result is a constraint on remote isotropy, which is equivalent to homogeneity.

In the third part, the possibility that Dark Matter(DM) is part of Gravity is investigated. This is done on a Cosmological, as well as on an astrophysical scale. In the former, I present a case study with a specific modified gravity model: Mimetic Dark Matter(MDM). By re-deriving the model's equations of motion, extra free functions and parameters appear in need of fine tuning to produce the observationally certified adiabatic initial conditions. To visualize this, I modify the Boltzmann code `CLASS` to include MDM, and then look at CMB correlation functions and matter power spectra, which show that deviations of at least 10% from adiabatic initial conditions fall beyond cosmic variance limits.

On an astrophysical scale, the hypothesis that DM is part of a modified gravity theory(MGT) is tested by examining DM devoid galaxies. The main argument is that if DM is part of a MGT, then this phenomenon should be found in every gravitational system. The fact that around 19 galaxies have been found with almost non-existing trace of DM, while other similar ones are DM dominated, constrains severely the above mentioned hypothesis. To quantify this, I derive a generalized Virial theorem for any MGT, and show that the extra term,

which should be associated to DM, when fitted to these 19 galaxies, gives inconsistent results. Therefore, unless fine-tuning is used, DM is more likely to be a non-baryonic particle, or a compact object such as primordial black holes, rather than part of a MGT.

The fourth part explores the realm of Quantum Field Theory(QFT) in a gravitational background, where the interaction between scalar and quantum spinor fields in curved spacetime is presented. The goal is to use neutrinos(spinors) as probes for Dark Energy(DE), to distinguish between its different models. After laying down a general formalism, I first investigate three types of interactions between the two fields, in a semi-classical way, and study the consequences on oscillations of neutrinos and their dynamics.

This framework is later generalized to a broader class of interactions between neutrinos, as quantum spinors, and DE, either in the form of a Cosmological Constant(CC) or a scalar field. I managed to show that, in principle, one can observe the difference DE models have on the transition probability between two neutrino flavors. This provides a proof of concept for using neutrino oscillations in curved spacetime as a tool to distinguish between models of the late acceleration of the Universe.

To put the above in an observational perspective, I conclude the fourth part by considering the full three-flavor neutrino oscillations within the ΛCDM paradigm. This results in ternary diagrams and flux plots that could be later compared to observations in neutrino observatories.

The fifth and final part summarizes the results and conclusions reached for each work. In addition, future perspectives and further developments are discussed in this section.

ACKNOWLEDGMENTS

I would like to start by thanking the person without whom I wouldn't be here writing this thesis, my supervisor Raúl Jiménez. It was perhaps the best coincidence ever that we met during your visit to Lebanon in the summer of 2017, which was the start of a great mentorship and friendship. I thank you for all the help, support, patience and advice you gave me during these years.

Second, A big thanks goes to Licia Verde, head of the Cosmology group at ICCUB, for the moral support I received from her through my PhD years, in addition to the help and advice she gave me on writing research statements and this very thesis. I would like to thank my dear friend Nicola Bellomo, whom I consider a cornerstone for my scientific journey. Thank you Nicola for spending time in helping and teaching me tricks that I will for sure use along my career.

I feel a deep sense of gratitude for the current and past members of our group, for the wonderful discussions, the nice gatherings and the willingness to help at every moment. So thank you José, Héctor, Davide Gualdi, Davide Bianchi, Nils, Alba and Katie. A special thanks goes to my good friends David Valcin and Samuel Brieden for sharing with me a great deal of the hardship of a PhD. I would also like to thank Roy Maartens for his much appreciated assistance with my first project, as well as for the, perhaps too many, reference letters for postdoc applications.

To the ICC PhD students of the 7th floor, Dani, Edgar, Alfred, Juan, Pau, Núria, thank you for the good time we spent together during lunch and the many gatherings we did.

A big round of applause goes to all the ICC personnel for always solving the unending problems of bureaucracy and technology. Thank you Miriam, Kayla, Dani, Gabi, Jordi, Joan and JR.

To my many friends in Barcelona, I thank you very much for the wonderful times we spent together and the never ending encouragement. Thank you for the laughs, gatherings and emotional support. You guys are my second family! Thank you dear Ettore, Omar L., Harry, Tomas, Omar M., Kevin, Abed, Alejandro, Miquel, Hind, Ziad Mroueh, Ahmad, Diana, Hiba, Soulafa, Shady, Joe, Riham, Haisam, Ziad Merhe, Mira, Christel, Alex, Monica and Farah.

Last, but most certainly not least, I would like to thank my family in Lebanon and Qatar. You're presence in my life was, and still is, motivating me to continue my quest in science. I would like to thank you for the support and encouragement you gave me, when the society didn't. Mama, Baba, Batoul and Hassouna, a special thanks goes for you! Hadhoud, Khalo-Hammoudi, Khalo-Bassem, Aya, Mohtadi,

Mahdi, Hadi, Sarah, Neemat, Chirine, Ali, Deaibes, Haitham, Albert, Abou Omar, George A., Michel, Andrew, Jad, George S, Lama, Sarah Maria, Zeineddine, Rodrigue, Wassim, Mahsha, Sally and Bahaa thank you for being part of my life.

RESUMEN EN ESPAÑOL

Nuestra comprensión del Universo ha avanzado enormemente en las últimas décadas. Tener una teoría de la gravedad bien establecida, la Relatividad General (GR), sentó las bases para un modelo exitoso para el Universo, ΛCDM. Sin embargo, a pesar del hecho de que GR y ΛCDM pasaron numerosas pruebas de observación, todavía hay algunas preguntas abiertas fundamentales sobre ellos que deben explorarse. Por tanto, el objetivo de esta tesis es resaltar algunas de estas cuestiones explorándolas desde una perspectiva teórica, además de presentar los medios actuales y futuros de explorarlas observacionalmente. Esta tesis consta de cinco partes. En la primera parte, la Introducción, presentaré una descripción general sobre los conceptos básicos en GR y ΛCDM que se necesitan para comprender las siguientes partes, además de algunos antecedentes históricos, convenciones y notaciones.

La segunda parte trata de probar una suposición esencial en Cosmología, el *Principio de Copérnico*, que establece que el Universo es homogéneo e isotrópico a gran escala. Teóricamente, al distinguir entre la línea de visión y las tasas de expansión transversal en el espaciotiempo más general posible, se pueden restringir las desviaciones del principio de Copérnico. Observacionalmente, esto se hace usando la polarización de fotones de fondo cósmico de microondas(CMB) que han sido dispersados en Compton inverso por cúmulos de galaxias. El resultado es una restricción sobre la isotropía remota, que es equivalente a la homogeneidad.

En la tercera parte, se investiga la posibilidad de que Dark Matter (DM) sea parte de Gravity. Esto se hace tanto a escala cosmológica como astrofísica. En el primero, presento un caso de estudio con un modelo de gravedad modificado específico: Mimetic Dark Matter (MDM). Al volver a derivar las ecuaciones de movimiento del modelo, aparecen funciones y parámetros libres adicionales que necesitan un ajuste fino para producir las condiciones iniciales adiabáticas certificadas por observación. Para visualizar esto, modifico el código de Boltzmann `CLASS` para incluir MDM, y luego observo las funciones de correlación CMB y los espectros de potencia de la materia, que muestran que las desviaciones de al menos un 10 % de las condiciones iniciales adiabáticas caen más allá de los límites de varianza cósmica.

A escala astrofísica, la hipótesis de que la DM es parte de una teoría de la gravedad modificada (MGT) se prueba examinando galaxias desprovistas de DM. El argumento principal es que si DM es parte de un MGT, entonces este fenómeno debería encontrarse en todos los sistemas gravitacionales. El hecho de que se hayan encontrado

alrededor de 19 galaxias con trazas casi inexistentes de DM, mientras que otras similares están dominadas por DM, limita severamente la hipótesis mencionada anteriormente. Para cuantificar esto, derivo un teorema de Virial generalizado para cualquier MGT y muestro que el término adicional, que debería estar asociado a DM, cuando se ajusta a estas 19 galaxias, da resultados inconsistentes. Por lo tanto, a menos que se utilice un ajuste fino, es más probable que DM sea una partícula no bariónica o un objeto compacto como agujeros negros primordiales, en lugar de parte de un MGT.

La cuarta parte explora el ámbito de la teoría cuántica de campos (QFT) en un trasfondo gravitacional, donde se presenta la interacción entre los campos de espino escalar y cuántico en el espacio-tiempo curvo. El objetivo es utilizar neutrinos (espinores) como sondas de Energía Oscura (DE), para distinguir entre sus diferentes modelos. Después de establecer un formalismo general, primero investigo tres tipos de interacciones entre los dos campos, de manera semiclásica, y estudio las consecuencias sobre las oscilaciones de los neutrinos y su dinámica.

Este marco se generaliza posteriormente a una clase más amplia de interacciones entre neutrinos, como espinores cuánticos, y DE, ya sea en forma de una constante cosmológica (CC) o un campo escalar. Logré demostrar que, en principio, se puede observar la diferencia que tienen los modelos DE sobre la probabilidad de transición entre dos sabores de neutrinos. Esto proporciona una prueba de concepto para el uso de oscilaciones de neutrinos en el espacio-tiempo curvo como una herramienta para distinguir entre modelos de la aceleración tardía del Universo.

La quinta y última parte resume los resultados y conclusiones alcanzados para cada trabajo. Además, en esta sección se analizan las perspectivas futuras y los desarrollos futuros.

PUBLICATIONS

Complete list of publications at the moment of thesis deposit.

Published articles in this thesis

- *"Distinguishing Dark Energy Models Using Neutrino Oscillations"*; **A.R. Khalifeh**, Raul Jimenez; Physics of the Dark Universe Journal 34(2021)100897; arXiv:2105.07973.
- *"Spinors and Scalars in curved spacetime: neutrino dark energy (DEν)"*; **A.R. Khalifeh**, Raul Jimenez; Physics of the Dark Universe 31(2021) 100777; arXiv:2010.08181.
- *"Can Dark Matter be Geometry? A Case Study with Mimetic Dark Matter"*; **A.R. Khalifeh**, Nicola Bellomo, José Luis Bernal, Raul Jimenez; Physics of the Dark Universe, 30(2020)100646; arXiv:1907.03660.
- *"Dwarf Galaxies without Dark Matter: constraints on Modified Gravity"*; **A.R. Khalifeh**, Raul Jimenez; Monthly Notices of the Royal Astronomical Society 501(2021)1, 254-260; arXiv:1912.08592.
- *"Measuring the Homogeneity of the Universe using Polarization Drift"*; Raul Jimenez, Roy Maartens, **A.R. Khalifeh**, Robert R Caldwell, Alan F Heavens, Licia Verde; Journal of Cosmology and Astroparticle Physics, 05, 048, 2019; arXiv:1902.11298.

Other articles submitted

- *"Using Neutrino Oscillations to Measure H_0"*; **A.R.Khalifeh** and Raul Jimenez; arXiv:2111.15249; Under review.

White papers

- *"EuCAPT White Paper: Opportunities and Challenges for Theoretical Astroparticle Physics in the Next Decade"*.arxiv:2110.10074

CONTENTS

1 INTRODUCTION

Spacetime tells matter how to move; matter tells spacetime how to curve. These were the twelve simple words John Wheeler used to summarize GR. Although it took Albert Einstein around 10 years to fully formalize the theory, we reached a stage in understanding it that we can sum it up like Wheeler did. GR is considered one of human kind's great achievements in the 20th century(along with quantum theory) and so far our best description for gravitational phenomena. Therefore, comprehending it is a basic first step in studying the Cosmos, i.e Cosmology.

In this chapter, I will present the main concepts and equations from GR that are necessary to explain our current status in Cosmology. This includes: the Equivalence Principle, the metric of spacetime and the Einstein-Hilbert action, along with the field equations that come out of it. Furthermore, to be specific for Cosmology, I will present the Friedmann-Lemaître-Robertson-Walker(FRW) metric, with the resulting Friedmann equations, in addition to a cursory description of the cosmic inventory and initial conditions of the Universe. Finally, a brief description of spinor fields in curved spacetime is presented, before giving an overview of this thesis. These topics are essential for understanding the works of chapters 2, 3 and 4. Most of the information can be found in references such as [1–4]

1.1 THE EQUIVALENCE PRINCIPLE

The story of GR starts in 1687, when Isaac Newton attempted to answer the question:"what determines an inertial frame?". According to Newton, inertial frames are coordinate systems in which equations of motion hold their "usual form", i.e the one given in Newton's first law of motion. From experiments presented in his *Principia* [5], Newton concluded that there's an absolute space in which inertial frames are at rest, or with respect to which they are in a state of uniform motion.

This argument was criticized by many for decades, with the most constructive one given my Ernest Mach in the 1880's [6]. Mach interpreted Newton's experiments as hinting at an interaction between us and the celestial bodies, which is now known as *Mach's Principle*. In other words, Mach believed that inertial frames now depend on the stars' positions and velocities with respect to us, i.e. they are not absolute. This left the community at a crossroad: either we believe Newton's absolute spacetime, with respect to which stars and galaxies

can be at rest or in uniform motion, or Mach's principle of our unity with the Cosmos.

As a first step in solving this dilemma [1], Albert Einstein established the *Principle of Special Relativity*(PSR) in 1905, which states that [7]:

> *Physical equations of motion are invariant under Lorentz, rather than Galilean, transformations.*

The importance of this principle is that it includes a bigger group of transformations that could leave the equations of motion invariant. Indeed, Newton only considered Galilean transformations in his definition of inertial frames, since he was focusing on his first law of motion. But Einstein showed that these equations are a limit of those of Special Relativity(SR), and that Galilean transformations are a subset of the Lorentz group. This results in a broader scope for the definition of inertial frames.

The next step was to generalize and incorporate the PSR with a relativistic gravitational theory, which Einstein did in 1907 by first introducing the *Principle of Equivalence of Gravitation and Inertia*(PoE) [8]. In its strong form, the principle states that:

> *At every point in spacetime, in an arbitrary gravitational field, it is possible to choose a coordinate system that is locally inertial, such that, in a small enough region around that point, the laws of nature are those of an unaccelerated Cartesian coordinate system in the absence of gravity.*

This means that inertial frames correspond to those that are freely falling in a gravitational field. Einstein's answer puts him close to Mach's, but the two answers are not quite the same. According to the PoE, in the absence of nearby matter, the gravitational field, and hence the inertial frame, is determined by the mean gravitational field produced by stars and galaxies far away. However, once a large mass(like the sun) is put near the observer, the inertial frames are now determined by the gravitational field of this mass, and not anymore by the rest of the Cosmos. The PoE has been tested in several ways and for many years(see [9] and references therein for past tests), and there's still interest in testing it nowadays [10]. These tests established the PoE as a concrete principle to define inertial coordinate systems, and thus end the dilemma first presented by Newton.

Having established the PoE, Einstein then continued working on formulating a relativistic theory of gravity, basing it on *Riemannian geometry*. The reason why this applies is the latter's similarity with the PoE: in Riemannian geometry, one can always define a set of locally Cartesian coordinates at any point in a curved space, which

1 It should be noted that, originally, the purpose of this work was to insure the invariance of Maxwell's equations under a coordinate transformation, thus preserving the universality of the speed of light.

is equivalent to say that, locally, matter satisfies the laws of SR. By noticing this resemblance between the PoE and Riemannian geometry, in a series of papers that resulted in a final one in 1916 [11], Einstein finally put forward his theory of gravity, GR, which we will now explore mathematically.

1.2 A MATHEMATICAL APPROACH TO GR

In this section, I will follow a practical introduction to GR, for the purpose of following up on the mathematics that appear later on in this thesis. For more details, the reader is advised to check [12].

The most fundamental entity in GR is the *metric tensor*, commonly symbolized by $g_{\mu\nu}$, which sets clocks and rulers in our four dimensional spacetime to define temporal and spatial distances. More specifically, the metric defines an invariant interval:

$$ds^2 = g_{\mu\nu} dx^\mu dx^\nu \tag{1.1}$$

where dx^μ is an infinitesimal of a general coordinate system x^μ, with μ, ν running from 0 to 3 for the 4 dimensions. For example, in Cartesian coordinates, $x^\mu = \{x^0, x^1, x^2, x^3\} = \{t, x, y, z\}$, with t being time and x, y, z are the three spatial coordinates. When we move to a coordinate system moving with a test particle, then $dx = dy = dz = 0$, and so ds becomes the *proper time* interval, $d\tau$, of these particles. Note that this does not apply for the case of light-like, i.e those that satisfy $ds^2 = 0$, since one cannot go to a frame in which light is at rest.

From the metric, one can then define the *Christoffel symbols*, or the affine connection:

$$\Gamma^\lambda_{\ \mu\nu} = \frac{1}{2} g^{\lambda\alpha} \left[\partial_\mu g_{\alpha\nu} + \partial_\nu g_{\alpha\mu} - \partial_\alpha g_{\mu\nu} \right] \tag{1.2}$$

where $g^{\lambda\alpha}$ is the inverse of $g_{\mu\nu}$ and $\partial_\alpha = \partial / \partial x^\alpha$. Mathematically, $\Gamma^\lambda_{\ \mu\nu}$ is not a tensor, i.e it does not transform as one under a coordinate transformation. Its purpose is to insure invariance of the equations of motion(EoM) under a general coordinate transformation. These EoM are generalized in GR from Newton's to the *geodesic equation*:

$$\frac{d^2 x^\alpha}{d\lambda^2} + \Gamma^\alpha_{\ \beta\gamma} \frac{dx^\beta}{d\lambda} \frac{dx^\gamma}{d\lambda} = 0 \tag{1.3}$$

where λ is an *affine parameter*, one that increases monotonically along the particle's path. Incidentally, in curved spacetime, particles no longer follow straight lines, rather they travel along *geodesics*, paths that extremize the action of a free particle,

$$S_{\text{free}} = \int \sqrt{g_{\mu\nu} \frac{dx^\mu}{d\lambda} \frac{dx^\nu}{d\lambda}} d\lambda, \tag{1.4}$$

where one can check that by extremizing eq. (1.4), we get eq. (1.3). Another useful way to write the geodesic equation is:

$$U^\alpha \nabla_\alpha U^\beta = 0 \tag{1.5}$$

where $U^\alpha = dx^\alpha/d\lambda$ is the 4-velocity of the particle and ∇_α is the *covariant derivative*. The latter generalizes ∂_α to one in curved spacetime, and so when it acts on a vector[2], it becomes:

$$\nabla_\alpha V^\beta = \partial_\alpha V^\beta + \Gamma^\beta_{\alpha\gamma} V^\gamma. \tag{1.6}$$

Having now the Christoffel symbols, one can then calculate the *Riemann Curvature Tensor*:

$$R^\alpha_{\beta\gamma\delta} = \partial_\gamma \Gamma^\alpha_{\beta\delta} - \partial_\delta \Gamma^\alpha_{\beta\gamma} + \Gamma^\alpha_{\gamma\lambda}\Gamma^\lambda_{\beta\delta} - \Gamma^\alpha_{\delta\lambda}\Gamma^\lambda_{\beta\gamma}. \tag{1.7}$$

As its name suggests, the Riemann tensor quantifies the local curvature at each point in our spacetime. One can also derive two useful quantities from eq. (1.7), the *Ricci tensor* and *Ricci Scalar* as

$$R_{\alpha\beta} = R^\lambda_{\alpha\lambda\beta} \quad \text{and} \quad R = g^{\alpha\beta} R_{\alpha\beta}, \tag{1.8}$$

respectively.

The last ingredient we need to finish our discussion on GR is the *Einstein field equations*. These are the result of extremizing the Einstein-Hilbert action,

$$S_{\text{GR}} = \int d^4x \sqrt{-g} \left[\frac{1}{2\kappa} R + \mathcal{L}_m \right], \tag{1.9}$$

where g is the determinant of the metric, $\kappa = c^4/8\pi G$, with c being the speed of light, G is Newton's constant, and $\mathcal{L}_m$ is the matter[3] Lagrangian density. By varying eq. (1.9) with respect to the metric, we finally get the Einstein field equations:

$$R_{\mu\nu} - \frac{1}{2} g_{\mu\nu} R = \frac{1}{\kappa} T_{\mu\nu} \tag{1.10}$$

where

$$T_{\mu\nu} = \frac{-1}{\sqrt{-g}} \frac{\delta(\sqrt{-g}\mathcal{L}_m)}{\delta g^{\mu\nu}} \tag{1.11}$$

is the *stress-energy tensor*, which quantifies the energy content of matter that modifies the spacetime curvature. One particular form of the stress-energy tensor which is very useful is that of a *perfect fluid*, which takes the form:

$$T_{\mu\nu} = (\rho + p) u_\mu u_\nu + p g_{\mu\nu} \tag{1.12}$$

2 To be more specific, a *contravariant* vector, one with an upper index. When it has a lower index, the quantity is called a *covariant* vector

3 In here, matter includes everything that is not geometrical in nature. We will see in the next section that there's a distinction between matter and radiation in Cosmology.

where ρ,p and u^μ are the energy density, pressure and 4-velocity of a certain type of fluid, respectively.

Eqs. (1.3) and (1.10) are what Wheeler's quote mentioned at the beginning of this chapter is about. Spacetime(encoded in the Christoffel symbol) tells matter how to move($d^2x^\alpha/d\lambda^2$); matter($T_{\mu\nu}$) tells spacetime how to curve($R_{\mu\nu} - \frac{1}{2}g_{\mu\nu}R$). The formalism presented here applies to any kind of spacetime and to any matter content, taking GR as the theory of gravity. We shall now see how a specific type of spacetime metric, when combined with every type of matter that we know (and don't know) of, can result in the field of Cosmology.

1.3 A BRIEF INTRODUCTION TO COSMOLOGY

Since the beginning of human civilizations, questions such as "Why are we here?", "How did we get here?" and "Where are we heading?" have been asked repeatedly. It wasn't until now that we were able to form scientific, testable answers to these questions, thanks to modern Cosmology.

In short, Cosmology is a discipline that combines GR and thermodynamics, resulting in a plethora of tools to describe our universe. In this section, we will go over the main equations and concepts that constitute pillars of modern Cosmology.

1.3.1 *FRW Metric*

To start our discussion, we need to find out what's the form of our Universe's metric. Two ingredients enter into determining this. The first one is the *Copernican Principle*, the assumption that our universe is homogeneous and isotropic on very large scales, i.e we do not occupy a very special place in the Universe. Many observational probes have been put to test this principle, and chapter 2 will be dedicated to this.

Mathematically, such a homogeneous and isotropic universe corresponds to two properties. First, hypersurfaces of constant time are maximally symmetric subspaces of the whole spacetime, which means that there are 6 transformations that leave their metric invariant (6 because the surfaces are 3 dimensional). Second, the global metric and matter components are invariant under the isometries of these subspaces, i.e they can depend only on time. These requirements result in the following general spacial line element(in spherical coordinates):

$$ds_3^2 = a^2(t)\left(\frac{dr^2}{1-Kr^2} + r^2 d\Omega^2\right) \tag{1.13}$$

where the subscript 3 stands for 3 dimensional space, r is the radial coordinate, $d\Omega^2 = d\theta^2 + \sin^2\theta d\phi^2$ is the solid angle given in terms of the angular coordinates θ and ϕ. We will get to the meaning of

$a(t)$ shortly. Moreover, K determines the type of curvature of such a subspace: if $K = 0$ it would be flat(Euclidean) space, if $K = 1$ it's positively curved(spherical) and if $K = -1$ then it's negatively curved(hyperbolic.)

The second ingredient that enters into determining the metric's form is the observational fact that our universe is expanding in an accelerating way. The first evidence for the expansion of the universe came from Edwin Hubble [13][4], by measuring the recession velocity of galaxies away from us. This means that if we grid our spacetime, points on this grid, which correspond to observers at rest, will be getting further away from each other as time advances. This is why we have an $a(t)$, the *scale factor*, in eq. (1.13): it quantifies this increasing distance between grid points. Incidentally, the term in parenthesis in eq. (1.13) defines the *comoving distance* between grid points, one that doesn't take into account the expansion, and thus remains constant.

Finally, we need to add the time coordinate, since we live(as we know so far) in a 4-dimensional spacetime, to get the FRW metric:

$$ds^2 = -c^2dt^2 + a^2(t)\left(\frac{dr^2}{1-Kr^2} + r^2d\Omega^2\right). \tag{1.14}$$

Note the minus sign next to the temporal distance. There should always be a sign difference between spacial and temporal coordinates in the metric to insure its invariance under Lorentz transformations. The coordinates' sign convention will be discussed at the end of this chapter.

Before deriving the equations of motion that will determine the Universe's evolution, it will prove advantageous to work with a re-scaled time variable, the *conformal time*, defined as:

$$d\eta^2 = \frac{dt^2}{a^2(t)}. \tag{1.15}$$

One of these advantages is that if we look at a flat FRW universe, inserting (1.15) in the metric (1.14), we get

$$ds^2 = a^2(\eta)\big(-c^2d\eta^2 + dr^2 + r^2d\Omega^2\big) \tag{1.16}$$

i.e a flat FRW metric described with conformal time becomes proportional to Minkowski (flat) spacetime. This is one way to see *Conformal flatness* of FRW spacetime, i.e. it can be transformed into Minkowski spacetime by a simple Weyl rescaling. This is a very important property to keep in mind for FRW metric.

4 There's some debate about whether Hubble should be accredited the first discovery of the expansion of the Universe. See [14, 15] for a historical discussion

1.3.2 *Equations of Motion*

Inserting eq. (1.14) in eq. (1.10), with the help of eqs. (1.8), (1.7) and (1.12), we get the first,

$$H^2 + \frac{Kc^2}{a^2} = \frac{c^4}{3\kappa}\rho, \tag{1.17}$$

and second,

$$\frac{\ddot{a}}{a} = -\frac{c^4}{6\kappa}\left(\rho + \frac{3p}{c^2}\right), \tag{1.18}$$

Friedmann equations. In eq. (1.17), $H = \dot{a}/a$, where " $\dot{}$ " denotes derivative with respect to t, is the *Hubble parameter*, which quantifies the relative change in scale factor with time.

As is evident from eqs. (1.17) and (1.18), the matter content of the universe(left hand side of those equations), determines its evolution(the right one). Therefore, we also need to know how the matter content evolves and the effect of gravity on this evolution. The latter is described by the *continuity equation*:

$$\dot{\rho} + 3H\left(\rho + \frac{P}{c^2}\right) = 0. \tag{1.19}$$

This is a consequence of energy-momentum conservation, i.e $\nabla_\alpha T_{\beta\gamma} = 0$, which is automatically satisfied due to the *Bianchi identity*:

$$\nabla_\alpha\left[R_{\beta\gamma} - \frac{1}{2}g_{\beta\gamma}R\right] = 0. \tag{1.20}$$

Furthermore, one can define an *equation of state* for a certain type of fluids, by writing

$$P = \omega\rho c^2. \tag{1.21}$$

This equation facilitates the analysis of different types of particles. For instance, if we assume ω is a constant, then eq. (1.19) is easily solved to give:

$$\rho = \rho_0 a^{-3(\omega+1)}, \tag{1.22}$$

where ρ_0 is the present value of the energy density of this specie. Fluids with $\omega = 0, 1/3$ and -1 correspond to non-relativistic matter, radiation and vacuum energy, respectively. The resulting energy densities depend on the scale factor as:

$$\rho_{rad} \propto a^{-4}; \quad \rho_m \propto a^{-3}; \text{ and } \rho_v = \text{constant}, \tag{1.23}$$

respectively. Incidentally, for species with $0 \leq \omega \leq 1/3$, we notice from eqs. (1.17) and (1.18) that this leads to $\dot{a} > 0$ and $\ddot{a} < 0$, i.e a decelerating expansion. On the other hand, if $\omega \leq -1$, we get an

accelerated expansion($\dot{a}, \ddot{a} > 0$). This shows the importance of eq. (1.21) in determining which species dominate the evolution of the universe, and therefore determining its thermal history.

Before delving into that, it is useful to define two parameters that are repeatedly used in Cosmology. The first is the *density parameter* of some specie i:

$$\Omega_i = \frac{\rho_i}{\rho_{cr}}, \tag{1.24}$$

where the *critical energy density* is $\rho_{cr} = 3\kappa H_0^2/c^4$, with H_0 being the value of the Hubble parameter today. It is evident from its definition that the sum over all density parameters should be 1, once we define a density parameter of K as

$$\Omega_K = -\frac{Kc^2}{H_0^2 a^2}. \tag{1.25}$$

This, combined with the strong observational evidence for a spatially flat Universe, i.e $K = 0$ [16, 17], is an indication for the existence of the *dark sector*, as we will see later.

The second useful parameter is the *redshift*, formally defined as the amount of stretching light's wavelength suffers due to the expansion of the universe. It is related to the scale factor by:

$$1 + z = \frac{a_0}{a(t)}, \tag{1.26}$$

where a_0 is the value of the scale factor today, usually set to 1. The redshift provides another way to measure time, and it is usually used in Cosmology for this purpose.

1.3.3 *Thermal History of the Universe*

In this part, I will briefly go over the main events, energy scales and content of interest in our Universe's thermal history, starting from a Big Bang singularity. More emphasis will be made on the characteristics of species we know must exist so far. For more details, see [1, 2, 18]

- **Planck Scale, Inflation and Grand Unified Theory:**
  The upper threshold in energy to which we can extend out classical theory of gravity(GR) is set by the Planck mass $M_{\rm pl}c^2 = 10^{19}$GeV. Beyond this threshold, we should start taking quantum gravity effects into account, which is still an active field of research.

  Another important event in the very early Universe is Inflation, which we will talk about in more detail in the next subsection. Inflation is expected to happen around the scale of Grand Unification, about 10^{16}GeV, i.e the scale at which electromagnetic, weak and strong forces were unified.

- **Baryo/Lepto-genesis:**
  A quark-antiquark and lepton-antilepton asymmetry occurred around the time inflation ended. If both species were created with equal abundance, they would have annihilated in the early universe, leaving nothing but radiation. However, we know that such an asymmetry must exist due to abundance of particles over anti-particles in the Universe, although we don't know yet how this asymmetry happened.

  Quantitatively, this asymmetry is translated by the fact that we have a small, yet non-vanishing, *baryon-to-photon ratio* $\equiv \eta_b = n_b/n_\gamma = 5.5 \times 10^{-10}$, where n_b and n_γ are the baryons and photon number densities, respectively.

- **Electro-weak phase transition:**
  The electromagnetic and weak interactions start to deviate from each other at thermal energies of around 100 GeV, or 10^{-12}s after the big bang. This happens when the weak interaction mediators, $W^{\pm}$ and Z^0 Bosons, gain their masses of around 80 and 90 GeV, respectively, through the Higgs mechanism.

- **QCD phase transition:**
  At thermal energy below 150 MeV, quarks become asymptotically free and start forming bound states of two (mesons) or three (baryons) of them. This corresponds to about 20 μs after the Big Bang.

- **Neutrino decoupling:**
  So far, there are a few things we know about neutrinos from the Standard Model(SM) of particle Physics. First, we know there are three types(generations) of them: electron, muon and tau neutrinos. Second, there's one degree of freedom for each anti-/neutrino generation (since there are no right handed neutrinos in the SM). Third, we know that they are fermions, and therefore they should follow the Fermi-Dirac thermal distribution. However, whether these particles are their own anti-particle or not, i.e whether they are of Dirac or Majorana type, is still debatable [19, 20].

  Strictly through weak interactions, neutrinos maintain thermal equilibrium with the sea of particles in the early universe, the *primordial plasma*. However, at around 1 MeV(or 1 s after the Big Bang) they start decoupling, i.e going out of equilibrium, from the primordial plasma. This happens when the expansion rate of the universe starts surpassing that of neutrino interactions. Since then, cosmic neutrinos have been traveling freely, interacting only gravitationally.

  From neutrino oscillation observations, we now know that neutrinos have mass and, from stringent cosmological constraints,

that $\sum_{i=0}^{3} m_i \lesssim 0.1 - 0.2$ eV [16, 21, 22], where the sum goes over the three neutrinos. This shows that neutrino decouples while being relativistic, which is important to keep in mind as we will see in chapter 4.

- **Electron-positron annihilation:**
  The reaction:

$$e^+ + e^- \leftrightarrow \gamma + \gamma \tag{1.27}$$

  remains balanced until the temperature of the universe drops below the electrons rest mass, $m_e c^2 = 511$KeV. After this, electrons and positrons start to annihilate. A major consequence of this is that neutrinos now travel with a temperature different from that of Photons:

$$T_\nu = \left(\frac{4}{11}\right)^{1/3} T_\gamma \tag{1.28}$$

  where T_ν and T_γ are the neutrinos and photon temperatures, respectively. This is why neutrino decoupling and electron-positron annihilation occur close to each other.

- **Big Bang Nucleosynthesis(BBN):**
  When the Universe's thermal energy was around 1 MeV or more, energetic radiation would destroy any newly formed atom or nucleus. Once the temperature drops below 0.1 MeV(about 3 minutes after the Big Bang), this radiation is not strong enough to overcome typical nuclear binding energies, and therefore Helium and Deuterium can start forming, initiating BBN.

  Predictions provided by this process puts restrictions on the baryons energy density, which at that time is composed of protons and neutrons. Moreover, these predictions, when combined with measurements of deuterium abundance from intergalactic media at large distances, result in $\Omega_{b0} \approx 0.05$, which means baryons constitute only 5% of the energy budget in the Universe.

  As we will see shortly, constraints from the CMB and large scale structure show that $\Omega_m \approx 0.3$, where the subscript "m" stands for matter. Therefore, BBN provides a compelling evidence for the existence of DM.

- **Matter-radiation equality:**
  All the events discussed so far(since the end of inflation) occurred in an era where radiation is dominating the energy budget of the universe. In Cosmology, radiation refers to ultra-relativistic species, i.e photons and neutrinos(only at that time). From eq. (1.23), we can see that the energy density of radiation decreases faster than that of matter, and then at thermal energy of 0.75 eV (or a redshift $z = 3400$) these two become equal. From

that point, matter, mainly DM, starts dominating the energy budget of the Universe.

There have been many astrophysical proofs for the existence of DM. These include: galaxy clusters dynamics [23], rotation curves of spiral galaxies [24], X-ray brightness in galaxy clusters [25] and weak lensing [26]. All these indicate that DM interacts only gravitationally with other species, in addition to it being cold, i.e non-relativistic. Moreover, as stated before, CMB observations, particularly peaks of its correlation functions, show that $\Omega_{\text{CDM}} \approx 0.3$, where CDM stands for *cold dark matter*. This means that, since DM decouples very early in the Universe's history, they provide gravitational wells which seed late structure formation, such as galaxies and their clusters.

Despite this plethora of information about DM, we still don't know what is its exact nature: a particle, compact object(such as primordial black holes [27]) or modified gravity. However, we will see in chapter 3 that it is more likely for DM to be either of the former two than the latter.

- **Recombination and photon decoupling:**
  At this stage in the Universe's evolution, ordinary matter in equilibrium contains: protons, electrons, photons, helium and a trace amount of heavier nuclei. Once Compton scattering between photons and electrons becomes unable to keep up with the Universe's expansion rate, electrons and protons start getting together to form the first hydrogen atoms. This is *recombination*, which happens at a thermal energy of roughly 0.3 eV(or at $z \approx 1200$).

  Approximately at the same time, because there are no longer free electrons available to scatter off, photons become free to travel without interactions. This is *photon decoupling*, which also defines the *last scattering surface* from which we see CMB photons.

  These mediators of the electromagnetic interaction, although dominating the number density in the Universe ($n_\gamma \approx 410$ photons/cm^3), they contribute the least to its energy budget, with $\Omega_\gamma \approx 5 \times 10^{-5}$. Moreover, after observing it for many years and through different probes, the CMB is now established as providing most of the radiation in the Universe (the rest coming for stars and galaxies) and that it has an almost perfect black-body spectrum with temperature $T_{\text{CMB}} = 2.723 \pm 0.001$ K.

- **Dark Energy domination:**

  As previously stated, in 1929 Hubble discovered that the Universe is expanding. However, an analysis of the emission spectra from supernovae-Ia showed that the Universe is in an accelerated

expansion [28–30]. Given what was already known about the content of the Universe at that time, this seemed problematic, for the attractive nature of gravity should result in a decelerating Universe.

The only way such accelerated expansion could happen is if the dominant constituent of the Universe has negative pressure. Such a mysterious component has been given the name *dark energy*(DE). Another evidence that comes in favor of DE is the fact that, as already mentioned, the sum of Ω_i for all species should be 1. Given that $\Omega_m \approx 0.3$, and that $K = 0$, then there must be something that compensates for the rest, which is precisely DE, thus having $\Omega_{DE} \approx 0.7$.

In order to explain this entity, the easiest way is to introduce a *cosmological constant*(CC) Λ to the cosmic inventory. This is the same CC used by Einstein to describe a static universe, but with an opposite sign, to insure a negative pressure, i.e $\omega_\Lambda = -1$. However, if one would attribute this type of energy to that of vacuum, calculations from quantum field theory results in an energy density, ρ_Λ, 60 orders of magnitude bigger than what is observed. This resulted in the *fine tuning problem* of cosmology.

Several proposals have been presented to circumvent this problem, such as a dynamical scalar field(*quintessence*) or a modification of GR. Nevertheless, the nature of DE is still an open question.

We have now reached the end of our cosmic inventory description, with the current state of our Universe being with DE dominating the energy budget since a redshift of about 0.5. The final topic in Cosmology, one of utmost importance, is the initial conditions of the Universe, will be addressed next.

1.3.4 *Initial conditions of the Universe and Inflation*

The Big Bang model of the Universe is successful in explaining the abundance of light elements, from which heavier ones started forming, leading to stars, galaxies, etc. However, this model needed a key ingredient in order to have the ability to predict these things: initial conditions(ICs). Of course one can always choose the ICs they want to match observations. The problem is, one would need to fine-tune these ICs too much in order to explain two main issues at the time: *the horizon and flatness problems.*

According to the aforementioned model, two points on the CMB sky separated by at least 1.2° didn't have time(from the Big Bang singularity) to be in causal contact. This means that these two points cannot have the same properties. Nevertheless, the CMB sky is very

smooth, up to one part in 10^5, and so the patches must have been in causal contact. This is the horizon problem.

On the other hand, the flatness problem stems from the fact that our Universe is spatially flat to a big degree, suggesting that the spatial curvature's initial conditions must be fixed at the level of 10^{-60}. This level pf precision requires a very high level of fine-tuning, something that Physicists like to avoid.

To solve these two problems in one hit, as well as provide the initial conditions needed is *Inflation*. This mechanism was first introduced by Alan Guth [31], later followed by Andrei Linde [32], Katsuhiko Sato [33], Alexei Starobinsky [34] and many others(see [35] for a recent review on Inflation). In its simplest forms, this mechanism assumes the presence of a homogeneous scalar field $\varphi(t)$ which slowly rolls down its almost flat potential, causing a rapid accelerated expansion of the Universe. This process would wipe out any initial curvature, resulting in the spatially flat universe we see today without the need of fine-tuning.

Moreover, by increasing the Universe's size 10^{27} times in less than 10^{-37}s, CMB patches would have ample of time to communicate and be in causal contact, which solves the horizon problem. Finally, by relating small perturbations of φ to those for matter, radiation and gravitational potentials, initial conditions are then provided, and Big Bang Nucleosynthesis can proceed as expected(see chapter 7 in [1] and chapter 8 in [2] for a quantitative description of Inflation).

The ability of Inflation to solve all these issue in one blow made it the most successful description of the early universe which, when combined with what has been described so far in this chapter, forms the concordance ΛCDM model. Nonetheless, there are other possible explanations for the state of the early universe that haven't been ruled out completely, such as Cyclic Universe [36, 37], string gas cosmology [38] and loop quantum cosmology [39, 40], to name a few.

As this thesis will not focus on Inflation and its alternatives, it would suffice the information presented so far to end this section on Cosmology. The next topic to be presented is one which has been gaining some attention recently, with a great possibility to enhance our understanding of gravity and cosmology at the fundamental level: *Quantum Spinors in Curved Spacetime.*

1.4 QUANTUM SPINORS IN CURVED SPACETIME

The study of quantum fields in curved spacetime proved to be very useful in Cosmology, specially for calculating the origin of CMB anisotropies and the seeds of large-scale structure during inflation [41]. Moreover, this subject is considered as an essential first step in the quest of understanding the quantum nature of gravity, with numerous attempts to tackle it were faced by its non-renormalizability [42].

Thus far, a great deal of work has been done on scalar and spin-2 fields in curved spacetime, targeting the dynamics of inflation and gravitational waves, respectively [4]. However, not much emphasis has been made on spin-1/2 fields, or *spinors*, traveling in a non-trivial gravitational field. In particular, when applied to the study of *neutrinos*, the study of quantum spinors in curved backgrounds could provide a plethora of gainful insights about our Universe, as this thesis tries to show(see chapter 4).

In this section, I present some of the basic concepts related to quantum spinors in curved spacetime, with the aim of making it easy for the non-expert reader to follow the discussion of chapter 4. This short review is based mainly on the work presented in [43]. Let's start with the most fundamental equation for spinors, the *Dirac equation*.

1.4.1 *Dirac Equation in Curved Spacetime*

Recall the Dirac equation in flat spacetime takes the form:

$$\left(i\hbar\eta_{\mu\nu}\gamma^{\mu}\partial^{\nu} - mc\right)\psi = 0, \tag{1.29}$$

where $\hbar$ is the reduced Planck constant, $\eta_{\mu\nu}$ is the Minkowski metric(diag[-1,1,1,1]), γ^{μ} are the Dirac matrices and m is the spinor's(ψ) mass. Naively, one would think that, to go to curved spacetime, one would simply substitute the above quantities with their curved spacetime correspondences:

$$\left(i\hbar g_{\mu\nu}\nabla^{\nu} - mc\right)\psi = 0. \tag{1.30}$$

However, the general covariance principle, which should allow us to go from (1.29) to (1.30), applies when the equation is written in terms of tensor fields, and spinors are not. Fundamentally, the reason for this hindrance lies in the fact that the general linear group in 4-dimension **GL**(4), which describes general coordinate transformations, doesn't have a spinorial representation [44, 45].

The solution to this impediment would be to work with *tetrad fields* [46], whereby one studies the dynamics of spinors with respect to local inertial observers. Recall that tetrad, or vierbein, field e^{μ}_{a} are defined in the entire spacetime and work by projecting a quantity from its general coordinates form, with index μ, to that in local coordinates a. Therefore, we can write the Dirac matrices as

$$\gamma^{\mu}(x) = e^{\mu}_{a}\gamma^{a}, \tag{1.31}$$

where γ^{a} are the usual Dirac matrices in flat spacetime, satisfying the commutation relation:

$$\gamma^{a}\gamma^{b} + \gamma^{b}\gamma^{a} = -2\eta^{ab}. \tag{1.32}$$

This relation gets generalized, using (1.31), to

$$\gamma^{\mu}(x)\gamma^{\nu}(x) + \gamma^{\nu}(x)\gamma^{\mu}(x) = -2g^{\mu\nu}. \tag{1.33}$$

Moreover, to take into account the spinorial nature of the field, the action of the covariant derivative on ψ can be defined as

$$\mathcal{D}_\mu \psi \equiv (\partial_\mu - \Gamma_\mu)\psi, \tag{1.34}$$

where we use the notation $\mathcal{D}$ for the covariant derivative of a spinor, and Γ_μ is the *spinorial affine connection*. To put it in simple words: the extra effects due to the spinorial nature of the field are summed in Γ_μ. It can be shown that the latter takes the form:

$$\Gamma_\mu(x) = -\frac{1}{4}\gamma_a\gamma_b e^{a\alpha}(x)\nabla_\mu e^b{}_\alpha(x), \tag{1.35}$$

which eventually results in the Dirac equation in curved spacetime to be:

$$\left[i\hbar\gamma^\mu\left(\partial_\mu + \frac{1}{4}\gamma_a\gamma_b e^{a\alpha}\nabla_\mu e^b{}_\alpha\right) - mc\right]\psi = 0. \tag{1.36}$$

Having this modified Dirac equation, along with a metric for gravity, forms the basis from which neutrino oscillations and dynamics in curved spacetime can be studied. This is explained and elaborated on in chapter 4.

1.5 OVERVIEW OF THE THESIS

We have reached a very advanced stage in our understanding of the Universe, both on large and small scales. This understanding is formulated in the ΛCDM concordance model within the context of GR as a theory of gravity. However, one cannot say that this understanding is complete, for a few of its basic constituents are still mysterious.

In particular, one cannot state with absolute certainty that our theory of gravity is given by GR. Although the latter has been successful in describing many phenomena, one must face the fact that its non-renormalizability at the beginning of the Universe is problematic. Moreover, almost 95% of the Universe's energy budget is given by the *dark sector*, with its nature still unknown till this day.

In an attempt to overcome these issues, several distinct models of *modified gravity* have been suggested in the literature. Some of these candidates for a new theory of gravity could cast away all the above issues in one hit, under certain conditions. However, these models are numerous, and it is becoming more important to derive new probes to constrain them, if not rule them out.

It is therefore the purpose of the current thesis to present new theoretical methods that derive observables which could distinguish some of these models. As we are now in the era of *precision Cosmology*, we have a golden opportunity to use this precise data to check the models and constrain their parameters.

The first chapter after the current one, chapter 2, is a prelude for such methodology. There, the polarization of CMB photons that have been

inverse Compton scattered off galaxy clusters is used as a probe for spatial homogeneity. This presents a new method to test the *Copernican Principle*.

Later, in chapter 3, the possibility of DM being part of a modified theory of gravity is investigated in two ways. The first is on cosmological scales, where a case study with a particular modified gravity model, *Mimetic Dark Matter* [47, 48], shows the amount of fine tuning this model needs to match the data. In particular, by re-deriving the equations of motion for this model, one finds additional free functions and constants that need to be fixed. Further, with lack of a built-in mechanism to generated adiabatic initial conditions, these free functions must be tuned to match CMB correlation functions, at least to around 10%. This puts great constraints on this model and its likes.

The second method presented in chapter 3 to test modified gravity is at astrophysical scales. The main argument there is: if DM is part of gravity, then such phenomenon should be present everywhere, by gravity's universality. However, the discovery of DM devoid dwarf galaxies [49–54] puts this hypothesis to question. To show this quantitatively, a generalized Virial theorem is derived for a wide class of modified gravity models. The result is that there is always an additional term in the generalized Virial theorem due to modifications of GR, even for the DM deficient galaxies. Therefore, unless high level of fine tuning is employed, the DM-modified gravity hypothesis is put to question.

In chapter 4, we make a turn towards quantum field theory in curved spacetime, particularly spinor fields. In the first part, a general formalism for the interaction of spinor and scalar fields in a generic spacetime is presented. Later, this formalism is specified to three different types of interactions between the two fields within flat FRW universe, and the dynamics of the spinor field is then studied.

The second part of chapter 4 is an application of the first one to neutrinos[5] interacting with a scalar field in curved spacetime. The purpose is to look at the effect of DE, be it a CC or a scalar field, on neutrino oscillations. To this end, we first present a general form of interaction between the two fields in a generic spacetime. This results in an evolution equation for the neutrino flavor state along its worldline, from which one gets the evolution of the transition amplitude between two flavor states. We then specify the spacetime to be flat FRW, and consider the case of a CC-DE (i.e. no scalar field involved) and a scalar field one coupled to neutrinos by a *linear derivative coupling*(LDC) [55].

The final conclusion from this work is that, depending on which DE model is being used, the transition probability between two flavor states will evolve differently with redshift. Once detected in neutrino

5 For simplicity, we look at two flavor neutrinos.

observatories, this work present the case for neutrino oscillations to be a new probe of DE models.

The final part of chapter 4 is an extension of the above formalism to three-flavor neutrinos, specifying ΛCDM as the model of the Universe. By looking at ternary diagrams and the neutrino fluxes' evolution with redshift, the presented method could be to measure the present acceleration rate of the Universe, H_0. Therefore, neutrino oscillations could provide new insights on the *Hubble tension*.

We finish the thesis with a summary of the results and future prospects in chapter 5.

Part I

TESTING THE COPERNICAN PRINCIPLE

2

MEASURING THE HOMOGENEITY OF THE UNIVERSE

One of modern Cosmology's pillars is the assumption of spatial homogeneity and isotropy of the Universe on large scales. This is known as the *Copernican Principle* which, stated differently, means that we do not live in a special place in the Universe. It is therefore paramount that we check the validity of this assumption as crudely as possible, in order to make sure that we are not missing anything in our analysis.

The spatial isotropy part of the Copernican Principle has been measured to a good extent with several probes. For instance, spatial variations in the CMB temperature with direction are constrained to about 10^{-4}, presenting a strong case for isotropy at the background level. However, spatial homogeneity is not as easily probed.

The fundamental reason for this difficulty is that to probe homogeneity, one must access the interior of our past lightcone, and check for spatial inhomogeneities within it. But that is not easy to do directly, since we can only observe the surface of the lightcone. Therefore, one will need a messenger from within the lightcone that leaves imprints on its surface which give us information about spatial homogeneity.

The following work [56], therefore, presents the case for CMB polarization to be such a probe of spatial homogeneity. To be specific, one must start the analysis without assuming any type of symmetry, i.e. in the most general spacetime possible. This results in having expansion rates in the longitudinal and transverse directions that, in principle, differ from each other. These quantities will then enter into equations of motion for any dynamical quantity. This is on the one hand.

On the other hand, as CMB photons travel from the last scattering surface, they get scattered off energetic electrons inside massive galactic clusters, affecting thereby their polarization. Then, the latter follows an equation of motion that depends on the expansion rates previously mentioned, as these photons travel towards us. By measuring CMB polarization over an extended period of time ($\mathcal{O}(10)$ years), and knowing that the longitudinal expansion rate can be measured with cosmic chronometers [57, 58], we finally get a measurement for the transverse expansion rate. The deviation of the latter from the longitudinal expansion rate is therefore a measure of distant spatial anisotropy, which is equivalent to homogeneity.

Below we present the work in its published form. We refer the unfamiliar reader to Appendix F in [12] for the basics of the first section, and [59] for those of the second one.

Journal of Cosmology and Astroparticle Physics
An IOP and SISSA journal

Measuring the homogeneity of the universe using polarization drift

Raul Jimenez,[a,b] **Roy Maartens,**[c,d] **Ali Rida Khalifeh,**[a,e] **Robert R. Caldwell,**[f] **Alan F. Heavens**[g] **and Licia Verde**[a,b]

[a]ICC, University of Barcelona,
Marti i Franques, 1, E08028 Barcelona, Spain
[b]ICREA,
Pg. Lluis Companys 23, Barcelona, 08010, Spain
[c]Department of Physics & Astronomy, University of the Western Cape,
Cape Town 7535, South Africa
[d]Institute of Cosmology & Gravitation, University of Portsmouth,
Portsmouth PO1 3FX, U.K.
[e]Dept. de Fisica Cuantica y Astrofisica, University of Barcelona,
Marti i Franques 1, E08028 Barcelona, Spain
[f]Department of Physics & Astronomy, Dartmouth College,
6127 Wilder Laboratory, Hanover, NH 03755, U.S.A.
[g]Imperial Centre for Inference and Cosmology, Imperial College London,
Prince Consort Road, London SW7 2AZ, U.K.

E-mail: raul.jimenez@icc.ub.edu, roy.maartens@gmail.com, ark93@icc.ub.edu, robert.r.caldwell@dartmouth.edu, a.heavens@imperial.ac.uk, liciaverde@icc.ub.edu

Received March 7, 2019
Accepted May 17, 2019
Published May 28, 2019

Abstract. We propose a method to probe the homogeneity of a general universe, without assuming symmetry. We show that isotropy can be tested at remote locations on the past lightcone by comparing the line-of-sight and transverse expansion rates, using the time dependence of the polarization of Cosmic Microwave Background photons that have been inverse-Compton scattered by the hot gas in massive clusters of galaxies. This probes a combination of remote transverse and parallel components of the expansion rate of the metric, and we may use radial baryon acoustic oscillations or cosmic clocks to measure the parallel expansion rate. Thus we can test remote isotropy, which is a key requirement of a homogeneous universe. We provide explicit formulas that connect observables and properties of the metric.

Keywords: CMBR polarisation, physics of the early universe, Sunyaev-Zeldovich effect

ArXiv ePrint: 1902.11298

https://doi.org/10.1088/1475-7516/2019/05/048

JCAP05(2019)048

Contents

JCAP05(2019)048

1 Introduction

Isotropy and homogeneity of the background are basic assumptions of the current standard model of the Universe. Within this expanding background, structure formation proceeds via small perturbations with a possible origin in quantum fluctuations of the vacuum. The homogeneous standard cosmological model is a simple, predictive model that successfully accommodates all observations up to now [1]. However, we should probe the foundations of this model as far as possible in order to understand if it holds and if new physics has not been dismissed because of our assumptions (see e.g. the reviews in [2–4]).

Isotropy is well confirmed by observations of the cosmic microwave background (CMB): the temperature of the CMB in its rest-frame shows isotropy at better than one part in 10^4 [1]. Homogeneity, on the other hand, is *not* established by observations of the CMB and the large-scale galaxy distribution — *we cannot directly observe homogeneity,* since we observe down the past lightcone, recording properties on 2-spheres of constant redshift and not on spatial surfaces that intersect that lightcone. What these observations can directly probe is isotropy about the observer. In order to link isotropy to homogeneity, we have to assume the Copernican Principle, i.e. that we are not at a special position in the Universe. The Copernican Principle is not observationally based; it is an expression of the intrinsic limitation of observations from one spacetime location.[1]

Of course, there is a rich literature of inhomogeneous cosmological models. In particular, void models aim at explaining the current acceleration of the Universe without the need of a cosmological constant (see e.g. [4] for a review) and while these models suffer from difficulties to fit all observations (e.g. [6, 7]), it is not ruled out that some better models could be built in the future. It is therefore important that we develop direct tests of homogeneity that do not assume the background spacetime. Checking whether galaxy number densities approach

[1] Nothing precludes that we are at a peculiar location. In fact, we are in the middle of a void with two massive galaxies, Andromeda and the Milky Way; this in itself is very peculiar [5].

homogeneity on large enough scales (for recent work, see e.g. [8–12]) is based on assuming a Friedmann background and is therefore a *consistency* test, not a direct test of homogeneity.

Direct tests of homogeneity need to access the *interior* of the observer's past lightcone. In the case of galaxy surveys, Bonnor and Ellis [13] formulated a conjecture about thermal histories in separated regions of the Universe. The conjecture was developed by some of us [14] into a direct probe of homogeneity, by using the "fossil" record (star formation history) of galaxies. This was then applied to find the first direct constraint on inhomogeneity in a galaxy survey, using the fossil record of SDSS galaxies [15]. The fossil record from the star formation history of galaxies was used as a proxy to probe inside the past lightcone, and led to constraints at the $\sim 10\%$ level on any deviation from the homogeneous Friedmann metric. While the fossil record provides already very interesting constraints, it is not a direct probe in the purest sense, as it uses a proxy to probe the metric. Furthermore, it is always useful to have several probes of the same measurement, so as to minimize possible systematic uncertainties. In this work we will present a method that uses photon geodesics to probe the metric, which is a more direct probe of homogeneity.

In the case of the CMB, the thermal Sunyaev-Zeldovich effect probes the remote CMB monopole as seen from the observed galaxy cluster, and thus can provide a direct test of remote isotropy and hence of homogeneity, as pointed out by [16] (subsequently used to test void models by [17–19]). Similarly, the kinetic SZ effect probes the remote dipole and was used by [20] to test void models. The kinetic SZ can be used as a probe of isotropy inside the past lightcone, and thereby as a probe of homogeneity, if we can observe photons that are multiple-scattered or if we can observe the CMB over an interval of cosmic time [21]. In fact, the long time baseline is critical to our plans: more spacetime geometry can be accessed by a patient cosmologist [22].

Polarization of the SZ effect provides further important tests. The polarized thermal SZ probes the remote quadrupole, allowing in principle for a reduction in cosmic variance in a perturbed Friedmann universe [23, 24]. (See [25–28] for recent work on reducing cosmic variance in perturbed Friedmann models via the kinetic and polarized thermal SZ effects.)

In this paper, we propose a new method to directly probe homogeneity, based on changes of the polarization of CMB photons generated by inverse Compton scattering of CMB photons off hot electrons in massive (proto)-halos, and the radial expansion history of the Universe. The new method enables a test of isotropy at remote positions on our past lightcone — a key test of homogeneity.

In section 2 we review the description of expansion rates in a general spacetime. This is a necessary step because to test homogeneity we have to work with space-time metrics that do not rely on homogeneity. For the same reason, in general cosmological spacetimes (i.e. without assuming a background or any large scale symmetries) we cannot describe polarisation as in homogeneous spacetime. This is presented in section 3. In section 3 we also describe the effect of scattering (by hot electrons) of CMB photons in generic metrics and the signature that inhomogeneities leave on the polarisation signal. Finally in Sec 4 we present an estimate of the observations needed to constrain homogeneity with the method developed above. We conclude in section 5.

2 Expansion rates in a general spacetime

Let us first recall how to reason in general spacetime metrics. The most efficient way is to use covariant language. A distant object, with worldline $\mathcal{E}$, emits photons at event E

JCAP05(2019)048

that we observe with redshift z_E at event O on our galaxy worldline $\mathcal{O}$. (See figure 1.) In order to compare the intrinsic properties of $\mathcal{E}$ and $\mathcal{O}$ at the same proper time, we need to compute the look-back time $t_O - t_E$, where t denotes proper time along galaxy worldlines. This is straightforward in a Friedmann model — but we cannot assume the geometry of the spacetime if our aim is to test directly for homogeneity. So we need to compute the look-back time in a covariant way, valid in a general spacetime [14].

The galaxy 4-velocity field is $u^\mu = dx^\mu/dt$. The past-pointing photon 4-momentum is $k^\mu = dx^\mu/dv$, where v is the null affine parameter with $v = 0$ at O. Then

$$1 + z = u_\mu k^\mu, \quad k^\mu = (1+z)(-u^\mu + n^\mu), \quad u_\mu n^\mu = 0, \; n_\mu n^\mu = 1\,, \tag{2.1}$$

where n^μ is a unit vector along the line of sight. For observers co-moving with the matter, an increment dv in null affine parameter corresponds to a time increment dt, where

$$dt = -u_\mu k^\mu dv = -(1+z)dv\,. \tag{2.2}$$

We need to relate v to z by (2.1):

$$\frac{dz}{dv} = k^\nu \nabla_\nu (u_\mu k^\mu) = k^\mu k^\nu \nabla_\mu u_\nu\,, \tag{2.3}$$

where the last equality follows since k^μ is a geodesic. The covariant derivative is split as

$$\nabla_\mu u_\nu = \frac{1}{3}\Theta h_{\mu\nu} + \sigma_{\mu\nu} + \omega_{\mu\nu} - u_\mu \dot{u}_\nu\,, \qquad h_{\mu\nu} = g_{\mu\nu} + u_\mu u_\nu\,, \tag{2.4}$$

where $h_{\mu\nu}$ projects into the galaxy instantaneous rest space, the dot indicates $u^\mu \nabla_\mu$, Θ is the volume expansion rate ($\Theta = 3H$ in a Friedmann model), $\sigma_{\mu\nu}$ is the shear, $\omega_{\mu\nu}$ is the vorticity and $\dot{u}_\mu$ is the acceleration. Now we will assume that the Universe is dominated by pressure-free matter, whereby $\dot{u}_\mu = 0$. Putting everything together, we get

$$\frac{dz}{dv} = (1+z)^2 \left[\frac{1}{3}\Theta + \sigma_{\mu\nu} n^\mu n^\nu\right]. \tag{2.5}$$

Now we integrate along the lightray from O to E, using (2.2) and (2.5):

$$t_O - t_E = \int_0^{z_E} \frac{dz}{(1+z)\left[\Theta(z)/3 + \sigma_{\mu\nu}(z) n^\mu n^\nu\right]}\,. \tag{2.6}$$

This will give us the look-back time — *provided that we can uniquely relate the time intervals along galaxy worldlines that cross the lightray to a time interval along our worldline* $\mathcal{O}$. In order to do this, we need the existence of spatial 3-surfaces that are everywhere orthogonal to u^μ; these will then be surfaces of constant proper time. The necessary and sufficient condition for these surfaces to exist is an irrotational flow:[2]

$$\omega_{\mu\nu} = 0\,. \tag{2.7}$$

Then we can uniquely identify the event E' where the constant proper time surface $t = t_E$ through E intersects $\mathcal{O}$. For rotating matter, it is not clear whether we can consistently define

[2]This condition is only required on scales where the dust model holds: it is violated on nonlinear scales due to multi-streaming and baryonic effects.

JCAP05(2019)048

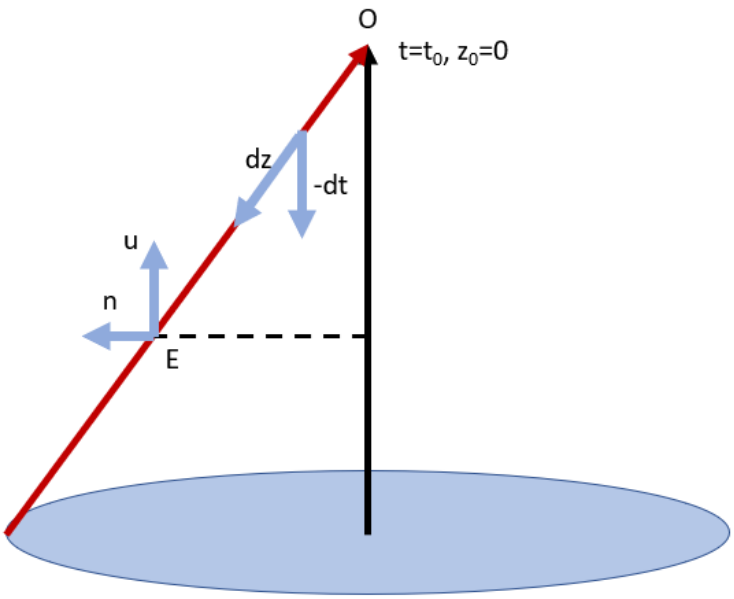

Figure 1. Schematic of the lookback time in a general spacetime.

a look-back time. From now on we assume that the general spacetime has irrotational cold matter and dark energy whose perturbations are negligible, together with standard baryonic and radiation content.

A clear target of observational cosmology should thus be to *measure* $\Theta(z)$ and $\sigma_{\mu\nu}(z)$ in order to probe homogeneity. In order to identify the line of sight and transverse expansion rates in a general spacetime, we start from the matter expansion tensor

$$\Theta_{\mu\nu} = \frac{1}{3}\Theta h_{\mu\nu} + \sigma_{\mu\nu}\,, \qquad \Theta = \Theta_{\mu\nu}h^{\mu\nu}\,, \tag{2.8}$$

where the average expansion rate is $\frac{1}{3}\Theta$. The line of sight (radial) expansion rate is

$$H_\parallel := \Theta_{\mu\nu}n^\mu n^\nu = \frac{1}{3}\Theta + \sigma_{\mu\nu}n^\mu n^\nu\,, \tag{2.9}$$

so that the lookback time from (2.6) is

$$t_O - t_E = \int_0^{z_E} \frac{dz}{(1+z)H_\parallel(z,n^\mu)}\,. \tag{2.10}$$

The transverse expansion tensor is

$$\Theta^\perp_{\mu\nu} = \Theta_{\alpha\beta}S^\alpha_\mu S^\beta_\nu = \frac{1}{3}\Theta_\perp S_{\mu\nu} + \sigma^\perp_{\mu\nu}\,, \qquad S_{\mu\nu} = h_{\mu\nu} - n_\mu n_\nu\,, \tag{2.11}$$

where $S_{\mu\nu}$ is the projector into the transverse space ("screen space"). Then the transverse expansion rate is

$$H_\perp = \frac{1}{2}\Theta_\perp = \frac{1}{2}\Theta^\perp_{\mu\nu}S^{\mu\nu} = \frac{1}{2}\Theta_{\mu\nu}S^{\mu\nu} = \frac{1}{3}\Theta - \frac{1}{2}\sigma_{\mu\nu}n^\mu n^\nu\,. \tag{2.12}$$

JCAP05(2019)048

Then it follows that, as required, the volume expansion rate is

$$\Theta(z) = H_{\parallel}(z, n^{\mu}) + 2H_{\perp}(z, n^{\mu}) \,, \tag{2.13}$$

while the radial shear is

$$\sigma_{\mu\nu}(z) n^{\mu} n^{\nu} = \frac{2}{3}\Big[H_{\parallel}(z, n^{\mu}) - H_{\perp}(z, n^{\mu})\Big] \,. \tag{2.14}$$

The shear can be split into transverse, radial and mixed parts:

$$\sigma_{\mu\nu} = \sigma^{\perp}_{\mu\nu} + A n_{\mu} n_{\nu} + 2B_{(\mu} n_{\nu)} \,, \quad B_{\mu} n^{\mu} = 0 \,, \tag{2.15}$$

where $\sigma^{\perp}_{\mu\nu}$ is defined by (2.11), and A, B_{μ} are found by suitable contractions of (2.15). This leads to

$$\sigma_{\mu\nu} = \sigma^{\perp}_{\mu\nu} + \frac{2}{3}\big(H_{\parallel} - H_{\perp}\big) n_{\mu} n_{\nu} + 2\sigma_{\alpha\beta} n^{\alpha} S^{\beta}_{(\mu} n_{\nu)} \,. \tag{2.16}$$

In principle, $H_{\parallel}$ is determined by baryon acoustic oscillation (BAO) measurements of a physical, radial length — a standard "ruler" — in galaxy clustering [29]:

$$H_{\parallel} = \frac{c}{(1+z)\Delta r_{\parallel}} \, \Delta z \,, \tag{2.17}$$

or by cosmic chronometers using a standard "clock" in the form of differential ages of ancient, elliptical galaxies [30, 31]:

$$H_{\parallel} = -\frac{\Delta z}{(1+z)\Delta t} \,, \tag{2.18}$$

which follows from (2.10). However, while the cosmic chronometer method is fully independent of the cosmological model, the radial length BAO needs to assume a value for $\Delta r_{\parallel}$ or obtain it through consistency with other measurements. These are the only[3] two routes to obtain $H_{\parallel}$.

Once $H_{\parallel}$ is determined, we would be able to find $H_{\perp}$ if we could probe the remote volume expansion Θ, using (2.13). By (2.14) or (2.16), an alternative would be available if we could probe the remote shear $\sigma_{\mu\nu}$. Then we would be able to test homogeneity by testing isotropy of the expansion rate at remote locations. The problem is to find a direct observational way to determine $H_{\perp}$ or Θ or $\sigma_{\mu\nu}$. In the absence of a direct solution, we turn to investigate the information contained in the evolution of polarization.

3 Polarization in a general cosmological spacetime

Polarization in a perturbed Friedmann model is well understood (see e.g. [32–34]). Linear polarization is described by the Stokes parameters Q, U. Note that these parameters have units of intensity per unit frequency, their measurement inevitably involve a quantity that is an integration of these parameters over a frequency range. In this sense the Q, U parameters should be seen as "differential" quantities. Under rotations through ϕ in the screen space, these parameters Q', U' are rotated by 2ϕ in parameter space, showing that linear polarization is described invariantly by a spin-2 object in the screen space. Thus Q, U are not physical invariants but depend on coordinates in the screen space. The invariants under rotation are

$$Q'^2 + U'^2 = Q^2 + U^2 \,, \tag{3.1}$$

[3] Observations of supernova as standarizable candles also give $H_{\parallel}$ but this depends on assuming the metric.

JCAP05(2019)048

whereas the direction defined by the polarization angle,

$$\alpha \equiv \frac{1}{2}\tan^{-1}\frac{U}{Q} \;\Rightarrow\; \alpha' = \alpha - \phi \tag{3.2}$$

is not invariant.

In a general cosmological spacetime (i.e. without assuming a background or any large-scale symmetries), we need to deal with the invariant objects. A general analysis was developed in a pioneering paper by Challinor [35] (see also [36, 37]): linear polarization is described by a symmetric trace-free tensor $\mathcal{P}^{\mu\nu}$ in the screen space, i.e. a spin-2 object in the screen space, which satisfies

$$\mathcal{P}^{\mu\nu}S_{\mu\nu} = 0 = \mathcal{P}^{\nu\mu} - \mathcal{P}^{\mu\nu} \quad \text{and} \quad \mathcal{P}^{\mu\nu}n_\nu = 0 = \mathcal{P}^{\mu\nu}u_\nu \;\big(\text{or} \quad \mathcal{P}^{\mu\nu} = \mathcal{P}^{\mu\nu}_{\perp} := S^\mu_\beta S^\nu_\gamma \mathcal{P}^{\beta\gamma}\big). \tag{3.3}$$

The magnitude of the polarization tensor is independent of coordinate choice and is given by the rotational invariant (3.1) [35]:

$$2\,\mathcal{P}_{\mu\nu}\,\mathcal{P}^{\mu\nu} = Q^2 + U^2\,. \tag{3.4}$$

After scattering by free electrons in a scatterer located at a given redshift z which is composed of a collapsed dark matter halo above a mass large enough to host high-energy free electrons that cause inverse Compton scattering on lower energy CMB photons, the linear polarization tensor in the screen space propagates along lightrays towards the observer according to conservation of $\nu^{-3}\,\mathcal{P}^{\mu\nu}$, where ν is the photon frequency [35]:

$$\big[k^\alpha\nabla_\alpha\big(\nu^{-3}\,\mathcal{P}^{\mu\nu}\big)\big]_\perp = S^\mu_\beta S^\nu_\gamma\, k^\alpha\nabla_\alpha\big(\nu^{-3}\,\mathcal{P}^{\beta\gamma}\big) = 0\,. \tag{3.5}$$

Note that we do not impose the stronger condition $k^\alpha\nabla_\alpha(\nu^{-3}\,\mathcal{P}^{\mu\nu}) = 0$, since in general lightray derivatives of screen-space quantities do not lie purely in the screen space. Polarization measurements implicitly involve a projection into the screen space, so that any components not in the screen space do not affect the measurement.

If we project (3.5) with $\nu^{-3}\,\mathcal{P}_{\mu\nu}$, we have

$$0 = k^\alpha\nabla_\alpha\big[\nu^{-3}\,\mathcal{P}_{\mu\nu}\big(\nu^{-3}\,\mathcal{P}^{\mu\nu}\big)\big] = \frac{1}{2}k^\alpha\nabla_\alpha\big[\nu^{-6}\big(Q^2+U^2\big)\big]\,. \tag{3.6}$$

It follows that for a source E observed by O at redshift $z = \nu_E/\nu_O - 1$, we have

$$Q_E^2 + U_E^2 = (1+z)^6(Q_O^2 + U_O^2)\,. \tag{3.7}$$

This is the expected scaling with redshift for the differential Stokes parameters.

3.1 Local coordinates for polarization

For matter that is irrotational and pressure-free on large scales, we have

$$\omega_{\mu\nu} = 0 = \dot{u}_\mu \quad\Leftrightarrow\quad u_{[\mu,\nu]} = 0 \quad\Leftrightarrow\quad u_\mu = -t_{,\mu}\,, \tag{3.8}$$

for some scalar t — which is then necessarily the proper time along matter worldlines. Therefore we can choose comoving coordinates (t, x^i) such that

$$\begin{aligned} ds^2 &= g_{\mu\nu}dx^\mu dx^\nu = -(u_\mu dx^\mu)^2 + h_{\mu\nu}dx^\mu dx^\nu \\ &= -dt^2 + (n_i dx^i)^2 + S_{ij}dx^i dx^j\,. \end{aligned} \tag{3.9}$$

JCAP05(2019)048

Locally, i.e., in a neighborhood of any point, we can choose $x^1 = x$ along n^i and then

$$ds^2\big|_{\rm loc} = -dt^2 + A_\parallel^2 dx^2 + S_{IJ}\, dx^I dx^J\,, \tag{3.10}$$

where $x^I = (y, z)$ and $n_i = A_\parallel \delta_i^1$. The area element in the screen space is $dV_\perp = \sqrt{\det S_{IJ}}\, d^2x$. Transverse areas expand as $A_\perp^2$, where $A_\perp$ is the transverse scale factor; since x^I are comoving (constant along the matter world-lines) this means that $\sqrt{\det S_{IJ}} \propto A_\perp^2$. We can normalize $A_\perp$ at some time $t = t_0$ so that $\sqrt{\det S_{IJ}} = A_\perp^2$, and then $S_{IJ} = A_\perp^2 s_{IJ}$, where $\det s_{IJ} = 1$. Thus

$$ds^2\big|_{\rm loc} = -dt^2 + A_\parallel^2 dx^2 + A_\perp^2\, s_{IJ}\, dx^I dx^J \quad \text{where} \quad \det s_{IJ} = 1\,. \tag{3.11}$$

The expansion rates are

$$H_\parallel = \frac{\dot A_\parallel}{A_\parallel}\,, \quad H_\perp = \frac{\dot A_\perp}{A_\perp}\,. \tag{3.12}$$

Note that $H_\perp$ is the geometric mean of the expansion rates in the local principal axis system of S_{IJ}.

In these coordinates, the polarization tensor has only screen-space components, and these components are the Stokes linear polarization parameters Q, U measured by the observer using the local coordinates in the screen space:

$$\mathcal{P}_{\mu\nu} = \mathcal{P}_{IJ}\, \delta^I_\mu\, \delta^J_\nu\,, \quad \mathcal{P}_{IJ} = \frac{1}{2}\begin{pmatrix} Q & U \\ U & -Q \end{pmatrix}. \tag{3.13}$$

We used $S^I_\mu = S^I_J \delta^J_\mu$ and $S^I_J = \delta^I_J$, which hold in the polarization coordinates of (3.11).

An alternative to local coordinates is an orthonormal tetrad. A polarization tetrad is briefly described in appendix A.

3.2 Drift of polarization

The time evolution of polarization at a scatterer is given in a general spacetime by the covariant derivative of the polarization tensor along the four-velocity of the scatterer, projected into the screen space, i.e. by $\big(\dot{\mathcal{P}}_{IJ}\big)_\perp$ at E. In the local coordinates of (3.11), both $S_{\mu\nu}$ and $\mathcal{P}_{\mu\nu}$ are zero if μ or ν is 0 or 1, and we find that

$$\big(\dot{\mathcal{P}}_{IJ}\big)_\perp := S^\mu_I S^\nu_J \left(u^\alpha \nabla_\alpha\, \mathcal{P}_{\mu\nu}\right) = \mathcal{P}_{IJ,0} - \Gamma^K_{I0}\, \mathcal{P}_{KJ} - \Gamma^K_{J0}\, \mathcal{P}_{IK}\,. \tag{3.14}$$

The Christoffel symbols in (3.14) encode the screen-space shear and the volume expansion rate:

$$\Gamma^K_{I0} = \sigma_{\perp}{}^K_I + \frac{1}{3}\big(H_\parallel + 2H_\perp\big)\delta^K_I\,. \tag{3.15}$$

This can be seen as follows. By (2.4), with $\omega_{\mu\nu} = 0$ and $u^\mu = \delta^\mu_0$, we have

$$\sigma^\mu_\nu = \nabla_\nu u^\mu - \frac{1}{3}\Theta\, \delta^\mu_\nu = \Gamma^\mu_{\nu 0} - \frac{1}{3}\Theta\, \delta^\mu_\nu\,. \tag{3.16}$$

Then we use (2.13) for Θ and project into the screen space to obtain (3.15). We can rewrite (3.14) as

$$\big(\dot{\mathcal{P}}_{IJ}\big)_\perp = \frac{d}{dt}\mathcal{P}_{IJ} - \frac{2}{3}\big(H_\parallel + 2H_\perp\big)\mathcal{P}_{IJ} - 2\sigma^\perp_{K(I}\, \mathcal{P}^K_{J)}\,. \tag{3.17}$$

JCAP05(2019)048

This equation can be derived also using the tetrad in the appendix without any need to use local coordinates. By the Equivalence Principle, $d\mathcal{P}_{IJ}/dt$ is given by the special relativistic scattering formula, which depends on the properties of the free electron distribution in the scatterer and of the CMB photons, both of which can be estimated from observations. The observable $(\dot{\mathcal{P}}_{IJ})_\perp$ is therefore determined by the local scattering physics (via $d\mathcal{P}_{IJ}/dt$) and by gravitational effects, which produce the expansion rate $(H_\parallel + 2H_\perp)/3$ and screen-space shear $\sigma^\perp_{IJ}$, of the matter field.

If we observe a scatterer over a proper time interval δt_O at the observer, where

$$\delta t_O = (1+z)\delta t_E\,, \tag{3.18}$$

then it follows from (3.7) that the change in polarization magnitude at the scatterer is related to the observed change in polarization magnitude by

$$\delta\big(Q^2+U^2\big)_E = (1+z)^6\,\delta\big(Q^2+U^2\big)_O + 6(1+z)^5\big(Q^2+U^2\big)_O\,\delta z\,, \tag{3.19}$$

where the redshift measured at the observer is $z+\delta z$ (see (B.5) in appendix B).

Equation (3.19) *predicts the polarization drift at the scatterer in terms of the measured polarization drift and redshift drift at the observer.* The polarization drift at the scatterer is also determined by (3.17):

$$\delta\mathcal{P}_{IJ}\big|_E = \big(\dot{\mathcal{P}}_{IJ}\big)_{\perp E}\delta t_E\,, \tag{3.20}$$

where δt_E is the proper time interval at the scatterer and $(\dot{\mathcal{P}}_{IJ})_{\perp E}$ is given by (3.17). By comparing the theoretical prediction for the polarization drift with the measurement (3.19), we can in principle deduce the local volume expansion rate and the screen-space shear at the scatterer. If we also find the radial expansion rate via the BAO, then we can deduce the transverse expansion rate at the scatterer. To be more specific, from local measurements of z and δt_O we can obtain δt_E as in (3.18). From measurements of the redshift drift δz (which can be measured directly from estimates of H_0 using the local distance ladder), $\mathcal{P}_O$ and $\delta\mathcal{P}_O$ we can use (3.19) and (3.20) to determine $\big(\dot{\mathcal{P}}_{IJ}\big)_{\perp E}$. Then we use the two equations in (3.17) and supply a theoretical prediction for $d\mathcal{P}_{IJ}/dt$ to get $H_\perp$ and $\sigma^\perp_{IJ}$. This is our procedure to measure homogeneity.

4 Observational strategy

We can provide an estimate of the observations needed to constrain homogeneity with the method developed above. It is beyond the scope of this paper to provide a detailed study of the experimental setup needed: this will be presented elsewhere.

Our proposed method relies on the difficult task of measuring the polarization drift, i.e., the time variation of the polarization tensor, at each scatterer position. The redshift drift (see appendix B) needs knowledge of H_0 which has already been obtained at the % level with the local distance ladder and the other relevant quantities are much easier to measure and have been discussed extensively in the literature. Effectively, one needs to "film" polarization (for a closely related idea see also [39]; also see [40, 41]).

While the polarized cosmological signal can be found in several observables, we seek a combination of detection method, observable and its scatterer that achieves the following:

JCAP05(2019)048

1. It is stable enough to be observed for a long time and thus to detect small drifts.
2. The polarization signal can be measured with exquisite signal to noise.
3. The scatterer is at cosmological distances and its redshift can be reliably measured (this does not need to be spectroscopic but can be photometric, which already exist).
4. It is abundant.
5. The signal can be easily accessible with current technology (but not necessarily with current experiments).

For this reason we focus on the polarized signal of CMB photons that have been inverse-Compton scattered by the hot intra-cluster gas of massive galaxy clusters. Consider a radio telescope with spatial resolution at the $\sim$ arcmin level. This is achievable as it is not too dissimilar to that of the Planck space mission. Consider also that measurements can be obtained over the time frame of $\mathcal{O}(10)$ years and that future CMB polarization experiments will be basically photon-noise limited because of the large number of detectors on the focal plane.

Halos of dark matter mass above 10^{13} $M_\odot$ are optimal scatterers, leaving their easily identifiable (Sunyaev-Zel'dovich [42]) signature on CMB high-resolution maps. An experiment to detect this signal is something like the more updated versions of CMB-S4 [43] considered by ref. [44], ($N_{\rm det} = 10^7$ detectors, $D = 12m$ mirror). Since the drift is linear in time, there is a considerable gain through having a longer experiment, with the error on the rate decreasing as $t_{\rm exp}^{-3/2}$. For a mission with improved detector sensitivitiy $s_{\rm det}$, from the CoRE proposal,[4] with a baseline $1.2m$ mirror, and mission length of $\delta t = 4yr$, the noise level is

$$c_{\rm noise} = 4.7\mu K{\rm arcmin}\left(\frac{4yr}{\delta t}\right)^{1/2}\left(\frac{400}{N_{\rm det}}\right)^{1/2}\left(\frac{s_{\rm det}}{50\mu K s^{1/2}}\right) \tag{4.1}$$

The S/N on the normalised drift rate a, defined such that the polarisation signals evolve from the initial observation P_0 at $t = 0$

$$P(t) = P_0\left(1 + a\frac{t}{t_*}\right) \tag{4.2}$$

(where t_* is the expansion timescale) is obtained through a Fisher analysis of the error on a, which yields an error

$$\sigma_a = \frac{\sqrt{6}}{N_{\rm pix}^{1/2} S}\left(\frac{\delta t\, t_*^2}{t_{\rm exp}^3}\right)^{1/2} \tag{4.3}$$

where $N_{\rm pix}$ is the number of pixels in the polarisation map, which we assume is repeatedly measured once every δt. Putting these together, assuming all-sky coverage, the signal-to-noise for the polarisation drift would make a detection challenging with the following S/N:

$$\frac{S}{N} = 66\left(\frac{N_{\rm det}}{10^7}\right)^{1/2}\left(\frac{D}{12m}\right)\left(\frac{s_{\rm det}}{0.1\,\mu K s^{1/2}}\right)^{-1}\left(\frac{t_{\rm exp}}{10\ yr}\right)^{3/2}\left(\frac{t_*}{Gyr}\right)^{-1} \tag{4.4}$$

Foreground variations are likely to be uncorrelated with the drift, but would constitute an additional source of noise. As pointed out in [44], the main contaminant is the E primordial

[4] http://www.core-mission.org/documents/CoreProposal_Final.pdf.

JCAP05(2019)048

mode. Our task is, on the other hand, easier as we only need to measure differential variations, which minimizes greatly many systematic effects.[5] Thus it is not unreasonable to assume that our differential measurement could have a S/N of $\mathcal{O}(100)$ in the integrated full sky. Assuming scatterers can all be identified in CMB maps and assuming the Stokes parameters can be reliably measured for all of them, we could limit variations of $H_{||}+2H_{\perp}$ via (3.19) and (3.17).

Recall that we need to measure $H_{||}$ independently of the metric to determine $H_{\perp}$. The BAO technique does require a value of the sound horizon that is usually assumed to be the one given by the CMB, which assumes homogeneity even when using only local measurements to obtain the ruler's length [38]. On the other, hand none of these assumptions are needed for the cosmic chronometer method, that is fully independent of the metric of space-time or the cosmological model. For the sake of the argument here we can assume that in future measurements $H_{||}$ can be measured at the percent level. This will be the degree that we can constrain homogeneity with future surveys. However, it is worth recalling that the Planck space mission already has observed 10^3 Sunyaev-Zel'dovich clusters for which the polarization drift could, in principle, be measured. This could give an interesting constraint on the degree of homogeneity; we will explore this elsewhere. We are fully aware that we have ignored many real-world effects, like foregrounds and other intrinsic time variable effects on Q and U, but we have shown that the method to measure homogeneity presented above is, in principle, feasible.

5 Conclusions

Measuring the degree of homogeneity of the space-time metric of the Universe remains an open question in cosmology. We have presented a method to measure homogeneity in general space-time metrics by "filming" the polarization signal of CMB photons inverse Compton scattered by the hot intra-cluster gas in galaxy clusters. In particular, the change in time of the Stokes parameters provides a measurement of the transverse expansion rate. The radial expansion rate is instead measured by more conventional probes like radial BAO or cosmic chronometers. We have estimated that a measurement of homogeneity at the $\sim$ percent level can be obtained with high resolution full sky CMB polarization maps in a period of years. Percent-level constraints on the degree of homogeneity may be achievable with the expected sensitivity of the proposed Simons Observatory [45] and CMB-S4 experiment [46].

Acknowledgments

We thank Anthony Challinor, Chris Clarkson and Julien Larena for helpful discussions. RJ and LV thank the Center Emile Borel for hospitality during the latest stages of this work. Funding for this work was partially provided by the Spanish MINECO under projects AYA2014-58747-P AEI/FEDER, UE, and MDM-2014-0369 of ICCUB (Unidad de Excelencia María de Maeztu). LV acknowledges support from the European Union Horizon 2020 research and innovation program ERC (BePreSySe, grant agreement 725327). RM acknowledges support from the South African SKA Project and the National Research Foundation of South Africa (Grant No. 75415). RM was also supported by the U.K. Science & Technology Facilities Council (Grant No. ST/N000668/1). The work of RC is supported in part by the US Department of Energy grant DE-SC0010386.

[5] Stacking galaxy clusters in the same redshift slice will eliminate any intrinsic variations in the cluster evolution.

JCAP05(2019)048

A Polarization tetrad

An orthonormal tetrad $\boldsymbol{e}_a = (\boldsymbol{u}, \boldsymbol{n}, \boldsymbol{e}_A)$, where $\boldsymbol{e}_A$ are orthogonal unit vectors spanning the screen space, is adapted to describe polarization, which is measured in the screen space by an observer $\boldsymbol{u}$. The tetrad components $\mathcal{P}_{ab} = \mathcal{P}_{\mu\nu}\, e^\mu_a\, e^\nu_b$ are then physical quantities. In this tetrad, the polarization tensor has nonzero components only in the screen space, and these components define the linear polarization Stokes quantities $\hat{Q}, \hat{U}$ that are measured by the observer:

$$\mathcal{P}_{AB} \equiv \mathcal{P}_{\mu\nu}\, e^\mu_A\, e^\nu_B = \frac{1}{2}\begin{pmatrix} \hat{Q} & \hat{U} \\ \hat{U} & -\hat{Q} \end{pmatrix}. \tag{A.1}$$

We use hats to distinguish the Stokes parameters in the polarization tetrad from those in the polarization coordinates of (3.13).

The orthonormal tetrad $\boldsymbol{e}_a$ has rotational freedom in the screen-space basis $\boldsymbol{e}_A$. By (3.5), a natural choice is that $\boldsymbol{e}_A$ propagates along the lightrays according to

$$\big(k^\alpha \nabla_\alpha e^\mu_A\big)_\perp = 0\,. \tag{A.2}$$

With this choice of the screen-space basis — which we can call the polarization basis — it follows from (3.5) that the tetrad components $\mathcal{P}_{AB}$ propagate according to

$$\frac{d}{dv}\big(\nu^{-3}\,\mathcal{P}_{AB}\big) = 0 \quad \text{equivalently} \quad \frac{d}{dv}\big(\nu^{-3}\,\hat{Q}\big) = 0 = \frac{d}{dv}\big(\nu^{-3}\,\hat{U}\big)\,. \tag{A.3}$$

A consequence of (A.3) is that the polarization at the scatterer is given in terms of the polarization measured at the observer by

$$\big(\hat{Q}_E\,,\,\hat{U}_E\big) = (1+z)^3\,\big(\hat{Q}_O\,,\,\hat{U}_O\big)\,, \tag{A.4}$$

where z is the observed redshift of the scatterer. In particular, this means that the polarization angle α is constant along each lightray:

$$\tan 2\hat{\alpha} \equiv \frac{\hat{U}}{\hat{Q}} \quad \Rightarrow \quad \frac{d\hat{\alpha}}{dv} = 0 \quad \Rightarrow \quad \hat{\alpha}_E = \hat{\alpha}_O \tag{A.5}$$

Note that (A.3)–(A.5) hold only in the polarization tetrad defined by (A.2).

B Redshift drift in a general cosmological spacetime

It follows from (2.2) and (2.5) that

$$1 + z = \exp \int_{t_E}^{t_O} dt\, H_\parallel(t, n^\mu) \tag{B.1}$$

Consider the small change δz in z over a proper time interval δt_O at the observer. The corresponding time interval along the u^μ world-line at the source is δt_E, and

$$(1 + z + \delta z) - (1 + z) = \exp \int_{t_E+\delta t_E}^{t_O+\delta t_O} dt\, H_\parallel - \exp \int_{t_E}^{t_O} dt\, H_\parallel \tag{B.2}$$

JCAP05(2019)048

We break up the total time interval $t_E \to t_O + \delta t_O$ into 4 segments,

$$\begin{aligned}\delta z &= \exp\left(\int_{t_E+\delta t_E}^{t_O} dt\, H_\parallel + \int_{t_O}^{t_O+\delta t_O} dt\, H_\parallel\right) - \exp\left(\int_{t_E}^{t_E+\delta t_E} dt\, H_\parallel + \int_{t_E+\delta t_E}^{t_O} dt\, H_\parallel\right) \\ &= \exp\int_{t_E+\delta t_E}^{t_O}\left[\exp\int_{t_O}^{t_O+\delta t_O} dt\, H_\parallel - \exp\int_{t_E}^{t_E+\delta t_E} dt\, H_\parallel\right] \end{aligned} \tag{B.3}$$

Now $\delta t_E = (1+z)^{-1}\delta t_O$, and working to lowest order in δt_O:

$$\begin{aligned}\delta z &\approx \exp\int_{t_E}^{t_O}\left[\exp\int_{t_O}^{t_O+\delta t_O} dt\, H_\parallel - \exp\int_{t_E}^{t_E+\delta t_E} dt\, H_\parallel\right] \\ &\approx (1+z)\Big\{\exp\left[\delta t_O H_\parallel(t_O, n_O^\mu)\right] - \exp\left[\delta t_E H_\parallel(t_E, n_E^\mu)\right]\Big\} \\ &\approx (1+z)\Big[1 + \delta t_O H_\parallel(t_O, n_O^\mu) - 1 - (1+z)^{-1}\delta t_O H_\parallel(t_E, n_E^\mu)\Big] \end{aligned} \tag{B.4}$$

Finally

$$\frac{\delta z}{\delta t_O} = (1+z)H_\parallel(t_O, n_O^\mu) - H_\parallel(t_E, n_E^\mu) + O(\delta t_O^2) \tag{B.5}$$

References

[1] Planck collaboration, *Planck* 2018 *results. VI. Cosmological parameters*, arXiv:1807.06209 [INSPIRE].

[2] C. Clarkson and R. Maartens, *Inhomogeneity and the foundations of concordance cosmology*, *Class. Quant. Grav.* **27** (2010) 124008 [arXiv:1005.2165] [INSPIRE].

[3] R. Maartens, *Is the universe homogeneous?*, *Phil. Trans. Roy. Soc. Lond.* **A 369** (2011) 5115 [arXiv:1104.1300] [INSPIRE].

[4] C. Clarkson, *Establishing homogeneity of the universe in the shadow of dark energy*, *Comptes Rendus Physique* **13** (2012) 682 [arXiv:1204.5505] [INSPIRE].

[5] A. Fattahi et al., *The Apostle project: local group kinematic mass constraints and simulation candidate selection*, *Mon. Not. Roy. Astron. Soc.* **457** (2016) 844 [arXiv:1507.03643].

[6] P. Bull, T. Clifton and P.G. Ferreira, *The kSZ effect as a test of general radial inhomogeneity in LTB cosmology*, *Phys. Rev.* **D 85** (2012) 024002 [arXiv:1108.2222] [INSPIRE].

[7] R. de Putter, L. Verde and R. Jimenez, *Testing LTB void models without the cosmic microwave background or large scale structure: new constraints from galaxy ages*, *JCAP* **02** (2013) 047 [arXiv:1208.4534] [INSPIRE].

[8] M. Scrimgeour et al., *The WiggleZ dark energy survey: the transition to large-scale cosmic homogeneity*, *Mon. Not. Roy. Astron. Soc.* **425** (2012) 116 [arXiv:1205.6812] [INSPIRE].

[9] P. Laurent et al., *A* $14\,h^{-3}$ *Gpc*^{3} *study of cosmic homogeneity using BOSS DR*12 *quasar sample*, *JCAP* **11** (2016) 060 [arXiv:1602.09010] [INSPIRE].

[10] C.-G. Park, H. Hyun, H. Noh and J.-C. Hwang, *The cosmological principle is not in the sky*, *Mon. Not. Roy. Astron. Soc.* **469** (2017) 1924 [arXiv:1611.02139] [INSPIRE].

[11] P. Ntelis et al., *Exploring cosmic homogeneity with the BOSS DR*12 *galaxy sample*, *JCAP* **06** (2017) 019 [arXiv:1702.02159] [INSPIRE].

[12] R.S. Gonçalves et al., *Cosmic homogeneity: a spectroscopic and model-independent measurement*, *Mon. Not. Roy. Astron. Soc.* **475** (2018) L20 [arXiv:1710.02496] [INSPIRE].

JCAP05(2019)048

[13] W.B. Bonnor and G.F.R. Ellis, *Observational homogeneity of the universe*, *Mon. Not. Roy. Astron. Soc.* **218** (1986) 605.

[14] A.F. Heavens, R. Jimenez and R. Maartens, *Testing homogeneity with the fossil record of galaxies*, *JCAP* **09** (2011) 035 [arXiv:1107.5910] [INSPIRE].

[15] B. Hoyle, R. Tojeiro, R. Jimenez, A. Heavens, C. Clarkson and R. Maartens, *Testing homogeneity with galaxy star formation history*, *Astrophys. J.* **762** (2013) L9 [arXiv:1209.6181] [INSPIRE].

[16] J. Goodman, *Geocentrism reexamined*, *Phys. Rev.* **D 52** (1995) 1821 [astro-ph/9506068] [INSPIRE].

[17] R.R. Caldwell and A. Stebbins, *A test of the Copernican principle*, *Phys. Rev. Lett.* **100** (2008) 191302 [arXiv:0711.3459] [INSPIRE].

[18] A. Moss, J.P. Zibin and D. Scott, *Precision cosmology defeats void models for acceleration*, *Phys. Rev.* **D 83** (2011) 103515 [arXiv:1007.3725] [INSPIRE].

[19] R.R. Caldwell and N.A. Maksimova, *Spectral distortion in a radially inhomogeneous cosmology*, *Phys. Rev.* **D 88** (2013) 103502 [arXiv:1309.4454] [INSPIRE].

[20] P. Zhang and A. Stebbins, *Confirmation of the Copernican principle at Gpc radial scale and above from the kinetic Sunyaev Zel'dovich effect power spectrum*, *Phys. Rev. Lett.* **107** (2011) 041301 [arXiv:1009.3967] [INSPIRE].

[21] T. Clifton, C. Clarkson and P. Bull, *The isotropic blackbody CMB as evidence for a homogeneous universe*, *Phys. Rev. Lett.* **109** (2012) 051303 [arXiv:1111.3794] [INSPIRE].

[22] A. Stebbins, *Measuring space-time geometry over the ages*, *Int. J. Mod. Phys.* **D 21** (2012) 1242017 [arXiv:1205.4201] [INSPIRE].

[23] M. Kamionkowski and A. Loeb, *Getting around cosmic variance*, *Phys. Rev.* **D 56** (1997) 4511 [astro-ph/9703118] [INSPIRE].

[24] N. Seto and M. Sasaki, *Polarization signal of distant clusters and reconstruction of primordial potential fluctuations*, *Phys. Rev.* **D 62** (2000) 123004 [astro-ph/0009222] [INSPIRE].

[25] G.-C. Liu, K. Ichiki, H. Tashiro and N. Sugiyama, *Reconstruction of CMB temperature anisotropies with primordial CMB induced polarization in galaxy clusters*, *Mon. Not. Roy. Astron. Soc.* **460** (2016) L104 [arXiv:1603.06166] [INSPIRE].

[26] A. Terrana, M.-J. Harris and M.C. Johnson, *Analyzing the cosmic variance limit of remote dipole measurements of the cosmic microwave background using the large-scale kinetic Sunyaev Zel'dovich effect*, *JCAP* **02** (2017) 040 [arXiv:1610.06919] [INSPIRE].

[27] A.-S. Deutsch, M.C. Johnson, M. Münchmeyer and A. Terrana, *Polarized Sunyaev Zel'dovich tomography*, *JCAP* **04** (2018) 034 [arXiv:1705.08907] [INSPIRE].

[28] A.-S. Deutsch, E. Dimastrogiovanni, M.C. Johnson, M. Münchmeyer and A. Terrana, *Reconstruction of the remote dipole and quadrupole fields from the kinetic Sunyaev Zel'dovich and polarized Sunyaev Zel'dovich effects*, *Phys. Rev.* **D 98** (2018) 123501 [arXiv:1707.08129] [INSPIRE].

[29] H.-J. Seo and D.J. Eisenstein, *Probing dark energy with baryonic acoustic oscillations from future large galaxy redshift surveys*, *Astrophys. J.* **598** (2003) 720 [astro-ph/0307460] [INSPIRE].

[30] R. Jimenez and A. Loeb, *Constraining cosmological parameters based on relative galaxy ages*, *Astrophys. J.* **573** (2002) 37 [astro-ph/0106145] [INSPIRE].

[31] J. Simon, L. Verde and R. Jimenez, *Constraints on the redshift dependence of the dark energy potential*, *Phys. Rev.* **D 71** (2005) 123001 [astro-ph/0412269] [INSPIRE].

JCAP05(2019)048

[32] A. Kosowsky, *Cosmic microwave background polarization*, *Annals Phys.* **246** (1996) 49 [astro-ph/9501045] [INSPIRE].

[33] M. Zaldarriaga and U. Seljak, *An all sky analysis of polarization in the microwave background*, *Phys. Rev.* **D 55** (1997) 1830 [astro-ph/9609170] [INSPIRE].

[34] M. Kamionkowski, A. Kosowsky and A. Stebbins, *Statistics of cosmic microwave background polarization*, *Phys. Rev.* **D 55** (1997) 7368 [astro-ph/9611125] [INSPIRE].

[35] A. Challinor, *Microwave background polarization in cosmological models*, *Phys. Rev.* **D 62** (2000) 043004 [astro-ph/9911481] [INSPIRE].

[36] A.M. Anile and R.A. Breuer, *Polarization transport in anisotropic universes*, *Astrophys. J.* **217** (1977) 353.

[37] C.G. Tsagas, A. Challinor and R. Maartens, *Relativistic cosmology and large-scale structure*, *Phys. Rept.* **465** (2008) 61 [arXiv:0705.4397] [INSPIRE].

[38] A. Heavens, R. Jimenez and L. Verde, *Standard rulers, candles and clocks from the low-redshift universe*, *Phys. Rev. Lett.* **113** (2014) 241302 [arXiv:1409.6217] [INSPIRE].

[39] S. Lange and L. Page, *Measuring the expansion of the universe through changes in the CMB photosphere*, *Astrophys. J.* **671** (2007) 1075 [arXiv:0706.3908] [INSPIRE].

[40] J.P. Zibin, A. Moss and D. Scott, *The evolution of the cosmic microwave background*, *Phys. Rev.* **D 76** (2007) 123010 [arXiv:0706.4482] [INSPIRE].

[41] A. Moss, J.P. Zibin and D. Scott, *Observing the evolution of the CMB*, *Phys. Rev.* **D 77** (2008) 043505 [arXiv:0709.4040] [INSPIRE].

[42] R.A. Sunyaev and Y.B. Zeldovich, *The observations of relic radiation as a test of the nature of X-ray radiation from the clusters of galaxies*, *Comments Astrophys. Space Phys.* **4** (1972) 173.

[43] CMB-S4 collaboration, *CMB-S4 technology book, first edition*, arXiv:1706.02464 [INSPIRE].

[44] T. Louis, E.F. Bunn, B. Wandelt and J. Silk, *Measuring polarized emission in clusters in the CMB S4 era*, *Phys. Rev.* **D 96** (2017) 123509 [arXiv:1707.04102] [INSPIRE].

[45] Simons Observatory collaboration, *The Simons observatory: science goals and forecasts*, *JCAP* **02** (2019) 056 [arXiv:1808.07445] [INSPIRE].

[46] CMB-S4 collaboration, *CMB-S4 science book, first edition*, arXiv:1610.02743 [INSPIRE].

JCAP05(2019)048

Part II

CAN DARK DARK MATTER BE GEOMETRY?

3

INVESTIGATING MODIFIED GRAVITY AS A DARK MATTER CANDIDATE

As was mentioned in the introduction 1, DM's existence has been proven with several observational probes [23–26], however its nature is still a mystery till this day. Several candidates have been proposed to explain this mysterious entity, including particles[60, 61] and primordial blackholes[27]. One suggestion, which will be the subject of this chapter, is *modified gravity* candidates of DM.

The idea that DM is part of a new, or modified, theory of gravity was initiated by Mordehai Milgrom in 1982-83 with what was called *Modified Newtonian Dynamics* (MOND) [62–64]. After many years of investigating this subject [65–68], relativistic modifications of gravity started to appear. These include *Tensor-Vector-Scalar* (TeVeS) model [69] and, relatively recently, *Mimetic Dark Matter* (MDM) [47, 48]. The latter will be the main focus of this chapter's first part [70]. It should be mentioned that MDM has been investigated greatly since its initiation and we direct the interested reader to a few of those works: [71–79].

In that part, we start by presenting a brief overview of MDM in its most simple form, highlighting the main concepts and equations. Then, we re-derive MDM's equations-of-motion (EoM) at the background level, and show that there is an additional parameter and function (of conformal time) that are not fixed by the model. These are related to the amount of DM in the Universe, and must be specified with observational data. Therefore, one can conclude that, at the background level, the model is at least at the same footing as ΛCDM.

Furthermore, we analyze the model at first order in perturbation theory. Again, we find an additional parameter and function that needs to be fixed by observations. We conjecture that there will always be one additional such combination in the model at each level in perturbation theory. The main reason for this freedom is that the model does not incorporate a mechanism to generate initial conditions, which are provided in ΛCDM by inflation. However, as we show in the work bellow, incorporating inflation with MDM does not cast away the fine-tuning problem, which is one of the main motivations for looking for an alternative to ΛCDM.

Finally, these results are incorporated into the Boltzmann code `CLASS` [80, 81] in order to see how the matter power spectrum and CMB correlation functions look like in MDM. From the latter, we find that a 20% change from adiabatic initial conditions puts MDM outside

the limits of cosmic variance[1]. On the other hand, from the matter power spectrum, a 10% deviation from adiabatic initial conditions can already cast it outside of the acceptable error range.

One can conclude from this work that, to explain DM with a modification of GR, one needs to incorporate a mechanism to generate adiabatic initial conditions within the model in a natural way. Otherwise, the model will be at an equal footing with ΛCDM and will face fine-tuning problems.

What has been described so far could be considered as a test for MG models of DM at the Cosmological level. However, one can also think of other tests at astrophysical scales, which is the subject of this chapter's second part [82].

It has been reported recently that there are a number of diffuse galaxies that do not show any trace of DM [49–54], with galaxy AGC 114905 recently added to that pool [83]. From here, the basic argument we present in our work is the following: if DM is part of a modification of GR, then, by gravity's universality, such an effect should appear in every system of similar properties. However, the existence of the aforementioned galaxies puts this premise to question, for other similar galaxies are in fact DM dominated, while these are not. In order to show this quantitatively, we derive a generalized Virial theorem for a substantial class of MG models.

In our main analysis, we use the 3+1 formalism of GR [84] and write down a general form of the EoM that includes a term describing DM. Moreover, we distinguish between MG models that satisfy the *Jebsen-Birkhoff theorem*[2] and those that do not. This distinction is crucial because in the derivation, one must assume asymptotic flatness at a certain point, which is not valid for some MG theories.

Having derived the Virial theorem with this method, we then moved on to constrain its additional term using observations of the Virial mass and radius from [49–54]. What we find is that, not only this term is never negligible, but there is also no consistency between the results. This means that the additional term in the generalized Virial theorem must be fine tuned to match the data of these galaxies.

After this general overview of both works, they are now presented in their published form below.

1 This is a fundamental uncertainty in the knowledge we may get about CMB correlation functions. It is more prominent for low values of the multipole expansion parameter l. See chapter 9 in [1]

2 The theorem states that all spherically symmetric vacuum solutions of the Einstein equation must be static and asymptotically flat [85].

Physics of the Dark Universe 30 (2020) 100646

Contents lists available at ScienceDirect

Physics of the Dark Universe

journal homepage: www.elsevier.com/locate/dark

Can dark matter be geometry? A case study with mimetic dark matter

Ali Rida Khalifeh [a,b,*], Nicola Bellomo [a,b], José Luis Bernal [d,a,b], Raul Jimenez [a,c]

[a] ICC, University of Barcelona, Marti i Franques, 1, E-08028 Barcelona, Spain
[b] Dept. de Fisica Quantica i Astrofisica, University of Barcelona, Marti i Franques 1, E-08028 Barcelona, Spain
[c] ICREA, Pg. Lluis Companys 23, Barcelona, E-08010, Spain
[d] Department of Physics and Astronomy, Johns Hopkins University, 3400 North Charles Street, Baltimore MD, 21218, USA

ARTICLE INFO

Article history:
Received 29 October 2019
Received in revised form 18 June 2020
Accepted 18 June 2020

ABSTRACT

We investigate the possibility of dark matter being a pure geometrical effect, rather than a particle or a compact object, by exploring a specific modified gravity model: mimetic dark matter. We present an alternative formulation of the theory, closer to the standard cosmological perturbation theory framework. We make manifest the presence of arbitrary parameters and extra functions, both at background level and at first order in perturbation theory. We present the full set of independent equations of motion for this model, and we discuss the amount of tuning needed to match predictions of the theory to actual data. By using the matter power spectrum and cosmic microwave background angular power spectra as benchmark observables, we explicitly show that since there is no natural mechanism to generate adiabatic initial conditions in this specific model, extra fine-tuning is required. We modify the publicly available Boltzmann code CLASS to make accurate predictions for the observables in mimetic dark matter. Our modified version of CLASS is available on GitHub[1]. We have used mimetic dark matter as an illustration of how much one is allowed to change the initial conditions before contradicting observations when modifying the laws of gravity as described by General Relativity. Moreover, we point out that modifying gravity without providing a natural mechanism to generate adiabatic initial conditions will always lead to highly fine-tuned models.

1. Introduction

The General Theory of Relativity (GR) has proven to be a very successful theory to describe and predict almost all of the gravitational phenomena observed to this date [1]. It has, so far, been tested over a wide range of scales, ranging from the weak field regime of our solar system, all the way to cosmological scales or to the strong regime (through recent detections of black holes coalescence events [2–4] and most recently the super-massive black hole imaging by the Event Horizon Telescope [5]).

On the other hand, explaining the universe using GR at galactic and cosmic scales requires additional non-baryonic components. These are cold dark matter (DM) and dark energy, and the model associated with these two in GR is henceforth known as ΛCDM, where Λ stands for the cosmological constant describing dark energy. The ΛCDM, according to state-of-the-art observational results [6,7], is able to describe with astonishing precision our Universe.

This model is still a phenomenological one, and suffers from a number of conceptual problems that prevents us yet from calling it the ultimate model describing the Universe. The nature of DM itself is still unknown, despite of the many DM candidates that have been proposed, including particles, compact objects and gravity effects, see e.g., Refs. [8,9] and Refs. therein. Typical modifications of GR have been driven by the presence of unsolved problems, and they typically address the issue of describing the dark energy sector by introducing a scalar field [10]. Since GR is extrapolated from solar system scales up to cosmological scales, it is not impossible that what we currently interpret as DM is in reality a pure gravitational effect.

In this work we analyse the Mimetic Dark Matter (MDM) model [11], in which DM, instead of being made of particle or compact objects, is described by gravity. In its original form, the model was a reformulation of GR, whereby the physical metric was rewritten in terms of an auxiliary one and a scalar field, while maintaining the language of differential geometry. The authors of Ref. [11] claim that GR is already able to describe DM without explicitly adding pressureless dust particles to the energy content of the universe: the scalar field is not a new dynamical degree of freedom, as stated in the footnote of Ref. [11]. The model has been investigated thoroughly: alternative formulations have been provided [12], the absence of ghosts has been proven [13,14], it

* Corresponding author at: Dept. de Fisica Quantica i Astrofisica, University of Barcelona, Marti i Franques 1, E-08028 Barcelona, Spain.
E-mail addresses: ark93@icc.ub.edu (A.R. Khalifeh), nicola.bellomo@icc.ub.edu (N. Bellomo), jbernal2@jhu.edu (J.L. Bernal), raul.jimenez@icc.ub.edu (R. Jimenez).

[1] https://github.com/ark93-cosmo/CLASS_Modified_MDM.

https://doi.org/10.1016/j.dark.2020.100646
2212-6864/

has been generalized to explain other cosmological phenomena, as inflation or dark energy [15], and to Horndeski theories of gravity [16–19]. We refer the interested reader to Ref. [20] and refs. therein to a complete discussion of different aspects of MDM.

However, some aspects of this theory remain unexplored, in particular the degree of tuning necessary to match the theory with current observations. In this work, we re-examine the derivation of the equations of motion for MDM, and show that the redundancy in the latter still provides the equivalent of Friedmann equations, but at the expense of new arbitrary functions that require tuning to match the observed Universe. Moreover, since the standard MDM model does not include a mechanism able to produce adiabatic initial conditions, further tuning is required.[2] In particular, we show that future cosmic-variance limited experiments are able to detect even a slight departure from adiabaticity, constraining the model unless some degree of fine tuning is assumed.

The paper is organized as follows: in Section 2 we review the mimetic dark matter model. In Section 3 we describe the structure of the model and its equations of motion, both at the background level and at first order in perturbation theory, describing the freedom in the choice of particular parameters of the theory. In Section 4 we investigate the observational consequences of this extra freedom, and we discuss the degree of tuning required by the theory. Finally we conclude in Section 5.

Throughout this work, we use the $(-,+,+,+)$ signature and units in which $\hbar = c = 1$. Spacetime indices are denoted by Greek letters and range from 0 to 3, while spatial indices are denoted by Latin letters and range from 1 to 3; repeated indices are summed over.

2. The mimetic dark matter model

The original MDM model proposed a reformulation of the physical metric $g_{\rho\sigma}$ as[3] [11]

$$g_{\rho\sigma} = -\frac{1}{\mu^4}\left(\tilde{g}^{\alpha\beta}\partial_\alpha\varphi\partial_\beta\varphi\right)\tilde{g}_{\rho\sigma}, \tag{1}$$

where $\tilde{g}_{\rho\sigma}$ is an auxiliary metric, φ is a scalar field, called mimetic field, and μ is an arbitrary factor we introduced here just to make explicit the freedom in rescaling the mimetic field by a constant factor. The physical metric corresponds to the auxiliary metric multiplied by a conformal factor that depends on the latter. In this way, one is said to express explicitly the conformal mode of gravity, which is manifested by the invariance of the physical metric under a conformal transformation of the auxiliary one. This conformal mode is now encoded in the scalar field φ, and therefore the auxiliary metric will no longer be used (see, e.g., Ref. [13] for more details on the conformal mode of gravity in these models). The mimetic field has to obey the so called constraint equation

$$g^{\rho\sigma}\partial_\rho\varphi\partial_\sigma\varphi + \mu^4 = 0, \tag{2}$$

obtained by contracting the mimetic field derivatives $\partial_\rho\varphi\partial_\sigma\varphi$ with the inverse of the physical metric, which reads as $g^{\rho\sigma} = P^{-1}\tilde{g}^{\rho\sigma}$, where $P = (\tilde{g}^{\alpha\beta}\partial_\alpha\varphi\partial_\beta\varphi)/\mu^4$.

The Einstein–Hilbert action reads as [11]

$$S = \int d^4x\sqrt{-g(\tilde{g},\varphi)}\left[\frac{M_p^2}{2}R(g_{\mu\nu}(\tilde{g}_{\mu\nu},\varphi)) + \mathcal{L}_{mr}[g_{\mu\nu},\psi_m,\psi_r]\right], \tag{3}$$

where g is the determinant of the physical metric, $M_p = (8\pi G)^{-1/2}$ is the reduced Planck mass, R is the Ricci scalar and $\mathcal{L}_{mr}$ is the Lagrangian that describes baryonic matter and radiation fields ψ_m and ψ_r, respectively. By varying the action with respect to the auxiliary metric, we get Einstein equations of the form:

$$M_p^2 G^{\mu\nu} = T^{\mu\nu} + \tilde{T}^{\mu\nu}, \tag{4}$$

where $G_{\mu\nu} = R_{\mu\nu} - (1/2)g_{\mu\nu}R$ is the Einstein tensor defined in terms of the Ricci tensor $R_{\mu\nu}$ and the Ricci scalar R, $T_{\mu\nu} = -(2/\sqrt{-g})\delta S_{mr}/\delta g^{\mu\nu}$ is the stress–energy tensor of the baryonic matter and radiation fields, with S_{mr} being their corresponding action, and $\tilde{T}^{\mu\nu}$ takes the form of the stress–energy tensor of dust [11]. Note also that a dynamical variable is any quantity by which the action is varied, which means that the auxiliary metric, as well as the physical metric, are dynamical variables. As can be seen from (4), the model predicts that the effects of DM, encoded in $\tilde{T}^{\mu\nu}$, can be generated without the need of adding extra species to the action. Moreover, as shown in Refs. [12,13], the MDM constraint (2) can be incorporated in the action with the use of a Lagrange multiplier λ. In addition, MDM can be modified (hence it becomes a modification of GR) by introducing into the action a potential for the scalar field, as has been first done in Refs. [15,23].[4] In that case, the action becomes[5]

$$S = \int d^4x\sqrt{-g}\left[\frac{M_p^2}{2}R(g_{\mu\nu}) - V(\varphi) - \lambda\left(g^{\mu\nu}\partial_\mu\varphi\partial_\nu\varphi + \mu^4\right) + \mathcal{L}_{mr}[g_{\mu\nu},\psi_m,\psi_r]\right], \tag{5}$$

where $V(\varphi)$ is a potential for the mimetic field. As done previously in [15], the variation of the action in Eq. (5) with respect to the physical metric gives the new Einstein equations which, after using its trace to substitute for λ, gives

$$M_p^2 G_{\mu\nu} - T_{\mu\nu} = -g_{\mu\nu}V(\varphi) + \left(T - M_p^2 G - 4V\right)\frac{\partial_\mu\varphi\partial_\nu\varphi - \frac{1}{2}g_{\mu\nu}\mathcal{C}}{\mathcal{C}+\mu^4}, \tag{6}$$

where $T = T^\mu_{\ \mu}$ and $G = G^\mu_{\ \mu}$ are the traces of $G_{\mu\nu}$ and $T_{\mu\nu}$, respectively, and

$$\mathcal{C} = g^{\alpha\beta}\partial_\alpha\varphi\partial_\beta\varphi + \mu^4. \tag{7}$$

The constraint equation (2) for the mimetic field, which incidentally can be derived by varying the action with respect to the Lagrange multiplier ($\delta S/\delta\lambda = 0$), is equivalent to $\mathcal{C} = 0$. Moreover, we will impose the constraint equation when we derive the Friedmann equations at the background level in the next section. This will allow us to track the quantities that are affected by it. The appearance of an opposite sign in Eq. (6) compared to equation (2.4) of Ref. [15] is due to our opposite choice of the metric signature. Moreover, if we compare the RHS of Eq. (6) to the stress–energy tensor of a perfect fluid:

$$\tilde{T}^\mu_{\ \nu} = pg^\mu_{\ \nu} + (\rho + p)u^\mu u_\nu, \tag{8}$$

where ρ is the energy density, p is the pressure and $u^\mu = dx^\mu/\sqrt{-ds^2}$ is the corresponding 4-velocity of the fluid, we see

[2] This issue was already mentioned in Ref. [11], and was also discussed in Refs. [21,22]. In the latter, adiabaticity was recovered by introducing extra specific functions.

[3] Note that there will be sign differences compared to [11] and [15] because we use an opposite metric signature.

[4] Notice that the mimetic field can be rescaled as $\varphi \to |\mu|\varphi$, hence it is possible to absorb the factor μ into the Lagrange multiplier λ at the level of the action. However, in the case of non-zero potential, the explicit form of the action may change under such rescaling.

[5] It is interesting to note that using the same action as in [11,15] with the current signature will result in an imaginary field. However the study of this case is beyond the scope of this work.

that we can re-obtain Eq. (4) by identifying as energy density, pressure and 4-velocity of the scalar field fluid, respectively with

$$\rho_\varphi = \left(1+\frac{1}{2}\mathcal{C}\right)\left(T - M_p^2 G - 4V(\varphi)\right) + V;$$
$$p_\varphi = -\frac{1}{2}\mathcal{C}\left(T - M_p^2 G - 4V(\varphi)\right) - V(\varphi);$$
$$u^\mu = \partial^\mu\varphi/\sqrt{\mathcal{C}+\mu^4}. \tag{9}$$

In this case Eq. (2) corresponds to the normalization equation $u^\mu u_\mu = -1$ for the 4-velocity. The equations of dynamics for matter and radiation fields ($\delta S/\delta\psi_m, \delta S/\delta\psi_r = 0$) do not change with respect to the standard ones in GR. Moreover, the stress–energy tensor of matter and radiation fields is conserved as in GR, namely we have $\nabla_\mu T^{\mu\nu} = 0$, even if Einstein equations (6) changed. For this reason we do not report them here and we refer the interested reader to Ref. [24].

3. Einstein equations

In the following we specify the general equations of the MDM model to the case of an Universe described by Friedman–Lemaître–Robertson–Walker metric. Since we are interested only in the description of scalar modes, we choose to work with the conformal Newtonian gauge described by the metric

$$ds^2 = g_{\mu\nu}dx^\mu dx^\nu = a^2(\tau)\left[-(1+2\Psi)d\tau^2 + (1-2\Phi)\delta_{ij}dx^i dx^j\right], \tag{10}$$

where a is the scale factor, τ is the conformal time, x^i are comoving spatial coordinates and the potentials Ψ and Φ are related to Bardeen gauge-invariant variables [25]. Throughout this section we follow notation and conventions of Ref. [24].

We assume that the matter and radiation content of the Universe can be described by an almost perfect fluid with stress–energy tensor given by

$$T^\mu_{\ \nu} = pg^\mu_{\ \nu} + (\rho+p)u^\mu u_\nu + \Sigma^\mu_{\ \nu}, \tag{11}$$

where $\Sigma^\mu_{\ \nu}$ contributes to the anisotropic stress only at first order in perturbation theory. Assuming that the fluid has some small density and pressure fluctuations $\delta\rho$ and δp, coordinate velocity $v^i = dx^i/d\tau$ and anisotropic stress $\Sigma^i_{\ j}$ (such that $\Sigma^i_{\ i} = 0$), the components of the stress–energy tensor, up to first order in perturbation theory, can be written as

$$T^0_{\ 0} = -(\bar\rho+\delta\rho), \qquad T^i_{\ 0} = -(\bar\rho+\bar p)v^i, \qquad T^i_{\ j} = (\bar p+\delta p)\delta^i_{\ j} + \Sigma^i_{\ j}, \tag{12}$$

where an over-bar denotes background quantities. In the following we use also the overdensity contrast $\delta = \delta\rho/\bar\rho$, the divergence of the velocity θ and of the traceless anisotropic stress σ, which read as

$$(\bar\rho+\bar p)\theta = ik^j\delta T^0_{\ j} = i(\bar\rho+\bar p)k^j v_j, \qquad (\bar\rho+\bar p)\sigma = -\left(\hat k_i\hat k_j - \frac{1}{3}\delta_{ij}\right)\Sigma^i_{\ j}. \tag{13}$$

3.1. Background evolution

At the background level, energy densities $\bar\rho(\tau)$, pressures $\bar p(\tau)$ and the scalar field $\bar\varphi(\tau)$ are only time-dependent. The constraint equation (2) reads, after fixing it for the appropriate metric signature, as

$$\mu^4 - \frac{\bar\varphi'^2}{a^2} = 0, \tag{14}$$

where " $'$ " denotes derivative with respect to the conformal time τ. As in GR, and as done in Ref. [15], Friedman equations are obtained from the $(0-0)$ and the trace of the spatial $(i-j)$ components of Eq. (6) and read as

$$\mathcal{A} = -\frac{1}{\mathcal{C}+\mu^4}\left[3\mathcal{B}-\mathcal{A}\right]\left[a^{-2}\bar\varphi'^2 + \frac{1}{2}\mathcal{C}\right], \tag{15}$$

$$\mathcal{B} = \frac{\mathcal{C}}{2(\mathcal{C}+\mu^4)}\left[3\mathcal{B}-\mathcal{A}\right], \tag{16}$$

where

$$\mathcal{A} = 3M_p^2\mathcal{H}^2 - a^2\bar\rho - a^2V, \quad \mathcal{B} = -M_p^2\left(2\mathcal{H}'+\mathcal{H}^2\right) - a^2\bar p + a^2V \tag{17}$$

and $\mathcal{H} = a'/a$ is the Hubble expansion parameter in conformal time. Note that these two equations are identical once the explicit form of $\mathcal{C}$, Eq. (7), is substituted. Therefore, the final form of either of them would be:

$$\left(a^2\mu^4 - \bar\varphi'^2\right)\mathcal{A} + \left(a^2\mu^4 + \bar\varphi'^2\right)\mathcal{B} = 0. \tag{18}$$

If we now impose the constraint equation (14) to (18), in order to make it consistent, we deduce that:

$$\mathcal{B} = 0 \quad \Rightarrow \quad M_p^2\left(2\mathcal{H}' + \mathcal{H}^2\right) + a^2\bar p - a^2V = 0 \tag{19}$$

and

$$\mathcal{A} = f(\tau) \quad \Rightarrow \quad 3M_p^2\mathcal{H}^2 - a^2\bar\rho - a^2V = f(\tau). \tag{20}$$

These two equations have the same form as the 2nd and 1st Friedmann equations, respectively. Therefore, although we have a redundancy at the level of Einstein equation's components, we still get the Friedmann equations. However, this is at the expense of getting an arbitrary function of conformal time, $f(\tau)$, which connects the expansion history of the universe to its energy. Indeed, as done before, if we identify the energy density of the scalar field with $\bar\rho_\varphi = a^{-2}f(\tau) + V$, Eqs. (9), (19) and (20) give the following definitions for the background density and pressure of the field, respectively:

$$\bar\rho_\varphi = T - M_p^2 G - 3V = f(\tau)a^{-2} + V; \quad \bar p_\varphi = -V. \tag{21}$$

Note that $f(\tau)$ function can be determined by taking the time derivative of Eq. (20), using the conservation equation, $\bar\rho' + 3\mathcal{H}(\bar\rho+\bar p) = 0$, and comparing the result to Eq. (19). We find that $f(\tau)$ has to satisfy the differential equation

$$f' + \mathcal{H}f + \left[(a^2V)' - 2\mathcal{H}(a^2V)\right] = 0. \tag{22}$$

The solution of the homogeneous equation reads $f = \kappa/a$, where κ is a space-independent integration constant because of homogeneity and isotropy. The general solution depends on the shape of the potential and is given by

$$f(\tau) = \frac{\kappa}{a} - a^2V(\varphi) + \frac{3}{a}\int_{\tau_0}^{\tau} d\tilde\tau\left(\mathcal{H}a^3V\right), \tag{23}$$

where τ_0 is some reference time, and which generalizes the result presented in Ref. [15] to an Universe filled with matter and radiation. Therefore, independently of the chosen shape of the potential, a fraction of the mimetic field energy density scales as κa^{-3}, i.e., as DM would do. The integration constant, κ, is an extra free parameter of the theory that has to be chosen properly to fit the observation. Notice that this additional parameter is not connected to any parameter in the action of the theory, hence apart from setting its value using current observational data, we cannot assign it any value motivated by the theory itself. Therefore, when it comes to the amount of DM in the universe, the model presents at least the same level of tuning needed as in ΛCDM. We discuss how this parameter was linked to the initial conditions of our Universe in Section 4.

We conclude by highlighting the solutions for two special cases: a zero potential ($V \equiv 0$) and a strictly negative constant potential ($V \equiv \bar{V} < 0$). In the first case we have that

$$\bar{\rho}_\varphi = fa^{-2} + V = \kappa a^{-3}, \qquad \bar{p}_\varphi = -V \equiv 0, \tag{24}$$

hence the mimetic field plays only the role of cold DM. In the second case we have both DM and dark energy at the same time, in fact $f(\tau) = \left[\kappa + \bar{V}a_0^3\right]/a = \tilde{\kappa}/a$, where $\tilde{\kappa}$ is a new integration constant and $a_0 = a(\tau_0)$, therefore

$$\bar{\rho}_\varphi = fa^{-2} + \bar{V} = \tilde{\kappa}a^{-3} + \bar{V}, \qquad \bar{p}_\varphi = -\bar{V}, \tag{25}$$

hence in this scenario the mimetic field plays the role both of DM and a cosmological constant, as in certain quartessence models [26] and as also shown in Ref. [23]. In both cases, see, e.g., Ref. [15], we can connect the energy density and pressure of the mimetic field to the background value of the Lagrange multiplier $2\bar{\lambda} = \bar{\rho}_\varphi + \bar{p}_\varphi = fa^{-2}$. Therefore the ambiguity in choosing the free parameter κ derives from the possibility of rescaling arbitrarily the mimetic field while reabsorbing any constant in the Lagrange multiplier.

3.2. Perturbative dynamics

In order to compare the predictions of this model to those of the traditional ΛCDM we need to compute the evolution of perturbations. In this section we present the equations of dynamics for the metric and scalar field fluctuations, while, as previously stated, we do not report those of matter and radiation fields since they are identical to those in GR. Moreover, the same machinery used to derive (19) and (20) applies to their perturbed equivalents, and therefore it will not be presented explicitly, rather simply the final results will be. Also, to simplify the expressions, we will impose the constraint equation (14), or equivalently $\mathcal{C} = 0$, at the level of the perturbation of Einstein equations (6). The result will be the same whether we take $\mathcal{C} = 0$ at this level or at very end. The results of this section apply to MDM models with an arbitrary shape of the potential, hence they can be applied to different scenarios.

The constraint equation (2) for the mimetic field fluctuation reads as

$$\delta\varphi' - \bar{\varphi}'\Psi = 0, \tag{26}$$

however, as done in Ref. [18], it is more convenient to introduce a new variable $v_\varphi = -\delta\varphi/\bar{\varphi}'$ whose equation of motion, invariant under rescaling of the mimetic field, is

$$v_\varphi' + \mathcal{H}v_\varphi + \Psi = 0. \tag{27}$$

Moreover, by defining the velocity divergence of the scalar field fluid as $\theta_\varphi = k^2 v_\varphi$, we find that Eq. (27) can be recast as

$$\theta_\varphi' + \mathcal{H}\theta_\varphi + k^2\Psi = 0, \tag{28}$$

which is the equation of motion of the velocity divergence for a non-relativistic and collisionless fluid. Therefore the theory itself, independently of the shape of the potential, is able to reproduce the equation of motion of DM velocity divergence.

At first order in perturbation theory we have four independent Einstein equations. In reporting these equations, we keep on the LHS of each equation all the terms unchanged with respect to the GR case, see e.g., Ref. [24], while on the RHS we put the new terms given by the MDM model.

By defining the pressure perturbation of the scalar field fluid as $\delta p_\varphi = v_\varphi \bar{\varphi}' V_{,\varphi}$, where $V_{,\varphi} = \partial V/\partial\varphi$, we find that the traceless part and the trace of the $(i-j)$ components of Einstein equations are given by

$$k^2(\Phi - \Psi) - \frac{3a^2}{2M_p^2}(\bar{\rho} + \bar{p})\sigma = 0, \tag{29}$$

$$\Phi'' + \mathcal{H}\left(\Psi' + 2\Phi'\right) + \left(2\mathcal{H}' + \mathcal{H}^2\right)\Psi + \frac{k^2}{3}(\Phi - \Psi) - \frac{a^2}{2M_p^2}\delta p = \frac{a^2}{2M_p^2}\delta p_\varphi. \tag{30}$$

Notice that the mimetic field cannot be a source of anisotropic stress, i.e., $\sigma_\varphi \equiv 0$, and only when the gradient of the potential $(\partial V/\partial\varphi)$ is non-zero the scalar field develops an isotropic pressure perturbation δp_φ.

Using Friedman equations (19) and (20), we find that the $(0-i)$ components of Einstein equations reads

$$\Phi' + \mathcal{H}\Psi - \frac{a^2}{2M_p^2k^2}(\bar{\rho} + \bar{p})\theta = \frac{a^2}{2M_p^2k^2}(\bar{\rho}_\varphi + \bar{p}_\varphi)\theta_\varphi, \tag{31}$$

which shows that not only in MDM we have an equation for velocity divergence identical to that of DM, but also this velocity contribution appears in the correct form in Einstein equations.

Finally, using the results we have found both in Section 3.1 and in Section 3.2 so far, we are able to write the perturbed equivalent of the 1st Friedmann equation as:

$$3\mathcal{H}\Phi' + 3\mathcal{H}^2\Psi + k^2\Phi + \frac{a^2}{2M_p^2}\bar{\rho}\delta = -\frac{a^2\bar{\rho}_\varphi}{2M_p^2}g(k,\tau), \tag{32}$$

where this specific form has been chosen for later convenience. It is important to emphasize again the fact that even if we have redundancy in the equations of motion, we can still find the equivalence of the perturbed Friedmann equations for this model, at the expense of getting an arbitrary function, which at 1st order in perturbation is $g(k,\tau)$. We argue that there is one of these functions at every level in perturbation theory, hence going to second order we would find an 60 arbitrary function, and so on.

By taking time derivatives of (32) and using the results of Sections 3.1 and 3.2, we get

$$g' = -(1 + \omega_\varphi)(\theta_\varphi - 3\Phi') - 3\mathcal{H}(c^2_{(\varphi),s} - \omega_\varphi)g \tag{33}$$

where $\omega_\varphi = \bar{p}_\varphi/\bar{\rho}_\varphi$ is the equation of state of the scalar field fluid, and $c^2_{(\varphi),s} = \delta p_\varphi/\delta\rho_\varphi$ is an effective sound-speed-like term of the mimetic field. If we compare Eq. (33) to equation (30) of Ref. [24], we notice that the function g evolves as the overdensity contrast of a fluid, therefore it can be thought as $g \equiv \delta_\varphi$. In the case of zero potential, i.e., in the case where the mimetic field describes DM, we recover the evolution equation for dust.

4. Initial conditions and observational constraints

We have shown that the MDM model, for any given potential V, shows a level of flexibility in the choice of the function $f(\tau)$ and in the choice of the initial conditions (ICs) for the mimetic field fluctuation and the function g at first order in perturbation theory. Notice that generalizations of the standard MDM model seems to be able to produce adiabatic ICs [21,22], however this feature depends on the form of the mimetic Lagrangian and it is not a general property of the MDM model.

At the background level, independently of the shape of the potential, we have a free parameter, κ, whose value in principle is set by ICs of the mimetic field and cannot be derived directly from the action written in Eq. (5). The authors of Ref. [11] suggested that if the mimetic field is coupled to the inflaton, a non-vanishing amount of DM can survive 60 e-folds of expansion without spoiling inflationary dynamics. Since the evolution of the mimetic field is fixed by the constraint equation (2), which does

not provide any attractor solution, the dynamics of the inflaton need to be fine-tuned to provide the correct amount of DM today. Moreover, in case the potential is non-zero, its shape and parameters have to be tuned to match observations, as we can see in the example in Eq. (25).

At the perturbation level, even if the g function and the mimetic field fluctuation evolve as an energy overdensity and a velocity, respectively, we have to set ICs for both quantities. This requires a second tuning because we know them to be adiabatic [27]. If the mimetic field is just a spectator field during inflation, as suggested above to fix the value of κ, then its presence can result in having also isocurvature ICs [28], which are largely ruled out [29]. However, having isocurvature initial conditions is not inevitable for MDM, rather it is a possibility without some level of fine-tuning. Moreover, even assuming no isocurvature ICs are generated, we still have to properly define the scalar field ICs, or, equivalently, to define an inflationary scenario able to generate adiabatic ICs also for the mimetic field.

To study the impact of ICs in this model, we consider the case study of MDM accounting only for DM, i.e., we consider the $V \equiv 0$ case. We fix κ to be the observed DM energy density today, we fix the ICs for g so that adiabaticity is preserved. We let vary only the IC of the mimetic field perturbation, i.e., the IC of the mimetic field fluid velocity divergence θ_φ, which in the adiabatic case is related to the gravitational potential by $\theta_\varphi = \frac{1}{2}(k^2\tau)\Psi$ [24]. Variations in κ and ICs for g, would result in larger departures from the ΛCDM case, hence we can consider our approach as conservative.

We modify the public code `CLASS` [30] to include the effects of the MDM model accounting for DM. We parametrize deviations from standard adiabatic ICs for the velocity divergence as

$$\theta_\varphi = \left[1 + \alpha \sin(\log_2 k)\right]\frac{1}{2}(k^2\tau)\Psi, \tag{34}$$

where α represents the maximum amplitude of the deviation from adiabatic initial conditions. Our choice in Eq. (34) has been made only for illustrative purposes, to make the plots clearer and easier to be interpreted; any other small deviation from adiabatic initial conditions would be equally valid to prove our point. This choice allows us to have variations between $[1-\alpha, 1+\alpha]$ with respect to adiabatic ICs. We check that for other wavenumber dependences, for instance randomly choosing a number in $[1-\alpha, 1+\alpha]$, our findings are unchanged. In the following we assume the Planck18 baseline cosmology assuming the best-fit parameters to the whole Planck dataset [6]: $\omega_{\rm b} = 0.0224$ is the physical baryon density today, $\omega_{\rm cdm} = 0.120$ is the physical cold dark matter density today, $h = 0.674$ is the reduced Hubble expansion rate today, $10^9 A_s = 2.101$ is the amplitude of the primordial scalar perturbations, $n_s = 0.965$ is the scalar spectral index and $\tau = 0.054$ is the optical depth to reionization. We use $\omega_\varphi = \kappa h^2 = 0.120$, where ω_φ is the physical density of the mimetic field today, instead of $\omega_{\rm cdm}$ when computing observables in MDM.

We compare the evolution of perturbations in ΛCDM and MDM in Fig. 1. As we can notice, even when we perfectly match the overdensity perturbation in the MDM model to the one of DM in ΛCDM and we assume for them the same initial conditions at early times, we observe deviations at late times generated by different ICs in the velocity sector. Hence any small change in ICs only in the velocities will generate in turn larger changes in cosmological observables.

These differences in the evolution of perturbations generate deviations in cosmological observables. We report them in Fig. 2 for the CMB temperature and polarization power spectra (C_ℓ^{TT}, C_ℓ^{EE}) and for the matter power spectrum (P_m). In all the cases, we analyse deviations up to 10%, 20% and 50% from adiabatic ICs, corresponding to $\alpha = 0.1,\ 0.2,\ 0.5$, respectively.

We compare these deviations to cosmic variance uncertainty. For the angular power spectra, the cosmic variance reads as [31]

$$\frac{\sigma_{C_\ell}}{C_\ell} = \sqrt{\frac{2}{f_{\rm sky}(2\ell+1)}} \tag{35}$$

where ℓ is the multipole and $f_{\rm sky}$ is the observed fraction of the sky, independently from the chosen experiment. On the other hand, in the case of the matter power spectrum we have a dependence on the chosen survey, in fact the error is given by, see, e.g., [32],

$$\frac{\sigma_{P_m}}{P_m} = \sqrt{\frac{4\pi^2}{V_S k^3 \Delta \log k}}\left(1 + \frac{1}{n_g P_m}\right), \tag{36}$$

where $\Delta \log k$ is the bin size in k-space, V_S is the volume of the survey and n_g is the number density of galaxies. For an Euclid-like survey, with average redshift $\bar{z} = 1$, redshift bin width $\Delta z = 0.1$ and uniform binning of $\log k$, we have an estimated volume of $V_S(\bar{z}) = 1.719\ {\rm Gpc}^3$ and number of galaxies of $n_g(\bar{z}) = 1.998 \times 10^{-3}\ {\rm Mpc}^{-3}$. Following Ref. [32], we further normalize the error bars to make them independent of the number of redshift bins and the width of the k bins.

As can be seen from Fig. 2, even fractional changes in the ICs generate deviations in the observable spectra which are detectable by cosmic variance limited experiments. Note that given the absence of a mechanism that automatically guarantees adiabatic ICs, a fractional change of less than 50% represents a very modest variation. In the CMB temperature and polarization correlation functions, current observations by the Planck mission (cosmic variance limited up to $\ell \sim 2000$), rule out deviations larger than 20% ($\alpha \gtrsim 0.2$) from the adiabatic initial conditions of ΛCDM. Furthermore, constraints by an Euclid-like mission will constrain any change at the percent level, as can be seen from the lower panel of Fig. 2. By allowing also the κ parameter, g function and its ICs, to vary we would expect much more significant deviations.

In other words, the free parameter κ and the ICs of the DM sector need to be fine-tuned at the 10% level with current observations and they will be constrained at better than percent level with Euclid-like observations. Note that the fine-tuning problem is more severe than it looks as it is a function and not a simple number that needs to be adjusted to reproduce exactly adiabaticity (thus the level of fine-tuning extends to infinite degrees of freedom). Our main finding is that modifications of gravity that do not naturally produce a mechanism to generate adiabatic initial conditions do suffer from serious fine-tuning issues in the form of fine-tuning of free functions.

5. Conclusions

Despite its great success in describing the Universe we live in, the ΛCDM model does not provide any insight into what actually is the nature of its two main constituents, DM and dark energy. In this work we have explored in detail the predictions of a modified gravity model where the phenomenology associated to DM is described by pure geometry rather than elementary particles or compact objects. In particular, as a proof of principle, we focused on the mimetic dark matter model.

After providing an alternative formulation to perturbation theory in this model, we found that this modified gravity model is naturally able to reproduce DM phenomenology, however it also contains free parameters and functions whose ICs need to be tuned in order to match observational data. Since the model

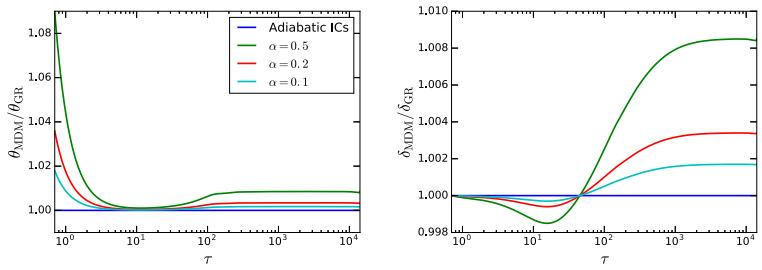

Fig. 1. Ratio of the mimetic field velocity divergence perturbation (left panel) and mimetic field density perturbation (right panel) in MDM (with $V = 0$) with respect to that of DM assuming ΛCDM for $k = 0.1$ hMpc^{-1}, as a function of conformal time. We consider different values of the parameter α (colour coded), which represents the maximum deviation from the adiabatic ICs case. (For interpretation of the references to colour in this figure legend, the reader is referred to the web version of this article.)

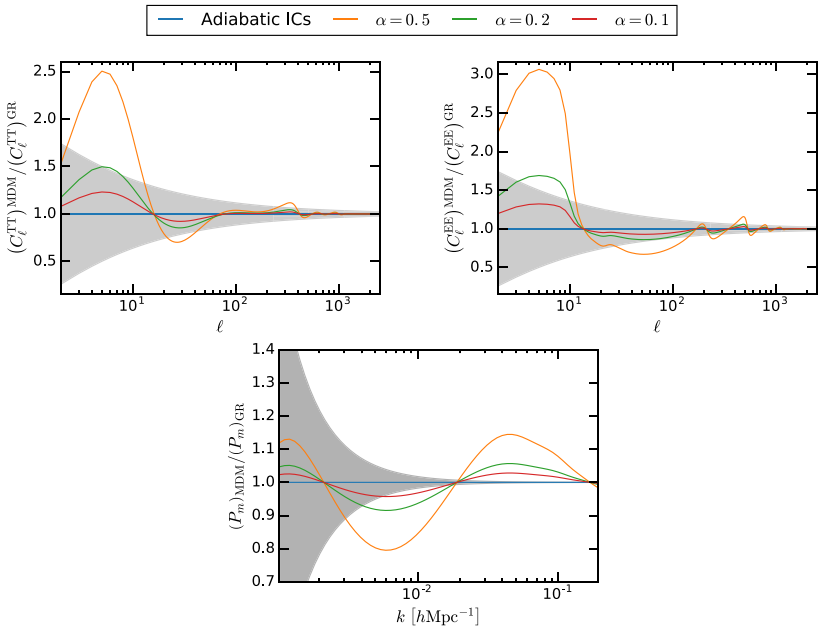

Fig. 2. Ratio of the CMB temperature angular power spectrum (upper left panel), the CMB E-mode polarization angular power spectrum (upper right panel) and the matter power spectrum at redshift $\bar{z} = 1$ (bottom panel), in the MDM model (with $V = 0$) with respect to the ΛCDM prediction, for the same cases considered in Fig. 1. In the three panels the grey regions represents the cosmic variance limit (normalized for P_m as explained under Eq. (36)).

does not naturally produce adiabatic initial conditions for the mimetic field, it requires extra tuning to reproduce observations. The purpose of this work was to highlight that this model, in its most basic form (i.e without a potential in the case of MDM), requires further development. In particular, to produce adiabatic initial conditions and, at the same time, to describe late time evolution of the universe, specific functions must be introduced at the level of the action. In other words, to reproduce observations, we do not have to tune only parameters, like in ΛCDM, but also the specific shape of functions.

We have modified the public Boltzmann code CLASS to compute both the evolution of perturbations and standard cosmological observables, as the matter power spectrum and cosmic microwave background temperature and polarization power spectrum, of the MDM model. Our modified version of CLASS is available on GitHub.[6] Several studies showed that ghosts and gradient instabilities may develop in an Universe filled only with the mimetic field [33,34]. In our numerical computations, which include matter and radiation, we did not impose by hand any extra stability requirement, hence we note that in a more realistic set-up this does not represent a problem of the model in its simplest version. However, if adding extra specific higher derivative couplings was needed to prevent these instabilities to emerge, as shown in Refs. [35–37], we would need a higher level of fine tuning. We proved that current and future cosmic variance dominated experiments are able to detect small deviations from perfect adiabatic ICs, even in the conservative case where only the ICs of the velocity perturbations were allowed to vary by a small fraction. If all the free parameters and functions of the theory were allowed to deviate from its ΛCDM analogue, deviations would be much larger and would have been detected, for instance by Planck.

We conclude by noticing that any modification of gravity that does not generically predict adiabatic ICs will suffer from severe fine tuning problems, since the degree of fine tuning for arbitrary functions is actually infinite and the model does not contain any attractor solution. This can be a route to restrict modifications

6 https://github.com/ark93-cosmo/CLASS_Modified_MDM

of gravity and guide model building when abandoning General Relativity.

CRediT authorship contribution statement

Ali Rida Khalifeh: Conceptualization, Methodology, Software, Validation, Formal analysis, Investigation, Resources, Data curation, Writing - original draft, Writing - review & editing, Visualization. **Nicola Bellomo:** Conceptualization, Methodology, Software, Validation, Formal analysis, Investigation, Resources, Data curation, Writing - original draft, Writing - review & editing, Visualization, Supervision, Project administration. **José Luis Bernal:** Supervision, Project administration. **Raul Jimenez:** Conceptualization, Methodology, Software, Validation, Formal analysis, Investigation, Resources, Data curation, Writing - original draft, Writing - review & editing, Visualization, Supervision, Project administration.

Declaration of competing interest

The authors declare that they have no known competing financial interests or personal relationships that could have appeared to influence the work reported in this paper.

Acknowledgements

ARK would like to thank Cyril Pitrou, Samuel Brieden and David Valcin for help and discussions. We thank Alexander Ganz, Justin Khoury, Sunny Vagnozzi and Alexander Vikman for useful comments on the draft. Funding for this work was partially provided by the Spanish MINECO under projects AYA2014-58747-P AEI/FEDER, UE, and MDM-2014-0369 of ICCUB, Spain (Unidad de Excelencia María de Maeztu). ARK is supported by project AYA2014-58747-P AEI/FEDER. NB is supported by the Spanish MINECO under grant BES-2015-073372. JLB was supported by the Spanish MINECO under grant BES-2015-071307, co-funded by the ESF, during most of the development of this work. Part of the calculations were done using the `xAct` package of Mathematica.

References

[1] C.M. Will, The confrontation between general relativity and experiment, Living Rev. Relativ. 17 (1) (2014) 4, arXiv:1403.7377.
[2] Scientific Collaboration and Virgo Collaboration, B.P. Abbott, et al., Observation of gravitational waves from a binary black hole merger, Phys. Rev. Lett. 116 (6) (2016) 061102, arXiv:1602.03837.
[3] B.P. Abbott, et al., Multi-messenger observations of a binary neutron star merger, Astrophys. J. 848 (2) (2017) L12, arXiv:1710.05833.
[4] B.P. Abbott, et al., GWTC-1: A gravitational-wave transient catalog of compact binary mergers observed by LIGO and virgo during the first and second observing runs, arXiv:1811.12907.
[5] The EHT Collaboration, First M87 event horizon telescope results. IV. Imaging the central supermassive black hole, ApJL 875 (2019) 4, arXiv:1906.11241.
[6] The Planck Collaboration, N. Aghanim, et al., Planck 2018 results. VI. Cosmological parameters, arXiv:1807.06209.
[7] The SDSS-III BOSS, S. Alam, et al., The clustering of galaxies in the completed SDSS-III Baryon oscillation spectroscopic survey: cosmological analysis of the DR12 galaxy sample, Mon. Not. R. Astron. Soc. 470 (2017) 2617–2652, arXiv:1607.03155.
[8] G. Bertone, D. Hooper, History of dark matter, Rev. Modern Phys. 90 (4) (2018) 045002, arXiv:1605.04909.
[9] G. Bertone, T.M.P. Tait, A new era in the search for dark matter, Nature 562 (2018) 51–56, arXiv:1810.01668.
[10] B. Ratra, P.J.E. Peebles, Cosmological consequences of a rolling homogeneous scalar field, Phys. Rev. D 37 (12) (1988) 3406–3427.
[11] A.H. Chamseddine, V. Mukhanov, Mimetic dark matter, J. High Energy Phys. 2013 (11) (2013) 135, arXiv:1308.5410.
[12] A. Golovnev, On the recently proposed mimetic dark matter, Phys. Lett. B 728 (2014) 39–40, arXiv:1310.2790.
[13] A.O. Barvinsky, Dark matter as a ghost free conformal extension of Einstein theory, J. Cosmol. Astropart. Phys. 1401 (2014) 014, arXiv:1311.3111.
[14] A. Ganz, P. Karmakar, S. Matarrese, D. Sorokin, Hamiltonian analysis of mimetic scalar gravity revisited, Phys. Rev. D 99 (6) (2019) 064009, arXiv:1812.02667.
[15] A.H. Chamseddine, V. Mukhanov, A. Vikman, Cosmology with mimetic matter, J. Cosmol. Astropart. Phys. 2014 (06) (2014) 017, arXiv:1403.3961.
[16] F. Arroja, N. Bartolo, P. Karmakar, S. Matarrese, The two faces of mimetic Horndeski gravity: disformal transformations and Lagrange multiplier, J. Cosmol. Astropart. Phys. 2015 (09) (2015) 051, arXiv:1506.08575.
[17] F. Arroja, N. Bartolo, P. Karmakar, S. Matarrese, Cosmological perturbations in mimetic Horndeski gravity, J. Cosmol. Astropart. Phys. 2016 (04) (2016) 042, arXiv:1512.09374.
[18] F. Arroja, T. Okumura, N. Bartolo, P. Karmakar, S. Matarrese, Large-scale structure in mimetic Horndeski gravity, J. Cosmol. Astropart. Phys. 2018 (05) (2018) 050, arXiv:1708.01850.
[19] A. Ganz, N. Bartolo, P. Karmakar, S. Matarrese, Gravity in mimetic scalar-tensor theories after GW170817, J. Cosmol. Astropart. Phys. 1901 (01) (2019) 056, arXiv:1809.03496.
[20] L. Sebastiani, S. Vagnozzi, R. Myrzakulov, Mimetic gravity: a review of recent developments and applications to cosmology and astrophysics, Adv. High Energy Phys. 2017 (2017) 3156915, arXiv:1612.08661.
[21] L. Mirzagholi, A. Vikman, Imperfect dark matter, J. Cosmol. Astropart. Phys. 2015 (06) (2015) 028, arXiv:1412.7136.
[22] S. Ramazanov, Initial conditions for imperfect dark matter, J. Cosmol. Astropart. Phys. 2015 (12) (2015) 007, arXiv:1507.00291.
[23] E.A. Lim, I. Sawicki, A. Vikman, Dust of dark energy, J. Cosmol. Astropart. Phys. 2010 (05) (2010) 012, arXiv:1003.5751.
[24] C.-P. Ma, E. Bertschinger, Cosmological perturbation theory in the synchronous and conformal Newtonian gauges, Agron. J. 455 (1995) 7, arXiv:astro-ph/9506072.
[25] J.M. Bardeen, Gauge-invariant cosmological perturbations, Phys. Rev. D 22 (1980) 1882–1905.
[26] J. Lima, J. Cunha, J. Alcaniz, Simplified quartessence cosmology, Astropart. Phys. 31 (3) (2009) 233–236, arXiv:astro-ph/0611007.
[27] H.V. Peiris, E. Komatsu, L. Verde, D.N. Spergel, C.L. Bennett, M. Halpern, G. Hinshaw, N. Jarosik, A. Kogut, M. Limon, S.S. Meyer, L. Page, G.S. Tucker, E. Wollack, E.L. Wright, First-year wilkinson microwave anisotropy probe (WMAP) observations: Implications for inflation, Astrophys. J. Suppl. Ser. 148 (2003) 213–231, arXiv:astro-ph/0302225.
[28] L.E. Padilla, J.A. Vázquez, T. Matos, G. Germán, Scalar field dark matter spectator during inflation: The effect of self-interaction, J. Cosmol. Astropart. Phys. 1905 (05) (2019) 056, arXiv:1901.00947.
[29] The Planck Collaboration, Y. Akrami, et al., Planck 2018 results. X. Constraints on inflation, arXiv:1807.06211.
[30] D. Blas, J. Lesgourgues, T. Tram, The cosmic linear anisotropy solving system (CLASS). Part II: Approximation schemes, J. Cosmol. Astropart. Phys. 2011 (07) (2011) 034, arXiv:1104.2933.
[31] M. Kamionkowski, A. Loeb, Getting around cosmic variance, Phys. Rev. D 56 (1997) 4511–4513, arXiv:astro-ph/9703118.
[32] B. Audren, J. Lesgourgues, S. Bird, M.G. Haehnelt, M. Viel, Neutrino masses and cosmological parameters from a Euclid-like survey: Markov chain Monte Carlo forecasts including theoretical errors, J. Cosmol. Astro-Part. Phys. 2013 (1) (2013) 026, arXiv:1210.2194.
[33] A. Ijjas, J. Ripley, P.J. Steinhardt, NEC violation in mimetic cosmology revisited, Phys. Lett. B 760 (2016) 132–138, arXiv:1604.08586 [gr-qc].
[34] H. Firouzjahi, M.A. Gorji, S.A. Hosseini Mansoori, Instabilities in mimetic matter perturbations, J. Cosmol. Astropart. Phys. 1707 (2017) 031, arXiv:1703.02923 [hep-th].
[35] Y. Zheng, L. Shen, Y. Mou, M. Li, On (in)stabilities of perturbations in mimetic models with higher derivatives, J. Cosmol. Astropart. Phys. 1708 (08) (2017) 040, arXiv:1704.06834 [gr-qc].
[36] S. Hirano, S. Nishi, T. Kobayashi, Healthy imperfect dark matter from effective theory of mimetic cosmological perturbations, J. Cosmol. Astropart. Phys. 1707 (07) (2017) 009, arXiv:1704.06031 [gr-qc].
[37] M.A. Gorji, S.A. Hosseini Mansoori, H. Firouzjahi, Higher derivative mimetic gravity, J. Cosmol. Astropart. Phys. 1801 (01) (2018) 020, arXiv:1709.09988 [astro-ph.CO].

Monthly Notices
of the
ROYAL ASTRONOMICAL SOCIETY

MNRAS **501,** 254–260 (2021)
Advance Access publication 2020 November 25

doi:10.1093/mnras/staa3653

Dwarf galaxies without dark matter: constraints on modified gravity

Ali Rida Khalifeh[1,2] and Raul Jimenez[2,3]★

[1]*Instituto de Ciencias del Cosmos, University of Barcelona, Marti i Franques, 1, E-08028 Barcelona, Spain*
[2]*Departamento de Fisica Cuantica y Astrofisica, University of Barcelona, Marti i Franques 1, E-08028 Barcelona, Spain*
[3]*Institució Catalana de Recerca i Estudis Avançats, Pg. Lluis Companys 23, E-08010 Barcelona, Spain*

Accepted 2020 November 18. Received 2020 November 18; in original form 2020 September 24

ABSTRACT

The discovery of 19 dwarf galaxies without dark matter (DM) provides, counterintuitively, strong support for the ΛCDM standard model of cosmology. Their presence is well accommodated in a scenario where the DM is in the form of cold dark particles. However, it is interesting to explore quantitatively what is needed from modified gravity models to accommodate the presence of these galaxies and what extra degree of freedom is needed in these models. To this end, we derive the dynamics at galaxy scales (Virial theorem) for a general class of modified gravity models. We distinguish between theories that satisfy the Jebsen–Birkhoff theorem, and those that do not. Our aim is to develop tests that can distinguish whether DM is part of the theory of gravity or a particle. The 19 dwarf galaxies discovered provide us with a stringent test for models of modified gravity. Our main finding is that there will always be an extra contribution to the Virial theorem coming from the modification of gravity, even if a certain galaxy shows very small, if not negligible, trace of DM, as has been reported recently. Thus, if these and more galaxies are confirmed as devoid (or negligible) of DM, while other similar galaxies have abundant DM, it seems interesting to find modifications of gravity to describe DM. Our result can be used by future astronomical surveys to put constraints on the parameters of modified gravity models at astrophysical scales where DM is described as such.

Key words: galaxies: dwarf – dark matter – cosmology: theory.

1 INTRODUCTION

The existence of dark matter (DM) has been demonstrated observationally in many occasions. Initially, at astrophysical scales, the virial mass of the Coma galaxy cluster was found by Zwicky (Zwicky 1933; Salucci et al. 2007) to be 500 times larger than the observed one. Later, the flat behaviour of stars' velocity curves in the outskirts of spiral galaxies was also another proof of the existence of additional unobserved matter (Persic, Salucci & Stel 1996; Sofue et al. 1999; Sofue & Rubin 2001). Moreover, from the cosmic microwave background structure at cosmological scales, there is a clear evidence for DM (Bennett et al. 2003; Komatsu et al. 2009); see Bertone & Hooper (2018) and Freese (2009) and references within for a detailed overview of DM. However, the nature of this unobserved entity is still an open question and an active field of research. In the context of the general theory of relativity (GR), this phenomenon is described by adding cold particles, that is pressurless non-relativistic ones, to the energy content of the universe. To describe the theory, given a metric of space–time $g_{\mu\nu}$, one would write an action of the form:

$$S = \int d^4x\sqrt{-g}\left[\frac{M_p^2}{2}R(g_{\mu\nu}) + \mathcal{L}_{m,r}(g_{\mu\nu},\psi_m,\psi_r) + \mathcal{L}_{\rm DM}\right], \quad (1)$$

where g is the determinant of $g_{\mu\nu}$, R is the Ricci scalar, the trace of the Ricci tensor $R_{\mu\nu}$, $M_p^2 = (8\pi G)^{-1}$ is the reduced Planck mass (in units for which the reduced Planck constant $\hbar$ and the speed of light c are 1), $\mathcal{L}_{m,r}$ is the Lagrangian density of matter and radiation, given as a function of the metric and the corresponding fields, ψ_m, ψ_r, and finally $\mathcal{L}_{\rm DM}$ is the Lagrangian density of DM particles. By setting the variation of (1) with respect to the metric to 0, we get the Einstein equations of motion:

$$\frac{1}{\sqrt{-g}}\frac{\delta S}{\delta g^{\mu\nu}} = 0 \Rightarrow R_{\mu\nu} - \frac{1}{2}g_{\mu\nu}R = \frac{1}{M_p^2}(T_{\mu\nu} + T_{\mu\nu}^{\rm DM}), \quad (2)$$

where $T_{\mu\nu}$ is the stress energy tensor of the baryonic and leptonic matter, as well as radiation, whereas $T_{\mu\nu}^{\rm DM}$ is that of the DM particles. From here, one can see how the gravitational phenomena observed (LHS of the above equation) is affected by the presence of DM particles (RHS). The particle nature proposal for DM has presented many candidates beyond the Standard Model of particle physics. These include sterile neutrinos (Dodelson & Widrow 1994), axions (Duffy & van Bibber 2009; Visinelli & Gondolo 2009), and WIMPs (weakly interacting massive particles), which include the lightest supersymmetric stable particle, the neutralino. For a detailed review on the different particle candidates for DM, see Silk et al. (2010) and Profumo, Giani & Piattella (2019).

Another explanation for these phenomena is to consider a theory of gravity other than GR, which is known as modified gravity theory (MGT). In this context, the gravitational laws of nature have specific geometrical properties that could result in the observed phenomena caused by DM, without the need for adding extra species to the particle content of the universe. For instance, one of the proposed MGTs is called $f(R)$ gravity, where $f(R)$ stands for an arbitrary (in the appropriate units) function of the Ricci scalar R. In this MGT, one

★ E-mail: raul.jimenez@gmail.com

generalizes the Einstein–Hilbert action to

$$S_{f(R)} = \int d^4x\sqrt{-g}\left[\frac{M_p^2}{2}f(R) + \mathcal{L}_{m,r}\right]. \quad (3)$$

The resulting Einstein equations would take the form:

$$R_{\mu\nu} - \frac{1}{2}g_{\mu\nu}R = \frac{1}{M_{P_{\rm eff}}^2}(T_{\mu\nu} + \tilde{T}_{\mu\nu}), \quad (4)$$

where the effective Planck mass is

$$M_{P_{\rm eff}}^2 = M_p^2 f'(R) \quad (5)$$

and $'$ denotes the derivative of a function with respect to its argument. The additional term on the RHS,

$$\tilde{T}_{\mu\nu} = M_P^2\left[\frac{f(R) - Rf'(R)}{2}g_{\mu\nu} + \nabla_\mu\nabla_\nu f'(R) - g_{\mu\nu}\Box f'(R)\right] \quad (6)$$

can now generate the gravitational phenomena observed associated with DM, but this term is not related to some type of particle, rather to gravity itself. In this way, one can provide an alternative explanation to the existence of DM. Another MGT that has been recently proposed is called mimetic dark matter (MDM; Chamseddine & Mukhanov 2013; Barvinsky 2014; Golovnev 2014). The original proposal of this work was to rewrite the physical metric in terms of an auxiliary one and the derivative of a scalar field. The resulting equation of motion will resemble (4) with a different $\tilde{T}_{\mu\nu}$ and $M_{P_{\rm eff}}^2$, but can describe the gravitational effects of DM. The model was further developed to incorporate other cosmological phenomena (Chamseddine, Mukhanov & Vikman 2014), as well as to avoid problems related to defining quantum fluctuations, adiabatic initial conditions, and cosmological singularities (Mirzagholi & Vikman 2015; Ramazanov 2015; Chamseddine & Mukhanov 2017). For further analysis and study of the model, see Ganz et al. (2019a, b), Arroja et al. (2015, 2016, 2018), Khalifeh (2015), and Khalifeh et al. (2020). More recently, the model has been developed to avoid the original singularity of the universe by having a running gravitational constant (Chamseddine, Mukhanov & Russ 2019). For more reviews on MGTs, see Clifton et al. (2012) and Nojiri, Odintsov & Oikonomou (2017).

The main purpose of this letter is to study the DM phenomena at astrophysical scales using the MGT approach. More specifically, we derive the virial theorem for a general class of MGTs, including the Horndeski model (Horndeski 1974; Kobayashi 2019), and see where the observed additional virial mass comes from. We distinguish, however, our derivation for theories that satisfy the Jebsen–Birkhoff theorem (JBT; Birkhoff & Langer 1923; Jebsen 1921) and those that do not, for reasons that will be explained below. We notice here that the additional virial mass term will exist irrespective of the system under consideration. Therefore, if one wants to associate $\tilde{T}_{\mu\nu}$ with DM, one would be claiming that their effects exist everywhere, by the universality of gravitational interactions. However, one might wonder what if there is a system in which there is no traceable amount of DM, as has been recently observed (Danieli et al. 2020a, b; Guo et al. 2020; Mancera et al. 2019; van Dokkum et al. 2019). Even though these results are still being further analysed, we use the possibility of having systems with no traceable amount of DM to put constraints on the parameters of MGTs in general.

2 VIRIAL THEOREM IN MGT

In this section, we derive the virial theorem for a class of MGTs that generate equations of motion with the form given in (4) within the 3 + 1 formalism of GR (Arnowitt, Deser & Misner 2008). A vital element in this derivation is the assumption of asymptotic flatness and stationarity (explained below in more detail), which is valid only if the MGT satisfies the JBT, such as in Brane cosmology or Palatini $f(R)$ gravity (see Dai, Maor & Starkman 2008; Faraoni 2010; Sotiriou & Faraoni 2010; Clifton et al. 2012, and references therein for more details on theories that do and do not satisfy the JBT). Therefore, the treatment in Section 2.1 will be applicable mainly to the former case, while a slight deviation from that will be presented in Section 2.2 for theories that violate the JBT. An alternative derivation of the virial theorem, using the Lagrangian formalism, will be briefly present in Appendix A. This method is applicable to both types of theories described here, for the virial theorem relies on the collisionless Boltzmann equation, and therefore it is a consequence of stress energy conservation. This means it should be applicable to any metric theory of gravity (Schmidt 2010).

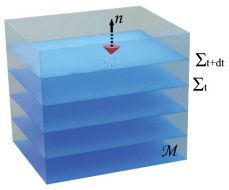

Figure 1. Illustration of foliating a manifold $\mathcal{M}$ with a set of hypersurfaces Σ_t in the 3 + 1 formalism of GR.

2.1 Theories satisfying the JBT

2.1.1 Formalism

Consider a stationary and asymptotically flat space–time[1] $\mathcal{M}$ with a metric g, and consider foliating $\mathcal{M}$ with a set of space-like hypersurfaces Σ_t, as illustrated in Fig. 1. Moreover, let n be a time-like 4-vector field, orthonormal to the Σ_ts and directed along increasing time t:

$$n_\alpha = -Nt_{,\alpha} \Rightarrow n_\alpha n^\alpha = -1, \quad (7)$$

where $_{,\alpha}$ means $\partial/\partial x^\alpha$, and N is the strictly positive lapse function. The latter measures the rate of flow of proper time τ with respect to coordinate time as one moves normally from one Σ_t to the next along n. Let

$$h_{\alpha\beta} = g_{\alpha\beta} + n_\alpha n_\beta \quad (8)$$

be the projection tensor orthogonally on to Σ_t and, when restricted to Σ_t, defines the positive definite induced 3-metric by g on Σ_t. Furthermore, define the shift vector N^α as the measure of how much the spatial coordinates shift as they move from one Σ_t to the next along n:

$$N^\alpha = -h^\alpha_{\ \beta}\xi^\beta, \quad (9)$$

[1]Mathematically, stationarity means that there exists a time-like Killing vector, at least at spatial infinity, that can be normalized to −1. Asymptotically flat, on the other hand, means two things: First, the Σ_ts contain a compact region P, such that $\Sigma_t - P$ is diffeomorphic to $\Re^3 - \{0\}$, where $\Re^3$ is the three-dimensional real space. Second, one can establish on each Σ_t a coordinate system in a way that the components of the metric differ from those of the Minkowski one by $\mathcal{O}(1/r)$ as $r \to \infty$, where r is the radial distance.

where $\xi^\alpha = (\partial/\partial t)^\alpha$ is the Killing vector associated with the stationarity of $\mathcal{M}$(see footnote 1). From these definitions, one can write the explicit components of n and N as

$$\begin{aligned} n_\alpha &= (-N, 0, 0, 0); \\ n^\alpha &= (1/N, N^1/N, N^2/N, N^3/N); \\ N^\alpha &= (0, N^1, N^2, N^3) \end{aligned} \tag{10}$$

and the metric components would be

$$g_{\mu\nu}\mathrm{d}x^\mu \mathrm{d}x^\nu = -(N^2 - N_i N^i)\mathrm{d}t^2 - 2N_i \mathrm{d}t\mathrm{d}x^i + h_{ij}\mathrm{d}x^i\mathrm{d}x^j. \tag{11}$$

The starting point in deriving the virial theorem is to contract the Einstein equation (4) with $h^{\mu\nu}$:

$$R_{\mu\nu}n^\mu n^\nu - \frac{1}{2}R = \frac{1}{M^2_{P\mathrm{eff}}}\left[S_\mu{}^\mu - \tilde{S}_\mu{}^\mu\right], \tag{12}$$

where

$$S_\mu{}^\mu\left(\tilde{S}_\mu{}^\mu\right) = h^{\mu\nu}T_{\mu\nu}(\tilde{T}_{\mu\nu}). \tag{13}$$

We can now use the Gauss–Codazzi–Mainardi equations, which relate the Ricci tensor of the 4-metric to that of the 3-metric $h_{\mu\nu}$, ${}^3R_{\mu\nu}$, the lapse function N, and the extrinsic curvature of Σ_t, $K_{\mu\nu}$ (see Gourgoulhon & Bonazzola 1993 for more details). The final result would be

$$\begin{aligned} &\nu^{|i}{}_{|i} - \frac{1}{4}{}^3R + \nu^{|i}\nu_{|i} - \frac{3}{4}(K_{ij}K^{ij} - K^2) + (Kn^\alpha)_{;\alpha} \\ &\quad = \frac{1}{2M^2_{P\mathrm{eff}}}\left[S_i{}^i - \tilde{S}_i{}^i\right], \end{aligned} \tag{14}$$

where '$_{|i}$' denotes the covariant derivative with respect to x^i associated with the 3-metric h, '$_{;\alpha}$' is the covariant derivative with respect to x^α associated with the 4-metric g, $\nu = \ln N$, and $K = -n^\alpha{}_{;\alpha}$ is the trace of $K_{\mu\nu}$. Now that we have done the first step, we can proceed to the second one, which is to integrate this result over space.

2.1.2 *Step 2: integration over space*

Integrating (14) over the space-like hypersurface Σ_t, and reshuffling some terms, gives

$$\begin{aligned} &\int_{\Sigma_t}\left[\frac{1}{2M^2_{P\mathrm{eff}}}\left(S_i{}^i - \tilde{S}_i{}^i\right) - \nu_{|i}\nu^{|i} + \frac{3}{4}\left(K_{ij}K^{ij} - K^2\right)\right]\sqrt{h}d^3x \\ &\quad = \int_{\Sigma_t}\left[(Kn^\alpha)_{;\alpha} + \nu^{|i}{}_{|i} - \frac{1}{4}{}^3R\right]\sqrt{h}d^3x. \end{aligned} \tag{15}$$

The first term inside the integral on the RHS of (16) is

$$(Kn^\alpha)_{;\alpha} = N^{-1}(KN^i)_{|i} = N^{-1}KN^i\nu_{|i} + (KN^i/N)_{|i} \tag{16}$$

where the first equality follows from equation (2.5) of Gourgoulhon & Bonazzola (1993). Therefore,

$$\begin{aligned} \int_{\Sigma_t}(Kn^\alpha)_{;\alpha}\sqrt{h}d^3x &= \int_{\Sigma_t}\frac{K}{N}N^i\nu_{|i}\sqrt{h}d^3x + \lim_{S\to\infty}\oint_S\frac{K}{N}N^i dS_i \\ &= \int_{\Sigma_t}\frac{K}{N}N^i\nu_{|i}\sqrt{h}\mathrm{d}^3x, \end{aligned} \tag{17}$$

where the integral over the 2-surface S, which is diffeomorphic to a 2-sphere, goes to 0 as the radius tends to ∞ (hence the meaning of the limit). Furthermore, the second integral of (16) is also a surface one, and in the limit considered, it is the total mass energy in Σ_t (Komar 1959; see appendix of Gourgoulhon & Bonazzola 1994 for proof):

$$\int_{\Sigma_t}\nu^{|i}{}_{|i}\sqrt{h}d^3x = \lim_{S\to\infty}\oint_S\nu^{|i}\mathrm{d}S_i = 4\pi M_{\Sigma_t}. \tag{18}$$

The final term on the RHS of (16),

$$\int_{\Sigma_t}{}^3R\sqrt{h}d^3x \tag{19}$$

needs to be considered carefully. The 3-Ricci scalar can be written as (Lifshitz & Landau 1980):

$${}^3R = -\frac{1}{\sqrt{h}}\frac{\partial}{\partial x^i}\left[\frac{1}{\sqrt{h}}\frac{\partial}{\partial x^j}(hh^{ij})\right] + h^{ij}\left[\Gamma^l{}_{im}\Gamma^m{}_{jl} - \Gamma^l{}_{lm}\Gamma^m{}_{ij}\right], \tag{20}$$

where $\Gamma^i{}_{jk}$ are the Christoffel symbols associated with h. The problem is that this is not a covariant form, and its convergence into a finite value depends on the coordinate system used, as one can check by comparing (19) in spherical coordinates to its form in Cartesian ones. But all the other terms of (16) are indeed finite. This means that (19) must also be finite. The solution to this dilemma is to express the Ricci scalar in a form valid in any coordinate system and corresponding to the sum of a convergent surface integral and a volume integral. The latter should be written in terms quadratic in the derivative of the metric, containing only its curvature part, and not the coordinate part like the Γs do. The key point in doing so is by introducing a flat background metric $\tilde{h}$, on to Σ_t along with h. The asymptotic flatness hypothesis insures that both metrics match at infinity, and then we can write ${}^3R$ in a way covariant with respect to $\tilde{h}$. In particular, the Christoffel terms of (19) will be replaced by a quadratic term covariant with respect to $\tilde{h}$, tending to 0 in the flat-space case. This procedure is known as the bimetric formalism (Cornish 1964; Nahmad-Achar & Schutz 1987; Katz & Ori 1990). The final form of (19) is[2]

$$\begin{aligned} \int_{\Sigma_t}{}^3R\sqrt{h}d^3x &= 16\pi M_{\Sigma_t} \\ &\quad + \int_{\Sigma_t}h^{ij}\left[\Delta^l{}_{im}\Delta^m{}_{jl} - \Delta^l{}_{lm}\Delta^m{}_{ij}\right]\sqrt{h}d^3x, \end{aligned} \tag{21}$$

where

$$\Delta^i{}_{jk} \equiv \frac{1}{2}h^{il}\left[h_{lk||j} + h_{ji||k} - h_{jk||l}\right] \tag{22}$$

is a covariant tensor on Σ_t, and $_{||j}$ denotes covariant derivative with respect to x^j corresponding to the 3-metric $\tilde{h}$.

Ultimately, the final form of the Virial theorem in an MGT satisfying the JBT:

$$\begin{aligned} &\int_{\Sigma_t}\left[\frac{1}{2M^2_{P\mathrm{eff}}}\left(S_i{}^i - \tilde{S}_i{}^i\right) - \nu_{|i}\nu^{|i}\right. \\ &\quad \left. + \frac{1}{4}h^{ij}\left(\Delta^l{}_{im}\Delta^m{}_{jl} - \Delta^l{}_{lm}\Delta^m{}_{ij}\right)\right]\sqrt{h}d^3x \\ &\quad + \int_{\Sigma_t}\left[\frac{3}{4}\left(K_{ij}K^{ij} - K^2\right) - \frac{K}{N}N^i\nu_{|i}\right]\sqrt{h}d^3x = 0. \end{aligned} \tag{23}$$

To see how this result corresponds to the known Newtonian form of the virial theorem, consider dust particles with a stress energy tensor of the form

$$T^{\alpha\beta} = \rho u^\alpha u^\beta, \tag{24}$$

where ρ is the energy density of the system and u^α is its 4-velocity vector. This means that

$$S_i{}^i = \gamma^2\rho u_i u^i, \tag{25}$$

[2]Note that M_{Σ_t} in (21) should be the total ADM mass energy, but because the two masses are equal in the stationary and asymptotically flat case, we skipped introducing it explicitly in the text.

where $\gamma = -n_\alpha u^\alpha$ is the Lorentz factor between the observer and the dust particles, and u^i is the velocity vector measured by the observer. In the Newtonian limit, one can choose a coordinate system in which the metric becomes

$$ds^2 = -(1+2\nu)dt^2 + (1-2\nu)\tilde{h}_{ij}dx^i dx^j. \tag{26}$$

Therefore, from (11) and the definition of $K_{\alpha\beta}$ (Gourgoulhon & Bonazzola 1993), one can show that $K_{ij} = K = 0$. Moreover, the $\Delta\Delta$ term of the integrand becomes $1/2\nu_{||i}\nu^{||i}$, so the net result is

$$2T + \Omega - \tilde{\Omega} = 0, \tag{27}$$

where the total kinetic energy is

$$T \equiv \frac{1}{2}\int_{\Sigma_t} \rho u^2 dV \tag{28}$$

with $u^2 = u^i u_i$ and $dV = \sqrt{\tilde{h}}d^3x$. Furthermore, the gravitational potential energy due to the dust particles is

$$\Omega \equiv -\int_{\Sigma_t} \frac{1}{M^2_{p_{\rm eff}}}(\nabla\nu)^2 dV, \tag{29}$$

where we put $M^2_{p_{\rm eff}}$ inside the integral because, depending on the MGT under consideration, this term can depend on space. Finally, the additional contribution to the theorem due to the MGT is

$$\tilde{\Omega} \equiv \int_{\Sigma_t} \tilde{h}^{ij}\tilde{T}_{ij} dV. \tag{30}$$

It is clear that the latter is always present, even if one considers the systems analysed in Danieli et al. (2020a, b), Guo et al. (2020), Mancera et al. (2019), and van Dokkum et al. (2019). By considering these galaxies in (27), one can then put constrains on the parameters of the MGT considered to make (30) vanishingly small.

2.2 Theories violating the JBT

Now we consider theories, such as the Dvali–Gabadaze–Porati model (Dvali, Gabadadze & Porrati 2000), which do not satisfy the JBT. Even in these theories, the equations of motion can be written in the from (4), and hence we start our analysis from equation (16).

First of all, the surface term in (18) will not go to zero, because we are no longer assuming asymptotic flatness. Furthermore, concerning the bimetric formalism trick used previously to write a covariant expression for (19), we can still use the same analysis. However, now the metric introduced $\tilde{h}$ on to the Σ_ts in no longer flat everywhere, rather it should match the form of h at infinity (which is not flat for the type of theories considered here), but remain flat where the dynamics is taking place. This is a mathematical trick to guarantee that (19) is written in a covariant way, and should not affect the physical result, specially when we take the Newtonian limit, as we will see shortly (see Cornish 1964; Nahmad-Achar & Schutz 1987; Katz & Ori 1990 for more details). Finally, since the mass term (18), which is known as the Komar mass (Komar 1959), does not cancel the ADM one appearing in (21), the final result of the generalized virial theorem (24) will have three additional terms on its RHS:

$$\lim_{S\to\infty}\oint_S \frac{K}{N}N^i dS_i + 4\pi(M_K - M_{\rm ADM}), \tag{31}$$

where M_K and $M_{\rm ADM}$ are the Komar and ADM masses, respectively.

From here, since we are interested in studying the dynamics of galaxies and galactic clusters, we need to take the Newtonian limit, as given by the metric (26). In this limit, it was shown in Abramowicz, Lasota & Muchotrzeb (1976) that the two mass terms in (31) do indeed match, and therefore cancel. Furthermore, the surface term cancels by definition from the form of the metric in this limit. Therefore, even for the case of theories that violate the JBT, in the Newtonian limit, the virial theorem takes the form (27), but away from that limit it has (31) as additional terms. It should be stressed that if an MGT does not produce the virial theorem at galactic scales, then such a theory fails in producing one of the observational proofs of the existence of DM, and therefore cannot be considered as a candidate for the latter in the first place.[3] Moreover, the unlikeliness of MGTs violating the JBT to be DM candidates has been studied previously (see Dai et al. 2008).

3 OBSERVATIONAL CONSTRAINTS

In this section, we link the quantities obtained in the generalized virial theorem (27) to those that could be observed, such as in Danieli et al. (2020a, b), van Dokkum et al. (2019), Guo et al. (2020), and Mancera et al. (2019). To this end, we can define masses and densities associated with the quantities Ω and $\tilde{\Omega}$, as written in (A19) and (A21). Note that the effect of MGT on $M_{p_{\rm eff}}$ has been absorbed into the masses. One can also define radii associated with the these two quantities:

$$R_V = -G\frac{M^2}{\Omega}, \quad R_M = \frac{G\tilde{M}^2}{\tilde{\Omega}}, \tag{32}$$

where R_V is the virial radius and R_M is the radius in which the MGT takes effect. According to Jackson (1970), the virial mass is defined as

$$2T = \frac{GM_V^2}{R_V}, \tag{33}$$

which, when inserted in (27), with the use of (32), gives the following relation between the virial, baryonic, and MGT masses:

$$\frac{M_V^2}{M^2} = 1 + \frac{\tilde{M}^2 R_V}{M^2 R_M} \tag{34}$$

and therefore one way of constraining the ratio $\tilde{M}^2/R_M$, i.e. a constrain on $\tilde{\Omega}$, is by measuring M, M_V, and R_V and using (34). In Table 1, we present the constraint on the ratio $\tilde{\Omega}/\Omega$ given by the measurements presented in Guo et al. (2020). This ratio is calculated using equations (32) inserted in (34). As we can see in Table 1 and Fig. 2, $\tilde{\Omega}$ is an appreciable multiple of Ω, when in fact, for these DM devoid galaxies, it should be negligible. This shows that, unless another mechanism is introduced specially for these galaxies to remove $\tilde{\Omega}$, it is very difficult for MGTs to account for these galaxies and for other DM rich ones that are similar in properties, such as AGC 8915, for instance (Guo et al. 2020).

In addition to that, another observable parameter that can be used is the velocity dispersion, σ, related to the virial mass and radius by (Munari et al. 2013; Owers et al. 2017)

$$M_V = \frac{3\sigma^2 R_V}{G}. \tag{35}$$

This can be used with (34) to put another constraint on a given MGT. Indeed, we can write (34) as

$$\frac{\sigma_g^4}{\sigma_{\rm int}^4} = 1 + \frac{\tilde{M}^2 R_V}{M^2 R_M}, \tag{36}$$

where $\sigma_{\rm int}$ and σ_g are the intrinsic and globular cluster's velocity dispersions, respectively. For instance, if we use the results of van

[3]But such a theory might still be a viable candidate for DE.

Table 1. Data from Guo et al. (2020). The second and third columns are the logarithm of the baryonic and virial masses, respectively. The ratio $|\tilde{\Omega}/\Omega|$ shows no obvious correlation or trend with the masses, which indicates modified gravity theories may need extra fine tuning as R will need to be adjusted on an object by object basis.

Galaxy name	$\log(M_b/M_\odot)$	$\log(M_V/M_\odot)$	$R = \lvert\tilde{\Omega}/\Omega\rvert$
AGC 6438	9.444	10.231	36.497
AGC 6980	9.592	9.876	2.698
AGC 7817	9.061	10.599	1190.242
AGC 7920	8.981	10.653	2207.005
AGC 7983	9.046	9.515	7.700
AGC 9500	9.092	9.712	16.378
AGC 191707	9.080	9.567	8.419
AGC 205215	9.706	9.984	2.597
AGC 213086	9.8	10.149	4.000
AGC 220901	8.864	9.363	8.954
AGC 241266	9.547	9.96	5.699
AGC 242440	9.467	10.098	17.281
AGC 258421	10.124	10.387	2.373
AGC 321435	9.204	9.593	4.998
AGC 331776	8.503	8.904	5.339
AGC 733302	9.042	9.489	6.834
AGC 749244	9.778	10.003	1.818
AGC 749445	9.264	9.708	6.727
AGC 749457	9.445	9.759	3.246

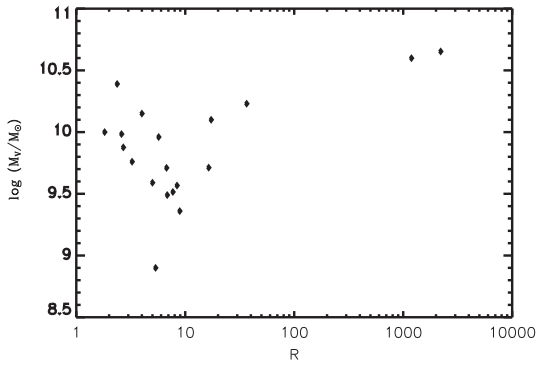

Figure 2. Virial mass as a function of R. There is no obvious correlation or trend with the masses, which indicates modified gravity theories may need extra fine tuning as R will need to be adjusted on an object by object basis.

Dokkum et al. (2019), where the velocity dispersion of DM devoid galaxy NGC 1052-DF2 has been measured, we find

$$\frac{\tilde{M}^2}{R_M} \approx 3\frac{M^2}{R_V} \Rightarrow \tilde{\Omega} \approx 3\Omega. \tag{37}$$

In other words, if DM is described by an MGT, the latter should produce a gravitational potential approximately 3 times that of baryonic matter for NGC 1052-DF2, where in reality it should not be present.

A third method to check the consequences of MGTs on DM devoid galaxies is by writing the mass in a radius r of a system as

$$M(r) = 4\pi \int_0^r (\rho_B + \tilde{\rho})r'^2 \mathrm{d}r' = M_B + \tilde{M}, \tag{38}$$

where ρ_B and M_B are the density and mass of baryonic matter, respectively, while, $\tilde{\rho}$ and $\tilde{M}$ are those of MGT. By measuring $M(r)$ and M_B one can therefore determine the amount of DM available as an MGT. Note that this is independent of whether a system is virialzed or not. For example, in Danieli et al. (2020b) the dynamical mass and that of the stars within the half-light radius for the ultradiffuse galaxy NGC 1052-DF2 have been measured to be very similar. This puts dire constraint on MGTs, which highlights the importance of such DM devoid galaxies in constraining these theories.

4 CONCLUSIONS

We have computed the virial theorem for MGTs that satisfy the JBT, as well as those that do not. Motivated by the recent discovery of a class of dwarf galaxies with no significant DM, we wanted to quantify what constraints these objects put on MGTs. In the same vein that the number of satellite dark matter haloes imposes severe constraints on the nature of particle DM, we have found an equivalent observable for the case when DM is a modification of gravity. Inspection of (24) and (27) shows that the virial theorem for MGT contains an extra term $\tilde{S}_i^i$ or $\tilde{\Omega}$. The existence of this term can be constrained by the DM devoid galaxies considered here. For instance, it was shown in Capozziello et al. (2013) that this extra mass term is proportional to the baryonic mass present in the system. If one then applies this model to the galaxies at hand, as is presented in Table 1, it would be difficult to see how the model matches the observations without fine tuning. On the other hand, trying to accommodate this term for MGT models will provide interesting insights into the nature of these models. If DM can indeed be part of the theory of gravity, one can think of two possibilities that $\tilde{S}_i^i$ can have in order to achieve that. The first is that $\tilde{S}_i{}^i$ should include specific coupling terms dependent on the environment and baryonic content of the considered galaxies in Danieli et al. (2020a, b), van Dokkum et al. (2019), Guo et al. (2020), and Mancera et al. (2019) such that they cancel the terms that generate DM effects in other galaxies. That is, the matter content and configuration of these galaxies should couple to gravity in a special way in order to make sure there's no DM effect. But this puts the universality of gravitational interactions into question. So another way is to look at a map of the sky for DM distribution, and have $\tilde{S}_i{}^i$ be the function that goes to 0 at the special positions where these galaxies are found, while it is not 0 in other locations. However, the difficulty arises from the fact that most dwarf galaxies do have DM, in fact are DM dominated, which makes the above suggested solution highly fine tuned. On the other hand, if DM was some type of particles, then accommodating its absence in these galaxies would be less fine tuned, by using, for instance, hydrodynamical events associated with galaxy formation. It will be interesting to see if non-fine-tuned MGT can be constructed to fulfill the existence of DM-free galaxies (Danieli et al. 2020a, b; van Dokkum et al. 2019).

ACKNOWLEDGEMENTS

We would like to thank Nicola Bellomo for interesting and fruitful discussions. We also thank the anonymous referee for a very positive and useful report. Funding for this work was partially provided by the Ministerio Ciencia under project PGC2018-098866-B-I00.

DATA AVAILABILITY

The data underlying this article are available in the article and references therein.

REFERENCES

Abramowicz M., Lasota J., Muchotrzeb B., 1976, Commun. Math. Phys., 47, 109

Arnowitt R., Deser S., Misner C. W., 2008, Gen. Relativ. Gravit., 40, 1997
Arroja F., Bartolo N., Karmakar P., Matarrese S., 2015, J. Cosmol. Astropart. Phys., 2015, 051
Arroja F., Bartolo N., Karmakar P., Matarrese S., 2016, J. Cosmol. Astropart. Phys., 2016, 042
Arroja F., Okumura T., Bartolo N., Karmakar P., Matarrese S., 2018, J. Cosmol. Astropart. Phys., 2018, 050
Barvinsky A. O., 2014, J. Cosmol. Astropart. Phys., 1401, 014
Bennett C. L. et al., 2003, ApJS, 148, 1
Bertone G., Hooper D., 2018, Rev. Mod. Phys., 90, 045002
Bildhauer S., 1989, Class. Quantum Gravity, 6, 1171
Birkhoff G. D., Langer R. E., 1923, Relativity and Modern Physics, Harvard Univ. Press, Cambridge MA, USA
Boehmer C. G., Harko T., Lobo F. S. N., 2008, J. Cosmol. Astropart. Phys., 0803, 024
Capozziello S., Harko T., Koivisto T. S., Lobo F. S., Olmo G. J., 2013, J. Cosmol. Astropart. Phys., 2013, 024
Chamseddine A. H., Mukhanov V., 2013, J. High Energy Phys., 2013, 135
Chamseddine A. H., Mukhanov V., 2017, J. Cosmol. Astropart. Phys., 1703, 009
Chamseddine A. H., Mukhanov V., Vikman A., 2014, J. Cosmol. Astropart. Phys., 2014, 017
Chamseddine A. H., Mukhanov V., Russ T. B., 2019, Eur. Phys. J., C79, 558
Clifton T., Ferreira P. G., Padilla A., Skordis C., 2012, Phys. Rep., 513, 1
Cornish F., 1964, Proc. R. Soc. A, 282, 358
Dai D.-C., Maor I., Starkman G., 2008, Phys. Rev. D, 77, 064016
Danieli S., van Dokkum P., Abraham R., Conroy C., Dolphin A. E., Romanowsky A. J., 2020a, ApJL, 895, 8
Danieli S., van Dokkum P., Conroy C., Abraham R., Romanowsky A. J., 2020b, ApJ, 874, L12
Dodelson S., Widrow L. M., 1994, Phys. Rev. Lett., 72, 17
Duffy L. D., van Bibber K., 2009, New J. Phys., 11, 105008
Dvali G. R., Gabadadze G., Porrati M., 2000, Phys. Lett., B485, 208
Faraoni V., 2010, Phys. Rev., D81, 044002
Freese K., 2009, EAS Publ. Ser. Vol. 36, Dark Matter and Dark Energy, Lyon, France. p. 113
Ganz A., Bartolo N., Karmakar P., Matarrese S., 2019a, JCAP, 56
Ganz A., Karmakar P., Matarrese S., Sorokin D., 2019b, Phys. Rev., D99, 064009
Golovnev A., 2014, Phys. Lett., B728, 39
Gourgoulhon E., Bonazzola S., 1993, Phys. Rev. D, 48, 2635
Gourgoulhon E., Bonazzola S., 1994, Class. Quantum Gravity, 11, 443
Guo Q. et al., 2020, Nature Astronomy, 4, 246
Horndeski G. W., 1974, Int. J. Theor. Phys., 10, 363
Jebsen J. T., 1921, Astronomy, 15, 1
Jackson J. C., 1970, MNRAS, 148, 249
Katz J., Ori A., 1990, Class. Quantum Gravity, 7, 787
Khalifeh A. R., 2015preprint (arXiv:1506.06250)
Khalifeh A. R., Bellomo N., Bernal J. L., Jimenez R., 2020, Physics of the Dark Universe, 30
Kobayashi T., 2019, Rep. Prog. Phys., 82, 086901
Komar A., 1959, Phys. Rev., 113, 934
Komatsu E. et al., 2009, ApJS, 180, 330
Lifshitz E., Landau L., 1980, Course of Theoretical Physics Series, Oxford: Pergamon Press, Vol. 2
Maartens R., Maharaj S. D., 1985, J. Math. Phys., 26, 2869
Mancera P. P. E. et al., 2019, ApJ, 883, L33
Mirzagholi L., Vikman A., 2015, J. Cosmol. Astropart. Phys., 1506, 028
Munari E., Biviano A., Borgani S., Murante G., Fabjan D., 2013, MNRAS, 430, 2638
Nahmad-Achar E., Schutz B. F., 1987, Gen. Relativ. Gravit., 19, 655
Nojiri S., Odintsov S. D., Oikonomou V. K., 2017, Phys. Rep., 692, 1
Owers M. S. et al., 2017, MNRAS, 468, 1824
Persic M., Salucci P., Stel F., 1996, MNRAS, 281, 27
Profumo S., Giani L., Piattella O. F., 2019, Universe, 5, 213
Ramazanov S., 2015, J. Cosmol. Astropart. Phys., 1512, 007
Salucci P., Lapi A., Tonini C., Gentile G., Yegorova I., Klein U., 2007, MNRAS, 378, 41
Schmidt F., 2010, Phys. Rev., D81, 103002
Silk J. et al., 2010, Particle Dark Matter: Observations, Models and Searches. Cambridge Univ. Press, Cambridge
Sofue Y., Rubin V., 2001, ARA&A, 39, 137
Sofue Y., Tutui Y., Honma M., Tomita A., Takamiya T., Koda J., Takeda Y., 1999, ApJ, 523, 136
Sotiriou T. P., Faraoni V., 2010, Rev. Mod. Phys., 82, 451
van Dokkum P., Danieli S., Abraham R., Conroy C., Romanowsky A. J., 2019, ApJ, 874, L5
Visinelli L., Gondolo P., 2009, Phys. Rev., D80, 035024
Zwicky F., 1933, Helv. Phys. Acta, 6, 110

APPENDIX A: ALTERNATIVE DERIVATION OF THE VIRIAL THEOREM

We present here another method for deriving the virial theorem (27), using the Lagrangian formalism and the relativistic Boltzmann equation. The method presented here should be applicable to any metric gravity theory, since it follows from energy–momentum conservation. Therefore, it applies to theories that violate the JBT as well. First, consider the equations of motion (4) and the metric in spherical coordinates:

$$ds^2 = -e^{2\nu(r)}dt^2 + e^{-2\nu(r)}dr^2 + r^2(d\theta^2 + \sin\theta^2 d\phi^2) \tag{A1}$$

(at the moment no approximations are being made. When we apply the Newtonian approximation, this metric reduces to 26). The $0-0$, $r-r$, $\theta-\theta$, and $\phi-\phi$ components of the field equations are, respectively:

$$-e^{2\nu}\left(\frac{1}{r^2}+\frac{2\nu'}{r}\right)+\frac{1}{r^2}=\frac{1}{M^2_{p\text{eff}}}\left(T_{00}+\tilde{T}_{00}\right), \tag{A2}$$

$$e^{2\nu}\left(\frac{2\nu'}{r}+\frac{1}{r^2}\right)-\frac{1}{r^2}=\frac{1}{M^2_{p\text{eff}}}\left(T_{rr}+\tilde{T}_{rr}\right), \tag{A3}$$

$$\frac{1}{2}e^{2\nu}\left(2\nu''+4\nu'^2+4\frac{\nu'}{r}\right)=\frac{1}{M^2_{p\text{eff}}}\left(T_{\theta\theta}+\tilde{T}_{\theta\theta}\right), \tag{A4}$$

$$\frac{1}{2}e^{2\nu}\left(2\nu''+4\nu'^2+4\frac{\nu'}{r}\right)=\frac{1}{M^2_{p\text{eff}}}\left(T_{\phi\phi}+\tilde{T}_{\phi\phi}\right). \tag{A5}$$

Summing these equations together, we get:

$$e^{2\nu}\left(2\nu''+\frac{4\nu'}{r}+4\nu'^2\right)=\frac{1}{M^2_{p\text{eff}}}\left(T_{\text{tot}}+\tilde{T}_{\text{tot}}\right), \tag{A6}$$

where T_{tot} and $\tilde{T}_{\text{tot}}$ are the sum of the components of T and $\tilde{T}$, respectively. Assuming that the deviation from GR is small, one can write $M^2_{p\text{eff}} = M^2_p(1+\epsilon\Psi)$, where ϵ is a small quantity and Ψ describes the deviation from GR due to the presence of $\tilde{T}_{\mu\nu}$. Equation (A6) becomes

$$e^{2\nu}\left(2\nu''+\frac{4\nu'}{r}+4\nu'^2\right)=\frac{1}{M^2_p}\left(T_{\text{tot}}+2\tilde{\rho}\right) \tag{A7}$$

and $2\tilde{\rho} = \tilde{T}_{\text{tot}}(1-\epsilon\Psi)$, written in this form for later convenience.

Next step, consider a system of collisionless point particles following a distribution function f_B. The stress energy tensor of such a system can be defined as

$$T_{\mu\nu} = \int f_B m u_\mu u_\nu du \tag{A8}$$

where m is the mass of a particle (galaxy, star...), u_μ its 4-velocity, and $du = du_r du_\theta du_\phi/u_t$ the invariant volume element in velocity space. From this definition, one can write

$$\frac{1}{M^2_p}T_{\text{tot}} = \frac{2}{M^2_p}\rho\langle u^2\rangle, \tag{A9}$$

where ρ is the mass density of the system, and $\langle u^2\rangle = \langle u_t^2\rangle + \langle u_r^2\rangle + \langle u_\theta^2\rangle + \langle u_\phi^2\rangle$, with $\langle . \rangle$ being the average in velocity space. The distribution function f_B follows the relativistic Boltzmann equation (Maartens & Maharaj 1985; Bildhauer 1989):

$$\left(p^\alpha \frac{\partial}{\partial x^\alpha} - p^\alpha p^\beta \Gamma^i{}_{\alpha\beta} \frac{\partial}{\partial p^i}\right) f_B = 0, \tag{A10}$$

where p^α is the particle's 4-momentum (see Boehmer, Harko & Lobo 2008 for further mathematical details). At this stage, it is more convenient to introduce a set of local tetrads $e^a_\mu(x)$, $a = 0, 1, 2, 3$, which can be chosen to be, for the current case of spherical symmetry:

$$e^0_\mu = e^\nu \delta^0_\mu, \quad e^1_\mu = e^{-\nu}\delta^1_\mu \tag{A11}$$

$$e^2_\mu = r\delta^2_\mu, \quad e^3_\mu = r\sin\theta\delta^3_\mu, \tag{A12}$$

where δ^a_μ is the Kronecker delta. Assuming that $f_B = f_B(r, u^a)$, where $u^a = u^\mu e^a_\mu$ are the velocity components in the tetrad frame, equation (A10) becomes (Jackson 1970)

$$u_1\frac{\partial f_B}{\partial r} - \left(u_0^2\frac{\partial \nu}{\partial r} - \frac{u_2^2+u_3^2}{r}\right)\frac{\partial f_B}{\partial u_1} - \frac{1}{r}u_1\left(u_2\frac{\partial f_B}{\partial u_2} + u_3\frac{\partial f_B}{\partial u_3}\right) - \frac{1}{r}e^{-\nu}u_3\cot\theta\left(u_2\frac{\partial f_B}{\partial u_3} - u_3\frac{\partial f_B}{\partial u_2}\right) = 0. \tag{A13}$$

Multiplying the above equation by $mu_r\mathrm{d}u$ and integrating over the velocity space (assuming that $f_B \to 0$ as $u \to \pm\infty$), then multiplying by $4\pi r^2\mathrm{d}r$ and integrating over the system, we get finally:

$$\int_0^R 4\pi\rho\left[\langle u_1^2\rangle + \langle u_2^2\rangle + \langle u_3^2\rangle\right]r^2\mathrm{d}r - \frac{1}{2}\int_0^R 4\pi\rho\left[\langle u_0^2\rangle + \langle u_1^2\rangle\right]r^3\frac{\partial \nu}{\partial r}\mathrm{d}r = 0. \tag{A14}$$

To simplify the problem, one can make two further approximations. First, assume ν to be small and slowly varying, hence $e^{2\nu} \approx 1 + 2\nu$ and all quadratic terms in ν or ν' drop. Second, assume the velocities to be much smaller than the speed of light, therefore $\langle u_1^2\rangle \approx \langle u_2^2\rangle \approx \langle u_3^2\rangle \ll \langle u_0^2\rangle \approx 1$. Thus, equations (A7; after using A9) and (A14) become

$$\frac{1}{r^2}\frac{\partial}{\partial r}\left(r^2\frac{\partial \nu}{\partial r}\right) = \frac{1}{M_p^2}(\rho + \tilde{\rho}) \tag{A15}$$

and

$$2T - \frac{1}{2}\int_0^R 4\pi\rho\frac{\partial \nu}{\partial r}r^3\mathrm{d}r = 0, \tag{A16}$$

respectively, where

$$T = \int_0^R 2\pi\rho\left[\langle u_1^2\rangle + \langle u_2^2\rangle + \langle u_3^2\rangle\right]r^2\mathrm{d}r \tag{A17}$$

is the total kinetic energy of the system. Multiplying (A15) by r^2 and integrating from 0 to r, we get, when using the explicit form of M_p^2 given in Section 1:

$$GM(r) = \frac{1}{2}r^2\frac{\partial \nu}{\partial r} - G\tilde{M}(r), \tag{A18}$$

where

$$M(r)\big(\tilde{M}(r)\big) = 4\pi\int_0^R \rho\big(\tilde{\rho}\big)r'^2\mathrm{d}r'. \tag{A19}$$

Finally, multiplying (A18) by $\mathrm{d}M(r)$ and integrating from 0 to R, after the use of (A16), we get the generalized virial theorem:

$$2T + \Omega + \tilde{\Omega} = 0, \tag{A20}$$

where

$$\Omega\big(\tilde{\Omega}\big) = -\int_0^R \frac{GM(r)\big(\tilde{M}(r)\big)}{r}\mathrm{d}M(r). \tag{A21}$$

This paper has been typeset from a TEX/LATEX file prepared by the author.

Part III

SPINOR FIELDS IN GRAVITATIONAL BACKGROUNDS

4

NEUTRINO-DARK ENERGY INTERACTION IN CURVED SPACETIME

It is now well established that *neutrinos* form part of *Multimessenger Astronomy*, along with electromagnetic and gravitational waves. Therefore, the more properties we uncover about neutrinos, the more we can discover about the universe from these messengers.

Studying neutrinos in Cosmology is not a recent subject and a great deal of literature on that is available, see [86, 87] for instance. However, most of the analysis has been made assuming neutrinos to be classical point particles. It would be therefore a natural step further to generalize our analysis by considering neutrinos to be *quantum spinors* traveling in gravitational fields. In this chapter, I present three projects I did where that generalizing step has been applied [88–90].

In the first work [88], I present a general formalism for studying the interaction of quantum spinor and scalar fields in curved spacetime. After writing down an action principle, I derive a generalized Dirac equation, such as (1.36) but including the scalar-spinor interaction. Following that, I specify the coupling term to three different interactions, and study their effect on neutrino dynamics in FRW spacetime. One of these coupling terms is particularly interesting: the linear derivative coupling(LDC), $\bar{\psi}\gamma^{\mu}\psi\partial_{\mu}\varphi$, where $\psi(\varphi)$ is the spinor(scalar)field.

This interaction is motivated by early universe symmetry breaking arguments [91, 92], and it was shown that it could play a role in explaining away DE [55]. The latter work focused on the scalar field part in this interaction, showing how it could produce a force that would "freeze" the scalar field and produces an equation fo state $\omega = -1$, thus mimicking DE. It is therefore natural to look at what would happen to neutrinos under such interaction, which is what I did in [89].

The ultimate goal of this work is to distinguish between DE models, mainly a cosmological constant(CC) and scalar field DE, using *neutrino oscillations*[1]. To do that, I first look at a particular form of general coupling between the two fields in a generic spacetime. This interaction will manifest itself in the spacetime evolution of neutrino flavor state, and thus in the transition amplitude between two flavors. Taking the latter's modulus squared gives the oscillation probability between two neutrino flavors in a generic spacetime.

Having done that, I then consider the case of a cosmological constant DE in a flat FRW spacetime. Then, I make contrast between the oscillation probability of this formalism and the one from flat

1 For simplicity, I consider a system of two neutrino flavors.

spacetime (eq.(38) in [89]), when using cosmological distances, e.g. the *luminosity distance*. The main message from this result is that there will be a huge difference between the two approaches as we go to higher redshifts. Thus, one should be careful when doing neutrino astronomy and use the formalism presented here, rather than simply substituting cosmological distances into flat spacetime oscillation probability formulae.

The next step would be to consider the case of scalar field DE, with the coupling between the two fields given by the LDC mentioned above. Again, a contrast between oscillation probabilities' evolution with redshift is made for this model and that of CC-DE. By varying the strength of the scalar-spinor coupling, a clear difference appears between the two models, showing thereby that neutrino oscillations could be used as probe to distinguish DE models.

While working on this project, I noticed that different values of H_0 in the Friedmann equation produce a slight shift in the evolution of the probabilities. This pushed me to study this effect in more detail in [90] by looking at the full three-flavor neutrino system in ΛCDM. The purpose would be to see if neutrino oscillation could be a probe of H_0 and therefore add some insight onto the *Hubble tension* [93–95]. Indeed, what I find is that there will be a difference of a few % in neutrino fluxes between early and late Universe probes of H_0. Although this shift might not be substantial to be detected with current neutrino observatories, there could be hints of its presence with future ones, such as *IceCube-Gen2* [96].

This chapter aims at demonstrating the potential of quantum field theory in curved spacetime to probe the Universe in a novel way. It would be a natural generalization of our current analysis, without the need of adding new forces or particles. With the advancement of detector technology, traces of these effects should start to appear, opening up a new era in our understanding of the Cosmos.

Physics of the Dark Universe 31 (2021) 100777

Contents lists available at ScienceDirect

Physics of the Dark Universe

journal homepage: www.elsevier.com/locate/dark

Spinors and Scalars in curved spacetime: Neutrino dark energy (DE_ν)

Ali Rida Khalifeh [a,b,*], Raul Jimenez [a,c]

[a] ICC, University of Barcelona, Marti i Franques, 1, E-08028 Barcelona, Spain
[b] Dept. de Fisica Cuantica y Astrofisica, University of Barcelona, Marti i Franques 1, E-08028 Barcelona, Spain
[c] ICREA, Pg. Lluis Companys 23, Barcelona, E-08010, Spain

ARTICLE INFO

Article history:
Received 19 October 2020
Received in revised form 11 January 2021
Accepted 18 January 2021

ABSTRACT

We study the interaction, in general curved spacetime, between a spinor and a scalar field describing dark energy; the so-called DE_ν model in curved space. The dominant term is the dimension 5 operator, which results in different energy shifts for the neutrino states: an Aharonov–Bohm-like effect. We study the phenomenology of this term and make observational predictions to detect dark energy interactions in the laboratory due to its effect on neutrino oscillation experiments, which opens up the possibility of designing underground experiments to detect dark energy. This dimension 5 operator beyond the Standard Model interaction is less suppressed than the widely discussed dimension 6 operator, which corresponds to mass varying neutrinos; the dimension 5 operator does not suffer from gravitational instabilities.

1. Introduction

The physical nature of the current phase of cosmic acceleration [1,2], associated to an entity called Dark Energy (DE), remains a major mystery. This is despite the fact that it has been observationally studied intensively and confirmed via very different cosmological observables, most notably, the cosmic microwave background (CMB) [3,4], supernovae [1,2], baryon acoustic oscillations (BAO) [5], large scale structure [6], cosmic chronometers [7–9] and weak lensing [10].

On the observational front, it is becoming clear that the effective equation of state of DE is compatible with a cosmological constant at the % level, i.e. $w = -1$ where $p = w\rho$ [3], with p and ρ being the pressure and energy density, respectively, of DE. Given how strongly the observations suggest that DE is a cosmological constant, it is interesting to explore possible alternatives, given the large difference between the value of the energy density of a cosmological constant (which is $\sim$ $(\text{meV})^4$) and the vacuum expectation value M_{p}^4, where M_{p} is the Planck mass (see e.g. Ref. [11,12]). Further, but not exclusive to the cosmological constant, there is the coincidence problem (see e.g., Ref. [13,14]), i.e., the fact that the redshift of equality between CDM and Λ is close to us in time.

In order to overcome all these problems, several alternatives have been proposed. One of the first ideas was that of a dynamic DE [15,16], which involves a minimally coupled dynamical scalar field (quintessence). The latter models have quickly gained popularity, as they alleviate the cosmological coincidence problem. Further extensions of quintessence models include the addition of a coupling with other sectors of the Universe, the so-called interacting quintessence. Most interacting models couple DE to the other "dark" component of the universe, Dark Matter (DM) (see for instance Refs. [17–20]). However, a coupling of the scalar field to DM in general induces effects akin to modifications of gravity beyond the simple description offered by General Relativity (GR). These modifications are being increasingly constrained by observations [21–35].

This shortcoming is avoided in a recently proposed alternative [36], where a generic scalar field is "frozen" in place by coupling with neutrinos (or any other particle, although neutrinos have several advantages; for one, we know they exist), and can thus act as DE. A coupling between neutrinos and the scalar field responsible for DE is motivated by the similarity in scale between neutrino rest-mass and the energy scale of dark energy ($\sim$ meV). Another advantage of neutrinos is that they become non-relativistic at relatively recent redshifts ($z \sim 10$) thus providing a possible alleviation of the "why now?" problem.

The main aim of this paper is to develop the formalism in curved space, using semi-classical effective field theory, for the lowest order interaction between spinor and scalar fields in order to constrain the possible interactions that could lead to momentum (and energy) transfer as in the phenomenological model of Ref. [36]. In order to do, so we explore all possible terms of interaction permitted by the symmetries in the standard model of particle physics (SM) to a scalar field. In this respect our model is very minimal as it only requires the current standard

* Corresponding author.
E-mail addresses: ark93@icc.ub.edu (A.R. Khalifeh), raul.jimenez@icc.ub.edu (R. Jimenez).

https://doi.org/10.1016/j.dark.2021.100777
2212-6864/

model, which we know exists, and one extra scalar field, the only postulated ingredient in this model. Our derivation is totally general and can be applied to any scenario in which a spinor and a scalar field interact in curved spacetime.

The structure of this paper is as follows: in Section 2 we derive, within the effective field theory framework, equations of motion due to a general type of interaction between a spinor and a scalar field that leads to momentum, and energy, transfer. We explore the dynamics (using a semi-classical approach) and phenomenology (the effect on neutrino oscillations) of the 5th dimension operator in Section 3. We summarize our results in Section 4. In an appendix, we solve the equations of motion of dimension operators 6 and 8 as to fully complete our analysis. Units in which $8\pi G = c = 1$, and a metric signature $(-+++)$ will be used.

2. General framework

In this section, we present the general framework used to study the interaction of a spinor field (particularly neutrino) and a scalar field in curved background. This will be applicable to any type of interaction between the two fields. In later sections we specify the type of interactions and study their consequences (see Ref. [37] for details on Spinors in curved spacetime).

What distinguishes neutrinos from other fields in curved spacetime, is the fact that the general linear group GL(4), which is that of general coordinate transformations, does not have a spinorial representation. This inhibits the generalization of equations of motion in the standard way (substituting partial derivatives with covariant ones, and the flat metric with that of curved background), and requires the use of tetrads, as we will see shortly.

The most general action for a real classical scalar field φ and a spinor field ψ, with its hermitian conjugate $\psi^\dagger$, interacting in a curved spacetime with a metric $g_{\mu\nu}$ takes the form:

$$S = S_{\text{gravity}} + S_{\text{scalar}} + S_{\text{spinor}} + S_{\text{interaction}} \tag{1}$$

where S_{gravity} is the gravitational action, S_{scalar} is that of the scalar field, S_{spinor} is the one of spinor fields and $S_{\text{interaction}}$ is for the interaction term. Note that both fields are coupled minimally to gravity, as a first step in studying the dynamics in curved spacetime. More explicitly, this action takes the form:

$$\begin{aligned} S = \int d^4x\sqrt{-g}\Big[&\frac{1}{2}R - \frac{1}{2}\mathcal{D}_\mu\varphi\mathcal{D}^\mu\varphi - V(\varphi) \\ &+ i\hbar\big(\bar\psi\gamma^\mu\mathcal{D}_\mu\psi - \mathcal{D}_\mu\bar\psi\gamma^\mu\psi\big) - 2m\bar\psi\psi + \lambda\Theta\Big] \end{aligned} \tag{2}$$

where g is the determinant of $g_{\mu\nu}$, $R = g^{\mu\nu}R_{\mu\nu}$ is the Ricci scalar, the trace of the Ricci tensor $R_{\mu\nu}$ and $\hbar$ is the reduced Planck constant. Moreover, $\mathcal{D}_\mu$ is the spacetime covariant derivative that takes into account the spin of the field. For instance, $\mathcal{D}_\mu$ reduces to a partial derivative ∂_μ when applied to a scalar field, or to the usual covariant derivative of GR, ∇_μ, when applied to a vector or tensor fields. The explicit form of the covariant derivative for a spinor field in curved spacetime will be introduced later. Furthermore, $V(\varphi)$ is the potential for the scalar field and $\bar\psi = \psi^\dagger\gamma^0$, with γ^0 being one of the Dirac gamma matrices γ^μ. Finally, m is the mass of the spinor field, λ is the coupling constant between the scalar and the spinor, as described by the interaction term $\Theta(\psi, \varphi, X_\psi, X_\varphi)$, with $X^\mu_\varphi\big(X^\mu_{\bar\psi}\big) = \nabla^\mu\varphi\big(\mathcal{D}^\mu\psi\big)$.

The equation of motion for the spinor field is obtained by varying (1) with respect to the spinor field:

$$\frac{1}{\sqrt{-g}}\frac{\delta S}{\delta\bar\psi} = 0 \quad\Rightarrow\quad i\hbar\gamma^\mu\mathcal{D}_\mu\psi - m\psi = -\frac{\lambda}{2}\left(\frac{\partial\Theta}{\partial\bar\psi} - \mathcal{D}^\mu\frac{\partial\Theta}{\partial X^\mu_{\bar\psi}}\right) \tag{3}$$

which will be our main focus in this work. The variation of the action with respect to ψ will give the complex conjugate of (3). For completeness, we state the equation of motion for the scalar field:

$$\Box\varphi - \frac{\partial V}{\partial\varphi} = -\lambda\left(\frac{\partial\Theta}{\partial\varphi} - \nabla^\mu\frac{\partial\Theta}{\partial X^\mu_\varphi}\right). \tag{4}$$

where $\Box = g^{\mu\nu}\nabla_\mu\nabla_\nu$.

3. Dimension 5 operator: Linear derivative coupling

In effective field theory, the lowest order interaction term beyond the SM interactions, between spinor and scalar fields which is allowed by the SM and GR symmetries, is[1]:

$$\Theta = J^\mu\nabla_\mu\varphi \tag{5}$$

where $J^\mu = \bar\psi\gamma^\mu\psi$. The Dirac equation in curved spacetime (3) is:

$$\big(i\hbar\gamma^\mu\mathcal{D}_\mu - m\big)\psi = -\frac{\lambda}{2}\gamma^\mu\psi\nabla_\mu\varphi. \tag{6}$$

If we focus on regions much smaller than the curvature scale, we can use the WKB approximation to study the dynamics of spinors in a gravitational field [38] (see Appendix A for a brief discussion on the WKB approximation). The strategy would be to expand the field in powers of $\hbar$, and then study the dynamics at each power. In this case, the spinor field can be written as[2]:

$$\psi(x) = e^{iS(x)/\hbar}\sum_{n=0}^{\infty}(-i\hbar)^n\psi_n(x) \tag{7}$$

where the ψ_ns are also spinors. Plugging this in (6), keeping terms up to first order, we get:

$$\begin{aligned} &\Big[-\big(\gamma^\mu\partial_\mu S + m\big) + \frac{\lambda}{2}\gamma^\mu\partial_\mu\varphi\Big]\psi_0 \\ &+ i\hbar\Big[\Big(\gamma^\mu\partial_\mu S + m - \frac{\lambda}{2}\gamma^\mu\partial_\mu\varphi\Big)\psi_1 + \gamma^\mu\mathcal{D}_\mu\psi_0\Big] = 0. \end{aligned} \tag{8}$$

3.1. Solution at 0th order in WKB expansion

From (8), we can read off the 0th order equation to be:

$$\big(\gamma^\mu\partial_\mu S + m\big)\psi_0 = \frac{\lambda}{2}\gamma^\mu\partial_\mu\varphi\psi_0. \tag{9}$$

A non-trivial solution for this algebraic set of equations exists if

$$\begin{aligned} &\det\left[\gamma^\mu\partial_\mu\left(S - \frac{\lambda}{2}\varphi\right) + m\right] = 0 \\ &\Rightarrow\quad \partial_\mu\left(S - \frac{\lambda}{2}\varphi\right)\partial^\mu\left(S - \frac{\lambda}{2}\varphi\right) = -m^2, \end{aligned} \tag{10}$$

which is the Hamilton–Jacobi equation for a spinless relativistic particle. Therefore, its canonical 4-momentum and 4-velocities are defined as:

$$p^\alpha = \partial^\alpha\left(S - \frac{\lambda}{2}\varphi\right); \quad u^\alpha = \frac{p^\alpha}{m} \tag{11}$$

giving the usual normalizations:

$$p^\alpha p_\alpha = -m^2; \quad u^\alpha u_\alpha = -1. \tag{12}$$

Notice that if we calculate the vorticity $\omega_{\alpha\beta} = \frac{1}{2}\big(\nabla_\alpha u_\beta - \nabla_\beta u_\alpha\big)$ by direct substitution of (11) we find that it is 0. Hence, at 0th

[1] Note that this interaction does not produce any gravitational instabilities, as already shown in Ref. [36]

[2] Note that here the phase $S(x)$ is slowly varying compared to ψ_n. Therefore there is no need to apply a WKB expansion on the phase.

order, the spinor field is equivalent to an irrotational fluid of spin 0 particles. This means that these particles follow the geodesic equation without alteration:

$$u^\alpha \nabla_\alpha u^\beta = 0 \quad \Rightarrow \quad \frac{dp^\alpha}{d\tau} + \frac{1}{m}\Gamma^\alpha_{\beta\gamma} p^\beta p^\gamma = 0 \tag{13}$$

where τ is the proper time of the particle. This result is consistent with the findings of Ref. [36], and it will be at every order in $\hbar$, as one can check by simply noticing that the equation of the scalar field does not change. Indeed the latter is:

$$g^{\mu\nu}\nabla_\mu\nabla_\nu\varphi - \frac{\partial V}{\partial\varphi} = -\lambda\left(\frac{\partial\Theta}{\partial\varphi} - \nabla^\mu\frac{\partial\Theta}{\partial X^\mu_\varphi}\right) = -\lambda\mathcal{D}_\mu J^\mu = 0 \tag{14}$$

where the last equality follows from (6) and its complex conjugate.

Although this type of interactions does not affect the dynamics, it still causes a shift in the energy of the neutrinos, as has been claimed previously in Ref. [36]. To see this quantitatively, consider the Lagrangian density for neutrinos:

$$\mathcal{L}_\nu = i\hbar\left(\bar\psi\gamma^\mu\mathcal{D}_\mu\psi - \mathcal{D}_\mu\bar\psi\gamma^\mu\psi\right) - 2m\bar\psi\psi + \lambda\bar\psi\gamma^\mu\psi\partial_\mu\varphi. \tag{15}$$

The conjugate momentum of the field would be:

$$\pi_\nu = \pi_\psi + \pi_{\bar\psi} = \frac{\delta\mathcal{L}_\nu}{\delta\mathcal{D}_t\psi} + \frac{\delta\mathcal{L}_\nu}{\delta\mathcal{D}_t\bar\psi} \tag{16}$$

and therefore the Hamiltonian density would be:

$$\begin{aligned}\mathcal{H} &= \pi_\psi\mathcal{D}_t\psi + \pi_{\bar\psi}\mathcal{D}_t\bar\psi - \mathcal{L}\\ &= i\hbar\left(\bar\psi\vec\gamma.\vec{\mathcal{D}}\psi - \vec{\mathcal{D}}\bar\psi.\vec\gamma\psi\right) + 2m\bar\psi\psi - \lambda\bar\psi\gamma^\mu\psi\partial_\mu\varphi.\end{aligned} \tag{17}$$

The last term is an additional contribution to the neutrino energy that comes from this interaction. If we consider a homogeneous and isotropic scalar field, i.e $\varphi = \varphi(t)$, then at 0th order in WKB expansion, this term would be of the form $\bar n_\nu\dot\varphi$, where $\bar n_\nu$ is the average number density of the neutrino particles, and a dot denotes derivative with respect to cosmic time. More interestingly, if the neutrino fluid is moving with a bulk velocity in a gravitational potential well, the additional term would take the form $\lambda\bar n_\nu\left(\dot\varphi + \vec v.\vec\nabla\varphi\right)$, where $\vec v$ is the bulk velocity. Of course this effect will be at perturbation level if we are considering a homogeneous and isotropic scalar field.

Let us see now in more detail the effect of this shift in energy on neutrino oscillations, and constrain the coupling λ to get an observable effect.

3.2. Phenomenology of 5th dim operator: Effect on neutrino oscillations

When studying neutrino oscillations, it is customary to write the neutrino state in terms of mass eigenstates and spacetime coordinates, as done for instance in Refs. [39,40]. However, since we are considering curved spacetime, it would be better to write things in a covariant way [41]:

$$|\Psi_\alpha(\lambda)\rangle = \sum_j U_{\alpha j} e^{i\int_{\lambda_0}^{\lambda}\vec P.\vec q\, d\lambda'}|\nu_j\rangle \tag{18}$$

where $|\Psi_\alpha\rangle$ is the neutrino state that was initially in a flavor α and λ is the affine parameter that characterizes the neutrino's world-line, with λ_0 its value today. Moreover, $U_{\alpha j}$ is the conversion matrix between flavor and mass eigenstates, $\vec P$ is the 4-momentum operator (generating spacetime translations) of the mass eigenstates $|\nu_j\rangle$ and $\vec q = d\vec x/d\lambda$ is a null vector tangent to the neutrino's world-line $\vec x(\lambda) = \left[t(\lambda), x(\lambda), y(\lambda), z(\lambda)\right]$. If we concentrate on transitions between electron neutrinos, ν_e, and muon neutrinos, ν_μ, we can define a vector of transition amplitudes:

$$\chi(\lambda) = \begin{bmatrix}\langle\nu_e|\Psi(\lambda)\rangle\\ \langle\nu_\mu|\Psi(\lambda)\rangle\end{bmatrix} \tag{19}$$

which satisfies the differential equation:

$$i\frac{d\chi}{d\lambda} = \vec P.\vec q\ \chi, \tag{20}$$

with the solution given in (18). Our goal is therefore to calculate the quantity $\vec P.\vec q$ for neutrinos traveling in curved spacetime and interacting with the scalar field φ, with an interaction given by (5). To this end, let us rewrite the Dirac equation (6) for a column vector of neutrino flavors ψ_f (we consider two neutrino flavors for simplicity):

$$\left[i\hbar\left(\gamma^\mu\mathcal{D}_\mu - \frac{i}{\hbar}A_{\varphi\mu}\mathcal{P}_L\right) - M_f\right]\psi_f = 0 \tag{21}$$

where

$$A_{\varphi\mu} = -\frac{1}{2}\partial^\mu\varphi\begin{pmatrix}\lambda_e & 0\\ 0 & \lambda_\mu\end{pmatrix} \tag{22}$$

and we are considering different coupling constants for the two flavors ν_e and ν_μ. Moreover, M_f is the vacuum mass matrix in flavor space, given by:

$$M_f^2 = U\begin{pmatrix}m_1^2 & 0\\ 0 & m_2^2\end{pmatrix}U^\dagger \tag{23}$$

where

$$U = \begin{pmatrix}\cos\theta & \sin\theta\\ -\sin\theta & \cos\theta\end{pmatrix} \tag{24}$$

is the mixing matrix, with mixing angle θ, that transforms from one basis to another, and m_1 and m_2 are eigenvalues for mass eigenstates. Finally, $\mathcal{P}_L = \frac{1}{2}(1-\gamma^5)$ is the left-handed projection operator. From now on we will focus on left-handed neutrinos only, and therefore drop this factor. Furthermore, the explicit form of the covariant derivative is [42]

$$\gamma^\mu\mathcal{D}_\mu = \gamma^a e^\mu_a\left(\partial_\mu + \Gamma_\mu\right) \tag{25}$$

where γ^a are the Dirac matrices in local inertial coordinates, e^μ_a are tetrad (or vierbein) fields that connect general coordinates to local ones, and

$$\Gamma_\mu = \frac{1}{8}\left[\gamma^b,\gamma^c\right]e^\nu_b\nabla_\mu e_{c\nu} \tag{26}$$

is the spin connection that describes the effect of gravity on the spin of the particle, with $\left[\gamma^a,\gamma^b\right]$ being the commutator of the two matrices γ^a and γ^b. We adopt the convention that Latin indices correspond to local inertial coordinates, while Greek ones correspond to general coordinates. From here, it can be shown that

$$\gamma^a e^\mu_a\Gamma_\mu = \frac{i}{\hbar}\gamma^a e^\mu_a A_{G\mu} \tag{27}$$

where

$$A^\mu_G = \frac{1}{4}\sqrt{-g}\,e^\mu_a\epsilon^{abcd}(\partial_\sigma e_{b\nu} - \partial_\nu e_{b\sigma})e^\nu_c e^\sigma_d \tag{28}$$

with ϵ^{abcd} being the Levi-Civita symbol in four dimensions. Hence, the Dirac equation will take the form:

$$\left[i\hbar\gamma^\mu\left(\partial_\mu - \frac{i}{\hbar}A_\mu\right) - M_f\right]\psi_f = 0 \tag{29}$$

with $A^\mu = A^\mu_G + A^\mu_\varphi$. For this equation to have a non-trivial solution, the mass-shell relation must be satisfied, i.e:

$$\left(P^\mu + A^\mu\right)\left(P_\mu + A_\mu\right) = M_f^2. \tag{30}$$

We already know what $\vec{q}$ is and that it satisfies the geodesic equation. Since we want to find $\vec{P}.\vec{q}$, we can construct $\vec{P}$ as done in [41]: First, take neutrinos to be energy eigenstates, that is $P^0 = q^0$. Second, assume $\vec{P}$ and $\vec{q}$ to be parallel (we do not really need the perpendicular component, since we are taking inner product of the two vectors in the end), which means we can write $P^i = q^i(1-\epsilon)$. Finally, for relativistic neutrinos, $\epsilon \ll 1$, and therefore (30) gives:

$$\vec{P}.\vec{q} = -\epsilon\left(g_{0i}q^0q^i + g_{ij}q^iq^j\right) = \frac{1}{2}M_f^2 - q^\mu A_\mu. \tag{31}$$

We can now write (18) as

$$|\Psi_\alpha(\lambda)\rangle = \sum_j U_{\alpha j}e^{i\Omega}|\nu_j\rangle \tag{32}$$

where

$$\Omega = \int_{\lambda_0}^{\lambda}\left(\frac{1}{2}M_f^2 - q^\mu A_\mu\right)d\lambda'. \tag{33}$$

For a flat FRW universe:

$$ds^2 = -dt^2 + a^2\delta_{ij}dx^idx^j. \tag{34}$$

A convenient choice for the tetrad fields is:

$$e_a^\mu = \mathrm{diag}\left[1, a^{-1}, a^{-1}, a^{-1}\right] \tag{35}$$

from which one can show, after some algebra, that A_G^μ=0. Physically, this can be seen as a consequence of having a homogeneous and isotropic spacetime, and therefore there would be no alteration in the spin direction. Furthermore, using (34), one can show that if neutrinos are traveling along null trajectories, which is convenient when studying oscillations, then the affine parameter is related to cosmic time by:

$$dt = Ed\lambda \tag{36}$$

where $E = q^0$ is the neutrino energy. From here, we can write (20) as

$$i\frac{d\chi}{dt} = -\frac{1}{2E}\left(M_f^2 + V_\varphi\right)\chi \tag{37}$$

where

$$V_\varphi = -2q^\mu A_{\varphi\mu} = E\dot{\varphi}\begin{pmatrix}\lambda_e & 0\\ 0 & \lambda_\mu\end{pmatrix} \tag{38}$$

and we have take into account that, at the background level, $\varphi = \varphi(t)$. On the other hand, when written explicitly from (23),

$$\begin{aligned} M_f^2 &= \begin{pmatrix} m_1^2 + \Delta\sin^2\theta & \frac{1}{2}\Delta\sin 2\theta \\ \frac{1}{2}\Delta\sin 2\theta & m_1^2 + \Delta\cos^2 2\theta\end{pmatrix} \\ &= \left(m_1^2 + \frac{1}{2}\Delta\right)I + \frac{1}{2}\Delta\begin{pmatrix}-\cos 2\theta & \sin 2\theta \\ \sin 2\theta & \cos 2\theta\end{pmatrix} \end{aligned} \tag{39}$$

where $\Delta = m_2^2 - m_1^2$ and I is the identity matrix. The term proportional to the identity matrix in the above will be a common phase factor for both transition amplitudes, hence we can ignore it for oscillation purposes. Moreover, if we want to measure this effect on Earth, we can consider distances small enough for us to safely assume a Minkowsky spacetime, in which case we can write $dt \approx dx$. In addition, to detect the effect of this interaction on neutrino oscillations, we look at the difference in frequency Ω between the presence of this interaction and its absence:

$$\Delta\Omega = \Omega - \Omega_{\mathrm{NoInt}} = \frac{1}{2E}\int_{x0}^{x} V_\varphi dx' \tag{40}$$

where Ω_{NoInt} is the frequency without interactions and x_0 is the position of Earth. So, for a specific flavor i,

$$\Delta\Omega_i = \frac{\lambda_i}{2E}\int_{x0}^{x} E\dot{\varphi}\, dx'. \tag{41}$$

Let us assume, for order of magnitude estimate purposes, that E and $\dot{\varphi}$ are roughly constants. Therefore

$$\lambda_i \sim \frac{\Delta\Omega_i}{\dot{\varphi}\Delta x} \tag{42}$$

where Δx is the distance traveled by the neutrino between its interaction and detection points. This will give us the order of magnitude of the interaction parameter depending on the nature of the scalar field under consideration. For instance, if φ is supposed to describe DE, then its energy scale is $\mathcal{O}$(meV), hence $\dot{\varphi} \sim 10^{-8}\mathrm{eV}^2$. If the distance traveled is of the size of our galaxy (around 50kpc), to get a difference in frequency $\mathcal{O}(\pi)$, then $\lambda_i \sim 10^{-9}\mathrm{GeV}^{-1}$. On the other hand, if the scalar field is the Higgs, which means its energy scale is $\mathcal{O}$(100GeV), then $\dot{\varphi} \sim 10^{20}\mathrm{eV}^2$, and so $\lambda_i \sim 10^{-37}\mathrm{GeV}^{-1}$. It is more likely therefore that this interaction to be relevant for DE rather than the Higgs. In other words, the DE cannot be the Higgs field in this model, but we need to postulate an extra scalar field. We will discuss elsewhere signatures of this models in specific neutrino oscillation experiments like IceCube. Here we only note that the effect is in principle measurable.

In the above discussion, we have not seen a direct effect on the equations of motion due to the curved gravitational field. This will be apparent at 1st order in the WKB expansion.

3.3. Solution at 1st order in WKB expansion

From (8), we can read off the 1st order equation of motion to be

$$\left(\gamma^\mu\partial_\mu\left(S - \frac{\lambda}{2}\varphi\right) + m\right)\psi_1 = -\gamma^\mu\mathcal{D}_\mu\psi_0. \tag{43}$$

Since this is a non-homogeneous linear algebraic equation, the solutions of the homogeneous equation for a Hermitian system, which is ψ_0, should be orthogonal to the inhomogeneity, i.e.[3]

$$\bar{\psi}_0\gamma^\mu\mathcal{D}_\mu\psi_0 = 0, \tag{44}$$

in order to insure non-trivial solutions at 1st order. This relation can be used to show that

$$u^\alpha\mathcal{D}_\alpha\psi_0 = -\frac{\theta}{2}\psi_0 \tag{45}$$

where $\theta = \mathcal{D}_\alpha u^\alpha$, which is equivalent to saying that ψ_0 follows a sourced geodesic in curved spacetime. Moreover, for later convenience, define a spinor ξ_0 such that

$$\psi_0 = f(x)\xi_0, \tag{46}$$

where $f(x)$ is a function of the coordinates. Therefore, the above relation translates into:

$$u^\alpha\partial_\alpha f = -\frac{\theta}{2}f; \quad u^\alpha\mathcal{D}_\alpha\xi_0 = 0. \tag{47}$$

As we will see shortly, these relations are useful when calculating the deviation from the 0th order geodesic motion due to curvature of spacetime. To this end, let us start by noticing that the Dirac current, $J^\mu = \bar{\psi}\gamma^\mu\psi$ can be decomposed into convection and magnetization currents[4]:

$$J^\mu = J_c^\mu + J_M^\mu \tag{48}$$

where

$$J_c^\mu = -\frac{\hbar}{2mi}\left[\left(\tilde{\mathcal{D}}^\mu\bar{\psi}\right)\psi - \bar{\psi}\tilde{\mathcal{D}}^\mu\psi\right]; \quad J_M^\mu = \frac{\hbar}{2m}\tilde{\mathcal{D}}_\nu\left(\bar{\psi}\sigma^{\mu\nu}\psi\right) \tag{49}$$

[3] This equation can be proved directly from the complex conjugate of (9) and (43).

[4] This relation can be derived by starting from the definition of the magnetization current and using the Dirac equation.

are the convective and magnetization currents, respectively, with $\tilde{\mathcal{D}}_\nu = \mathcal{D}_\nu - i\frac{\lambda}{2}\partial_\nu\varphi$ and $\sigma^{\mu\nu} = \frac{i}{2}[\gamma^\mu, \gamma^\nu]$. Using the WKB expansions (7) and (46), we get the convection current to be, to 1st order in $\hbar$:

$$J^\mu_c = f^2\left[u^\mu - \frac{\hbar}{2mi}\left(\tilde{\mathcal{D}}^\mu\bar{\xi}_0\xi_0 - \bar{\xi}_0\tilde{\mathcal{D}}^\mu\xi_0\right)\right] + \mathcal{O}(\hbar^2). \tag{50}$$

Moreover, the convection current describes the probability flow of a particle moving with a velocity v^μ, i.e it is proportional to the latter, which is

$$v^\mu = u^\mu - \frac{\hbar}{2mi}\left(\tilde{\mathcal{D}}^\mu\bar{\xi}_0\xi_0 - \bar{\xi}_0\tilde{\mathcal{D}}^\mu\xi_0\right). \tag{51}$$

Therefore the deviation from geodesic motion at order $\hbar$ is

$$\delta u^\mu = \frac{\hbar}{2mi}\left(\tilde{\mathcal{D}}^\mu\bar{\xi}_0\xi_0 - \bar{\xi}_0\tilde{\mathcal{D}}^\mu\xi_0\right) = \frac{\hbar}{2mi}\left(\mathcal{D}^\mu\bar{\xi}_0\xi_0 - \bar{\xi}_0\mathcal{D}^\mu\xi_0\right) \tag{52}$$

where the last equality shows that the linear derivative coupling has no effect on the dynamics, as expected. Note that this deviation from geodesic motion can be interpreted in terms of an additional force due to the spin-curvature coupling, which can be written as

$$f^\mu = m\frac{\mathcal{D}v^\mu}{\mathcal{D}\tau} = mv^\nu\mathcal{D}_\nu v^\mu = \frac{\hbar}{4}g^{\mu\nu}u^\alpha R_{\nu\alpha\gamma\delta}\bar{\xi}_0\sigma^{\gamma\delta}\xi_0 \tag{53}$$

where $R_{\nu\alpha\gamma\delta}$ is the Riemann curvature tensor (see [42] for details about the derivation). What this means is that there will be a force due to the interaction of the spinor neutrino field with gravity, at order $\hbar$. This force will result in a change of the neutrino momentum that appears in Section 3.2, and therefore will affect the resulting neutrino oscillations. Furthermore, this additional force will change the scaling of the momentum with the scale factor. However, observationally, it would be difficult to detect such a change with current technologies due to the fact that this extra term is $\mathcal{O}(\hbar)$ smaller than the other terms in the geodesic equation. We will leave the details of this result for future work. Note also that this force will not alter the dynamics of the scalar field for two reasons: first, this force exists irrespective of whether there is an interaction between the spinor and the scalar fields (as we have shown above), and second, as the scalar field is a classical field, such an effect would not alter its motion.

This concludes the results for the linear derivative coupling between the neutrino spinor and a scalar field. As we can see, this type of interaction affects the energy density of the spinor field, but does not alter the dynamics. The latter change due to the spin-curvature coupling at order $\hbar$.

4. Discussion and summary

We have studied the interactions between spinor and scalar fields in curved spacetime, respecting all symmetries allowed by the SM of particle physics. We have studied the most dominant interaction beyond the SM ones in a semi-classical manner, using the WKB approximation. This term is the 5th dimension interaction which causes a shift in the energy of neutrinos. This shift is similar to the Aharonov–Bohm effect, as the one described qualitatively in section 5 of the DE$_\nu$ model [36], and therefore we were able to confirm this quantitatively. We have studied the phenomenology of this effect on neutrinos oscillations and provided a test for underground laboratories to detect this interaction. This could open the possibility of detecting dark energy in the laboratory.

Declaration of competing interest

The authors declare that they have no known competing financial interests or personal relationships that could have appeared to influence the work reported in this paper.

Acknowledgments

Funding for this work was partially provided by the Spanish ministry of science under project PGC2018-098866-B-I00. We thank Carlos Pena-Garay for useful discussions and feedback.

Appendix A. WKB approximation

The Wentzel, Kramers, Brillouin (WKB) approximation is a method for obtaining a global approximation to the solution of a linear differential equation whose highest derivative is multiplied by a small parameter [43]. In Quantum Mechanics, it is usually used to solve for the wave function of the Schrödinger equation in regions where the wavelength is much smaller than the typical distance over which the potential energy varies [44]. This is the key requirement for the applicability of the WKB approximation, which allows one then to assume a solution $\psi(x)$ of the form

$$\psi(x) = e^{if(x)/\hbar} \tag{A.1}$$

where $f(x)$ is a complex function. By expanding $f(x)$ in powers of $\hbar$, plugging in the Schrödinger equation, and solving at each level in powers of $\hbar$, one can then get an approximate solution to the problem considered(see, for instance, problem 8.2 in [45]. The 0th order solution will give the classical solution to the Hamilton–Jacobi equation, which shows why the WKB method is a semi-classical approximation. For the situation discussed in our paper, the same concept applies, where we focus on regions such that the wavelength is much smaller than the typical distance over which the curvature varies (in the case of an FLRW universe, we would be interested in cases where $k \gg H$, with k being the wavenumber). As a generalization of (A.1), one can use the solution presented earlier in this work, Eq. (7), as has been done in [46–49].

Appendix B. 6th dimension operator: Non-linear coupling

In these two appendices we give some details on the sub-dominant interaction terms to the 5th-dimension one. The purpose is to provide details for other sub-dominant physical effects that can occur at different epochs.

Consider the case where the coupling is

$$\Theta = i\hbar\bar{\psi}\gamma^\mu\mathcal{D}_\mu\psi\varphi^2. \tag{B.1}$$

Inserting this in (3), we get

$$\left(i\hbar\not{\mathcal{D}} - m\right)\psi = \frac{i\hbar\lambda}{2}\not{\mathcal{D}}\psi\varphi^2 \tag{B.2}$$

where $\not{\mathcal{D}} = \gamma^\mu\mathcal{D}_\mu$, a notation that applies to any slashed 4-vector. Note that this coupling will be an order of magnitude weaker than the dimension 5 for the same coupling constant, and so its effect on neutrino oscillations would be suppressed. Applying the WKB approximation (7) to this equation gives, up to order $\hbar$:

$$\begin{aligned}&\left[\left(1 - \frac{\lambda\varphi^2}{2}\right)\not{\partial}S + m\right]\psi_0 \\ &- i\hbar\left\{\left[\left(1 - \frac{\lambda\varphi^2}{2}\right)\not{\partial}S + m\right]\psi_1 + \left(1 - \frac{\lambda}{2}\varphi^2\right)\not{\mathcal{D}}\psi_0\right\} = 0\end{aligned} \tag{B.3}$$

from which we can start our analysis at each order in $\hbar$.

B.1. Solution at order $\hbar^0$

We can read off the equation of motion at this order from (B.3) to be

$$\left[\left(1 - \frac{\lambda\varphi^2}{2}\right)\not{\partial}S + m\right]\psi_0 = 0. \tag{B.4}$$

The evolution equation of the 4-momentum along the world line would be

$$\frac{dp^\alpha}{d\tau}+\frac{1}{m}\Gamma^\alpha_{\beta\gamma}p^\beta p^\gamma=-\frac{\lambda\varphi}{m\left(1-\frac{\lambda\varphi^2}{2}\right)}\left(m^2X^\alpha_\varphi+p^\alpha p_\beta X^\beta_\varphi\right). \tag{B.5}$$

Out of curiosity, if we multiply (B.5) by m and define $m^2_{\rm eff}=2m^2\ln\left(1-\lambda\varphi^2/2\right)$, (B.5) becomes

$$m\frac{dp^\alpha}{d\tau}+\Gamma^\alpha_{\beta\gamma}p^\beta p^\gamma=m_{\rm eff}\frac{dm_{\rm eff}}{d\varphi}\tilde\partial^\alpha\varphi \tag{B.6}$$

where $\tilde\partial^\alpha=\partial^\alpha+u^\alpha u_\beta\partial^\beta$, which can be interpreted as resulting from a boost in spacetime. This result is very similar to the one coming from mass varying neutrinos [50,51], thus we will not delve much into it in detail. Before going to the order $\hbar$ solution, let us study the consequences of this interaction in a flat FRW universe.

B.1.1. Solution at order $\hbar^0$ in a flat FRW universe

Consider the metric of spacetime (34). The 0th component of (B.5) gives

$$\frac{1}{p}\frac{dp}{dt}+\frac{1}{a}\frac{da}{dt}=-\frac{1}{1-\frac{\lambda\varphi^2}{2}}\frac{d}{dt}\left(1-\frac{\lambda\varphi^2}{2}\right), \tag{B.7}$$

where we have used the fact that $p^0=E=\sqrt{p^2+m^2}$ and therefore $dp^0/d\tau=(p/m)dp/dt$. Note again, due to homogeneity and isotropy, at the background level, $\varphi=\varphi(t)$. The solution for (B.7) is simply

$$p=\frac{p_0}{\tilde a};\quad \tilde a=a\left(1-\frac{\lambda\varphi^2}{2}\right). \tag{B.8}$$

where p_0 is a positive integration constant. This result shows a shift in the momentum of the neutrino when approximated as a classical particle with spin 0. This shift involves a φ^2 term, which is similar to a mass term for the scalar field. Moreover, since p is a non-negative quantity, this means that $\lambda\varphi^2<2$ in our units. This also avoids a divergence in the amplitude of the momentum.

We can use this result to see the effect this interaction has on neutrino decoupling and Matter–radiation equality redshift. If we assume that our effective field theory approach can be extended to energies $\mathcal{O}$ (1 MeV), then, since at those energies neutrinos are still relativistic, and that for a relativistic particle $p\propto T$, where T is the temperature, then:

$$\frac{T_\nu}{T_\gamma}=\left(\frac{8}{11}\right)^{1/3}\left(1-\frac{\lambda\varphi^2}{2}\right)^{-1}, \tag{B.9}$$

with T_ν and T_γ are the temperatures of neutrinos and photons, respectively. Note that the factor $(8/11)^{1/3}$ appears instead of the usual $(4/11)^{1/3}$ is because, at this level in our WKB expansion, neutrinos are approximated as spin 0 particles, therefore Bosons. This result will then change the radiation content today, to be:

$$\Omega_{r0}=\Omega_{\gamma0}\left(1+N_\nu\left(\frac{8}{11}\right)^{1/3}\left(1-\frac{\lambda\varphi^2}{2}\right)^{-1}\right), \tag{B.10}$$

where Ω_{r0} and $\Omega_{\gamma0}$ are the radiation and photon density parameters today, respectively, which are explicitly defined as $\Omega_i=8\pi G\rho_i/3H_0^2$ for a specie i with energy density ρ_i. Matter–radiation equality occurs when

$$\frac{\Omega_{r0}}{a^4_{eq}}=\frac{\Omega_{m0}}{a^3_{eq}}, \tag{B.11}$$

with Ω_{m0} being the density parameter of matter today, and a_{eq} is the scale factor at equilibrium. This gives the redshift at matter–radiation equality to be:

$$1+z_{eq}=\frac{\Omega_{m0}}{\Omega_{\gamma0}}\left[1+N_\nu\left(\frac{8}{11}\right)^{1/3}\left(1-\frac{\lambda\varphi^2}{2}\right)^{-1}\right]^{-1}. \tag{B.12}$$

If we use the latest Planck results [3] for the density parameters, z_{eq} and N_ν, we find $\lambda\varphi^2/2\sim\mathcal{O}(1)$.

B.2. Solution at order $\hbar^1$

At this order, from (B.3), the equation of motion is:

$$\left[\left(1-\frac{\lambda\varphi^2}{2}\right)\not\partial S+m\right]\psi_1=-\left(1-\frac{\lambda\varphi^2}{2}\right)\not p\psi_0 \tag{B.13}$$

which can be used along with the complex conjugate of (B.4) to find that, also with this type of coupling, ψ_0 satisfies (44). However, when written as in (46), the equation that $f(x)$ satisfies is slightly altered:

$$u^\alpha\partial_\alpha f=-\frac{1}{2}\left(1-\frac{\lambda\varphi^2}{2}\right)\tilde\theta f;\quad \tilde\theta=\nabla_\alpha\left[\left(1-\frac{\lambda\varphi^2}{2}\right)^{-1}u^\alpha\right] \tag{B.14}$$

while the one for $\xi_0(x)$ is still the same.

As has been done for the case of the 5th dimensional operator, we divide the Dirac current into convection and magnetization ones, and find the former to be in this case:

$$J^\mu=f^2\left[u^\mu+\frac{\hbar}{2mi}\left(\bar\xi_0\tilde{\mathcal{D}}^\mu\xi_0-\tilde{\mathcal{D}}^\mu\bar\xi_0\xi_0\right)\right]+\mathcal{O}(\hbar^2) \tag{B.15}$$

but now $\tilde{\mathcal{D}}^\mu=\left(1-\frac{\lambda\varphi^2}{2}\right)\mathcal{D}^\mu$. From here, the velocity would be:

$$v^\mu=u^\mu+\frac{\hbar}{2mi}\left(\bar\xi_0\tilde{\mathcal{D}}^\mu\xi_0-\tilde{\mathcal{D}}^\mu\bar\xi_0\xi_0\right) \tag{B.16}$$

and therefore the force that will alter the motion of the $\hbar^0$ order would be:

$$\begin{aligned}\frac{f^\mu}{m}=&\frac{\hbar}{4m}u^\nu g^{\mu\alpha}\left(1-\frac{\lambda\varphi^2}{2}\right)R_{\alpha\nu\gamma\delta}\bar\xi_0\sigma^{\gamma\delta}\xi_0\\&+\frac{u^\nu g^{\mu\alpha}}{\left(1-\frac{\lambda\varphi^2}{2}\right)}\lambda\varphi\left(\partial_\alpha\varphi\delta u_\nu-\partial_\nu\varphi\delta u_\alpha\right)\\&+\frac{\delta u^\beta g^{\mu\alpha}}{2\left(1-\frac{\lambda\varphi^2}{2}\right)}\lambda\varphi\left(u_\alpha\partial_\beta\varphi-\partial_\alpha\varphi u_\beta\right)\end{aligned} \tag{B.17}$$

where

$$\delta u^\mu=\frac{\hbar}{2mi}\left(\bar\xi_0\tilde{\mathcal{D}}^\mu\xi_0-\tilde{\mathcal{D}}^\mu\bar\xi_0\xi_0\right). \tag{B.18}$$

We can see the difference between this interaction and that of the 5th dimension operator. Because the former does alter the dynamics of the species involved, this alteration is manifested as well at first order in WKB, albeit in a slightly complicated way. Note also that there will be no divergence in this force, as we can see from the definition of $\tilde{\mathcal{D}}^\mu$.

We will now consider the last possible operator beyond the SM. We will focus only on the order $\hbar^0$ solution and its implications on the dynamics.

Appendix C. 8 dimensional operator: Non-linear derivative coupling

Consider the case where

$$\Theta=i\hbar\bar\psi\not p\psi\,\partial_\mu\varphi\partial^\mu\varphi \tag{C.1}$$

which gives the equation of motion:

$$\left(i\hbar\not{\partial} - m\right)\psi = \frac{i\hbar\lambda}{2}\psi\,\partial_\mu\varphi\partial^\mu\varphi. \tag{C.2}$$

One can see that the result is very similar to the one in the previous section, under the substitution of φ^2 with $\partial_\mu\varphi\partial^\mu\varphi$. Therefore we will avoid repeating the procedure explained above, and restrict to listing the final relevant results.

At $\hbar^0$ order, the spinor follows:

$$\left[\left(1 - \lambda/2\partial_\mu\varphi\partial^\mu\varphi\right)\not{\partial}S + m\right]\psi_0 = 0 \tag{C.3}$$

and therefore the resulting 4-momentum will take the form:

$$p^\alpha = \left(1 - \lambda/2\partial_\mu\varphi\partial^\mu\varphi\right)\partial^\alpha S. \tag{C.4}$$

Again, with this type of interactions, the vorticity would be non-zero:

$$\omega_{\alpha\beta} = \frac{\lambda X^\gamma_\varphi}{2m\left(1 - \lambda/2(X_\varphi)_\delta X^\delta_\varphi\right)}\left[\nabla_\beta X^\gamma_\varphi p_\alpha - \nabla_\alpha X^\gamma_\varphi p_\beta\right]. \tag{C.5}$$

This results in the following evolution equation for the 4-momentum:

$$\frac{dp^\alpha}{d\tau} + \frac{1}{m}\Gamma^\alpha_{\beta\gamma}p^\beta p^\gamma = -\frac{\lambda(X_\varphi)_\gamma}{m\left(1 - \lambda/2(X_\varphi)_\delta X^\delta_\varphi\right)}\left(m^2 g^{\alpha\beta} + p^\alpha p^\beta\right)\nabla_\beta X^\gamma_\varphi. \tag{C.6}$$

As we did for the 6th dimension operator, we can multiply the above by m and define an $m^2_{\rm eff} = 2m^2\ln\left[1 - \lambda X^\gamma_\varphi(X_\varphi)_\gamma/2\right]$ to get

$$m\frac{dp^\alpha}{d\tau} + \Gamma^\alpha_{\beta\gamma}p^\beta p^\gamma = m_{\rm eff}\frac{dm_{\rm eff}}{dX^\gamma_\varphi}\tilde\nabla^\alpha X^\gamma_\varphi \tag{C.7}$$

where $\tilde\nabla^\alpha = \nabla^\alpha + u^\alpha u^\beta\nabla_\beta$ (boost like operator). This again can be interpreted in terms of mass varying neutrinos, however this time the variation is coming from a kinetic term, i.e thermal motion, while in the 6th dimension case it was due to a potential term of the scalar field. If we now study the dynamics in a flat FRW universe (34), we find the evolution equation for the amplitude of the momentum in cosmic time to be

$$\frac{1}{p}\frac{dp}{dt} + \frac{1}{a}\frac{da}{dt} = -\frac{1}{1 + \frac{\lambda\dot\varphi^2}{2}}\frac{d}{dt}\left(1 + \frac{\lambda\dot\varphi^2}{2}\right), \tag{C.8}$$

and the solution

$$p = \frac{p_0}{\tilde a};\quad \tilde a = a\left(1 + \lambda\dot\varphi^2/2\right). \tag{C.9}$$

The same shift in the evolution of the momentum is happening here as in the 6 dimensional operator, but now the shift is due to a kinetic-like term. The existence of this kinetic term allows us to interpret this redshift in the momentum of the neutrino as being due to the thermal motion of the scalar "particles".

References

[1] A.G. Riess, et al., Observational evidence from supernovae for an accelerating universe and a cosmological constant, Astron. J. 116 (1998) 1009–1038, http://dx.doi.org/10.1086/300499, arXiv:astro-ph/9805201.

[2] S. Perlmutter, et al., Measurements of Omega and Lambda from 42 high redshift supernovae, Astrophys. J. 517 (1999) 565–586, http://dx.doi.org/10.1086/307221, arXiv:astro-ph/9812133.

[3] N. Aghanim, et al., Planck 2018 results. VI. Cosmological parameters, arXiv:1807.06209.

[4] D.N. Spergel, et al., Wilkinson Microwave anisotropy probe (WMAP) three year results: Implications for cosmology, Astrophys. J. Suppl. 170 (2007) 377, http://dx.doi.org/10.1086/513700, arXiv:astro-ph/0603449.

[5] D.J. Eisenstein, et al., Detection of the Baryon acoustic peak in the large-scale correlation function of SDSS luminous red galaxies, Astrophys. J. 633 (2005) 560–574, http://dx.doi.org/10.1086/466512, arXiv:astro-ph/0501171.

[6] M. Colless, et al., The 2dF galaxy redshift survey: Spectra and redshifts, Mon. Not. R. Astron. Soc. 328 (2001) 1039, http://dx.doi.org/10.1046/j.1365-8711.2001.04902.x, arXiv:astro-ph/0106498.

[7] J. Simon, L. Verde, R. Jimenez, Constraints on the redshift dependence of the dark energy potential, Phys. Rev. D 71 (2005) 123001, http://dx.doi.org/10.1103/PhysRevD.71.123001, URL https://link.aps.org/doi/10.1103/PhysRevD.71.123001.

[8] M. Moresco, A. Cimatti, R. Jimenez, L. Pozzetti, G. Zamorani, M. Bolzonella, J. Dunlop, F. Lamareille, M. Mignoli, H. Pearce, Improved constraints on the expansion rate of the Universe up to $z \sim 1.1$ from the spectroscopic evolution of cosmic chronometers, J. Cosmol. Astropart. Phys. 2012 (8) (2012) 006, http://dx.doi.org/10.1088/1475-7516/2012/08/006, arXiv:1201.3609.

[9] M. Moresco, L. Pozzetti, A. Cimatti, R. Jimenez, C. Maraston, L. Verde, D. Thomas, A. Citro, R. Tojeiro, D. Wilkinson, A 6% measurement of the Hubble parameter at $z \sim 0.45$: Direct evidence of the epoch of cosmic re-acceleration, J. Cosmol. Astropart. Phys. 1605 (05) (2016) 014, http://dx.doi.org/10.1088/1475-7516/2016/05/014, arXiv:1601.01701.

[10] C.R. Contaldi, H. Hoekstra, A. Lewis, Joint cosmic microwave background and weak lensing analysis: Constraints on cosmological parameters, Phys. Rev. Lett. 90 (2003) 221303, http://dx.doi.org/10.1103/PhysRevLett.90.221303, arXiv:astro-ph/0302435.

[11] S. Weinberg, The cosmological constant problem, Rev. Modern Phys. 61 (1989) 1–23, http://dx.doi.org/10.1103/RevModPhys.61.1.

[12] S. Weinberg, Theories of the cosmological constant, in: Critical Dialogues in Cosmology, 1996, pp. 195–203, arXiv:astro-ph/9610044.

[13] I. Zlatev, L. Wang, P.J. Steinhardt, Quintessence, cosmic coincidence and the cosmological constant, Phys. Rev. Lett. 82 (1999) 896–899, http://dx.doi.org/10.1103/PhysRevLett.82.896, arXiv:astro-ph/9807002.

[14] H.E.S. Velten, R.F. vom Marttens, W. Zimdahl, Aspects of the cosmological ?coincidence problem? Eur. Phys. J. C 74 (11) (2014) 3160, http://dx.doi.org/10.1140/epjc/s10052-014-3160-4, arXiv:1410.2509.

[15] B. Ratra, P.J.E. Peebles, Cosmological consequences of a rolling homogeneous scalar field, Phys. Rev. D 37 (1988) 3406–3427, http://dx.doi.org/10.1103/PhysRevD.37.3406, URL https://link.aps.org/doi/10.1103/PhysRevD.37.3406.

[16] R.R. Caldwell, R. Dave, P.J. Steinhardt, Cosmological imprint of an energy component with general equation of state, Phys. Rev. Lett. 80 (1998) 1582–1585, http://dx.doi.org/10.1103/PhysRevLett.80.1582, arXiv:astro-ph/9708069.

[17] S. Micheletti, E. Abdalla, B. Wang, A field theory model for dark matter and dark energy in interaction, Phys. Rev. D 79 (2009) 123506, http://dx.doi.org/10.1103/PhysRevD.79.123506, arXiv:0902.0318.

[18] B. Wang, E. Abdalla, F. Atrio-Barandela, D. Pavon, Dark matter and dark energy interactions: Theoretical challenges, cosmological implications and observational signatures, Rep. Progr. Phys. 79 (9) (2016) 096901, http://dx.doi.org/10.1088/0034-4885/79/9/096901, arXiv:1603.08299.

[19] C.G. Böhmer, G. Caldera-Cabral, R. Lazkoz, R. Maartens, Dynamics of dark energy with a coupling to dark matter, Phys. Rev. D 78 (2008) 023505, http://dx.doi.org/10.1103/PhysRevD.78.023505, arXiv:0801.1565.

[20] L. Lopez Honorez, B.A. Reid, O. Mena, L. Verde, R. Jimenez, Coupled dark matter-dark energy in light of near universe observations, J. Cosmol. Astropart. Phys. 2010 (9) (2010) 029, http://dx.doi.org/10.1088/1475-7516/2010/09/029, arXiv:1006.0877.

[21] C. Wetterich, An asymptotically vanishing time-dependent cosmological constant, Astron. Astrophys. 301 (1995) 321, arXiv:hep-th/9408025.

[22] J. Väliviita, E. Majerotto, R. Maartens, Large-scale instability in interacting dark energy and dark matter fluids, J. Cosmol. Astropart. Phys. 2008 (7) (2008) 020, http://dx.doi.org/10.1088/1475-7516/2008/07/020, arXiv:0804.0232.

[23] E. Majerotto, J. Väliviita, R. Maartens, Instability in interacting dark energy and dark matter fluids, Nucl. Phys. B 194 (2009) 260–265, http://dx.doi.org/10.1016/j.nuclphysbps.2009.07.089.

[24] E. Majerotto, J. Väliviita, R. Maartens, Adiabatic initial conditions for perturbations in interacting dark energy models, Mon. Not. R. Astron. Soc. 402 (4) (2010) 2344–2354, http://dx.doi.org/10.1111/j.1365-2966.2009.16140.x, arXiv:0907.4981.

[25] J. Väliviita, R. Maartens, E. Majerotto, Observational constraints on an interacting dark energy model, Mon. Not. R. Astron. Soc. 402 (4) (2010) 2355–2368, http://dx.doi.org/10.1111/j.1365-2966.2009.16115.x, arXiv:0907.4987.

[26] L. Amendola, Perturbations in a coupled scalar field cosmology, Mon. Not. R. Astron. Soc. 312 (3) (2000) 521–530, http://dx.doi.org/10.1046/j.1365-8711.2000.03165.x, arXiv:astro-ph/9906073.

[27] L. Amendola, Coupled quintessence, Phys. Rev. D 62 (4) (2000) 043511, http://dx.doi.org/10.1103/PhysRevD.62.043511, arXiv:astro-ph/9908023.

[28] A.V. Macciò, C. Quercellini, R. Mainini, L. Amendola, S.A. Bonometto, Coupled dark energy: Parameter constraints from N-body simulations, Phys. Rev. D 69 (12) (2004) 123516, http://dx.doi.org/10.1103/PhysRevD.69.123516, arXiv:astro-ph/0309671.

[29] L. Amendola, M. Baldi, C. Wetterich, Quintessence cosmologies with a growing matter component, Phys. Rev. D 78 (2) (2008) 023015, http://dx.doi.org/10.1103/PhysRevD.78.023015, arXiv:0706.3064.
[30] V. Pettorino, L. Amendola, C. Baccigalupi, C. Quercellini, Constraints on coupled dark energy using cmb data from WMAP and South pole telescope, Phys. Rev. D 86 (10) (2012) 103507, http://dx.doi.org/10.1103/PhysRevD.86.103507, arXiv:1207.3293.
[31] L. Lopez Honorez, O. Mena, Instabilities in dark coupled models and constraints from cosmological data, in: J.-M. Alimi, A. Fuözfa (Eds.), in: American Institute of Physics Conference Series, vol. 1241, 2010, pp. 1016–1024, http://dx.doi.org/10.1063/1.3462595, arXiv:0911.3269.
[32] L. Lopez Honorez, B.A. Reid, O. Mena, L. Verde, R. Jimenez, Coupled dark matter-dark energy in light of near universe observations, J. Cosmol. Astropart. Phys. 2010 (9) (2010) 029, http://dx.doi.org/10.1088/1475-7516/2010/09/029, arXiv:1006.0877.
[33] V. Salvatelli, A. Marchini, L. Lopez-Honorez, O. Mena, New constraints on coupled dark energy from the Planck satellite experiment, Phys. Rev. D 88 (2) (2013) 023531, http://dx.doi.org/10.1103/PhysRevD.88.023531, arXiv:1304.7119.
[34] M. Escudero, L. Lopez-Honorez, O. Mena, S. Palomares-Ruiz, P. Villanueva-Domingo, A fresh look into the interacting dark matter scenario, J. Cosmol. Astropart. Phys. 2018 (6) (2018) 007, http://dx.doi.org/10.1088/1475-7516/2018/06/007, arXiv:1803.08427.
[35] M.B. Gavela, D. Hernández, L. Lopez Honorez, O. Mena, S. Rigolin, Dark coupling, J. Cosmol. Astropart. Phys. 2009 (7) (2009) 034, http://dx.doi.org/10.1088/1475-7516/2009/07/034, arXiv:0901.1611.
[36] F. Simpson, R. Jimenez, C. Pena-Garay, L. Verde, Dark energy from the motions of neutrinos, Phys. Dark Universe 20 (2018) 72, http://dx.doi.org/10.1016/j.dark.2018.04.002, arXiv:1607.02515.
[37] N. Birrell, P. Davies, Quantum Fields in Curved Space, in: Cambridge Monographs on Mathematical Physics, Cambridge Univ. Press, Cambridge, UK, 1984, http://dx.doi.org/10.1017/CBO9780511622632, chapter 3.8.
[38] V. Mukhanov, S. Winitzki, Introduction to Quantum Effects in Gravity, Cambridge University Press, 2007.
[39] B. Kayser, On the quantum mechanics of neutrino oscillation, Phys. Rev. D 24 (1981) 110–116, http://dx.doi.org/10.1103/PhysRevD.24.110, URL https://link.aps.org/doi/10.1103/PhysRevD.24.110.
[40] C. Giunti, C.W. Kim, Fundamentals of Neutrino Physics and Astrophysics, 2007.
[41] C.Y. Cardall, G.M. Fuller, Neutrino oscillations in curved spacetime: A heuristic treatment, Phys. Rev. D 55 (1997) 7960–7966, http://dx.doi.org/10.1103/PhysRevD.55.7960, URL https://link.aps.org/doi/10.1103/PhysRevD.55.7960.
[42] M. Lanzagorta, Quantum Information in Gravitational Fields, Morgan & Claypool Publishers, 2014, pp. 2053–2571, http://dx.doi.org/10.1088/978-1-627-05330-3, chapter 5.
[43] Carl M. Bender, Steven A. Orszag, Advanced Mathematical Methods for Scientists and Engineers, Springer NY, New York, 1999, chapter 10.
[44] Jun John Sakurai, Jim Napolitano, Modern Quantum Mechanics, in: Quantum Physics, Quantum Information and Quantum Computation, Cambridge University Press, chapter 2.5.
[45] David J. Griffiths, Introduction to Quantum Mechanics, Pearson Prentice Hall, Upper Saddle River, NJ, 2005, Print.
[46] O.K. Reity, V.Y. Lazur, WKB method for the dirac equation with the central-symmetrical potential and its application to the theory of two dimensional supercritical atoms, in: eConf C0107094, 2001, pp. 676–682.
[47] O.K. Reity, V.V. Rubish, S.I. Myhalyna, The WKB method for the Dirac equation with vector-scalar potentials in 2+1 and 3+1 dimensions, in: eConf C0306234, 2003, pp. 1429–1434.
[48] J.W. Van Orden, S. Jeschonnek, J. Tjon, Scaling of Dirac fermions and the WKB approximation, Phys. Rev. D 72 (2005) 054020, http://dx.doi.org/10.1103/PhysRevD.72.054020.
[49] J. Bolte, S. Keppeler, Ann. Physics 274 (125) (1999) http://dx.doi.org/10.1006/aphy.1999.5912.
[50] R. Fardon, A.E. Nelson, N. Weiner, Dark energy from mass varying neutrinos, J. Cosmol. Astropart. Phys. 2004 (10) (2004) 005, http://dx.doi.org/10.1088/1475-7516/2004/10/005.
[51] A.W. Brookfield, C. van de Bruck, D.F. Mota, D. Tocchini-Valentini, Cosmology of mass-varying neutrinos driven by quintessence: Theory and observations, Phys. Rev. D 73 (2006) 083515, http://dx.doi.org/10.1103/PhysRevD.73.083515, URL https://link.aps.org/doi/10.1103/PhysRevD.73.083515.

Physics of the Dark Universe 34 (2021) 100897

Contents lists available at ScienceDirect

Physics of the Dark Universe

journal homepage: www.elsevier.com/locate/dark

Distinguishing Dark Energy models with neutrino oscillations

Ali Rida Khalifeh [a,b,*], Raul Jimenez [a,c]

[a] ICC, University of Barcelona, Marti i Franques, 1, E-08028 Barcelona, Spain
[b] Dept. de Fisica Cuantica y Astrofisica, University of Barcelona, Marti i Franques 1, E-08028 Barcelona, Spain
[c] ICREA, Pg. Lluis Companys 23, Barcelona, E-08010, Spain

ARTICLE INFO

Article history:
Received 28 May 2021
Received in revised form 30 August 2021
Accepted 12 October 2021

Keywords:
Spinors in curved spacetime
Neutrino oscillation
Dark Energy

ABSTRACT

Dark Energy models are numerous and distinguishing between them is becoming difficult. However, using distinct observational probes can ease this quest and gives better assessment to the nature of Dark energy. To this end, the plausibility of neutrino oscillations to be a probe of Dark Energy models is investigated. First, a generalized formalism of neutrino (spinor field) interaction with a classical scalar field in curved space–time is presented. This formalism is then applied to two classes of Dark Energy models in a flat Friedman–Lemaître–Robertson–Walker metric: a Cosmological Constant and scalar field Dark Energy coupled to neutrinos. By looking at the neutrino oscillation probability's evolution with redshift, these models can be distinguished, for certain neutrino and scalar field coupling properties. This evolution could be traced by neutrino flux measurements in future underground, terrestrial or extraterrestrial, neutrino telescopes which would assess probing Dark Energy models with this technique.

1. Introduction

Since the discovery of the accelerated expansion of the Universe [1,2], one of the most interesting open questions in Astrophysics and Cosmology is to understand if Dark Energy(DE) is dynamic, or instead strictly a constant. Indeed, if DE was shown to be dynamical, this would be a major revolution, as it would indicate a great deal of new physics. However, recent observational constraints indicate that DE is consistent with a cosmological constant, with a few percent uncertainty [3]. Current and upcoming cosmological surveys, such as DESI [4] and Euclid [5] will decrease this level of uncertainty to the % level [6]. Nevertheless, theoretical arguments have been presented over the years in favor of a dynamical DE, due to fundamental issues accompanied by a constant one, such as the coincidence problem [7], see also [8–10].

In order to lift this dilemma, one could combine several probes and techniques to constraint DE models. In addition to the already mentioned probes, as well as Gravitational Waves surveys [11–13], looking at neutrinos could open a new window to the nature of DE. Several Cosmological probes have been used to constrain neutrino properties in the context of a flat Friedman–Lemaître–Robertson–Walker(FLRW) Universe [14–19]. However, neutrinos have been mostly considered as classical point particles, rather than quantum spinor fields traveling in curved spacetime, which could provide novel insights for both neutrinos and DE. An interaction between spinor and scalar fields is sensible to our spacetime's curved geometry, which could leave observational imprints. This shows the advantage of using Cosmology to understand properties of the Universe, for it can thus give information on both Gravity and neutrinos.

Studying neutrinos as quantum spinors in curved spacetime have been done in several theoretical contexts, such as near Schwarzschild Blackholes [20], in extended theories of gravity [21] or to derive fundamental uncertainty relations [22,23]. More specifically to dynamical DE, neutrinos have been investigated in the context of mass-varying neutrinos [24–28], pseudo-Dirac particles [29,30] or Lorentz/*CPT* violating theories [31,32], where *CPT* stands for Charge Conjugation(C), Parity(P) and Time reversal(T) symmetries. It would be interesting therefore to expand on these works to produce an observational trace of this kind of interactions.

As a first step along this way, one of us proposed a model, called DE_ν, in which a scalar field is "frozen" in place via an interaction with neutrino [33]. This model, by construction, mimics a cosmological constant from the point of view of cosmological observables (expansion history and perturbations) and thus it does not leave any significant imprint in these classical observables. We then expanded upon that work [34], and looked at DE_ν in the context of quantum spinors in curved spacetime, in addition to beyond Standard Model scalar–spinor interactions.

* Corresponding author at: ICC, University of Barcelona, Marti i Franques, 1, E-08028 Barcelona, Spain.
E-mail addresses: ark93@icc.ub.edu (A.R. Khalifeh), raul.jimenez@icc.ub.edu (R. Jimenez).

https://doi.org/10.1016/j.dark.2021.100897

In this work, we further develop Ref. [34], as well as the works previously mentioned, to produce an observable that could be measured experimentally, which can then differentiate between DE models. We look at a more general massive spinor–scalar field interaction(Section 2), and then derive a generalized formula for the oscillation probability in an arbitrary spacetime(Section 3). Although a scalar field DE scenario does not include all types of DE, nevertheless it incorporates a large class of DE models, including scalar–tensor theories of gravity such as Horndeski [35,36]. That is the reason why we focus on such an interaction here. Afterwards, we specify to cosmological constant DE(Section 4.1), what is known as ΛCDM model, and quintessence [37,38] with a neutrino–scalar interaction as presented in the DE$_\nu$ model (Section 4.2). For the latter, we look at various neutrino and DE$_\nu$ properties and compare them to the former model. We finish by presenting a summary and future prospects(Section 5).

Throughout the paper, we use units in which $\hbar = c = 1$, where c is the speed of light and $\hbar$ is the reduced Planck constant. Moreover, the metric signature we use is the mostly positive one, $(-,+,+,+)$, and Greek indices will be used for spacetime coordinates $(0,1,2,3)$, while Latin ones are dedicated for spatial coordinates only, $(1,2,3)$. In addition, for neutrino states notations, we use Greek and Latin indices to describe flavor and mass states, respectively.

2. Generalized formalism

Let us consider a general interaction of a spinor field, ψ, with a classical scalar field, φ, in curved spacetime with metric $g_{\mu\nu}$. This is described by the following action:

$$S = \int d^4x\sqrt{-g}\Big[\frac{1}{2}R - \frac{1}{2}\mathcal{D}_\mu\varphi D^\mu\varphi - V(\varphi) + i\big(\bar\psi\gamma^\mu\mathcal{D}_\mu\psi - \mathcal{D}_\mu\bar\psi\gamma^\mu\psi\big) - 2m\bar\psi\psi + \zeta\Theta\Big]. \tag{1}$$

In here, g is the determinant of $g_{\mu\nu}$ and R is the Ricci scalar, the trace of the Ricci tensor $R_{\mu\nu}$. Moreover, $\mathcal{D}_\mu$ is a generalized covariant derivative for fields with different spins in curved spacetime (see Ref.[39–41] for more details on quantum fields in curved backgrounds). For example, when acting a particle of spin 0, $\mathcal{D}_\mu$ reduces to ∂_μ, the usual partial derivative in flat spacetime. We will see shortly the form it takes when acting on spinors. Another term that appears in (1) is the scalar field potential $V(\varphi)$, which describes self interactions of φ. Furthermore, $\gamma^\mu = \{\gamma^0,\gamma^1,\gamma^2,\gamma^3\}$ are the four Dirac matrices, $\bar\psi = \psi^\dagger\gamma^0$, with $\psi^\dagger$ being the complex transpose of ψ, and m is the spinor field's mass. Finally, ζ is the coupling constant for the general interaction term between ψ and φ, $\Theta\big(\psi,\bar\psi,\varphi,X^\mu_\psi,X^\mu_{\bar\psi},X^\mu_\varphi\big)$, with $X^\mu_\psi\big(X^\mu_{\bar\psi}\big) = \mathcal{D}^\mu\psi\big(\mathcal{D}^\mu\bar\psi\big)$ and $X^\mu_\varphi = \partial^\mu\varphi$.

By setting the variational derivative of the action (1) with respect to(w.r.t) $\bar\psi$ to 0, we get the modified Dirac equation for ψ, i.e.

$$\frac{1}{\sqrt{-g}}\frac{\delta S}{\delta\bar\psi} = 0 \quad\Rightarrow\quad \big(i\gamma^\mu\mathcal{D}_\mu - m\big)\psi = -\frac{\zeta}{2}\left(\frac{\partial\Theta}{\partial\bar\psi} - \mathcal{D}^\mu\frac{\partial\Theta}{\partial X^\mu_{\bar\psi}}\right) \equiv -\frac{\zeta}{2}\frac{\delta\Theta}{\delta\bar\psi}. \tag{2}$$

At this stage, one could say that the interaction is of the most general form, for neither Θ nor the metric have been specified. However, as we are considering a more phenomenological approach to the question at hand, it would be more useful to look for a practical form of the variational derivative of Θ w.r.t $\bar\psi$. This would allow us to calculate observables that could be eventually measured by experiments. Moreover, it would prove useful to divide the interaction term into flavor-invariant and flavor-dependent parts, to study how each would affect the transition probability from one flavor state to another. Intuitively, one would expect that the former should not modify this flavor oscillation probability, since by definition the latter is a transition between flavors. However, as we will see in the next section, this is not always the case.

There are several ways in which one can implement these considerations. For instance, in order to have the right hand side(r.h.s) of (2) mathematically and dimensionally consistent with its left hand side(l.h.s), one possibility is:

$$-\frac{\zeta}{2}\frac{\delta\Theta}{\delta\bar\psi} = \big(\xi\gamma^\mu F_\mu(\varphi,X^\mu_\varphi) + \xi_f G(\varphi,X^\mu_\varphi)\big)\psi. \tag{3}$$

The first term on the r.h.s is a global interaction in flavor space, i.e. it couples to all flavors with the same strength ξ. On the other hand, the second term is a flavor-specific term, with the coupling strength ξ_f depending on which flavor is being considered. Another term that could be added is a kinetic coupling, such as $\xi F(\varphi,X^\mu_\varphi)\gamma^\mu\mathcal{D}_\mu\psi$. However, as such a term could produce effects on other Cosmological observables(see appendix in [34]), we will not be considering it here. Finally, for the purpose we seek of studying ΛCDM and quintessence(in the context of DE$_\nu$), it turns out that having

$$-\frac{\zeta}{2}\frac{\delta\Theta}{\delta\bar\psi} = \big(\xi F(\varphi,X^\mu_\varphi) + \xi_f\gamma^\mu G_\mu(\varphi,X^\mu_\varphi)\big)\psi. \tag{4}$$

is more useful, and will therefore be used in the following sections

3. Neutrino oscillation

In this section, for simplicity, we will be studying two-flavor neutrino oscillation in curved space–time, although one could generalize the analysis to three-flavor oscillations (see Ref. [20–22] for more details on neutrino oscillations in curved space–time). In addition, a more stringent study of neutrino oscillations in curved backgrounds would rely on the full quantum field theoretic treatment (see Ref. [23,42] and references within for further details). However, for the purpose of studying neutrino interaction with DE, the quantum mechanical treatment presented here is sufficient for comparison with observations. We will look at the quantum field theoretic treatment for both fields in future works.

3.1. Transition amplitude's evolution

The first step in studying neutrino oscillations is to expand a state of flavor α, $|\nu_\alpha\rangle$, in terms of mass eigenstates, $|\nu_j\rangle$:

$$|\nu_\alpha(\lambda)\rangle = \sum_{j=1,2} U_{\alpha j}e^{i\Phi(\lambda)}|\nu_j\rangle, \tag{5}$$

where λ is the monotonically increasing affine parameter along the neutrino world-line and $U_{\alpha j}$ is the two-flavor mixing matrix, given by:

$$U = \begin{pmatrix}\cos\theta & \sin\theta\\ -\sin\theta & \cos\theta\end{pmatrix} \tag{6}$$

with θ being the mixing angle. Moreover, $\Phi(\lambda)$ is the mass eigenstate's evolution operator [20]:

$$\Phi(\lambda) = \int_{\lambda_0}^{\lambda} P_\mu\frac{dx^\mu}{d\lambda'}d\lambda' \tag{7}$$

where P^μ is the 4-momentum operator, $dx^\mu/d\lambda$ is a null vector tangent to the neutrino world-line, and $\lambda_0(\lambda)$ is the affine parameter's value at the observer(source).

One can see that Eq. (5) is a solution for the Schrödinger like equation

$$i\frac{d}{d\lambda}|\nu_\alpha(\lambda)\rangle = \Phi(\lambda)|\nu_\alpha(\lambda)\rangle, \tag{8}$$

and therefore the transition amplitude between states α and β,

$$\Psi_{\alpha\beta} = \langle\nu_\beta|\nu_\alpha(\lambda)\rangle, \tag{9}$$

satisfies

$$i\frac{d}{d\lambda}\Psi_{\alpha\beta} = \Phi(\lambda)\Psi_{\alpha\beta}. \tag{10}$$

The ultimate goal is to find the transition probability between flavors α and β, i.e.

$$P_{\beta\to\alpha} = |\Psi_{\alpha\beta}|^2 = |\langle\nu_\beta|\nu_\alpha(\lambda)\rangle|^2, \tag{11}$$

and therefore we need to calculate $\Phi(\lambda)$, or more specifically, $P_\mu dx^\mu/d\lambda$, as has been pointed out before [20,34].

For the purpose at hand, let us start with a system of two-flavors, electron and muon neutrinos ν_e and ν_μ, respectively, that is $\alpha, \beta = e, \mu$. Let

$$\boldsymbol{\psi} = \begin{pmatrix}\psi_e\\ \psi_\mu\end{pmatrix}, \tag{12}$$

be a vector of spinor fields. The modified Dirac equation (2) for this system becomes:

$$\left(i\gamma^\mu\mathcal{D}_\mu - \mathcal{M}_f\right)\boldsymbol{\psi} = \left(\xi F(\varphi, X^\mu_\varphi) + \xi_f\gamma^\mu G_\mu(\varphi, X^\mu_\varphi)\right)\boldsymbol{\psi} \tag{13}$$

where the vacuum mass matrix in flavor space is given by

$$\mathcal{M}_f^2 = U\begin{pmatrix}m_1^2 & 0\\ 0 & m_2^2\end{pmatrix}U^\dagger \tag{14}$$

with m_1, m_2 being the masses of mass states $|\nu_1\rangle, |\nu_2\rangle$, respectively.

Now we introduce the explicit form of the covariant derivative $\mathcal{D}_\mu$. As explained in Ref. [39,40], when studying spinors in curved spacetime, one needs to introduce a local inertial coordinate system, with its own set of Dirac matrices γ^a, and link it to the general one using tetrad fields e^μ_a, where Greek indices correspond to general coordinates, while Latin ones for the local system. With this, we can write

$$\gamma^\mu\mathcal{D}_\mu = \gamma^a e^\mu_a\left(\partial_\mu + \Gamma_\mu\right) \tag{15}$$

where

$$\Gamma_\mu = \frac{1}{8}\left[\gamma^b, \gamma^c\right]e^\nu_b\nabla_\mu e_{c\nu} \tag{16}$$

is called the spin-connection which takes into account the gravitational effect on the particle's spin. In Eq. (16), $[\gamma^b, \gamma^c]$ is the commutator of γ^a and γ^b, and ∇_μ is the usual covariant derivative of General Relativity [43]. With these relations, one can then show that

$$\gamma^a e^\mu_a\Gamma_\mu = i\gamma^a e^\mu_a A_{G\mu} \tag{17}$$

with

$$A^\mu_G = \frac{1}{4}\sqrt{-g}e^\mu_a\epsilon^{abcd}(\partial_\sigma e_{b\nu} - \partial_\nu e_{b\sigma})e^\nu_c e^\sigma_d \tag{18}$$

where ϵ^{abcd} is the local four dimensional Levi-Civita symbol. Inserting Eqs. (15), (17) and (18) in Eq. (13) and moving all terms to the l.h.s, we get:

$$\left\{i\gamma^\mu\left[\partial_\mu + i\left(A_{G\mu} + \xi_f G_\mu\right)\right] - \left[\mathcal{M}_f - \xi F\right]\right\}\boldsymbol{\psi} = 0. \tag{19}$$

In order to get non-trivial solutions for the above system, the determinant of the braces must be 0. This results in a modified mass–shell relation:

$$\left(P^\mu + A^\mu\right)\left(P_\mu + A_\mu\right) = \tilde{\mathcal{M}}_f^2, \tag{20}$$

where $A^\mu = A^\mu_G + \xi_f G_\mu$ and

$$\tilde{\mathcal{M}}_f^2 = U\begin{pmatrix}\tilde{m}_1^2 & 0\\ 0 & \tilde{m}_2^2\end{pmatrix}U^\dagger \tag{21}$$

with $\tilde{m}_i = m_i - \xi F$ for $i = 1, 2$. It should be noted here that $\tilde{m}$ is not a mass-varying neutrino, rather an effective mass due to the interaction with another field (see [24–26] for comparison). From Eq. (20), one can show that

$$P_\mu\frac{dx^\mu}{d\lambda} = \frac{1}{2}\tilde{\mathcal{M}}_f^2 - \frac{dx^\mu}{d\lambda}A_\mu, \tag{22}$$

which finally implies, from Eqs. (7) and (10), that

$$i\frac{d}{d\lambda}\Psi_{\alpha\beta} = \left[\frac{1}{2}\tilde{\mathcal{M}}_f^2 + V_I\right]\Psi_{\alpha\beta}, \tag{23}$$

with $V_I = -A_\mu dx^\mu/d\lambda$. In deriving Eq. (22), two well motivated assumptions have been made based on the fact that we are focusing on high energy neutrinos [20,34]. First, we consider neutrinos as energy eigenstates, i.e. $P^0 = dx^0/d\lambda$, and second, P^i and $dx^i/d\lambda$ are assumed parallel, that is $P^i = (1-\varepsilon)dx^i/d\lambda$, with $\varepsilon \ll 1$ for high-energy neutrinos.[1]

3.2. Transition probability

Let us now be more explicit, and look at each component of Eq. (23). With some matrix algebra, it can be shown that

$$\tilde{\mathcal{M}}_f^2 = \left(\tilde{m}_1^2 + \frac{1}{2}\tilde{\Delta}\right)I + \frac{1}{2}\tilde{\Delta}\begin{pmatrix}-\cos 2\theta & \sin 2\theta\\ \sin 2\theta & \cos 2\theta\end{pmatrix}, \tag{24}$$

where I is the 2×2 identity matrix in flavor space and $\tilde{\Delta}^2_m = \tilde{m}_2^2 - \tilde{m}_1^2 = \Delta^2_m - 2\xi F\Delta_m$(up to 1^{st} order in ξ), with $\Delta^2_m = m_2^2 - m_1^2$ and $\Delta_m = (m_2 - m_1)$. Note the resemblance to the MSW effect [44,45], with the difference being that interactions with matter are substituted by those with spacetime and DE. Also, it is safe to ignore the term proportional to I in Eq. (24), since it is common for both transition amplitudes, and therefore will cancel when we calculate the probability. If we start initially from a ν_e state, for instance, the evolution equation for the transition amplitudes becomes:

$$\begin{aligned} i\frac{d}{d\lambda}\begin{pmatrix}\Psi_{ee}\\ \Psi_{e\mu}\end{pmatrix} &= \begin{pmatrix}-\frac{1}{4}\tilde{\Delta}^2_m\cos 2\theta + \xi_e V_I & \frac{1}{4}\tilde{\Delta}^2_m\sin 2\theta\\ \frac{1}{4}\tilde{\Delta}^2_m\sin 2\theta & \frac{1}{4}\tilde{\Delta}^2_m\cos 2\theta + \xi_\mu V_I\end{pmatrix}\\ &\quad\times\begin{pmatrix}\Psi_{ee}\\ \Psi_{e\mu}\end{pmatrix}\\ &\equiv \boldsymbol{M}\begin{pmatrix}\Psi_{ee}\\ \Psi_{e\mu}\end{pmatrix}. \end{aligned} \tag{25}$$

Notice that the gravitational contribution $A_{G\mu}$ has been dropped from the interaction term. This is because it is proportional to I in flavor space, and therefore does not contribute to the oscillation probability [20]. In addition to that, in spatially homogeneous and isotropic universes, such as FRW, this term is 0 identically [34].

[1] The second condition can be relaxed since we are eventually taking the inner product of the two vectors, so that the perpendicular part does not contribute.

From Eq. (25), we can proceed by diagonalizing $\boldsymbol{M}$, which has

$$v_{\pm} = \frac{1}{4}\Big[2\big(\xi_e+\xi_\mu\big)V_l \pm \sqrt{\big[\tilde{\Delta}_m^2\cos 2\theta - 2V_l(\xi_e-\xi_\mu)\big]^2 + (\tilde{\Delta}_m^2)^2\sin^2 2\theta}\Big] \tag{26}$$

as eigenvalues, and

$$\tilde{U} = \begin{pmatrix} \cos\tilde{\theta} & \sin\tilde{\theta} \\ -\sin\tilde{\theta} & \cos\tilde{\theta} \end{pmatrix} \tag{27}$$

as the unitary matrix that diagonalizes it, with[2]

$$\cos 2\tilde{\theta} = \frac{\tilde{\Delta}_m^2\cos 2\theta - 2V_l\big(\xi_e-\xi_\mu\big)}{\sqrt{\big[\tilde{\Delta}_m^2\cos 2\theta - 2V_l\big(\xi_e-\xi_\mu\big)\big]^2 + (\tilde{\Delta}_m^2)^2\sin^2 2\theta}};$$
$$\sin 2\tilde{\theta} = \frac{\tilde{\Delta}_m^2\sin 2\theta}{\sqrt{\big[\tilde{\Delta}_m^2\cos 2\theta - 2V_l\big(\xi_e-\xi_\mu\big)\big]^2 + (\tilde{\Delta}_m^2)^2\sin^2 2\theta}}. \tag{28}$$

In analogy with the flavor–mass bases transformation, let us define

$$\boldsymbol{\phi}_e \equiv \begin{pmatrix}\phi_{e-}\\ \phi_{e+}\end{pmatrix} = \tilde{U}^T\begin{pmatrix}\Psi_{ee}\\ \Psi_{e\mu}\end{pmatrix}, \tag{29}$$

as a vector of transition amplitudes in an effective mass basis, $\{v_-, v_+\}$, that takes into account the neutrino interaction with gravity and DE. Using the unitarity of $\tilde{U}$ and Eq. (25), it can be shown that $\boldsymbol{\phi}_e$ satisfies:

$$i\frac{d}{d\lambda}\begin{pmatrix}\phi_{e-}\\ \phi_{e+}\end{pmatrix} = \begin{pmatrix} v_- & -i\frac{d\tilde{\theta}}{d\lambda} \\ i\frac{d\tilde{\theta}}{d\lambda} & v_+ \end{pmatrix}\begin{pmatrix}\phi_{e-}\\ \phi_{e+}\end{pmatrix}. \tag{30}$$

Notice that the off-diagonal terms come from transforming the l.h.s of Eq. (25). Also, in the case where there is no mixing between effective mass states, then $d\tilde{\theta}/d\lambda = 0$, and the transition amplitudes evolve as:

$$\phi_{ej} = \big(\cos\omega_j + i\sin\omega_j\big)\phi_{ej}(0) \tag{31}$$

for $j = +, -$, where $\phi_{ej}(0)$ is the initial condition and

$$\omega_j(\lambda) = \int_{\lambda_0}^{\lambda} v_j d\lambda'. \tag{32}$$

This is known as the adiabatic evolution condition which, as we will see in the next section, applies to the DE scenarios we will examine. Further, one important consequence of adiabaticity is that the flavor-specific interaction will be constant along the neutrino's world-line. To see this, differentiate $\cos 2\tilde{\theta}$ from Eq. (28) w.r.t λ:

$$\frac{d\tilde{\theta}}{d\lambda} = \frac{\sin 2\tilde{\theta}}{\Delta_m}\left\{-2\xi\,\Delta_m\frac{dF}{d\lambda}\left[\frac{\cos 2\tilde{\theta}\sin 2\theta}{\sin 2\tilde{\theta}} - \cos 2\theta\right] + \frac{dV_l}{d\lambda}(\xi_e-\xi_\mu)\right\}. \tag{33}$$

Since we expect gravitational and DE effects to be small compared to the vacuum oscillations, that is $\xi, \xi_f \ll 1$, we can keep terms up to first order in these coupling constants. With this assumption, by setting Eq. (33) to 0, we find that $dV_l/d\lambda = 0$. This is again another analogy with the MSW effect, where in adiabatic oscillations the interaction term is constant along the path [46].

The final ingredient we need to get the oscillation probability is initial conditions. As we are considering an initial ν_e state, we can write

$$\boldsymbol{\phi}_e(0) \equiv \begin{pmatrix}\phi_{e-}(0)\\ \phi_{e+}(0)\end{pmatrix} = \begin{pmatrix}\cos\tilde{\theta} & -\sin\tilde{\theta}\\ \sin\tilde{\theta} & \cos\tilde{\theta}\end{pmatrix}\begin{pmatrix}1\\0\end{pmatrix} = \begin{pmatrix}\cos\tilde{\theta}\\ \sin\tilde{\theta}\end{pmatrix}, \tag{34}$$

where, by construction, an initial ν_e state corresponds to $\Psi_{ee}(0) = 1$ and $\Psi_{e\mu}(0) = 0$. By acting with the inverse transformation of Eq. (29), we can calculate the amplitude $\Psi_{e\mu}$, and thus, with the initial conditions Eq. (34), we finally obtain the $\nu_e \to \nu_\mu$ transition probability:

$$P_{\nu_e\to\nu_\mu} = |\Psi_{e\mu}|^2 = \sin^2 2\tilde{\theta}\sin^2\left(\frac{\omega_- - \omega_+}{2}\right). \tag{35}$$

Let us now look in more detail into the oscillating term in Eq. (35). If we use the above mentioned approximation ($\xi, \xi_f \ll 1$), one can show that

$$\begin{aligned}\omega_- - \omega_+ &= \int_{\lambda_0}^{\lambda}(v_- - v_+)d\lambda' \\ &\approx \frac{\Delta_m^2}{2}(\lambda_0-\lambda) + V_l\cos 2\theta(\xi_e-\xi_\mu)(\lambda-\lambda_0) \\ &\quad + \xi\,\Delta_m\int_{\lambda_0}^{\lambda} F d\lambda'.\end{aligned} \tag{36}$$

The first term in Eq. (36) corresponds to the usual vacuum oscillation term. Indeed, if one neglects the interactions completely, i.e. $F = G = 0$, and consider Minkowski spacetime, that is $d\lambda = dt/E = dx/E$, we get

$$\omega_- - \omega_+ = \omega_{\rm std} \equiv \frac{\Delta_m^2 L}{2E} \tag{37}$$

where L is the distance traveled by the neutrinos. This results in

$$P^{\rm std}_{\nu_e\to\nu_\mu} = \sin^2 2\theta\sin^2\left(\frac{\Delta_m^2 L}{4E}\right). \tag{38}$$

which is the standard vacuum transition probability in flat spacetime [46]. The second term in Eq. (36) is the flavor-specific correction, and the third term is an integrated correction from the flavor-invariant interaction. This is where we see that the latter does affect the transition probability, both in amplitude, through $\sin 2\tilde{\theta}$ in Eq. (35), and in period.

Let us finish the analysis by writing a Signal-to-Noise-like expression for the oscillation probability Eq. (35). If we substitute the expression for $\sin 2\tilde{\theta}$ from Eq. (28) into Eq. (35), and then expand all functions of the interactions up to 1st order, we get

$$\frac{\delta P}{P} \equiv \frac{P_{\nu_e\to\nu_\mu} - P^{\rm vac}_{\nu_e\to\nu_\mu}}{P^{\rm vac}_{\nu_e\to\nu_\mu}} = \frac{4V_l(\xi_e-\xi_\mu)}{\Delta_m^2} + \cot\left(\frac{1}{2}\omega_{\rm vac}\right)\omega_{\rm DE}, \tag{39}$$

where

$$P^{\rm vac}_{\nu_e\to\nu_\mu} = \sin^2 2\theta\sin^2\omega_{\rm vac} \tag{40}$$

is the transition probability in vacuum, with frequency

$$\omega_{\rm vac} = \frac{\Delta_m^2}{2}(\lambda_0-\lambda), \tag{41}$$

and

$$\omega_{\rm DE} = V_l\cos 2\theta(\xi_e-\xi_\mu)(\lambda-\lambda_0) + \xi\,\Delta_m\int_{\lambda_0}^{\lambda} F d\lambda' \tag{42}$$

is the additional contribution to the oscillation frequency due to the interaction with DE.

In this section, we looked at how a type of general interactions between neutrinos and DE, in a generic spacetime, can affect the probability of oscillations, with the final result given in Eq. (35).

[2] One way of deriving Eq. (28) is to perform the matrix product $\tilde{U}^T\boldsymbol{M}\tilde{U}$, and equate it to diag$\{v_-, v_+\}$.

Now we can specify the interaction to known DE models, particularly a cosmological constant and scalar field based DE, and thus establish the distinction between them.

4. Oscillation probability for specific DE models

As mentioned in the Introduction 1, we have focused on the interaction of neutrinos with scalar fields since the latter includes a large class of DE models, such as some modified gravity scenarios and Quintessence. Having established a general formalism for the interaction of neutrinos with a scalar field in the previous section, we will now focus on two DE energy models: a Cosmological Constant Λ and Quintessence.

4.1. ΛCDM

This model is the simplest model describing our Universe, and has sustained a great deal of observational test [3,47]. Taking GR as the theory of gravity, ΛCDM has two main components in the late universe: a cosmological constant DE, Λ, and cold Dark Matter(CDM). The metric of spacetime that best describes it is FLRW:

$$ds^2 = -dt^2 + a^2(t)\delta_{ij}dx^i dx^j, \tag{43}$$

where t is cosmic time, x^i, for $i = 1, 2, 3$, are comoving spatial coordinates, δ_{ij} is the Kronecker delta and $a(t)$ is the scale factor that incorporates the universe's expansion. The resulting evolution equation for the scale factor will be the usual first Friedmann equation:

$$H^2 = H_0^2\left(\Omega_{m_0}a^{-3} + \Omega_{\Lambda_0}\right), \tag{44}$$

where $H = \dot{a}/a$ is the Hubble parameter, with H_0 being its value today and Ω_{m0}, $\Omega_{\Lambda 0}$ are today's matter and Λ density parameters, respectively, with the most recent measurement given by the Planck Collaboration [3]. Note that this equation is not altered for two reasons. First, we are considering gravity in terms of the background spacetime, and not from a quantum perspective, hence Einstein equations, from which Eq. (44) is derived, are still the same. Second, the neutrino density parameter has not been added since it is small compared to that of matter and Λ [48].

To see the effect of DE in this model on neutrino oscillations, let us start by noting that when DE is Λ, $\xi = \xi_f = 0$ in Eq. (4), implying the automatic satisfaction of the adiabaticity condition, $d\tilde{\theta}/d\lambda = 0$, from Eq. (33), and thus $\sin\tilde{\theta}(\cos\tilde{\theta}) = \sin\theta(\cos\theta)$. Therefore, from the first equality in Eq. (36), we define

$$\omega_\Lambda \equiv \omega_- - \omega_+\big|_{DE=\Lambda} = \frac{\Delta_m^2}{2}\int_{t_{\rm em}}^{t_0}\frac{1}{E}dt, \tag{45}$$

with the second equality meaning Eq. (36) when DE is Λ. Here, t_0 is today, $t_{\rm em}$ is the time of neutrino emission and $E = dt/d\lambda$ is the $0^{\rm th}$ component of the null tangent vector $dx^\mu/d\lambda$, which is also the neutrino's energy. Since the latter follows the geodesic equation, as shown in [20,34], then $E = E_0/a$, with E_0 being the neutrino energy at detection, and thus, using Eq. (44),

$$\begin{aligned}\omega_\Lambda &= \frac{\Delta_m^2}{2H_0E_0}\int_{a_{\rm em}}^{1}\left(\Omega_{m_0}a^{-3} + \Omega_{\Lambda_0}\right)^{-1/2}da \\ &= \frac{\Delta_m^2}{2H_0E_0}\int_0^{z_{\rm em}}\left(\Omega_{m_0}(1+z)^7 + \Omega_{\Lambda_0}(1+z)^4\right)^{-1/2}dz,\end{aligned} \tag{46}$$

where $a_{\rm em}(z_{\rm em})$ is the scale factor(redshift) at neutrino emission, and with the usual normalization $a_0 = 1$ and $z_0 = 0$. On the other hand, if one takes a simple approach (SA) to neutrino oscillations in an expanding universe, and substitutes L and E in Eq. (38) by the luminosity distance,

$$D_L = (1+z_e)H_0^{-1}\int_0^{z_e}\left(\Omega_{m_0}(1+z)^3 + \Omega_{\Lambda_0}\right)^{-1/2}dz \tag{47}$$

and $E = E_0(1+z_e)$, respectively, we get,

$$\omega_{\rm SA} = \frac{\Delta_m^2}{2H_0E_0}\int_0^{z_e}\left(\Omega_{m_0}(1+z)^3 + \Omega_{\Lambda_0}\right)^{-1/2}dz. \tag{48}$$

Finally, inserting Eqs. (46) and (48) in Eq. (35) gives the two-flavor neutrino oscillation probability in the ΛCDM model,

$$P_\Lambda = \sin^2 2\theta \sin^2\omega_\Lambda, \tag{49}$$

and in the SA,

$$P_{\rm SA} = \sin^2 2\theta \sin^2\omega_{\rm SA}. \tag{50}$$

In Fig. 1, we plot the evolution of P_Λ(solid black curve) and $P_{\rm SA}$(dotted blue curve) as a function of redshift, to compare the two approaches. To this end, we took $\Delta_m^2 = 7.53\times10^{-5}{\rm eV}^2$[3] and $E_0 = 10^{16}$ eV, a value to which neutrino detectors are on average sensitive to [50]. Further, we used $\Omega_{m_0} = 0.315$, $\Omega_{\Lambda_0} = 0.685$ and $H_0 = 1.44\times10^{-33}$ eV as reported in [3]. For redshifts higher than ~ 2, the difference between the two probabilities stabilizes at around 80%, as can be seen from Fig. 2. On the other hand, the latter shows, for the observationally more interesting range of redshifts ($0 \le z \le 0.5$), the difference can reach up to 50% while they coincide for redshift 0, as expected.

The difference between Eqs. (46), (49) and Eqs. (48), (50) is being highlighted here to insure that, when doing neutrino observations, one cannot directly substitute $D_L(z)$ and $E(z)$ as neutrino traveling length and energy, respectively. This will not properly take into account the evolution of a spin 1/2 particle in a curved background. Rather, one should use the formalism presented in Section 3, for a more general interaction with a scalar field in curved spacetime, or Eqs. (46), (49) for ΛCDM. The same idea applies to other models of DE, however there will be differences in the evolution of the oscillation probability, as we will see next.

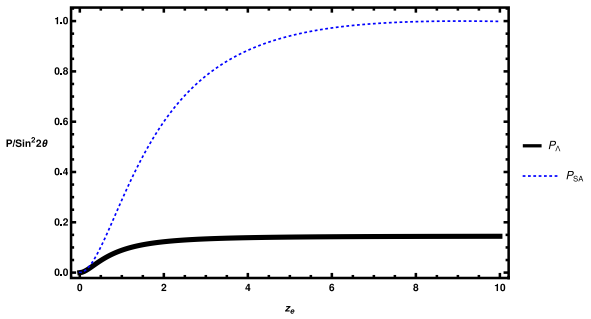

Fig. 1. The two-flavor neutrino oscillation probability, divided by $\sin^2 2\theta$, as a function of redshift of emission, $z_e \in [0, 10]$, for the two cases P_Λ(solid black curve) and $P_{\rm SA}$(dotted blue line), given by Eqs. (45),(49) and Eqs. (48),(50), respectively. To be specific, due to the large value of $C = \Delta_m^2/(2H_0E_0)$, we used $\omega \mod 2\pi C$ as the argument of $\sin^2$ in Eqs. (49)–(50) to avoid numerical instabilities. The values of different parameters used in these equations is given in the text below Eq. (50).

[3] Here we used mass states 1 and 2 from Ref. [49] as ours. One can check that other values of Δ_m^2 reported there does not alter the evolution of the frequencies Eqs. (46), (48). Physically, this is due to the absence of a direct interaction between DE and neutrinos. Mathematically, this is because the coefficient multiplying the integrals in Eqs. (46), (48) includes $H_0^{-1} \sim \mathcal{O}(10^{33})$ eV, which wipes out the $\mathcal{O}(10^2){\rm eV}^2$ difference between Δ_m^2s.

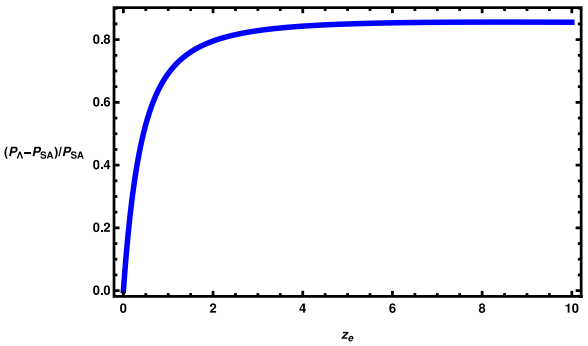

Fig. 2. Absolute value of the fractional difference between the oscillation probabilities P_Λ and P_{SA}, given by Eqs. (45),(49) and Eqs. (48),(50), respectively, as a function of emission redshift, $z_e \in [0, 10]$. To be specific, due to the large value of $C = \Delta_m^2/(2H_0E_0)$, we used $\omega \mod 2\pi C$ as the argument of $\sin^2$ in Eqs. (49)–(50) to avoid numerical instabilities. Moreover, we shifted both P_Λ and P_{SA} by 10^{-5} to avoid the singularity when they are 0 at $z_e = 0$. The values of different parameters used in these equations is given in the text below Eq. (50).

4.2. Quintessence

As a homogeneous canonical scalar field minimally coupled to gravity, Quintessence could be an explanation to the late time accelerated expansion [8,37,51–53]. One of the main reasons for introducing quintessence as an alternative to a cosmological constant is to make DE dynamical, thereby avoiding the cosmological constant and coincidence problems(see [38] and references therein for more information on Quintessence).

In order to probe this model using neutrino oscillations, a coupling between the scalar and spinor fields has to be introduced, otherwise the difference in effect of quintessence and Λ on the oscillation probability will be difficult to observe. We consider the coupling introduced in [33], given the name DE_ν model, and which we analyzed in [34]. In the present formalism, DE_ν translates to $F = 0$ and $G_\mu = \partial_\mu\varphi$ in Eq. (4). As mentioned in [33], such a derivative coupling is a low energy limit of the model presented in [54], with the scalar field being a Nambu–Goldstone boson resulting from the spontaneous symmetry breaking of Lepton number symmetry [55–57]. This shows that such a coupling is motivated both from Particle Physics and Cosmology points of view, hence it is being further analyzed here.

To start the analysis, recall that since the scalar field is homogeneous, its energy density would be

$$\rho_\varphi = \frac{1}{2}\dot\varphi^2 + V(\varphi) \tag{51}$$

where $\dot\varphi = \partial_t\varphi$ and $V(\varphi)$ is the potential energy of φ. Therefore, Eq. (44) becomes

$$H^2 = H_0^2\left(\Omega_{m_0}a^{-3} + \Omega_\varphi\right), \tag{52}$$

where

$$\Omega_\varphi = \frac{8\pi G}{3H_0^2}\rho_\varphi \tag{53}$$

is the density parameter of quintessence. Moreover, as already shown in [34], this type of interactions does not affect the Klein–Gordon equation, which can be written as:

$$\frac{d}{da}\left(a^6\dot\varphi^2\right) = 2a^6\frac{dV}{da}. \tag{54}$$

For φ to produce an accelerated expansion, it should satisfy the condition:

$$\dot\varphi^2 \ll V(\varphi) \approx \rho_{\Lambda_0}, \tag{55}$$

where ρ_{Λ_0} is the energy density of a cosmological constant today. This means that, first, in Eq. (52), $\Omega_\varphi \approx \Omega_{\Lambda_0}$, and second, we can write[4]

$$\frac{dV}{da} \equiv \frac{7}{2}\epsilon, \tag{56}$$

where $\epsilon < \rho_{\Lambda_0} \sim \mathcal{O}(10^{-11}\text{eV}^4)$,[5] and thus, from Eq. (54), we get

$$\dot\varphi = \sqrt{\epsilon a}. \tag{57}$$

On the neutrino's side, this type of interaction results in

$$V_l = -\frac{dx^\mu}{d\lambda}G_\mu = -E\dot\varphi = -E_0\sqrt{\epsilon(1+z)}, \tag{58}$$

from which one can show, using Eqs. (26), (28) and (33), that

$$v_\pm = \frac{1}{2}V_l\left[\xi_e + \xi_\mu \mp \cos 2\theta(\xi_e - \xi_\mu)\right] \pm \Delta_m^2, \tag{59}$$

$$\sin 2\tilde\theta = \sin 2\theta\left[1 + \frac{4E_0\sqrt{\epsilon(1+z)}}{\Delta_m^2}\cos 2\theta(\xi_e - \xi_\mu)\right]^{-1/2} \tag{60}$$

and

$$\frac{d\tilde\theta}{d\lambda} = \frac{\sin 2\tilde\theta}{\Delta_m}(\xi_e - \xi_\mu)\frac{dV_l}{d\lambda}, \tag{61}$$

respectively. To check if the adiabaticity condition is satisfied for the current case, differentiate Eq. (58) w.r.t λ and insert it in Eq. (61), to find

$$\frac{d\tilde\theta}{d\lambda} \approx \frac{\sin 2\theta(\xi_e - \xi_\mu)}{2\Delta_m}E_0^2\epsilon^{1/2}H_0\sqrt{\Omega_{m_0}(1+z)^6 + \Omega_{\varphi_0}(1+z)^3}. \tag{62}$$

From the fact that $H_0 \sim \mathcal{O}(10^{-33})$eV [48], $E_0 \sim \mathcal{O}(10^{16})$ eV(typical value for high-energy neutrinos [50]), $\xi_{e,\mu} \sim \mathcal{O}(10^{-14})\text{eV}^{-1}$ [34] and $\epsilon \sim \mathcal{O}(10^{-11})\text{eV}^4$, one can see that $d\tilde\theta/d\lambda \ll v_\pm$, and therefore the adiabaticity condition still holds, resulting in an oscillation frequency

$$\omega_Q \approx \frac{\Delta_m^2}{2E_0H_0}\int_0^{z_e}\sqrt{\frac{1 + \frac{4E_0\sqrt{\epsilon(1+z)}}{\Delta_m^2}\cos 2\theta(\xi_e - \xi_\mu)}{\Omega_{m_0}(1+z)^7 + \Omega_{\varphi_0}(1+z)^4}}dz. \tag{63}$$

Finally, from Eq. (35), the two-flavor oscillation probability in the case when DE is quintessence is:

$$P_Q = \frac{\sin^2 2\theta}{1 + \frac{4E_0\sqrt{\epsilon(1+z)}}{\Delta_m^2}\cos 2\theta(\xi_e - \xi_\mu)}\sin^2(\omega_Q/2). \tag{64}$$

To study the difference between this model and ΛCDM, we plot (Fig. 3) Eq. (64) for values of ξ_i, $i = e, \mu$, ranging from 10^{-17} to 10^{-14} eV^{-1}, in addition to Eq. (49) for the ΛCDM case. We have checked that smaller values of ξ_i do not produce any noticeable deviation from ΛCDM, while already at 10^{-14} we can see from Fig. 3 that the deviation is $\sim 50\%$ at $z = 2$. That is the reason why we focus on this range of values of the couplings ξ_i. Moreover, we use the same parameters used to produce Figs. 1 and 2(see text after Eq. (50)), in addition to $\cos 2\theta = 0.4$ [49]. As the strength of the coupling increases, the difference between the two models starts to become apparent at redshift ~ 0.5, which is expected since then DE is becoming more dynamical than in the case of ΛCDM.

[4] The 7/2 factor is to reduce numerical factors clustering.

[5] Note that ϵ is not exactly the slow-roll parameter $\varepsilon = d(H^{-1})/dt$, but one can show that $\varepsilon \approx 3\epsilon a/V$.

In order to make the distinction between the different DE scenarios more concrete, we study in more detail the dependence of P_Q in Eq. (64) on the parameters ϵ and ξ_f of this particular DE model. First, if quintessence is slow-rolling, but not ultra slow-rolling, then ε (see footnote 5) cannot be too small [58]. Taking $\epsilon \in [10^{-14}, 10^{-12}]$, which corresponds to $\varepsilon \in [10^{-3}, 10^{-1}]$, we find that $\xi_f \in [10^{-15}, 10^{-13}]$ gives distinguishable stable results. On the other hand, values beyond this interval would lead to unstable transition probabilities. This shows that, in principle, the presented method here could provide a complementary theoretical constraint to this type of coupling.

Second, if we now fix $\epsilon \sim \mathcal{O}(10^{-13})$, for instance, we find that the difference between quintessence and ΛCDM starts to become appreciable(i.e. more that a few %) for $\xi_f \sim \mathcal{O}(10^{-14} - 10^{-13})$. This is still consistent with Particle Physics constraints for this type of coupling, which is $\xi_f \lesssim 10^{-7}$ eV^{-1} [59,60]. Moreover, for values of ξ_f that differ from each other by at least half an order of magnitude, the transition probabilities start deviating from each other by more than a few %. One may conclude from this that there is a small window for fine-tuning in this model, but not a too small one.

On another note, we can also explore how the results might change for different neutrino parameters. Unlike for ΛCDM, the neutrino–quintessence interaction is affected by the value of Δ^2_m and its hierarchy, which is evident from the denominator of Eq. (64). To see this, we plot in the upper panel of Fig. 4 the probabilities shown in Fig. 3, but for $\Delta^2_m = 2.51 \times 10^{-3}$ eV^2 (normal hierarchy), while in the lower panel we use $\Delta^2_m = -2.56 \times 10^{-3}$ eV^2 (inverted hierarchy), with $\cos 2\theta \sim 0.2$ for both. These values of Δ^2_m correspond to the difference between neutrino mass states 3 and 2 of the standard neutrino oscillation treatment [49].

There are a few things to be noted from these plots. First, if our neutrino mass states are 3 and 2 from [49], it is more difficult to distinguish ΛCDM from the quintessence model considered here for coupling constants smaller than 10^{-14}. This difficulty can be evaded once we consider the full 3-flavor neutrino oscillations, which will be done in future works. Our purpose here is merely to show that different DE models affect neutrino oscillations differently. Second, even when we include all three neutrino flavors, there will be a noticeable difference between the two hierarchies for larger values of the coupling($\sim 10^{-14}$), as is apparent from the two panels of Fig. 4. Therefore, such a neutrino–quintessence interaction could require some fine-tuning to match future observations, which puts it at equal, or less, footing with ΛCDM.[6]

4.3. Observational strategy

Let us now comment on the relationship between our findings and observable quantities. Note that, due to the fact that we are considering a two-flavor neutrino system, direct comparison with neutrino observations would not be very beneficial. Nevertheless, our main results, presented in Figs. 1 to 4, do affect neutrino observations, and we will be exploring this in more detail for three-flavor neutrinos in future work.

The main quantities observed at neutrino observatories, such as IceCube [50], are neutrino fluxes. For instance, the electron neutrino flux, F_{ν_e} can be expressed as [61,62]:

$$F_{\nu_e} = \sum_{\alpha=e,\mu\tau} P_{\nu_\alpha \to \nu_e} F^0_{\nu_\alpha}, \tag{65}$$

where $F^0_{\nu_\alpha}$ is the flux of neutrinos with flavor α at the source. It is in this expression that our results could affect neutrino observations. The interaction of spinor neutrinos with curved spacetime will alter this expression through the transition probability $P_{\nu_\alpha \to \nu_e}$. More specifically to our case, depending on which DE model is considered, Eqs. (49) and (64) will give different $P_{\nu_\alpha \to \nu_e}$ as a function of redshift, and thus the neutrino flux detected will be different. Therefore, by calculating the neutrino flux for each DE model, and compare it with observations, one can distinguish between these models.

Another observational aspect worth mentioning is the experimental sensitivity available for such effects to be observed. We would like first to highlight that, when analyzing neutrino data, the usual emphasis is on the probability and flux's dependence on the neutrino's energy. However, in addition to this dependence, we are drawing attention here to the non-trivial effect of spacetime curvature on the observational results, which in an FLRW context translates into the dependence on the redshift. That is why in the analysis above a value for the energy of$\sim$10 PeV has been chosen. Such a value is within reach of next generation neutrino detector IceCube-Gen2, which will have a 5 times better sensitivity than IceCube [63].

5. Conclusions

In this paper, we have provided a proof of concept that distinct DE models can be distinguished using neutrino oscillations, particularly through the evolution of the oscillation probability with redshift. We first looked at a more general interaction between two-flavor neutrinos, as quantum spinor fields, and a classical scalar field in general spacetime. We focused on the interaction with a scalar field since it comprises a large class of models for DE, including ΛCDM, quintessence and some modified gravity scenarios (such as Horndeski theory [35,36]). Moreover, the interaction term considered includes a part that couples equally to both neutrino flavors, a flavor–global interaction, and another which is flavor dependent (see Eq. (4)). The purpose is to examine the different effect these two terms have on the oscillation probability, which can be seen from the main result Eqs. (35), (36) in Section 3.2.

Furthermore, we applied this general formalism to two specific DE models, ΛCDM and quintessence, to produce observable contrast between them using neutrino oscillations. In the former model, we showed in Fig. 1 the evolution of the oscillation probability with redshift when DE is a cosmological constant. We also show in that figure the oscillation probability in case of a direct substitution of the cosmological distance traveled by neutrinos(such as the luminosity distance) and their energy in the standard formula for neutrino oscillations Eq. (38), what we called SA. The point of this contrast is that, if we detect ν_e from a type Ia supernova(SN), for example, and we want to calculate their flux (which depends on the ν_e's survival probability), SA would give a result $\sim 50-80$%(depending on the SN's redshift, see Fig. 2) more than the actual value. This should be taken into account when doing neutrino observations in the future [63,64].

On the other hand, for quintessence, we looked at a derivative coupling between neutrinos and the scalar field that is motivated by symmetry breaking arguments [55–57], which was referred to in [33] as the DE$_\nu$ model. This coupling, and others, have been already studied in [34], but we focused in this work on the observational consequences of such a coupling which, without it, ΛCDM and quintessence would be indistinguishable. In Fig. 3, we show the oscillation probability's evolution with redshift for the two models, with the DE$_\nu$ coupling varied from 10^{-17} to 10^{-14} eV^{-1}. We also investigated the effect several Δ^2_m values from Particle Physics have on the probabilities, which in Fig. 3 was

[6] Unless the value of the coupling constant is derived from a more fundamental theory, which establishes a fixed distinction between this model and ΛCDM.

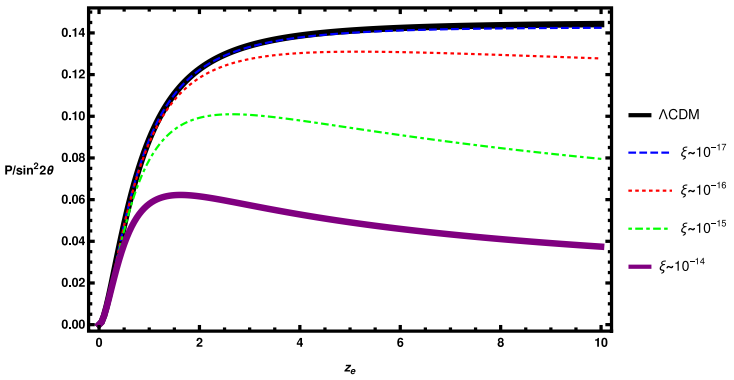

Fig. 3. Evolution of the neutrino oscillation probability with redshift in the case of ΛCDM(solid black line) and quintessence, for neutrino–quintessence coupling $\sim \mathcal{O}(10^{-17})$(dashed blue), 10^{-16}(dotted red), 10^{-15}(dot–dash green) and 10^{-14}(solid purple line). The parameters used are given in the text, after Eq. (50).

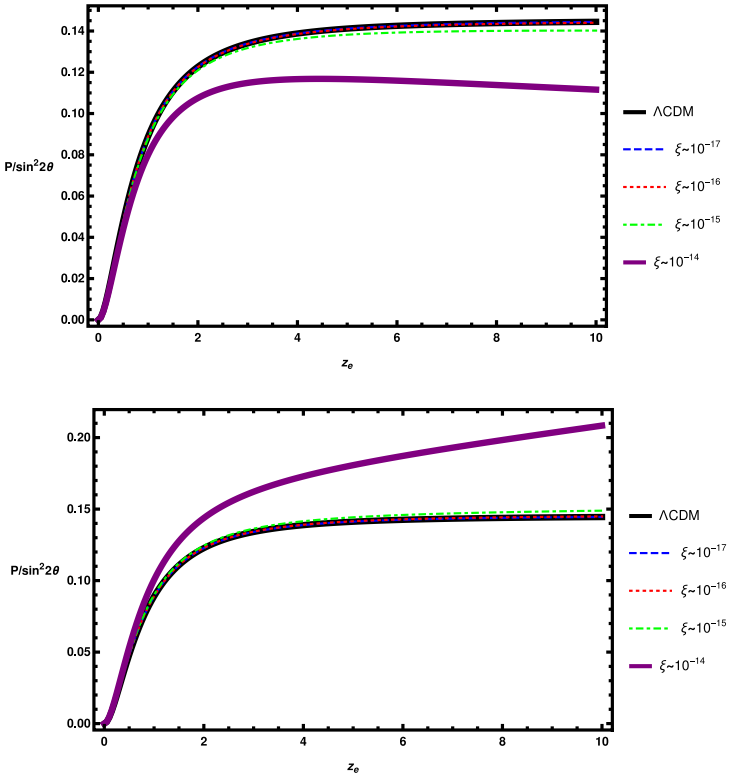

Fig. 4. Evolution of the neutrino oscillation probability with redshift in the case of ΛCDM(solid black line) and quintessence, for neutrino–quintessence coupling $\sim \mathcal{O}(10^{-17})$(dashed blue), 10^{-16}(dotted red), 10^{-15}(dot–dash green) and 10^{-14}(solid purple line). The parameters used are given in the text after Eq. (50), except for $\cos 2\theta \sim 0.2$ and Δ^2_m, which is 2.51×10^{-3} eV^2(upper panel) for normal hierarchy, and -2.56×10^{-3} eV^2(lower panel) for the inverted one.

produced assuming mass states 1 and 2 from [49] as ours. This plot shows a clear distinction between ΛCDM and quintessence for several values of the DE$_\nu$ coupling. However, if we consider states 2 and 3 as our mass states, it would become more difficult to distinguish the two DE models, unless the DE$_\nu$ coupling is at least $\mathcal{O}(10^{-14})$, as seen in Fig. 4. Nevertheless, one can see from the latter a difference in the probability's evolution between the normal and inverted hierarchies, specially for high values of the DE$_\nu$ coupling.

In the future, we would like to generalize the present work further, by looking at the full three-flavor neutrino scenario, which should alleviate the distinction between mass states choice previously mentioned. However, we expect the difference between hierarchies' choice to remain even in this case, which prompts investigating its possible degeneracy with parameters of DE models. Furthermore, one could also look at another type of general interaction that could include other modified gravity models for DE, such as extended gravity [65] or higher dimensions [66]. Finally, with the advancement in neutrino detection

techniques, we would expect these signals to appear in near future terrestrial experiments [63,64], or perhaps underground lunar ones.

CRediT authorship contribution statement

Ali Rida Khalifeh: Conceptualization, Methodology, Software, Validation, Formal analysis, Investigation, Resources, Data curation, Writing - original draft, Writing - review & editing, Visualization, Project administration, Funding acquisition. **Raul Jimenez:** Conceptualization, Methodology, Software, Validation, Formal analysis, Investigation, Resources, Data curation, Writing - original draft, Writing - review & editing, Visualization, Supervision, Project administration, Funding acquisition.

Declaration of competing interest

The authors declare that they have no known competing financial interests or personal relationships that could have appeared to influence the work reported in this paper.

Acknowledgments

We would like to thank David Valcin and Nicola Bellomo for very helpful discussions. The work of ARK and RJ is supported by MINECO, Spain grant PGC2018-098866-B-I00 FEDER, UE. ARK and RJ acknowledge "Center of Excellence Maria de Maeztu 2020-2023" award to the ICCUB (CEX2019- 000918-M).

References

[1] S. Perlmutter, et al., Measurements of omega and lambda from 42 high redshift supernovae, Astrophys. J. 517 (1999) 565–586, http://dx.doi.org/10.1086/307221, arXiv:astro-ph/9812133.
[2] A.G. Riess, et al., Observational evidence from supernovae for an accelerating universe and a cosmological constant, Astron. J. 116 (1998) 1009–1038, http://dx.doi.org/10.1086/300499, arXiv:astro-ph/9805201.
[3] N. Aghanim, et al., Planck Collaboration Collaboration, Planck 2018 results. VI. Cosmological parameters, Astron. Astrophys. 641 (2020) A6, http://dx.doi.org/10.1051/0004-6361/201833910, arXiv:1807.06209.
[4] DESI collaboration, The dark energy spectroscopic instrument (DESI), in: Bulletin of the American Astronomical Society, Vol. 51, 2019, p. 57, arXiv:1907.10688.
[5] R. Laureijs, G. Racca, L. Stagnaro, J.-C. Salvignol, J.L. Alvarez, G.S. Criado, L.G. Venancio, A. Short, P. Strada, C. Colombo, G. Buenadicha, J. Hoar, R. Kohley, R. Vavrek, Y. Mellier, M. Berthe, J. Amiaux, M. Cropper, S. Niemi, S. Pottinger, A. Ealet, K. Jahnke, T. Maciaszek, F. Pasian, M. Sauvage, S. Wachter, U. Israelsson, W. Holmes, M. Seiffert, V. Cazaubiel, A. Anselmi, P. Musi, Euclid mission status, in: J.M. Oschmann Jr., M. Clampin, G.G. Fazio, H.A. MacEwen (Eds.), Space Telescopes and Instrumentation 2014: Optical, Infrared, and Millimeter Wave, 9143, International Society for Optics and Photonics, SPIE, 2014, pp. 132–139, http://dx.doi.org/10.1117/12.2054883.
[6] L. Amendola, et al., Cosmology and fundamental physics with the euclid satellite, Living Rev. Rel. 21 (1) (2018) 2, http://dx.doi.org/10.1007/s41114-017-0010-3, arXiv:1606.00180.
[7] H. Velten, R. vom Marttens, W. Zimdahl, Aspects of the cosmological "coincidence problem", Eur. Phys. J. C74 (11) (2014) 3160, http://dx.doi.org/10.1140/epjc/s10052-014-3160-4, arXiv:1410.2509.
[8] I. Zlatev, L. Wang, P.J. Steinhardt, Quintessence, cosmic coincidence, and the cosmological constant, Phys. Rev. Lett. 82 (1999) 896–899, http://dx.doi.org/10.1103/PhysRevLett.82.896, arXiv:astro-ph/9807002.
[9] S. Weinberg, The cosmological constant problem, Rev. Modern Phys. 61 (1989) 1–23, http://dx.doi.org/10.1103/RevModPhys.61.1.
[10] S. Weinberg, Theories of the cosmological constant, in: Critical Dialogues in Cosmology, 1996, pp. 195–203, arXiv:astro-ph/9610044.
[11] LIGO Scientific Collaboration and Virgo Collaboration, Observation of gravitational waves from a binary black hole merger, Phys. Rev. Lett. 116 (2016) 061102, http://dx.doi.org/10.1103/PhysRevLett.116.061102, URL https://link.aps.org/doi/10.1103/PhysRevLett.116.061102.
[12] C. de Rham, S. Melville, Gravitational rainbows: LIGO and dark energy at its cutoff, Phys. Rev. Lett. 121 (2018) 221101, http://dx.doi.org/10.1103/PhysRevLett.121.221101, URL https://link.aps.org/doi/10.1103/PhysRevLett.121.221101.
[13] P. Creminelli, F. Vernizzi, Dark energy after GW170817 and GRB170817a, Phys. Rev. Lett. 119 (2017) 251302, http://dx.doi.org/10.1103/PhysRevLett.119.251302, URL https://link.aps.org/doi/10.1103/PhysRevLett.119.251302.
[14] J. Lesgourgues, S. Pastor, Massive neutrinos and cosmology, Phys. Rep. 429 (2006) 307–379, http://dx.doi.org/10.1016/j.physrep.2006.04.001, arXiv:astro-ph/0603494.
[15] M. Betti, et al., PTOLEMY Collaboration, Neutrino physics with the PTOLEMY project: active neutrino properties and the light sterile case, J. Cosmol. Astropart. Phys. 1907 (2019) 047, http://dx.doi.org/10.1088/1475-7516/2019/07/047, arXiv:1902.05508.
[16] M. Takada, E. Komatsu, T. Futamase, Cosmology with high-redshift galaxy survey: neutrino mass and inflation, Phys. Rev. D73 (2006) 083520, http://dx.doi.org/10.1103/PhysRevD.73.083520, arXiv:astro-ph/0512374.
[17] R. Jimenez, C.P.n. Garay, L. Verde, Neutrino footprint in large scale structure, Phys. Dark Univ. 15 (2017) 31–34, http://dx.doi.org/10.1016/j.dark.2016.11.004, arXiv:1602.08430.
[18] M. Moresco, R. Jimenez, L. Verde, A. Cimatti, L. Pozzetti, C. Maraston, D. Thomas, Constraining the time evolution of dark energy, curvature and neutrino properties with cosmic chronometers, J. Cosmol. Astropart. Phys. 1612 (12) (2016) 039, http://dx.doi.org/10.1088/1475-7516/2016/12/039, arXiv:1604.00183.
[19] C. Wetterich, Growing neutrinos and cosmological selection, Phys. Lett. B 655 (5–6) (2007) 201–208, http://dx.doi.org/10.1016/j.physletb.2007.08.060, arXiv:0706.4427.
[20] C.Y. Cardall, G.M. Fuller, Neutrino oscillations in curved spacetime: A heuristic treatment, Phys. Rev. D 55 (1997) 7960–7966, http://dx.doi.org/10.1103/PhysRevD.55.7960, URL https://link.aps.org/doi/10.1103/PhysRevD.55.7960.
[21] L. Buoninfante, G.G. Luciano, L. Petruzziello, L. Smaldone, Neutrino oscillations in extended theories of gravity, Phys. Rev. D 101 (2) (2020) 024016, http://dx.doi.org/10.1103/PhysRevD.101.024016, arXiv:1906.03131.
[22] M. Blasone, G. Lambiase, G.G. Luciano, L. Petruzziello, L. Smaldone, Time-energy uncertainty relation for neutrino oscillations in curved spacetime, Classical Quantum Gravity 37 (15) (2020) 155004, http://dx.doi.org/10.1088/1361-6382/ab995c, arXiv:1904.05261.
[23] M. Blasone, P. Jizba, L. Smaldone, Flavor energy uncertainty relations for neutrino oscillations in quantum field theory, Phys. Rev. D 99 (1) (2019) 016014, http://dx.doi.org/10.1103/PhysRevD.99.016014, arXiv:1810.01648.
[24] A.W. Brookfield, C. van de Bruck, D.F. Mota, D. Tocchini-Valentini, Cosmology of mass-varying neutrinos driven by quintessence: Theory and observations, Phys. Rev. D 73 (2006) 083515, http://dx.doi.org/10.1103/PhysRevD.73.083515, URL https://link.aps.org/doi/10.1103/PhysRevD.73.083515.
[25] R. Fardon, A.E. Nelson, N. Weiner, Dark energy from mass varying neutrinos, J. Cosmol. Astropart. Phys. 2004 (10) (2004) 005, http://dx.doi.org/10.1088/1475-7516/2004/10/005.
[26] D.B. Kaplan, A.E. Nelson, N. Weiner, Neutrino oscillations as a probe of dark energy, Phys. Rev. Lett. 93 (2004) 091801, http://dx.doi.org/10.1103/PhysRevLett.93.091801, URL https://link.aps.org/doi/10.1103/PhysRevLett.93.091801.
[27] H. Mohseni Sadjadi, H. Yazdani Ahmadabadi, Damped neutrino oscillations in a conformal coupling model, Phys. Rev. D 103 (2021) 065012, http://dx.doi.org/10.1103/PhysRevD.103.065012, URL https://link.aps.org/doi/10.1103/PhysRevD.103.065012.
[28] H. Mohseni Sadjadi, A.P. Khosravi, Symmetry breaking, and the effect of matter density on neutrino oscillation, J. Cosmol. Astropart. Phys. 04 (2018) 008, http://dx.doi.org/10.1088/1475-7516/2018/04/008, arXiv:1711.06607.
[29] A. Esmaili, Y. Farzan, Implications of the pseudo-Dirac scenario for ultra high energy neutrinos from GRBs, J. Cosmol. Astropart. Phys. 12 (2012) 014, http://dx.doi.org/10.1088/1475-7516/2012/12/014, arXiv:1208.6012.
[30] J.F. Beacom, N.F. Bell, D. Hooper, J.G. Learned, S. Pakvasa, T.J. Weiler, Pseudo-Dirac neutrinos: A challenge for neutrino telescopes, Phys. Rev. Lett. 92 (2004) 011101, http://dx.doi.org/10.1103/PhysRevLett.92.011101, URL https://link.aps.org/doi/10.1103/PhysRevLett.92.011101.
[31] S. Ando, M. Kamionkowski, I. Mocioiu, Neutrino oscillations, lorentz/CPT violation, and dark energy, Phys. Rev. D 80 (2009) 123522, http://dx.doi.org/10.1103/PhysRevD.80.123522, URL https://link.aps.org/doi/10.1103/PhysRevD.80.123522.
[32] N. Klop, S. Ando, Effects of a neutrino-dark energy coupling on oscillations of high-energy neutrinos, Phys. Rev. D 97 (2018) 063006, http://dx.doi.org/10.1103/PhysRevD.97.063006, URL https://link.aps.org/doi/10.1103/PhysRevD.97.063006.
[33] F. Simpson, R. Jimenez, C. Pena-Garay, L. Verde, Dark energy from the motions of neutrinos, Phys. Dark Univ. 20 (2018) 72, http://dx.doi.org/10.1016/j.dark.2018.04.002, arXiv:1607.02515.
[34] A.R. Khalifeh, R. Jimenez, Spinors and scalars in curved spacetime: Neutrino dark energy (DE_ν), Phys. Dark Univ. 31 (2021) 100777, http://dx.doi.org/10.1016/j.dark.2021.100777, arXiv:2010.08181.
[35] G.W. Horndeski, Second-order scalar-tensor field equations in a four-dimensional space, Internat. J. Theoret. Phys. 10 (1974) 363–384, http://dx.doi.org/10.1007/BF01807638.

[36] T. Kobayashi, Horndeski theory and beyond: a review, Rep. Progr. Phys. 82 (8) (2019) 086901, http://dx.doi.org/10.1088/1361-6633/ab2429, arXiv:1901.07183.
[37] B. Ratra, P.J.E. Peebles, Cosmological consequences of a rolling homogeneous scalar field, Phys. Rev. D 37 (1988) 3406–3427, http://dx.doi.org/10.1103/PhysRevD.37.3406, URL https://link.aps.org/doi/10.1103/PhysRevD.37.3406.
[38] S. Tsujikawa, Quintessence: A review, Classical Quantum Gravity 30 (2013) 214003, http://dx.doi.org/10.1088/0264-9381/30/21/214003, arXiv:1304.1961.
[39] N. Birrell, P. Davies, Quantum Fields in Curved Space, in: Cambridge Monographs on Mathematical Physics, Cambridge Univ. Press, Cambridge, UK, 1984, http://dx.doi.org/10.1017/CBO9780511622632, (Chapter 3.8).
[40] M. Lanzagorta, Quantum Information in Gravitational Fields, in: 2053-2571, Morgan & Claypool Publishers, 2014, http://dx.doi.org/10.1088/978-1-627-05330-3, (Chapter 5).
[41] V. Mukhanov, S. Winitzki, Introduction to Quantum Effects in Gravity, Cambridge University Press, 2007.
[42] A. Capolupo, G. Lambiase, A. Quaranta, Neutrinos in curved spacetime: Particle mixing and flavor oscillations, Phys. Rev. D 101 (2020) 095022, http://dx.doi.org/10.1103/PhysRevD.101.095022, URL https://link.aps.org/doi/10.1103/PhysRevD.101.095022.
[43] S.M. Carroll, Spacetime and Geometry, Cambridge University Press, 2019.
[44] S. Mikheyev, A.Y. Smirnov, Resonance amplification of oscillations in matter and spectroscopy of solar neutrinos, Sov. J. Nucl. Phys. 42 (1985) 913–917.
[45] S. Mikheev, A.I. Smirnov, Resonant amplification of ν oscillations in matter and solar-neutrino spectroscopy., Nuovo Cimento C Geophys. Space Phys. C 9 (1986) 17–26, http://dx.doi.org/10.1007/BF02508049.
[46] C. Giunti, C.W. Kim, Fundamentals of Neutrino Physics and Astrophysics, Oxford University Press, 2007, (Chapter9.3).
[47] S. Alam, M. Ata, S. Bailey, F. Beutler, D. Bizyaev, J.A. Blazek, A.S. Bolton, J.R. Brownstein, A. Burden, C.-H. Chuang, J. Comparat, A.J. Cuesta, K.S. Dawson, D.J. Eisenstein, S. Escoffier, H. Gil-Marín, J.N. Grieb, N. Hand, S. Ho, K. Kinemuchi, D. Kirkby, F. Kitaura, E. Malanushenko, V. Malanushenko, C. Maraston, C.K. McBride, R.C. Nichol, M.D. Olmstead, D. Oravetz, N. Padmanabhan, N. Palanque-Delabrouille, K. Pan, M. Pellejero-Ibanez, W.J. Percival, P. Petitjean, F. Prada, A.M. Price-Whelan, B.A. Reid, S.A. Rodríguez-Torres, N.A. Roe, A.J. Ross, N.P. Ross, G. Rossi, J.A. Rubiño Martín, S. Saito, S. Salazar-Albornoz, L. Samushia, A.G. Sánchez, S. Satpathy, D.J. Schlegel, D.P. Schneider, C.G. Scóccola, H.-J. Seo, E.S. Sheldon, A. Simmons, A. Slosar, M.A. Strauss, M.E. Swanson, D. Thomas, J.L. Tinker, R. Tojeiro, M.V. Magaña, J.A. Vazquez, L. Verde, D.A. Wake, Y. Wang, D.H. Weinberg, M. White, W.M. Wood-Vasey, C. Yèche, I. Zehavi, Z. Zhai, G.-B. Zhao, The clustering of galaxies in the completed SDSS-III baryon oscillation spectroscopic survey: cosmological analysis of the DR12 galaxy sample, Mon. Not. R. Astron. Soc. 470 (3) (2017) 2617–2652, http://dx.doi.org/10.1093/mnras/stx721, arXiv:https://academic.oup.com/mnras/article-pdf/470/3/2617/18315003/stx721.pdf.
[48] S. Dodelson, F. Schmidt, Modern Cosmology, second ed., Academic Press, 2020.
[49] Particle Data Group Collaboration Collaboration, Review of particle physics, Phys. Rev. D 98 (2018) 030001, http://dx.doi.org/10.1103/PhysRevD.98.030001, URL https://link.aps.org/doi/10.1103/PhysRevD.98.030001.
[50] IceCube Collaboration Collaboration, The detection of a sn iin in optical follow-up observations of icecube neutrino events, Astrophys. J. 811 (1) (2015) 52, http://dx.doi.org/10.1088/0004-637x/811/1/52.
[51] C. Wetterich, Cosmology and the fate of dilatation symmetry, Nuclear Phys. B 302 (1988) 668–696, http://dx.doi.org/10.1016/0550-3213(88)90193-9, arXiv:1711.03844.
[52] Y. Fujii, Origin of the gravitational constant and particle masses in a scale-invariant scalar-tensor theory, Phys. Rev. D 26 (1982) 2580–2588, http://dx.doi.org/10.1103/PhysRevD.26.2580, URL https://link.aps.org/doi/10.1103/PhysRevD.26.2580.
[53] L.H. Ford, Cosmological-constant damping by unstable scalar fields, Phys. Rev. D 35 (1987) 2339–2344, http://dx.doi.org/10.1103/PhysRevD.35.2339, URL https://link.aps.org/doi/10.1103/PhysRevD.35.2339.
[54] M. Fukugita, S. Watamura, M. Yoshimura, Light pseudoscalar particle and stellar energy loss, Phys. Rev. Lett. 48 (1982) 1522–1525, http://dx.doi.org/10.1103/PhysRevLett.48.1522, URL https://link.aps.org/doi/10.1103/PhysRevLett.48.1522.
[55] C.P. Burgess, J.M. Cline, New class of majoron-emitting double-β decays, Phys. Rev. D 49 (1994) 5925–5944, http://dx.doi.org/10.1103/PhysRevD.49.5925, arXiv:hep-ph/9307316.
[56] E. Witten, Lepton number and neutrino masses, in: J. Law, R.W. Ollerhead, J.J. Simpson (Eds.), Nucl. Phys. B Proc. Suppl. 91 (2001) 3–8, http://dx.doi.org/10.1016/S0920-5632(00)00916-6, arXiv:hep-ph/0006332.
[57] Y. Chikashige, R.N. Mohapatra, R.D. Peccei, Are there real goldstone bosons associated with broken lepton number? Phys. Lett. B 98 (1981) 265–268, http://dx.doi.org/10.1016/0370-2693(81)90011-3.
[58] D. Chowdhury, J. Martin, C. Ringeval, V. Vennin, Assessing the scientific status of inflation after Planck, Phys. Rev. D 100 (8) (2019) 083537, http://dx.doi.org/10.1103/PhysRevD.100.083537, arXiv:1902.03951.
[59] A. Gando, Y. Gando, H. Hanakago, H. Ikeda, K. Inoue, R. Kato, M. Koga, S. Matsuda, T. Mitsui, T. Nakada, et al., Limits on majoron-emitting double-β decays of136xe in the kamland-zen experiment, Phys. Rev. C 86 (2) (2012) http://dx.doi.org/10.1103/physrevc.86.021601.
[60] K.J. Kelly, P.A.N. Machado, Multimessenger astronomy and new neutrino physics, J. Cosmol. Astropart. Phys. 2018 (10) (2018) 048, http://dx.doi.org/10.1088/1475-7516/2018/10/048.
[61] H. Athar, J.F. Nieves, Matter effects on neutrino oscillations in gravitational and magnetic fields, Phys. Rev. D 61 (2000) 103001, http://dx.doi.org/10.1103/PhysRevD.61.103001, arXiv:hep-ph/0001069.
[62] M. Lei, N. Steinberg, J.D. Wells, Probing non-standard neutrino interactions with supernova neutrinos at hyper-k, J. High Energy Phys. 01 (2020) 179, http://dx.doi.org/10.1007/JHEP01(2020)179, arXiv:1907.01059.
[63] M.G. Aartsen, et al., IceCube-Gen2 Collaboration Collaboration, IceCube-Gen2: The window to the extreme universe, J. Phys. G 48 (6) (2021) 060501, http://dx.doi.org/10.1088/1361-6471/abbd48, arXiv:2008.04323.
[64] S. Böser, M. Kowalski, L. Schulte, N.L. Strotjohann, M. Voge, Detecting extra-galactic supernova neutrinos in the antarctic ice, Astropart. Phys. 62 (2015) 54–65, http://dx.doi.org/10.1016/j.astropartphys.2014.07.010, arXiv:1304.2553.
[65] S. Capozziello, M. De Laurentis, Extended theories of gravity, Phys. Rep. 509 (2011) 167–321, http://dx.doi.org/10.1016/j.physrep.2011.09.003, arXiv:1108.6266.
[66] R. Maartens, K. Koyama, Brane-world gravity, Living Rev. Rel. 13 (2010) 5, http://dx.doi.org/10.12942/lrr-2010-5, arXiv:1004.3962.

Using Neutrino Oscillations to Measure H_0

Ali Rida Khalifeh[a,b,*], Raul Jimenez[a,c]

[a] *ICC, University of Barcelona, Marti i Franques, 1, E-08028 Barcelona, Spain.*
[b] *Dept. de Fisica Cuantica y Astrofisica, University of Barcelona, Marti i Franques 1, E-08028 Barcelona, Spain.*
[c] *ICREA, Pg. Lluis Companys 23, Barcelona, E-08010, Spain.*

Abstract

The tension between late and early universe probes of today's expansion rate, the Hubble parameter H_0, remains a challenge for the standard model of cosmology ΛCDM. There are many theoretical proposals to remove the tension, with work still needed on that front. However, by looking at new probes of the H_0 parameter one can get new insights that might ease the tension. Here, we argue that neutrino oscillations could be such a probe. We expand on previous work and study the full three-flavor neutrino oscillations within the ΛCDM paradigm. We show how the oscillation probabilities evolve differently with redshift for different values of H_0 and neutrino mass hierarchies. We also point out how this affects neutrino fluxes which, from their measurements at neutrino telescopes, would determine which value of H_0 is probed by this technique, thus establishing the aforementioned aim.

1. Introduction

The Hubble tension, the discrepancy between early and late universe measurements of the Hubble parameter H_0, is still persisting [1, 2]. Early universe probes are mainly from Cosmic Microwave Background (CMB) experiments, such as the ones from [3, 4]. This parameter is determined assuming Λ Cold Dark Matter (ΛCDM) as the fiducial cosmological model, combined with measurements independent from it. On the other hand, late universe ones use the local distance ladder method [5, 6] on Cepheids, type-Ia supernovae and tip of the red giant branch in a way independent from the cosmological model [7, 8].

To solve this tension, several theoretical models have been proposed, including early dark energy [9, 10] and modified gravity [11] (see [12] for a recent and thorough review on the subject). However, one can gain new insight on this tension by developing new observables, being late or early universe ones, that are affected by today's expansion rate.

*Corresponding author
Email addresses: ark93@icc.ub.edu (Ali Rida Khalifeh), raul.jimenez@icc.ub.edu (Raul Jimenez)

In this work, we build on previous ones [13, 14] and show the possibility of using neutrino oscillations as a new probe for the Hubble tension. Although the latter has been looked at in connection with neutrinos previously [15], our approach is quite different. We consider a system of three-flavor neutrinos, $(\nu_e, \nu_\mu, \nu_\tau)$, traveling in a flat Friedmann-Lemaître-Robertson-Walker (FRW) spacetime with a cosmological constant Dark energy (DE) Λ. By studying the transition probabilities' evolution from one flavor to another as a function of redshift, we show how different values of H_0 affect the detected neutrino fluxes, making the latter a potential probe for H_0. In our analysis, we consider different initial conditions (ICs) for neutrino flavor decomposition, and distinguish between their mass hierarchies.

It should be noted that there have been a great deal of work in the literature done on neutrinos as spinors in curved spacetime. We direct the interested reader to a few of them and references therein [16, 17, 18, 19, 20, 21, 22, 23, 24, 25, 26].

The organization of the paper is as follows: we briefly present the necessary principles and equations for the analysis in section 2. Then, we present and discuss the main results, given as triangular plots, what is called ternary diagrams, and fluxes' evolution with redshift, in section 3. We finish with some concluding remarks in section 4.

We use units in which $\hbar = c = 1$ and a metric signature $(-,+,+,+)$. Moreover, data from [3] is used to get an early universe (EU) value of H_0, what we call $H_0^{EU} = 2.13 \times 10^{-33} h^{\mathrm{EU}}$eV, where $h^{\mathrm{EU}} = 0.674$. In addition to that, matter and DE density parameters $\Omega_{m(\Lambda)} = 8\pi G/(3H_0^2)\rho_{m(\Lambda)}$, where ρ_m, ρ_Λ are the energy densities of matter and DE, respectively, are also taken from [3]. For the late universe (LU) value of H_0, H_0^{LU}, we use results from [27], which gives $H_0^{LU} = 2.13 \times 10^{-33} h^{\mathrm{LU}}$ eV, with $h^{\mathrm{LU}} = 0.740$.

Notation wise, neutrino flavor states will be denoted by Greek indices, while Latin ones denote mass eigenstates.

2. Neutrinos in flat FLRW Universe

In this section, we will follow a practical approach in which we briefly describe the relevant equations and principles needed for the case under study. We refer the unfamiliar reader to [13, 14] and references therein for a more thorough derivation.

In the concordance ΛCDM model, spacetime is best described by a flat FLRW metric $g_{\mu\nu}$, given by the line element

$$ds^2 = g_{\mu\nu}dx^\mu dx^\nu = -dt^2 + a^2(t)\big(dr^2 + r^2 d\theta^2 + r^2 \sin^2\theta d\phi^2\big) \tag{1}$$

in terms of cosmic time t and spherical coordinates $\{r, \theta, \phi\}$. Moreover, $a(t)$, the scale factor, is independent of spatial coordinates due to homogeneity and isotropy of FRW. Following the usual machinery in Cosmology [28, 29], one gets the first Friedmann equation

$$H^2(z) = \frac{8\pi G}{3}\big(\rho_m + \rho_\Lambda\big) = H_0^2\Big(\Omega_m(1+z)^3 + \Omega_\Lambda\Big) \tag{2}$$

where $1+z=a_0/a$ is the redshift, with a_0 being today's value of $a(t)$.

This is what we will be needing from the gravity side. On the neutrino part, to study their oscillations in curved spacetime, we are mainly interested in the transition amplitude between two flavor states $|\nu_\alpha\rangle$ and $|\nu_\beta\rangle$, $\Psi_{\alpha\beta}$, from which we get the oscillation probability $P_{\alpha\beta}$:

$$\Psi_{\alpha\beta} \equiv \langle \nu_\beta | \nu_\alpha \rangle \Rightarrow P_{\alpha\beta} = |\Psi_{\alpha\beta}|^2. \tag{3}$$

As was shown previously [14], $\Psi_{\alpha\beta}$ evolves with the affine parameter λ for the case of ΛCDM as:

$$i\frac{d}{d\lambda}\Psi_{\alpha\beta} = \frac{1}{2}\mathcal{M}_f^2\Psi_{\alpha\beta}, \tag{4}$$

where

$$\mathcal{M}_f^2 = U \begin{pmatrix} m_1^2 & 0 & 0 \\ 0 & m_2^2 & 0 \\ 0 & 0 & m_3^2 \end{pmatrix} U^\dagger \tag{5}$$

is the square of the vacuum mass matrix in flavor space. In the above equation, m_i, for $i=1,2,3$, are the eigenvalues of the neutrino mass states, $|\nu_i\rangle$, and $U_{\alpha j}$ is the Pontecorvo-Maki-Nakagawa-Sakata(PMNS) matrix for neutrino mixing [30, 31]. More explicitly, the latter can be written in terms of mixing angles θ_{ij}, for $\{i,j\}=1,2,3$, as [32]

$$U = \begin{pmatrix} c_{12}c_{13} & s_{12}c_{13} & s_{13}e^{-i\delta} \\ -s_{12}c_{23} - s_{13}s_{23}c_{12}e^{i\delta} & c_{12}c_{23} - s_{12}s_{23}s_{13}e^{i\delta} & s_{23}c_{13} \\ s_{12}s_{23} - s_{13}c_{12}c_{23}e^{i\delta} & -s_{23}c_{12} - s_{12}s_{13}c_{23}e^{i\delta} & c_{13}c_{23} \end{pmatrix} \tag{6}$$

where $c_{ij} \equiv \cos\theta_{ij}$, $s_{ij} \equiv \sin\theta_{ij}$ and δ is the Charge Conjugation-Parity (CP) violating phase. Incidentally, here we are considering neutrinos to be of the Dirac type, hence there is one CP violating phase (see [33, 34] for a review on CP violation and the nature of neutrinos).

If we start with an initial state $|\nu_\alpha\rangle$, then eq. (4) can be written explicitly as

$$i\frac{d}{d\lambda}\begin{pmatrix} \Psi_{\alpha e} \\ \Psi_{\alpha\mu} \\ \Psi_{\alpha\tau} \end{pmatrix} = \frac{1}{2}U \begin{pmatrix} m_1^2 & 0 & 0 \\ 0 & m_2^2 & 0 \\ 0 & 0 & m_3^2 \end{pmatrix} U^\dagger \begin{pmatrix} \Psi_{\alpha e} \\ \Psi_{\alpha\mu} \\ \Psi_{\alpha\tau} \end{pmatrix} \tag{7}$$

for the transition of α to any of the three flavors e, μ and τ. By defining

$$\Phi_\alpha \equiv U^\dagger \Psi_\alpha, \tag{8}$$

eq. (7) becomes, after multiplying it with $U^\dagger$ from the left,

$$i\frac{d}{d\lambda}\begin{pmatrix} \Phi_{\alpha 1} \\ \Phi_{\alpha 2} \\ \Phi_{\alpha 3} \end{pmatrix} = \frac{1}{2}\begin{pmatrix} m_1^2 & 0 & 0 \\ 0 & m_2^2 & 0 \\ 0 & 0 & m_3^2 \end{pmatrix} \begin{pmatrix} \Phi_{\alpha 1} \\ \Phi_{\alpha 2} \\ \Phi_{\alpha 3} \end{pmatrix}. \tag{9}$$

Here, we have used the unitarity condition of the PMNS, $U^\dagger U = I$, where I is the 3×3 identity matrix. As one can see, by going from eq. (7) to eq. (9) we

have simply changed from flavor to mass basis. This will make it easier to solve the evolution equation, and then we can simply transform back to the flavor basis by the inverse of (8).

The solution to each $\Phi_{\alpha i}$ is

$$\Phi_{\alpha i}(\lambda) = \Phi_{\alpha}^{\rm ini} e^{-i\frac{1}{2}m_i^2\Delta\lambda} \tag{10}$$

where $\Phi_{\alpha}^{\rm ini}$ is the initial neutrino composition at emission in mass basis, and [14]

$$\Delta\lambda \equiv \frac{1}{E_0}\int_0^{z_e} \frac{dz}{H(z)(1+z)^2}, \tag{11}$$

with E_0 being the detected neutrino energy on Earth (corresponding to $z = 0$), z_e is the source's redshift and $H(z)$ is given in eq. (2).

Finally, to get the probability $P_{\alpha\beta}$, there are three steps that need to be done. First, starting from an initial neutrino flavor composition, $\Psi^{\rm ini}$, we apply eq (8) to get $\Phi_{\alpha}^{\rm ini}$. Second, we plug the latter in the solution eq. (10) and apply the inverse of eq. (8) to get the evolution of $\Psi_{\alpha\beta}$. Third, we take the modulus square of that to get an expression for the $\alpha \to \beta$ transition probability of the form:

$$P_{\alpha\beta} = \delta_{\alpha\beta} + \sum_{i<j}\left[a_{\alpha\beta;ij}\sin^2\left(\frac{\Delta m_{ij}^2\Delta\lambda}{4}\right) + b_{\alpha\beta;ij}\sin\left(\frac{\Delta m_{ij}^2\Delta\lambda}{2}\right)\right] \tag{12}$$

where $\delta_{\alpha\beta}$ is the Kronecker delta, $\Delta m_{ij}^2 \equiv m_i^2 - m_j^2$, and the $a_{\alpha\beta;ij}$s[1] and $b_{\alpha\beta;ij}$s are numerical factors resulting from different combinations of PMNS components. In particular, this combination depends on which states α and β are being considered (see eq. (13.9) in [35] for the equivalent form in Minkowski spacetime).

From here, we can apply the above machinery to several initial conditions and see how it affects the probability's evolution with redshift, in addition to that of the flux, which will be the subject of the next section.

3. Observational Results for Different Initial Conditions

The space of initial conditions (ICs) for neutrino oscillations, i.e. initial decomposition, has many elements. However, there are three that are more relevant observationally: Neutron decay (ND), Muon damping (MD) and Pion decay (PD). In the representation $(\nu_e : \nu_\mu : \nu_\tau)$ for the initial ratios, these three conditions correspond to $(1:0:0)$, $(0:1:0)$ and $(1/3:2/3:0)$, respectively. In terms of $\Psi_{\alpha}^{\rm ini}$, this corresponds to

[1] To avoid confusion, we note that the semicolon does not correspond to any kind of derivative, but it's used just to seperate flavor from mass indicies.

Parameter	Normal Hierarchy (NH)	Inverted Hierarchy (IH)
$\sin^2(\theta_{12})$	0.307 ± 0.013	0.307 ± 0.013
Δm^2_{21}	$(7.53 \pm 0.18) \times 10^{-5}\text{eV}^2$	$(7.53 \pm 0.18) \times 10^{-5}\text{eV}^2$
$\sin^2(\theta_{13})$	$(2.18 \pm 0.07) \times 10^{-2}$	$(2.18 \pm 0.07) \times 10^{-2}$
$\sin^2(\theta_{23})$	0.545 ± 0.021	0.547 ± 0.021
Δm^2_{32}	$2.453 \times 10^{-3}\text{eV}^2$	$-2.546 \times 10^{-3}\text{eV}^2$
δ	$1.36 \pm 0.36\pi$ rad(2σ)	$1.36 \pm 0.36\pi$ rad(2σ)

Table 1: Neutrino oscillation parameters used in the analysis as reported in [32]

$$\Psi^{\text{ini}}_{\text{ND}} = \begin{pmatrix} 1 \\ 0 \\ 0 \end{pmatrix}, \quad \Psi^{\text{ini}}_{\text{MD}} = \begin{pmatrix} 0 \\ 1 \\ 0 \end{pmatrix}, \quad \Psi^{\text{ini}}_{\text{PD}} = \begin{pmatrix} \frac{1}{\sqrt{5}} \\ \frac{2}{\sqrt{5}} \\ 0 \end{pmatrix}, \tag{13}$$

normalized such that the sum of probabilities is 1.

Our purpose in this section is to see observational differences between H_0^{EU} and H_0^{LU} in neutrino oscillations. In addition to that, we distinguish between inverted hierarchy (IH) for neutrinos masses, as well as the normal one (NH). This will result in a total of four cases for each initial neutrino composition eq. (13): NH-EU, NH-LU, IH-EU and IH-LU. For instance, NH-EU corresponds to having neutrinos in the NH with today's rate of acceleration given by H_0^{EU}. In table 1, we list the values of the different neutrino parameters for both hierarchies as reported in [32].

One thing we can look at observationally is flavor ternary plots. These are triangular diagrams, with each side indicating the percentage of neutrinos from a certain flavor detected. In other words, each side corresponds to the probability of detecting neutrinos with certain flavor, with the sum being always equal to 1. These are shown in figure 1. The first, second and third rows correspond to ND, MD and PD initial conditions, respectively. Moreover, the left side plots correspond to NH, while the right side ones to IH. Finally, in each diagram, different colors represent the indicated redshifts of emission, diamonds correspond to using H_0^{EU} in the analysis of the previous section, while stars correspond to using H_0^{LU}.

The first thing to note when looking at these diagrams is the difference between the left and right side ones for each IC. There is a slight distinction between hierarchies throughout their evolution with redshift. Therefore there is no degeneracy between NH and IH as neutrinos travel in an expanding universe, as expected. Second, once can notice an appreciable difference in evolution between different ICs, and therefore we see no degeneracy between them as well. Third, in every diagram, the distinction between EU and LU starts to become

appreciable at around $z_e \sim 0.2$[2]. To give a concrete example on this distinction, let's look at the middle-right diagram of figure 1, particularly the points corresponding to z=2. If at some point we detect at neutrino observatories, such as IceCube [36], neutrinos coming from a source with known redshift z=2, then we should find the flavor fraction given by the green star if the true value of H_0 is $H_0^{\rm LU}$. However, if the detected flavor-fraction is given by the green diamond, and we are certain about the source's redshift, then we deduce that $H_0 = H_0^{\rm EU}$.

Another observable that we can consider is the total neutrino flux. For a given flavor β, the total flux received at the detector, φ_{β_0}, is given by:

$$\begin{aligned}\varphi_{\beta_0} &= \sum_\alpha P_{\alpha\beta}\varphi_{\alpha_e} \\ &= \varphi_{\beta_e} + \sum_{\alpha;i<j}\left[a_{\alpha\beta;ij}\sin^2\left(\frac{\Delta m^2_{ij}\Delta\lambda}{4}\right) + b_{\alpha\beta;ij}\sin\left(\frac{\Delta m^2_{ij}\Delta\lambda}{2}\right)\right]\varphi_{\alpha_e} \quad (14)\end{aligned}$$

where eq. (12) has been used in the second line and φ_{α_e} is the flux at emission. When analyzing astrophysical neutrino fluxes, it is usually assumed that it takes an empirical form $\varphi_{\alpha_e} \sim AE_\nu^{-\gamma}$, where A is a normalization constant and γ is the spectral index, for any flavor [39, 40, 41]. Therefore, the φ_{α_e}s on the right hand side (r.h.s) of eq. (14) can be factorized, allowing us to form a fractional difference,

$$\delta\varphi_{\nu\beta} = \frac{\varphi_{\beta_0} - \varphi_{\beta_e}}{\varphi_{\beta_e}}, \quad (15)$$

between the observed and emitted fluxes, figure 2. Note that in these plots, the total flux for each flavor is being presented, i.e. summing over all ICs eq. (13).

Let us now make a few comments about these plots. First, all diagrams of figure 2 show noticeable differences between hierarchies and EU/ LU values of H_0. To see this more clearly, we plot in figure 3 the fractional difference between EU and LU for each of the quantities appearing in figure 2 and for both hierarchies. That is, we look at

$$\delta\varphi_\alpha^{\rm EU-LU} = \frac{\varphi_{\alpha_0}^{\rm EU} - \varphi_{\alpha_0}^{\rm LU}}{\rm Max[\varphi_{\alpha_0}^{\rm EU}, \varphi_{\alpha_0}^{\rm LU}]} \quad (16)$$

for each hierarchy and flavor α, as a function of redshift. Even at relatively small redshifts ($z_e \sim 0.1$), using $H_0^{\rm EU}$ or $H_0^{\rm LU}$ makes a difference of a few % on the flux received.

Second, the starting values of figure 2's diagrams is related to the fact that our ICs eq. (13) are mainly of ν_e and ν_μ type. As they evolve with redshift, neutrinos start changing flavor to one another. In particular, ν_e and ν_μ are

[2]On the other hand, there is a clear distinction between the two for ND initial conditions. The fact that there is very little change for ND in the LU case is a distinctive feature compared to the other cases.

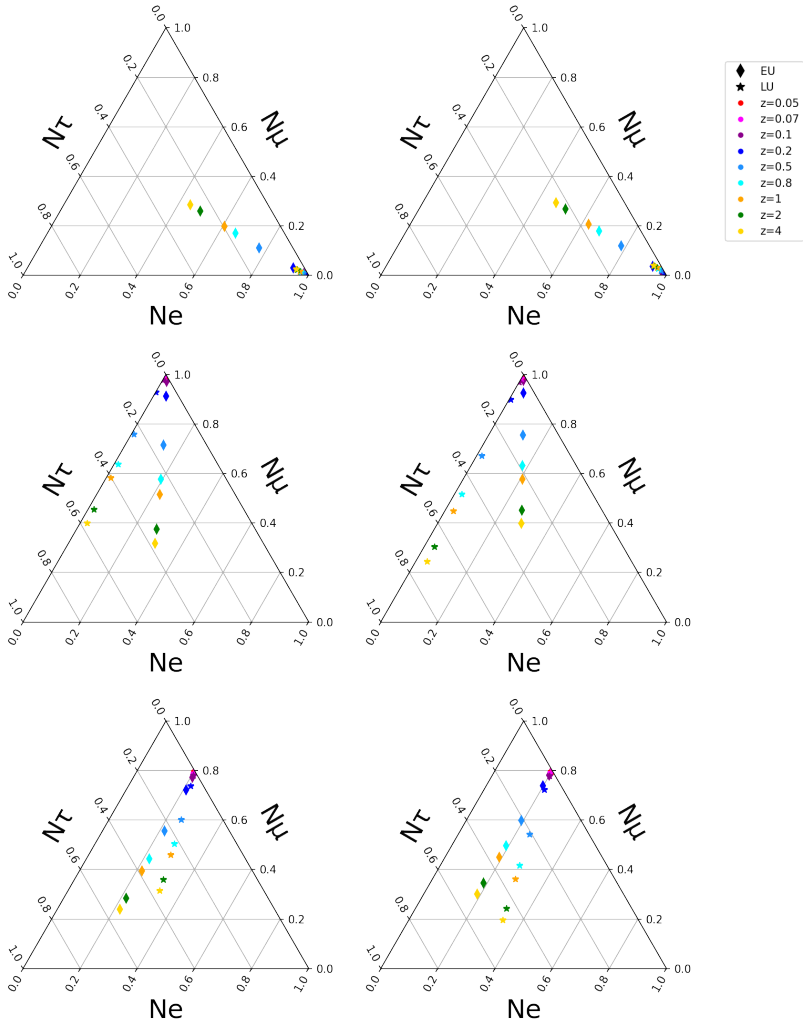

Figure 1: Ternary plots of ND (top), MD (middle) and PD (bottom) initial neutrino flavor decomposition, eq.(13), for NH (left) and IH (right). Diamond shaped points correspond to having $H_0^{\rm EU}$ as today's rate of expansion, while star shaped ones for $H_0^{\rm LU}$. Different colors correspond to emission redshifts, as given by the legend above. The python script to produce these is available in [37], which was written using [38].

mostly transitioning to ν_τ, explaining the negative values of the top diagrams in figure 2. Moreover, there is a $\nu_\mu \to \nu_\tau$ transition as well, which can be seen from the decreasing (increasing) character of the middle (bottom) diagram in the aforementioned figure. However, since we started with more ν_μ than ν_e, in addition to $\nu_{e,\mu} \to \nu_\mu$ being more dominant than the other transitions, then we have $\varphi_{\mu_0} > \varphi_{\mu_e}$.

To give a more complete picture of how the difference between H_0^{EU} and H_0^{LU} affects neutrino oscillations, we can also look at the evolution of individual transition probabilities with redshift, as was done in [14]. However, in order to avoid clustering of diagrams, we report those in a GitHub repository [37].

4. Conclusion

With the persistence of a tension between early and late universe probes of today's expansion rate, H_0, using additional probes could shed some new light on the matter. In this work, which is an extension of previous ones [13, 14], we demonstrated how neutrino oscillations can be such a probe.

We considered a system of three-flavors neutrinos as spinors in a flat FRW universe, with a cosmological constant DE, Λ. We use neutrino parameters, table 1, and initial conditions eq. (13) to study the evolution of transition probabilities and neutrino fluxes with redshift. In particular, for each IC, figure 1 shows the detected flavor composition, distinguishing between H_0^{EU} and H_0^{LU} on the one hand, and between hierarchies on the other. Moreover, this distinction is presented for several redshifts of emission, demonstrating how the probability evolves with it. We can conclude from this that using H_0^{EU} or H_0^{LU} creates a difference of about 10% on neutrino oscillations, starting from a redshift of emission of about 0.2.

Concerning detected neutrino fluxes, we consider the sum of all initial conditions in eq. (13) for each neutrino flavor ν_e, ν_μ and ν_τ. Fractional difference between detected and emitted fluxes is shown in figure 2, for the four different combinations of hierarchies and early/late universe values of H_0. On the other hand, the fractional difference of the latter's effect on the fluxes is presented in figure 3. The same conclusion previously reached applies here as well, showing the potential of using neutrino oscillations as a new probe of the Hubble tension.

It is worth emphasizing that the considerations of this work are a mere generalization of neutrino oscillation studies to curved spacetime. No new entity or force have been added, rather a simple combination of distinct, well established, phenomena: neutrino oscillations and the Universe's accelerated expansion. Therefore, such an effect must be observed at some point in neutrino observatories [36, 42], if it wasn't already in disguise. If this effect is not detected, even with the increasing performance of neutrino observatories [43], then this could hint to new Physics in the neutrino or gravitational sectors.

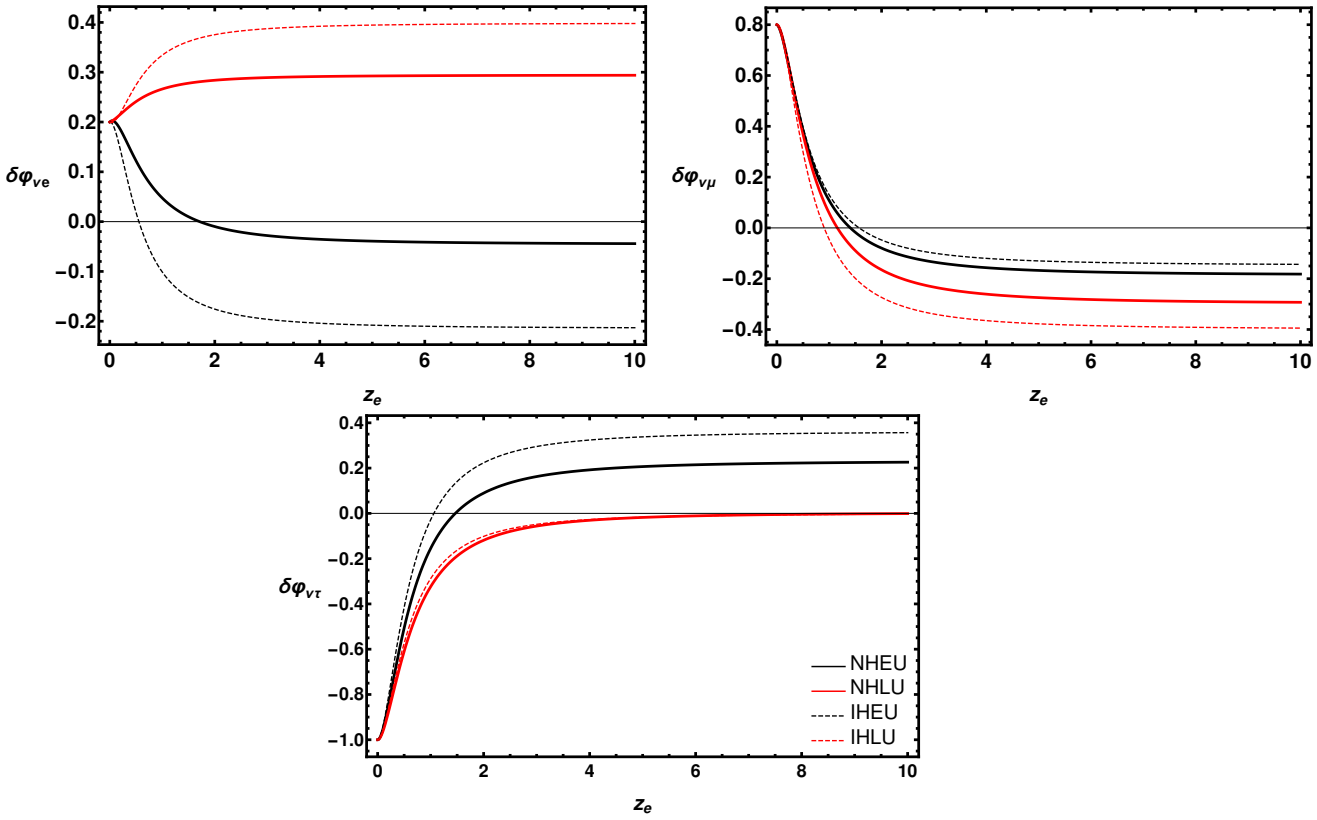

Figure 2: Fractional difference, eq. (15), between observed and emitted neutrino fluxes as a function of redshift. The presented δ_φs are for ν_e(top-left), ν_μ(top-right) and ν_τ(bottom). Black curves correspond to having $H_0^{\rm EU}$, while red ones to $H_0^{\rm LU}$. On the other hand, solid lines refer to NH, while dashed ones to IH. The `Mathematica` script used to produce these is available in [37].

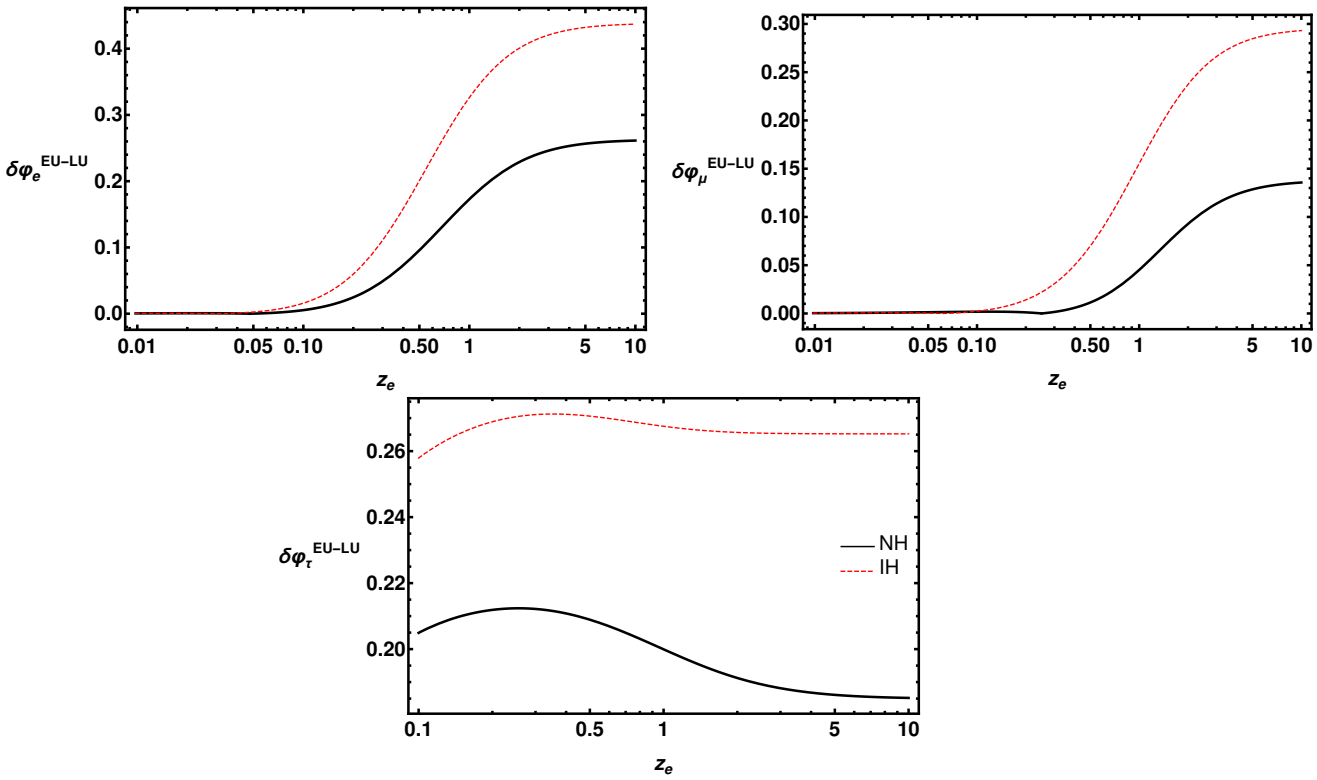

Figure 3: Log-Linear plots of the fractional difference between EU and LU for each flavor flux as given in eq. (16). The differences presented in each plot are for both hierarchies and correspond to ν_e(top-left), ν_μ(top-right) and ν_τ(bottom). The black-solid line correspond to having NH, while the red-dashed one to IH. The `Mathematica` script used to produce these is available in [37].

5. Acknowledgment

We would like to thank Samuel Brieden for insightful discussions. The work of ARK and RJ is supported by MINECO grant PGC2018-098866-B-I00 FEDER, UE. ARK and RJ acknowledge "Center of Excellence Maria de Maeztu 2020-2023" award to the ICCUB (CEX2019- 000918-M).

References

[1] A. G. Riess, et al., A 2.4% Determination of the Local Value of the Hubble Constant, Astrophys. J. 826 (1) (2016) 56. arXiv:1604.01424, doi:10.3847/0004-637X/826/1/56.

[2] L. Verde, T. Treu, A. G. Riess, Tensions between the early and late Universe, Nature Astronomy 3 (2019) 891–895. arXiv:1907.10625, doi:10.1038/s41550-019-0902-0.

[3] N. Aghanim, et al., Planck 2018 results. VI. Cosmological parameters, Astron. Astrophys. 641 (2020) A6. arXiv:1807.06209, doi:10.1051/0004-6361/201833910.

[4] T. M. C. Abbott, et al., Dark Energy Survey Year 3 Results: Cosmological Constraints from Galaxy Clustering and Weak Lensing (5 2021). arXiv:2105.13549.

[5] N. Jackson, The Hubble Constant, Section 3, Living Rev. Rel. 10 (2007) 4. arXiv:0709.3924, doi:10.12942/lrr-2007-4.

[6] M. Rowan-Robinson, Cosmological Distance Ladder: Distance and Time in the Universe, W.H.Freeman & Co, New York, NY(USA).

[7] A. G. Riess, et al., Observational evidence from supernovae for an accelerating universe and a cosmological constant, Astron. J. 116 (1998) 1009–1038. arXiv:astro-ph/9805201, doi:10.1086/300499.

[8] K. C. Wong, et al., H0LiCOW – XIII. A 2.4 per cent measurement of H0 from lensed quasars: 5.3σ tension between early- and late-Universe probes, Mon. Not. Roy. Astron. Soc. 498 (1) (2020) 1420–1439. arXiv:1907.04869, doi:10.1093/mnras/stz3094.

[9] T. Karwal, M. Kamionkowski, Dark energy at early times, the Hubble parameter, and the string axiverse, Phys. Rev. D 94 (10) (2016) 103523. arXiv:1608.01309, doi:10.1103/PhysRevD.94.103523.

[10] F. Niedermann, M. S. Sloth, Resolving the Hubble tension with new early dark energy, Phys. Rev. D 102 (6) (2020) 063527. arXiv:2006.06686, doi:10.1103/PhysRevD.102.063527.

[11] M. Ballardini, M. Braglia, F. Finelli, D. Paoletti, A. A. Starobinsky, C. Umiltà, Scalar-tensor theories of gravity, neutrino physics, and the H_0 tension, JCAP 10 (2020) 044. arXiv:2004.14349, doi:10.1088/1475-7516/2020/10/044.

[12] N. Schöneberg, G. Franco Abellán, A. Pérez Sánchez, S. J. Witte, V. Poulin, J. Lesgourgues, The H_0 Olympics: A fair ranking of proposed models (7 2021). arXiv:2107.10291.

[13] A. R. Khalifeh, R. Jimenez, Spinors and Scalars in curved spacetime: Neutrino dark energy (DE_ν), Phys. Dark Univ. 31 (2021) 100777. arXiv:2010.08181, doi:10.1016/j.dark.2021.100777.

[14] A. R. Khalifeh, R. Jimenez, Distinguishing Dark Energy models with neutrino oscillations, Phys. Dark Univ. 34 (2021) 100897. arXiv:2105.07973, doi:10.1016/j.dark.2021.100897.

[15] M. Escudero, S. J. Witte, A CMB search for the neutrino mass mechanism and its relation to the Hubble tension, Eur. Phys. J. C 80 (4) (2020) 294. arXiv:1909.04044, doi:10.1140/epjc/s10052-020-7854-5.

[16] M. Blasone, P. Jizba, L. Smaldone, Flavor Energy uncertainty relations for neutrino oscillations in quantum field theory, Phys. Rev. D 99 (1) (2019) 016014. arXiv:1810.01648, doi:10.1103/PhysRevD.99.016014.

[17] M. Blasone, G. Lambiase, G. G. Luciano, L. Petruzziello, L. Smaldone, Time-energy uncertainty relation for neutrino oscillations in curved spacetime, Class. Quant. Grav. 37 (15) (2020) 155004. arXiv:1904.05261, doi:10.1088/1361-6382/ab995c.

[18] L. Buoninfante, G. G. Luciano, L. Petruzziello, L. Smaldone, Neutrino oscillations in extended theories of gravity, Phys. Rev. D 101 (2) (2020) 024016. arXiv:1906.03131, doi:10.1103/PhysRevD.101.024016.

[19] A. Capolupo, G. Lambiase, A. Quaranta, Neutrinos in curved spacetime: Particle mixing and flavor oscillations, Phys. Rev. D 101 (2020) 095022. doi:10.1103/PhysRevD.101.095022.
URL https://link.aps.org/doi/10.1103/PhysRevD.101.095022

[20] C. Y. Cardall, G. M. Fuller, Neutrino oscillations in curved spacetime: A heuristic treatment, Phys. Rev. D 55 (1997) 7960–7966. doi:10.1103/PhysRevD.55.7960.
URL https://link.aps.org/doi/10.1103/PhysRevD.55.7960

[21] D. B. Kaplan, A. E. Nelson, N. Weiner, Neutrino oscillations as a probe of dark energy, Phys. Rev. Lett. 93 (2004) 091801. doi:10.1103/PhysRevLett.93.091801.
URL https://link.aps.org/doi/10.1103/PhysRevLett.93.091801

[22] S. Ando, M. Kamionkowski, I. Mocioiu, Neutrino oscillations, lorentz/*cpt* violation, and dark energy, Phys. Rev. D 80 (2009) 123522. doi:10.1103/PhysRevD.80.123522.
URL https://link.aps.org/doi/10.1103/PhysRevD.80.123522

[23] N. Klop, S. Ando, Effects of a neutrino-dark energy coupling on oscillations of high-energy neutrinos, Phys. Rev. D 97 (2018) 063006. doi:10.1103/PhysRevD.97.063006.
URL https://link.aps.org/doi/10.1103/PhysRevD.97.063006

[24] H. Mohseni Sadjadi, H. Yazdani Ahmadabadi, Damped neutrino oscillations in a conformal coupling model, Phys. Rev. D 103 (2021) 065012. doi:10.1103/PhysRevD.103.065012.
URL https://link.aps.org/doi/10.1103/PhysRevD.103.065012

[25] H. Mohseni Sadjadi, A. P. Khosravi, Symmetry breaking, and the effect of matter density on neutrino oscillation, JCAP 04 (2018) 008. arXiv:1711.06607, doi:10.1088/1475-7516/2018/04/008.

[26] G. G. Luciano, M. Blasone, Gravitational Effects on Neutrino Decoherence in the Lense–Thirring Metric, Universe 7 (11) (2021) 417. arXiv:2110.00971, doi:10.3390/universe7110417.

[27] A. G. Riess, S. Casertano, W. Yuan, L. M. Macri, D. Scolnic, Large Magellanic Cloud Cepheid Standards Provide a 1% Foundation for the Determination of the Hubble Constant and Stronger Evidence for Physics beyond ΛCDM, Astrophys. J. 876 (1) (2019) 85. arXiv:1903.07603, doi:10.3847/1538-4357/ab1422.

[28] S. Dodelson, F. Schmidt, Modern Cosmology, 2nd edition, Academic Press, 2020.

[29] O. F. Piattella, Lecture Notes in Cosmology, UNITEXT for Physics, Springer, Cham, 2018. arXiv:1803.00070, doi:10.1007/978-3-319-95570-4.

[30] B. Pontecorvo, Neutrino Experiments and the Problem of Conservation of Leptonic Charge, Zh. Eksp. Teor. Fiz. 53 (1967) 1717–1725.

[31] Z. Maki, M. Nakagawa, S. Sakata, Remarks on the Unified Model of Elementary Particles, Progress of Theoretical Physics 28 (5) (1962) 870–880. arXiv:https://academic.oup.com/ptp/article-pdf/28/5/870/5258750/28-5-870.pdf, doi:10.1143/PTP.28.870.
URL https://doi.org/10.1143/PTP.28.870

[32] P. D. Group, Review of Particle Physics, Chapter 14.3, Progress of Theoretical and Experimental Physics 2020 (8), 083C01 (08 2020). arXiv:https://academic.oup.com/ptep/article-pdf/2020/8/083C01/34673722/ptaa104.pdf, doi:10.1093/ptep/ptaa104.
URL https://doi.org/10.1093/ptep/ptaa104

[33] H. Nunokawa, S. J. Parke, J. W. F. Valle, CP Violation and Neutrino Oscillations, Prog. Part. Nucl. Phys. 60 (2008) 338–402. arXiv:0710.0554, doi:10.1016/j.ppnp.2007.10.001.

[34] A. Baha Balantekin, B. Kayser, On the Properties of Neutrinos, Ann. Rev. Nucl. Part. Sci. 68 (2018) 313–338. arXiv:1805.00922, doi:10.1146/annurev-nucl-101916-123044.

[35] C. Giunti, C. W. Kim, Fundamentals of Neutrino Physics and Astrophysics, chapter 13.1, Oxford University Press, 2007.

[36] The detection of a sn iin in optical follow-up observations of icecube neutrino events, The Astrophysical Journal 811 (1) (2015) 52. doi:10.1088/0004-637x/811/1/52.
URL https://doi.org/10.1088/0004-637x/811/1/52

[37] A. R. Khalifeh, NeutrinoOscillation-H0Tension (11 2021). doi:10.5281/zenodo.1234.
URL https://github.com/ark93-cosmo/NeutrinoOscillation-H0Tension

[38] Y. Ikeda, B. Grabowski, F. Körmann, mpltern 0.3.0: ternary plots as projections of Matplotlib (Nov. 2019). doi:10.5281/zenodo.3528355.
URL https://doi.org/10.5281/zenodo.3528355

[39] R. Abbasi, et al., The IceCube high-energy starting event sample: Description and flux characterization with 7.5 years of data, Phys. Rev. D 104 (2021) 022002. arXiv:2011.03545, doi:10.1103/PhysRevD.104.022002.

[40] M. G. e. a. Aartsen, Evidence for astrophysical muon neutrinos from the northern sky with icecube, Phys. Rev. Lett. 115 (2015) 081102. doi:10.1103/PhysRevLett.115.081102.
URL https://link.aps.org/doi/10.1103/PhysRevLett.115.081102

[41] C. A. Argüelles, K. Farrag, T. Katori, R. Khandelwal, S. Mandalia, J. Salvado, Sterile neutrinos in astrophysical neutrino flavor, JCAP 02 (2020) 015. arXiv:1909.05341, doi:10.1088/1475-7516/2020/02/015.

[42] M. G. Aartsen, et al., IceCube-Gen2: The Window to the Extreme Universe, J. Phys. G 48 (6) (2021) 060501. arXiv:2008.04323, doi:10.1088/1361-6471/abbd48.

[43] S. Böser, M. Kowalski, L. Schulte, N. L. Strotjohann, M. Voge, Detecting extra-galactic supernova neutrinos in the Antarctic ice, Astropart. Phys. 62 (2015) 54–65. arXiv:1304.2553, doi:10.1016/j.astropartphys.2014.07.010.

Part IV

SUMMARY OF RESULTS AND FUTURE PROSPECTS

5 SUMMARY OF RESULTS AND FUTURE PROSPECTS

During the last two decades, Cosmology has evolved to become a concrete and well established field of research. With technological advancements pushing the frontiers of our observational capabilities, this motivates for harder work on the theoretical side to answer our fundamental question about the Universe. This thesis provides several examples where theoretical analysis can result in new observables to answer these questions.

To conclude this work, I will present a summary of the results obtained above, in addition to describing potential future projects for each one of them.

5.1 TESTING THE COPERNICAN PRINCIPLE

In this work, entitled *"Measuring the Homogeneity of the Universe Using Polarization Drift"* [56], we present a new method to assess spatial homogeneity of the Universe. This technique, which is presented in chapter 2 above, is based on measuring polarization of CMB photons that were inverse-Compton scattered in galaxy clusters.

In order to do that, we first look at the most general spacetime possible, i.e. metric, for an expanding universe. This results in having expansion rates in the line-of-sight (radial) and transverse directions (see eqs. (3.11) and (3.12) in [56])[1]. On the other hand, we also look at the evolution of the polarization tensor along lightrays propagating towards the observer. This equation involves covariant derivatives, therefore Christoffel symbols where the two expansion rates appear. Moreover, this evolution also depends on the scatterer's properties through the polarization tensor's temporal evolution(see eq. (3.17) in [56] and discussion after it). By using the coordinate invariance of the polarization amplitude, we establish a relation between the observed and emitted one. The latter will depend on local properties of the scatterer, while its propagation towards the observer will depend on the expansion rates.

Finally, given that the radial expansion rate can be measured using standard rulers [97] or cosmic chronometers [98, 99], by measuring this *polarization drift* in the amplitude described above, one establishes a way to determine the transverse expansion rate. By comparing the two rates at high enough redshifts, one can then constrain deviations from isotropy at remote locations, which is equivalent to homogeneity.

1 In a homogeneous and isotropic Universe, these two quantities are equal.

Constraining spatial isotropy and homogeneity using polarization drift provides therefore an novel way to test the extent of applicability of the Copernican principle. This test is made assuming GR to be our theory of gravity. However, one might consider this not to be the case, given the motivations presented in the previous chapters on modified theories of gravity. Therefore, a natural next step for this project is to use this technique to test modified gravity models.

Depending on the model considered, there will be additional scalar and tensor modes appearing in the corresponding metric. These will induce changes to the E and B polarization modes that we measure. We can therefore use the polarization drift techniques described above to put constrains on these additional modes, and then establish which gravity models are more viable.

5.2 MODIFIED GRAVITY FOR DARK MATTER

The hypothesis that DM is part of a new theory of gravity has been tested on cosmological and astrophysical scales in chapter 3, which is based on [70, 82].

In the first part [70], *"Can Dark Matter be Geometry? A Case Study with Mimetic Dark Matter"*, we re-derive the equations of motion for a specific MG model, *Mimetic Dark Matter* [47, 48]. There, we find that there are additional functions and parameters in the model that need to be fine tuned to match observations. We showed that this is the case at background and first order in perturbation levels. Therefore, one can conclude that this model is at most on the same footing as ΛCDM. To show this explicitly, we modified the Boltzmann code `CLASS` [80, 81] to include MDM, and then we plot the matter power spectrum and CMB correlation functions in this model. What we found is that a 20%(10%) change in adiabatic initial conditions will set the CMB correlation functions(matter power spectrum) off the cosmic variance limit. Therefore, without a builtin mechanism to generate adiabatic initial conditions, such as inflation in ΛCDM, one would need to fine tune functions and parameters in this model to at least 10% level.

The fact that MDM is based on modifications of GR that include a scalar field makes it similar to other MG models that are based on such field. Therefore, the next step beyond this work would be to consider these other MG models that incorporate effects of DM within them, and study how much fine-tuning, if any, would be needed to match CMB and large-scale-structure observations. With upcoming advanced surveys, such as *LiteBIRD* [100] or *DESI* [101], constraining these models will become possible at the 1% level.

Having studied its implications on cosmological scales, we then went on to study the MG-DM hypothesis on astrophysical scales [82]. In particular, we look at a collection of ultra-diffuse dwarf galaxies that have been observed to be negligible of DM [49–54]. The main

argument of out work is the following: if DM is part of a MG, then by the universality of gravitational interactions, this effect should be present in any system of similar properties. However, the fact that such galaxies exist, while others similar ones are in fact DM dominated puts this hypothesis to question. Therefore, unless one is willing to abandon gravity's universality, there would be a great deal of fine tuning needed in these MGs to include both types of galaxies.

To prove this argument quantitatively, we derive a generalized Virial theorem for a broad class of MG models. Within the ADM formalism of GR, and while distinguishing between MGs that do and don't satisfy the Jebsen-Birkhoff theorem, we found that there is always an additional term in the Virial theorem due to modifications of GR. This term is present irrespective of the system under consideration, in particular, even for the DM-devoid galaxies previously mentioned. Therefore, unless this additional term vanishes at the location of these galaxies, while it would be non-vanishing for others, i.e. fine-tuned, the MG-DM hypothesis is now put to question.

The basic principle described above can be applied to other observables to test the DM-MG hypothesis, particularly to *gravitational lensing potentials*. In the future, I will work on deriving the latter from first principle, providing thus a scheme to check how much fine-tuning would MGs need to match *EUCLID* data [102] , for instance, specially for regions where there's DM deficiency.

Another method to constrain the DM-MG hypothesis is with *direct DM detection* experiments. The latter, such as *XENON* [103], is based on DM particles scattering off xenon ones. However, if DM is part of a MG, such a detection is unlikely to occur, specially when the MG is accompanied by a *screening mechanism* [104]. As a next step from the above, I would like to study the plausibility of such scattering in MGs, with and without screening effects.

These techniques described above, once compared with experiments and observations, could get us closer to knowing whether DM is an elementary particle, a compact object or a manifestation of gravity.

5.3 NEUTRINO OSCILLATIONS IN CURVED SPACETIME

In chapter 4, we looked at how neutrinos, when considered as quantum spinor fields in curved backgrounds, can give us a great deal of insight about the Universe's properties. This fact adds more information to *Multimessenger Astronomy*, since neutrinos are part of it, and thus makes it more beneficial.

In the first part of this chapter, which is based on [88], we lay down a general formalism for quantum spinor-scalar interactions in an arbitrary background. This formalism is then applied to three specific couplings, and neutrino dynamics are studied in an FRW spacetime using the WKB technique. By deriving and solving a generalized

geodesic equation, we found that, depending on the interaction, there could be a shift in the neutrino's momentum, which might be noticeable at least at 0^{th} order in WKB. Moreover, a particular focus has been made on one of these couplings, the LDC, due to its potential to explain the effect of DE [55].

This was the motivation to start the second part of this chapter [89]. There, we consider a special type of general interactions between neutrino[2] and a scalar field. The ultimate goal is to see the effect of DE, manifested by this scalar field, on neutrino oscillations. To this end, we look at the evolution of a neutrino flavor state in flat FRW spacetime with redshift, and see the modifications this coupling has on it. Incidentally, this type of interaction includes a cosmological constant DE automatically, which thus allows us to compare between the two models.

Therefore, from the flavor state, we calculate the probability of transition between two neutrino flavors in both DE models: cosmological constant and scalar field DE, with the latter coupled to neutrinos by the LDC. In the former case, we emphasis the importance of using the formalism presented here, rather than using neutrino transition probability in Minkowski spacetime and substituting the distance traveled with the Luminosity one, for instance. The difference between the two approaches reaches 80% at redshift of about 2, making this distinction the more important to consider.

On the other hand, for the case of scalar field DE coupled to neutrinos via a LDC, the difference between it and CC-DE increases with the neutrino-scalar coupling constant. These results provide a proof of concept that neutrino observations could be used to distinguish between some DE models.

In order to link these results directly with observations, the final part of chapter 4 considers the full three-flavor neutrino oscillation within the ΛCDM paradigm [90]. Moreover, a distinction in the neutrino transition probabilities' evolution with redshift between the two mass hierarchies is presented. In addition to that, we look at the effect of using different values for H_0 on this evolution. By presenting these differences in ternary diagrams and neutrino flux plots, we show how neutrino observations could be used as a new probe for H_0, and therefore an additional insight on the *Hubble Tension*.

From here, one might think of another way to use neutrino observations to distinguish between DE models in the future. In particular, this technique can be extended onto specific MGs describing DE. The latter, which could also be models of *Inflation*, will not only affect neutrino flavor, but will also alter its scattering cross section in a way that depends on the MG model. From these measurements at *IceCube-Gen2* [96], for instance, we might be able to constrain more of these MGs, if not ruling out some of them.

2 For simplicity, we focus here on a two-flavor neutrino system.

Another application to the quantum field theory in curved spacetime technique is in DM. Being a valuable player in *large scale structure formation*, uncovering more of DM's properties is crucial to better understand this process. In particular, as quantum fields, DM particles' coupling to gravity will affect their *distribution function* within galaxy clusters, in turn affecting structure formation. Therefore, a detailed theoretical analysis might hint for a noticeable shift in *Euclid* data.

Finally, a further interesting application for the above technique might be in *Gravitational Waves*(GW). Similarly to neutrinos, GW, or graviton's, *polarization* can exhibit an oscillation mechanism in some MGs. As quantum fields, their probability of transition between one polarization to another will be affected by the surrounding background, i.e. on the source of GW. I would like therefore to apply this machinery to *GW oscillations* [105–107], and find its potential detectability with future data from *LIGO-Virgo-Kagra*, or *LISA*. This might uncover a new feature of GW that can test models of gravity.

These techniques, therefore, could provide hints for gravitational interactions at the quantum level, and reduce the space of possible DM, DE and MGs candidates, bringing new insights to Physical Cosmology in the epoch of large surveys.

BIBLIOGRAPHY

[1] Scott Dodelson. *Modern Cosmology*. Amsterdam: Academic Press, 2003. ISBN: 978-0-12-219141-1.

[2] Oliver F. Piattella. *Lecture Notes in Cosmology*. UNITEXT for Physics. Cham: Springer, 2018. DOI: 10.1007/978-3-319-95570-4. arXiv: 1803.00070 [astro-ph.CO].

[3] Steven Weinberg. *Gravitation and Cosmology: Principles and Applications of the General Theory of Relativity*. New York: John Wiley and Sons, 1972. ISBN: 978-0-471-92567-5, 978-0-471-92567-5.

[4] Viatcheslav Mukhanov and Sergei Winitzki. *Introduction to quantum effects in gravity*. Cambridge University Press, June 2007. ISBN: 978-0-521-86834-1, 978-1-139-78594-5.

[5] Sir Isaac Newton. Translated by I. Bernard Cohen and Anne Whitman. *The Principia: Mathematical Principles of Natural Philosophy*. University of California Press, 1999. ISBN: 978-0-520-08816-0, 978-520-08817-7.

[6] Ernst Mach. *The Science of Mechanics: A Critical and Historical Account of Its Development*. 4th ed. The Open Court Publishing Company, 1919. ISBN: 0875482023.

[7] Albert Einstein. "On the electrodynamics of moving bodies." In: *Annalen Phys.* 17 (1905), pp. 891–921. DOI: 10.1002/andp.200590006.

[8] Albert Einstein. "Über das Relativitätsprinzip und die aus demselben gezogenen Folgerungen." In: *Jahrbuch der Radioaktivität und Elektronik* 4 (Jan. 1908), pp. 411–462.

[9] Thibault Damour. "Testing the equivalence principle: why and how?" In: *Classical and Quantum Gravity* 13.11A (1996), A33–A41. DOI: 10.1088/0264-9381/13/11a/005. URL: https://doi.org/10.1088/0264-9381/13/11a/005.

[10] Obinna Umeh, Kazuya Koyama, and Robert Crittenden. "Testing the equivalence principle on cosmological scales using the odd multipoles of galaxy cross-power spectrum and bispectrum." In: *arXiv e-prints*, arXiv:2011.05876 (Nov. 2020), arXiv:2011.05876. arXiv: 2011.05876 [astro-ph.CO].

[11] Albert Einstein. "The Foundation of the General Theory of Relativity." In: *Annalen Phys.* 49.7 (1916). Ed. by Jong-Ping Hsu and D. Fine, pp. 769–822. DOI: 10.1002/andp.200590044.

[12] Sean M. Carroll. *Spacetime and Geometry*. Cambridge University Press, July 2019. ISBN: 978-0-8053-8732-2, 978-1-108-48839-6, 978-1-108-77555-7.

[13] Edwin Hubble. "A relation between distance and radial velocity among extra-galactic nebulae." In: *Proc. Nat. Acad. Sci.* 15 (1929), pp. 168–173. DOI: 10.1073/pnas.15.3.168.

[14] M. J. Way and Harry Nussbaumer. "Lema\^{i}tre's Hubble relationship." In: *Phys. Today* 64N8 (2011), p. 8. DOI: 10.1063/PT.3.1194. arXiv: 1104.3031 [physics.hist-ph].

[15] Sidney van den Bergh. "The Curious Case of Lemaitre's Equation No. 24." In: *J. Roy. Astron. Soc. Canada* 105 (2011), p. 151. arXiv: 1106.1195 [physics.hist-ph].

[16] N. Aghanim et al. "Planck 2018 results. VI. Cosmological parameters." In: *Astron. Astrophys.* 641 (2020), A6. DOI: 10.1051/0004-6361/201833910. arXiv: 1807.06209 [astro-ph.CO].

[17] G. Hinshaw et al. "Nine-Year Wilkinson Microwave Anisotropy Probe (WMAP) Observations: Cosmological Parameter Results." In: *Astrophys. J. Suppl.* 208 (2013), p. 19. DOI: 10.1088/0067-0049/208/2/19. arXiv: 1212.5226 [astro-ph.CO].

[18] Steven Weinberg. *Cosmology*. 2008. ISBN: 978-0-19-852682-7.

[19] A. Baha Balantekin and Boris Kayser. "On the Properties of Neutrinos." In: *Ann. Rev. Nucl. Part. Sci.* 68 (2018), pp. 313–338. DOI: 10.1146/annurev-nucl-101916-123044. arXiv: 1805.00922 [hep-ph].

[20] Hiroshi Nunokawa, Stephen J. Parke, and Jose W. F. Valle. "CP Violation and Neutrino Oscillations." In: *Prog. Part. Nucl. Phys.* 60 (2008), pp. 338–402. DOI: 10.1016/j.ppnp.2007.10.001. arXiv: 0710.0554 [hep-ph].

[21] Nathalie Palanque-Delabrouille et al. "Neutrino masses and cosmology with Lyman-alpha forest power spectrum." In: *Journal of Cosmology and Astroparticle Physics* 2015.11 (2015), p. 011. DOI: 10.1088/1475-7516/2015/11/011. arXiv: 1506.05976.

[22] Elena Giusarma, Sunny Vagnozzi, Shirley Ho, Simone Ferraro, Katherine Freese, Rocky Kamen-Rubio, and Kam-Biu Luk. "Scale-dependent galaxy bias, CMB lensing-galaxy cross-correlation, and neutrino masses." In: *Phys. Rev. D* 98 (2018), p. 123526. DOI: 10.1103/PhysRevD.98.123526. arXiv: 1802.08694.

[23] F. Zwicky. "Die Rotverschiebung von extragalaktischen Nebeln." In: *Helv. Phys. Acta* 6 (1933), pp. 110–127. DOI: 10.1007/s10714-008-0707-4.

[24] Yoshiaki Sofue and Vera Rubin. "Rotation curves of spiral galaxies." In: *Ann. Rev. Astron. Astrophys.* 39 (2001), pp. 137–174. DOI: 10.1146/annurev.astro.39.1.137. arXiv: astro-ph/0010594.

[25] Douglas Clowe, Marusa Bradac, Anthony H. Gonzalez, Maxim Markevitch, Scott W. Randall, Christine Jones, and Dennis Zaritsky. "A direct empirical proof of the existence of dark matter." In: *Astrophys. J. Lett.* 648 (2006), pp. L109–L113. DOI: 10.1086/508162. arXiv: astro-ph/0608407.

[26] Scott Dodelson. *Gravitational Lensing*. UK: Cambridge University Press, 2017.

[27] Nicola Bellomo, José Luis Bernal, Alvise Raccanelli, and Licia Verde. "Primordial Black Holes as Dark Matter: Converting Constraints from Monochromatic to Extended Mass Distributions." In: *JCAP* 01 (2018), p. 004. DOI: 10.1088/1475-7516/2018/01/004. arXiv: 1709.07467 [astro-ph.CO].

[28] Robert E. Williams et al. "The Hubble Deep Field: Observations, data reduction, and galaxy photometry." In: *Astron. J.* 112 (1996), p. 1335. DOI: 10.1086/118105. arXiv: astro-ph/9607174.

[29] S. Perlmutter et al. "Measurements of Ω and Λ from 42 high redshift supernovae." In: *Astrophys. J.* 517 (1999), pp. 565–586. DOI: 10.1086/307221. arXiv: astro-ph/9812133.

[30] Adam G. Riess et al. "Observational evidence from supernovae for an accelerating universe and a cosmological constant." In: *Astron. J.* 116 (1998), pp. 1009–1038. DOI: 10.1086/300499. arXiv: astro-ph/9805201.

[31] Alan H. Guth. "The Inflationary Universe: A Possible Solution to the Horizon and Flatness Problems." In: *Phys. Rev. D* 23 (1981). Ed. by Li-Zhi Fang and R. Ruffini, pp. 347–356. DOI: 10.1103/PhysRevD.23.347.

[32] Andrei D. Linde. "A New Inflationary Universe Scenario: A Possible Solution of the Horizon, Flatness, Homogeneity, Isotropy and Primordial Monopole Problems." In: *Phys. Lett. B* 108 (1982). Ed. by Li-Zhi Fang and R. Ruffini, pp. 389–393. DOI: 10.1016/0370-2693(82)91219-9.

[33] K. Sato. "First Order Phase Transition of a Vacuum and Expansion of the Universe." In: *Mon. Not. Roy. Astron. Soc.* 195 (1981), pp. 467–479.

[34] Alexei A. Starobinsky. "Dynamics of Phase Transition in the New Inflationary Universe Scenario and Generation of Perturbations." In: *Phys. Lett. B* 117 (1982), pp. 175–178. DOI: 10.1016/0370-2693(82)90541-X.

[35] Debika Chowdhury, Jérôme Martin, Christophe Ringeval, and Vincent Vennin. "Assessing the scientific status of inflation after Planck." In: *Phys. Rev. D* 100.8 (2019), p. 083537. DOI: 10.1103/PhysRevD.100.083537. arXiv: 1902.03951 [astro-ph.CO].

[36] Paul J. Steinhardt and Neil Turok. "The Cyclic universe: An Informal introduction." In: *Nucl. Phys. B Proc. Suppl.* 124 (2003). Ed. by D. B. Cline, pp. 38–49. DOI: 10.1016/S0920-5632(03)02075-9. arXiv: astro-ph/0204479.

[37] Paul J. Steinhardt, Neil Turok, and N. Turok. "A Cyclic model of the universe." In: *Science* 296 (2002), pp. 1436–1439. DOI: 10.1126/science.1070462. arXiv: hep-th/0111030.

[38] Robert H. Brandenberger. "Alternatives to the inflationary paradigm of structure formation." In: *Int. J. Mod. Phys. Conf. Ser.* 01 (2011). Ed. by Sang Pyo Kim, pp. 67–79. DOI: 10.1142/S2010194511000109. arXiv: 0902.4731 [hep-th].

[39] Abhay Ashtekar. "New Variables for Classical and Quantum Gravity." In: *Phys. Rev. Lett.* 57 (18 1986), pp. 2244–2247. DOI: 10.1103/PhysRevLett.57.2244. URL: https://link.aps.org/doi/10.1103/PhysRevLett.57.2244.

[40] Ted Jacobson and Lee Smolin. "Nonperturbative Quantum Geometries." In: *Nucl. Phys. B* 299 (1988), pp. 295–345. DOI: 10.1016/0550-3213(88)90286-6.

[41] Leonard E. Parker and D. Toms. *Quantum Field Theory in Curved Spacetime: Quantized Field and Gravity*. Cambridge Monographs on Mathematical Physics. Cambridge University Press, Aug. 2009. ISBN: 978-0-521-87787-9, 978-0-521-87787-9, 978-0-511-60155-2. DOI: 10.1017/CBO9780511813924.

[42] N. D. Birrell and P. C. W. Davies. *Quantum Fields in Curved Space*. Cambridge Monographs on Mathematical Physics. Cambridge, UK: Cambridge Univ. Press, Feb. 1984. ISBN: 978-0-521-27858-4, 978-0-521-27858-4. DOI: 10.1017/CBO9780511622632.

[43] Marco Lanzagorta. *Quantum Information in Gravitational Fields*. 2053-2571. Morgan and Claypool Publishers, 2014. ISBN: 978-1-627-05330-3. DOI: 10.1088/978-1-627-05330-3. URL: http://dx.doi.org/10.1088/978-1-627-05330-3.

[44] M. Carmeli. *Group theory and general relativity: Representations of the Lorentz group and their applications to the gravitational field*. 2000.

[45] E. Cartan. *The Theory of Spinors*. New York:Dover, 1981.

[46] Peter Collas and David Klein. *The Dirac Equation in Curved Spacetime: A Guide for Calculations, Appendix A*. SpringerBriefs in Physics. Springer, 2019. ISBN: 978-3-030-14825-6. DOI: 10.1007/978-3-030-14825-6. arXiv: 1809.02764 [gr-qc].

[47] Ali H. Chamseddine and Viatcheslav Mukhanov. "Mimetic Dark Matter." In: *JHEP* 11 (2013), p. 135. DOI: 10.1007/JHEP11(2013)135. arXiv: 1308.5410 [astro-ph.CO].

[48] Ali H. Chamseddine, Viatcheslav Mukhanov, and Alexander Vikman. "Cosmology with Mimetic Matter." In: *JCAP* 06 (2014), p. 017. DOI: 10.1088/1475-7516/2014/06/017. arXiv: 1403.3961 [astro-ph.CO].

[49] Zili Shen, Shany Danieli, Pieter van Dokkum, Roberto Abraham, Jean P. Brodie, Charlie Conroy, Andrew E. Dolphin, Aaron J. Romanowsky, J. M. Diederik Kruijssen, and Dhruba Dutta Chowdhury. "A Tip of the Red Giant Branch Distance of 22.1 ± 1.2 Mpc to the Dark Matter Deficient Galaxy NGC 1052–DF2 from 40 Orbits of Hubble Space Telescope Imaging." In: *Astrophys. J. Lett.* 914.1 (2021), p. L12. DOI: 10.3847/2041-8213/ac0335. arXiv: 2104.03319 [astro-ph.GA].

[50] Pavel E. Mancera Piña et al. "Off the Baryonic Tully–Fisher Relation: A Population of Baryon-dominated Ultra-diffuse Galaxies." In: *Astrophys. J. Lett.* 883.2 (2019), p. L33. DOI: 10.3847/2041-8213/ab40c7. arXiv: 1909.01363 [astro-ph.GA].

[51] Qi Guo et al. "Further evidence for a population of dark-matter-deficient dwarf galaxies." In: *Nature Astron.* 4.3 (2019), pp. 246–251. DOI: 10.1038/s41550-019-0930-9. arXiv: 1908.00046 [astro-ph.GA].

[52] Pieter van Dokkum et al. "A galaxy lacking dark matter." In: *Nature* 555.7698 (2018), pp. 629–632. DOI: 10.1038/nature25767. arXiv: 1803.10237 [astro-ph.GA].

[53] Asher Wasserman, Aaron J. Romanowsky, Jean Brodie, Pieter van Dokkum, Charlie Conroy, Roberto Abraham, Yotam Cohen, and Shany Danieli. "A Deficit of Dark Matter from Jeans Modeling of the Ultra-diffuse Galaxy NGC 1052-DF2." In: *Astrophys. J. Lett.* 863.2 (2018), p. L15. DOI: 10.3847/2041-8213/aad779. arXiv: 1807.07069 [astro-ph.GA].

[54] Shany Danieli, Pieter van Dokkum, Charlie Conroy, Roberto Abraham, and Aaron J. Romanowsky. "Still Missing Dark Matter: KCWI High-Resolution Stellar Kinematics of NGC1052-DF2." In: *Astrophys. J. Lett.* 874.2 (2019), p. L12. DOI: 10.3847/2041-8213/ab0e8c. arXiv: 1901.03711 [astro-ph.GA].

[55] Fergus Simpson, Raul Jimenez, Carlos Pena-Garay, and Licia Verde. "Dark energy from the motions of neutrinos." In: *Phys. Dark Univ.* 20 (2018), pp. 72–77. DOI: 10.1016/j.dark.2018.04.002. arXiv: 1607.02515 [astro-ph.CO].

[56] Raul Jimenez, Roy Maartens, Ali Rida Khalifeh, Robert R. Caldwell, Alan F. Heavens, and Licia Verde. "Measuring the Homogeneity of the Universe Using Polarization Drift." In: *JCAP* 05 (2019), p. 048. DOI: 10.1088/1475-7516/2019/05/048. arXiv: 1902.11298 [astro-ph.CO].

[57] Raul Jimenez and Abraham Loeb. "Constraining cosmological parameters based on relative galaxy ages." In: *Astrophys. J.* 573 (2002), pp. 37–42. DOI: 10.1086/340549. arXiv: astro-ph/0106145.

[58] Joan Simon, Licia Verde, and Raul Jimenez. "Constraints on the redshift dependence of the dark energy potential." In: *Phys. Rev. D* 71 (2005), p. 123001. DOI: 10.1103/PhysRevD.71.123001. arXiv: astro-ph/0412269.

[59] Anthony Challinor. "Microwave background polarization in cosmological models." In: *Phys. Rev. D* 62 (2000), p. 043004. DOI: 10.1103/PhysRevD.62.043004. arXiv: astro-ph/9911481.

[60] Gianfranco Bertone and Dan Hooper. "History of dark matter." In: *Rev. Mod. Phys.* 90.4 (2018), p. 045002. DOI: 10.1103/RevModPhys.90.045002. arXiv: 1605.04909 [astro-ph.CO].

[61] Stefano Profumo. *An Introduction to Particle Dark Matter*. World Scientific, 2017. ISBN: 978-1-78634-000-9, 978-1-78634-001-6, 978-1-78634-001-6. DOI: 10.1142/q0001.

[62] M. Milgrom. "A Modification of the Newtonian dynamics as a possible alternative to the hidden mass hypothesis." In: *Astrophys. J.* 270 (1983), pp. 365–370. DOI: 10.1086/161130.

[63] M. Milgrom. "A modification of the Newtonian dynamics: implications for galaxy systems." In: *Astrophys. J.* 270 (1983), pp. 384–389. DOI: 10.1086/161132.

[64] M. Milgrom. "A Modification of the Newtonian dynamics: Implications for galaxies." In: *Astrophys. J.* 270 (1983), pp. 371–383. DOI: 10.1086/161131.

[65] J. Bekenstein and Mordehai Milgrom. "Does the missing mass problem signal the breakdown of Newtonian gravity?" In: *Astrophys. J.* 286 (1984), pp. 7–14. DOI: 10.1086/162570.

[66] Mordehai Milgrom. "Solutions for the modified Newtonian dynamics field equation." In: *Astrophys. J.* 302 (1986), pp. 617–625. DOI: 10.1086/164021.

[67] Jacob D. Bekenstein and Robert H. Sanders. "Gravitational lenses and unconventional gravity theories." In: *Astrophys. J.* 429 (1994), p. 480. DOI: 10.1086/174337. arXiv: astro-ph/9311062.

[68] R. H. Sanders. "The published extended rotation curves of spiral galaxies: confrontation with modified dynamics." In: *Astrophys. J.* 473 (1996), p. 117. DOI: 10.1086/178131. arXiv: astro-ph/9606089.

[69] Jacob D. Bekenstein. "Relativistic gravitation theory for the modified Newtonian dynamics paradigm." In: *Phys. Rev. D* 70 (8 2004), p. 083509. DOI: 10.1103/PhysRevD.70.083509. URL: https://link.aps.org/doi/10.1103/PhysRevD.70.083509.

[70] Ali Rida Khalifeh, Nicola Bellomo, José Luis Bernal, and Raul Jimenez. "Can Dark Matter be Geometry? A Case Study with Mimetic Dark Matter." In: *Phys. Dark Univ.* 30 (2020), p. 100646. DOI: 10.1016/j.dark.2020.100646. arXiv: 1907.03660 [astro-ph.CO].

[71] A. O. Barvinsky. "Dark matter as a ghost free conformal extension of Einstein theory." In: *JCAP* 01 (2014), p. 014. DOI: 10.1088/1475-7516/2014/01/014. arXiv: 1311.3111 [hep-th].

[72] Ali Rida Khalifeh. "Quintessential Inflation in Mimetic Dark Matter." In: (June 2015). arXiv: 1506.06250 [gr-qc].

[73] Frederico Arroja, Nicola Bartolo, Purnendu Karmakar, and Sabino Matarrese. "The two faces of mimetic Horndeski gravity: disformal transformations and Lagrange multiplier." In: *JCAP* 09 (2015), p. 051. DOI: 10.1088/1475-7516/2015/09/051. arXiv: 1506.08575 [gr-qc].

[74] Jiro Matsumoto, Sergei D. Odintsov, and Sergey V. Sushkov. "Cosmological perturbations in a mimetic matter model." In: *Phys. Rev. D* 91.6 (2015), p. 064062. DOI: 10.1103/PhysRevD.91.064062. arXiv: 1501.02149 [gr-qc].

[75] Ratbay Myrzakulov, Lorenzo Sebastiani, Sunny Vagnozzi, and Sergio Zerbini. "Static spherically symmetric solutions in mimetic gravity: rotation curves and wormholes." In: *Class. Quant. Grav.* 33.12 (2016), p. 125005. DOI: 10.1088/0264-9381/33/12/125005. arXiv: 1510.02284 [gr-qc].

[76] L. Sebastiani, S. Vagnozzi, and R. Myrzakulov. "Mimetic gravity: a review of recent developments and applications to cosmology and astrophysics." In: *Adv. High Energy Phys.* 2017 (2017), p. 3156915. DOI: 10.1155/2017/3156915. arXiv: 1612.08661 [gr-qc].

[77] Frederico Arroja. "The Two Faces of Mimetic Horndeski Gravity: Disformal Transformations and Lagrange Multiplier." In: *2nd LeCosPA Symposium: Everything about Gravity, Celebrating the Centenary of Einstein's General Relativity*. 2017. DOI: 10.1142/9789813203952_0056.

[78] Hassan Firouzjahi, Mohammad Ali Gorji, and Seyed Ali Hosseini Mansoori. "Instabilities in Mimetic Matter Perturbations." In: *JCAP* 07 (2017), p. 031. DOI: 10.1088/1475-7516/2017/07/031. arXiv: 1703.02923 [hep-th].

[79] Sunny Vagnozzi. "Recovering a MOND-like acceleration law in mimetic gravity." In: *Class. Quant. Grav.* 34.18 (2017), p. 185006. DOI: 10.1088/1361-6382/aa838b. arXiv: 1708.00603 [gr-qc].

[80] Julien Lesgourgues. "The Cosmic Linear Anisotropy Solving System (CLASS) I: Overview." In: (Apr. 2011). arXiv: 1104.2932 [astro-ph.IM].

[81] Diego Blas, Julien Lesgourgues, and Thomas Tram. "The Cosmic Linear Anisotropy Solving System (CLASS) II: Approximation schemes." In: *JCAP* 07 (2011), p. 034. DOI: 10.1088/1475-7516/2011/07/034. arXiv: 1104.2933 [astro-ph.CO].

[82] Ali Rida Khalifeh and Raul Jimenez. "Dwarf Galaxies without Dark Matter: constraints on Modified Gravity." In: *Mon. Not. Roy. Astron. Soc.* 501.1 (2021), pp. 254–260. DOI: 10.1093/mnras/staa3653. arXiv: 1912.08592 [gr-qc].

[83] Pavel E. Mancera Piña, Filippo Fraternali, Tom Oosterloo, Elizabeth A. K. Adams, Kyle A. Oman, and Lukas Leisman. "No need for dark matter: resolved kinematics of the ultra-diffuse galaxy AGC 114905." In: (Nov. 2021). arXiv: 2112.00017 [astro-ph.GA].

[84] Richard L. Arnowitt, Stanley Deser, and Charles W. Misner. "The Dynamics of general relativity." In: *Gen. Rel. Grav.* 40 (2008), pp. 1997–2027. DOI: 10.1007/s10714-008-0661-1. arXiv: gr-qc/0405109.

[85] Timothy Clifton, Pedro G. Ferreira, Antonio Padilla, and Constantinos Skordis. "Modified Gravity and Cosmology." In: *Phys. Rept.* 513 (2012), pp. 1–189. DOI: 10.1016/j.physrep.2012.01.001. arXiv: 1106.2476 [astro-ph.CO].

[86] Julien Lesgourgues, Gianpiero Mangano, Gennaro Miele, and Sergio Pastor. *Neutrino Cosmology*. Cambridge University Press, Feb. 2013. ISBN: 978-1-108-70501-1, 978-1-139-60341-6.

[87] Massimiliano Lattanzi and Martina Gerbino. "Status of neutrino properties and future prospects - Cosmological and astrophysical constraints." In: *Front. in Phys.* 5 (2018), p. 70. DOI: 10.3389/fphy.2017.00070. arXiv: 1712.07109 [astro-ph.CO].

[88] Ali Rida Khalifeh and Raul Jimenez. "Spinors and Scalars in curved spacetime: Neutrino dark energy (DEν)." In: *Phys. Dark Univ.* 31 (2021), p. 100777. DOI: 10.1016/j.dark.2021.100777. arXiv: 2010.08181 [gr-qc].

[89] Ali Rida Khalifeh and Raul Jimenez. "Distinguishing Dark Energy models with neutrino oscillations." In: *Phys. Dark Univ.* 34 (2021), p. 100897. DOI: 10.1016/j.dark.2021.100897. arXiv: 2105.07973 [astro-ph.CO].

[90] Ali Rida Khalifeh and Raul Jimenez. "Using Neutrino Oscillations to Measure H_0." In: (Nov. 2021). arXiv: 2111.15249 [astro-ph.CO].

[91] Y. Chikashige, Rabindra N. Mohapatra, and R. D. Peccei. "Are There Real Goldstone Bosons Associated with Broken Lepton Number?" In: *Phys. Lett. B* 98 (1981), pp. 265–268. DOI: 10.1016/0370-2693(81)90011-3.

[92] M. Fukugita, S. Watamura, and M. Yoshimura. "Light Pseudoscalar Particle and Stellar Energy Loss." In: *Phys. Rev. Lett.* 48 (22 1982), pp. 1522–1525. DOI: 10.1103/PhysRevLett.48.1522. URL: https://link.aps.org/doi/10.1103/PhysRevLett.48.1522.

[93] Licia Verde, Tommaso Treu, and Adam G. Riess. "Tensions between the early and late Universe." In: *Nature Astronomy* 3 (2019), pp. 891–895. DOI: 10.1038/s41550-019-0902-0. arXiv: 1907.10625 [astro-ph.CO].

[94] Adam G. Riess, Stefano Casertano, Wenlong Yuan, Lucas M. Macri, and Dan Scolnic. "Large Magellanic Cloud Cepheid Standards Provide a 1% Foundation for the Determination of the Hubble Constant and Stronger Evidence for Physics beyond ΛCDM." In: *Astrophys. J.* 876.1 (2019), p. 85. DOI: 10.3847/1538-4357/ab1422. arXiv: 1903.07603 [astro-ph.CO].

[95] Adam G. Riess et al. "A 2.4% Determination of the Local Value of the Hubble Constant." In: *Astrophys. J.* 826.1 (2016), p. 56. DOI: 10.3847/0004-637X/826/1/56. arXiv: 1604.01424 [astro-ph.CO].

[96] M. G. Aartsen et al. "IceCube-Gen2: The Window to the Extreme Universe." In: *J. Phys. G* 48.6 (2021), p. 060501. DOI: 10.1088/1361-6471/abbd48. arXiv: 2008.04323 [astro-ph.HE].

[97] Hee-Jong Seo and Daniel J. Eisenstein. "Probing dark energy with baryonic acoustic oscillations from future large galaxy redshift surveys." In: *Astrophys. J.* 598 (2003), pp. 720–740. DOI: 10.1086/379122. arXiv: astro-ph/0307460.

[98] Raul Jimenez and Abraham Loeb. "Constraining cosmological parameters based on relative galaxy ages." In: *Astrophys. J.* 573 (2002), pp. 37–42. DOI: 10.1086/340549. arXiv: astro-ph/0106145.

[99] Joan Simon, Licia Verde, and Raul Jimenez. "Constraints on the redshift dependence of the dark energy potential." In: *Phys. Rev. D* 71 (2005), p. 123001. DOI: 10.1103/PhysRevD.71.123001. arXiv: astro-ph/0412269.

[100] M. Hazumi et al. "LiteBIRD: JAXA's new strategic L-class mission for all-sky surveys of cosmic microwave background polarization." In: *Proc. SPIE Int. Soc. Opt. Eng.* 11443 (2020), 114432F. DOI: 10.1117/12.2563050. arXiv: 2101.12449 [astro-ph.IM].

[101] Arjun Dey et al. "Overview of the DESI Legacy Imaging Surveys." In: *Astron. J.* 157.5 (2019), p. 168. DOI: 10.3847/1538-3881/ab089d. arXiv: 1804.08657 [astro-ph.IM].

[102] A. Cimatti, R. Laureijs, B. Leibundgut, S. Lilly, R. Nichol, A. Refregier, P. Rosati, M. Steinmetz, N. Thatte, and E. Valentijn. "Euclid Assessment Study Report for the ESA Cosmic Visions." In: (Dec. 2009). arXiv: 0912.0914 [astro-ph.CO].

[103] Elena Aprile. "The XENON Dark Matter Experiment." In: (Feb. 2005). arXiv: astro-ph/0502279.

[104] Philippe Brax. "Screening mechanisms in modified gravity." In: *Class. Quant. Grav.* 30 (2013), p. 214005. DOI: 10.1088/0264-9381/30/21/214005.

[105] Kevin Max, Moritz Platscher, and Juri Smirnov. "Gravitational Wave Oscillations in Bigravity." In: *Phys. Rev. Lett.* 119 (11 2017), p. 111101. DOI: 10.1103/PhysRevLett.119.111101. URL: https://link.aps.org/doi/10.1103/PhysRevLett.119.111101.

[106] Kevin Max, Moritz Platscher, and Juri Smirnov. "Decoherence of gravitational wave oscillations in bigravity." In: *Phys. Rev. D* 97 (6 2018), p. 064009. DOI: 10.1103/PhysRevD.97.064009. URL: https://link.aps.org/doi/10.1103/PhysRevD.97.064009.

[107] Tatsuya Narikawa, Koh Ueno, Hideyuki Tagoshi, Takahiro Tanaka, Nobuyuki Kanda, and Takashi Nakamura. "Detectability of bigravity with graviton oscillations using gravitational wave observations." In: *Phys. Rev. D* 91 (6 2015), p. 062007. DOI: 10.1103/PhysRevD.91.062007. URL: https://link.aps.org/doi/10.1103/PhysRevD.91.062007.

The bibliography printed above refers to citations in the Introduction, in individual chapter introductions and in Summary of Results, Discussions and Conclusions. Citations in each individual publication can be found listed within the corresponding publication.

COLOPHON

This document was typeset using the typographical look-and-feel `classicthesis` developed by André Miede and Ivo Pletikosić. The style was inspired by Robert Bringhurst's seminal book on typography "*The Elements of Typographic Style*". `classicthesis` is available for both LaTeX and LyX:

https://bitbucket.org/amiede/classicthesis/

Happy users of `classicthesis` usually send a real postcard to the author, a collection of postcards received so far is featured here:

http://postcards.miede.de/

Thank you very much for your feedback and contribution.

Final Version as of January 3, 2022 (classicthesis v4.6).